CCMS-87-09
VPI-E-87-10

VIRGINIA TECH

CENTER FOR COMPOSITE MATERIALS AND STRUCTURES

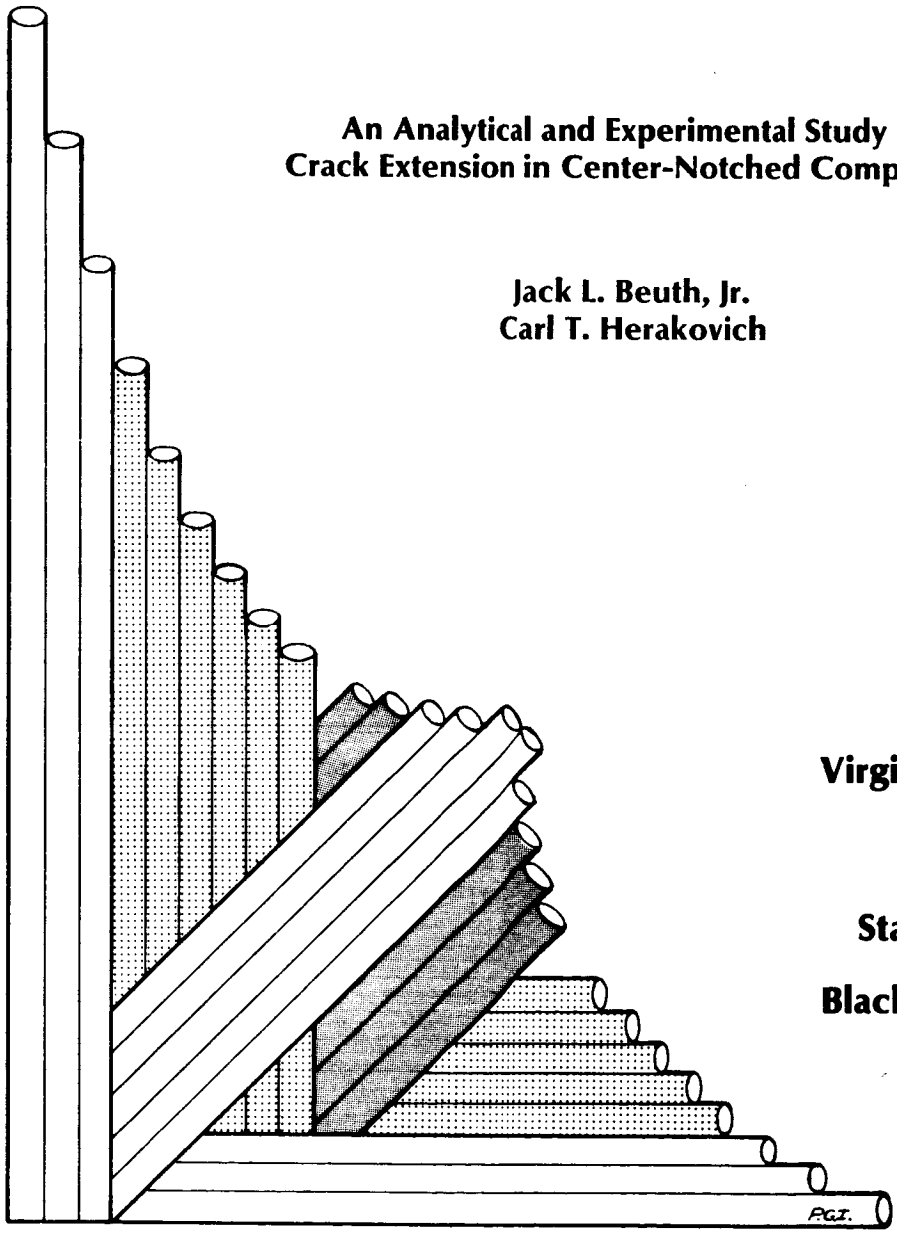

An Analytical and Experimental Study of Crack Extension in Center-Notched Composites

Jack L. Beuth, Jr.
Carl T. Herakovich

Virginia Polytechnic Institute and State University

Blacksburg, Virginia 24061

College of Engineering
Virginia Polytechnic Institute and State University
Blacksburg, Virginia 24061

July 1987

CCMS-87-09
VPI-E-87-10

An Analytical and Experimental Study of Crack Extension in Center-Notched Composites

Jack L. Beuth, Jr.[1]
Carl T. Herakovich[2]

Department of Engineering Science & Mechanics

Interim Report 61
The NASA-Virginia Tech Composites Program
NASA Grant NAG-1-343

Prepared for:

National Aeronautics and Space Administration
Langley Research Center
Hampton, Virginia 23665

Hercules Inc.
Composite Structures Group
Bacchus Works
Magna, Utah 84044

Center for Innovative Technology
Hallmark Bldg, Suite 201
13873 Park Center Road
Herndon, Virginia 22071

---

[1] Graduate Student, Department of Engineering Science & Mechanics

[2] Professor, Department of Engineering Science & Mechanics

An Analytical and Experimental Study of Crack Extension in Center-Notched Composites

by

Jack. L. Beuth, Jr.

Carl T. Herakovich, Chairman

Engineering Mechanics

(ABSTRACT)

The normal stress ratio theory for crack extension in anisotropic materials is studied analytically and experimentally in order to evaluate its validity. The theory is applied within a macroscopic-level analysis of a single center notch of arbitrary orientation in a unidirectional composite material. The bulk of the analytical work of this study applies an elasticity solution for an infinite plate with a center line crack to obtain critical stress and crack growth direction predictions. An elasticity solution for an infinite plate with a center elliptical flaw is also used to obtain qualitative predictions of the location of crack initiation around the border of an actual rounded notch tip. The analytical portion of the study includes the formulation of a new crack growth theory that includes local shear stress. Predictions of the normal stress ratio theory are obtained for the problems of a unidirectional tensile coupon with a horizontal center notch and a unidirectional Iosipescu shear specimen with a vertical center notch, each with an arbitrary fiber orientation. These predictions are subsequently compared to experimental results.

It is shown that the normal stress ratio theory exhibits a strong ability to correctly predict crack extension direction. Predicted critical stresses correlated well with experimental stresses at crack initiation. Use of the elliptical flaw analysis resulted in significant agreement with observed locations of crack extension, while still providing correct crack extension direction predictions. It is suggested that future analytical studies include application of the normal stress ratio theory as a predictor of critical stresses and its application within a rounded notch tip analysis. Also, future experimental efforts should include performing the critical shear tests identified in this study which could not be performed using the Iosipescu specimen.

Acknowledgements

This study was supported by the NASA-Virginia Tech Composites Program under the NASA Grant NAG-1-343, Hercules, Inc. and the Center for Innovative Technology. Special acknowledgement must be given to Gaurang Choksi who spent countless hours providing finite element results to compare with the analytical work of this study.

Table of Contents

List of Illustrations

List of Tables

1.0 Introduction and Survey of Fracture Theories

The existence of cracks and crack-like flaws can significantly reduce the strength of any engineering material. For isotropic materials containing such flaws, the methods of classical fracture mechanics have been developed and can be used to obtain reasonable estimates of cracked material strength. For composite materials, however, classical fracture mechanics principles can only be applied to a small class of problems. As a result, there is currently a great need for a theoretical method that is applicable to and accurate in predicting generalized notched composite strength behavior. Until such a method is proposed and verified, composite designs will continue to be inefficient, due to the need to compensate for a lack of reliable notched material strength predictions. This study represents an initial attempt at evaluating and extending an existing crack growth theory and correlating its predictions with experiment.

1.1 Isotropic Fracture Theories

1.1.1 Classical Methods

Because of the strong need for the ability to predict cracked material strength, a great number of researchers have proposed a number of analytical methods for approaching the problem. For isotropic materials, the most fundamental and by far the most widely applied and accepted are the methods of classical fracture mechanics, originally investigated by Griffith [1] and refined and expanded by Irwin [2]. The equivalent methods of critical strain energy release rate and critical stress intensity factor were derived for application to isotropic materials by making the assumption that crack extension will be collinear with an original flaw regardless of the far-field applied stress state. For such crack extension, the near-crack-tip stress state is the same both before and after crack growth. In obtaining the near-crack-tip stress field, a crack is modelled as an ellipse with a zero minor axis dimension. As a result, a crack is modelled as a line crack having an infinitely sharp tip. Under the constraint of these assumptions, stress-based and energetic analyses of the near-crack-tip stress field independently yield a monumental finding. They indicate that a cracked isotropic material subjected to a specific far-field stress state will have a unique critical far-field stress state value that is a function of the crack length only. This conclusion, expressed in the form of a critical stress intensity factor or critical strain energy release rate, represents the foundation of modern fracture mechanics principles.

Crack extension collinear with an original notch is observed experimentally for isotropic materials subjected to pure mode I far-field loading. For mode II and particularly mixed-mode applied far-field loading conditions, however, crack extension has consistently been shown to occur at an angle to an original crack. This observed behavior directly contradicts the theoretical assumption of self-similar crack growth used in deriving classical fracture mechanics principles. Despite this, classical fracture mechanics principles are currently used to obtain rough estimates of the effect of

an existing crack on the strength of isotropic materials subjected to mode II and mixed-mode far-field applied loads. This is possible because isotropic material strength is not directionally dependent. As a result, the strength of a cracked isotropic material is not a strong function of the direction of crack extension. The strength estimates that result from the use of classical fracture mechanics principles are reliable enough to be useful as a guide for design engineers, but are not highly accurate. Also, from a research standpoint it is essential that linear fracture mechanics principles be extended or modified in a way to allow them to account for non-collinear crack extension. Only in this way can a fundamental understanding of fracture mechanics behavior be obtained.

1.1.2 Mixed-Mode Fracture Theories

In an attempt to correct the contradiction between the assumption of crack extension collinear with an original flaw made in deriving classical fracture mechanics principles and observations made of mode II and mixed-mode crack extension, and to provide more accurate mixed-mode strength predictions, a number of theories have been proposed to solve the mode II and mixed-mode crack extension problems in isotropic materials. In this report, four of the most prominent of such theories will be briefly outlined and compared. Application of each of these theories yields not only a prediction of cracked material strength, but also a prediction of the direction of crack extension.

1.1.2.1 Maximum Normal Stress Theory

The first isotropic crack growth theory to take into account non-collinear crack extension was the maximum normal stress theory developed by Erdogan and Sih [3]. The maximum normal stress theory assumes that crack extension occurs in the direction of maximum normal stress, $\sigma_{\theta\theta}$,

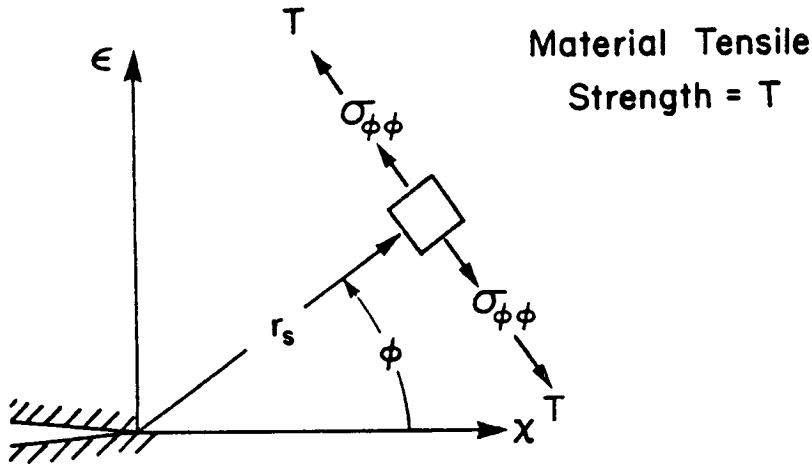

Figure 1. Maximum Normal Stress Theory Parameters

evaluated at a specified distance, r_s, from the crack tip, when the maximum value of $\sigma_{\varphi\varphi}$ reaches the material tensile strength, T (Figure 1). The theory is based upon the assumption that crack extension behavior is principally controlled by mode I (opening) crack displacement.

1.1.2.2 Strain Energy Density Theory

The strain energy density theory [4] represents an attempt to predict crack growth behavior in isotropic materials by evaluating the strain energy per unit volume around the crack tip, in a pointwise manner. It is based upon the local variation of the strain energy density factor, S, defined for plane stress problems as

$$S = \frac{r_s}{2}(\sigma_x\varepsilon_x + \sigma_y\varepsilon_y + \tau_{xy}\gamma_{xy}) \ . \tag{1}$$

The theory proposes that crack extension occurs in the direction of maximum potential energy density, corresponding to a minimum value of the strain energy density factor, evaluated at a specified distance, r_s , from the crack tip. Crack extension is hypothesized to occur when the minimum value of S reaches a critical value. For an isotropic material, the strain energy density factor can be separated into dilatational and distortional components. It is shown in [5] that, when this is done, the direction of minimum S generally has a larger value of dilatational strain energy density than distortional strain energy density. As pointed out in [5], this suggests that the theory corresponds with observations that crack growth often occurs as the result of material elements breaking up ahead of the crack tip and then joining with it.

1.1.2.3 Maximum Dilatational Strain Energy Density Theory

Another theory used to model mixed-mode crack extension on the basis of the local distribution of stress around a sharp crack tip is the maximum dilatational strain energy density theory,

originally proposed in [6,7] and modified to predict critical stresses in [8]. The theory is highly similar to the strain energy density theory, except for two important differences. First, instead of considering the total strain energy density functional at a specified distance from the crack tip, only the dilatational component is considered. As previously mentioned, for isotropic materials, the dilatational and distortional components of the strain energy per unit volume can be separated. The expression that results for the dilatational strain energy density under plane stress conditions is

$$(\frac{\partial W}{\partial V})_D = \frac{1-2\nu}{6E}(\sigma_x + \sigma_y)^2 \ . \tag{2}$$

In this theory, it is assumed that only this portion of the strain energy density around the crack tip contributes to crack extension. The second difference between this theory and the strain energy density theory is that, unlike the strain energy density theory, the region around the crack tip along the periphery of which the dilatational strain energy density is evaluated is not a circle. It is instead the elastic-plastic boundary defined by the Von-Mises yield theory. As a result, the distance from the crack tip at which the dilatational strain energy density is evaluated is a function of both far-field loading conditions and angle around the crack tip.

The maximum dilatational strain energy density theory hypothesizes that a crack will extend from an existing flaw in an isotropic material in the direction of maximum $(\frac{\partial W}{\partial V})_D$. It can be shown that, because of the way in which the theory is formulated, as far-field stresses applied to the material are proportionally increased, the value of $(\frac{\partial W}{\partial V})_D$ in a given direction remains a constant. The value of r_s in the direction of maximum dilatational strain energy density does increase, however, in order to satisfy the Von Mises yield criterion. Because of this, the theory states that crack extension will occur when the value of r_s in the direction of maximum dilatational strain energy density reaches a critical value.

The maximum dilatational strain energy density theory is obviously formulated in an attempt to account for material elements breaking up ahead of the crack tip, as the strain energy density theory does. It does so, however, in a much more direct way, by considering the dilatational

component of the strain energy density functional only. The theory also represents an advancement over both the maximum normal stress theory and the strain energy density theory in that it allows a non-circular core region around the crack tip, along the boundary of which the theory is applied. This is an important step, because the core region around the analytically modelled sharp crack tip should roughly correspond to the plastic region around an actual crack tip. Experiments clearly indicate that the crack tip plastic region is generally not circular in shape in isotropic materials. The maximum dilatational strain energy density theory thus has the potential for defining the shape of the actual crack tip plastic region. It is along this boundary that the elastic stresses reach their highest value and an elastic fracture theory should be applied.

1.1.2.4 Energy Release Rate Criterion

The final theory outlined in this study for the prediction of mixed-mode isotropic material fracture behavior is an energy release rate criterion formulated by Nuismer [9]. Instead of looking at the local distribution of stresses around a sharp crack tip, the theory uses the classical fracture mechanics expression for the energy release rate for a sharp crack propagating in its own plane,

$$G_o = \frac{\pi(\kappa + 1)}{8\mu}(k_1^2 + k_2^2) \ , \tag{3}$$

where k_1 and k_2 are the cracked material stress intensity factors, μ is the material shear modulus, and $\kappa = (3 - 4\nu)$ for plane strain and $\frac{(3 - \nu)}{(1 + \nu)}$ for generalized plane stress. It is assumed that the energy release rate for a crack propagating out of its plane (branch crack) will also be defined by the above expression, except that the stress intensity factors will be changed. The stress intensity factors for the branch crack are then derived by making a continuity assumption, assuming that the stress field at the tip of the branch crack must approach the stress field at the tip of the original crack, in the limit, as the branch crack length approaches zero. The resulting expression for the energy release rate due to the initiation of a branch crack is a function of the stress state before crack extension occurs and the direction of crack extension only.

The energy release rate theory of Nuismer postulates that crack extension will occur in the direction of maximum energy release rate, when the maximum reaches a critical value. This theory is attractive in that it is a direct extension of classical fracture mechanics principles to the problem of non-collinear crack extension. It is also important to note that in [9] it is shown that the expression for energy release rate that results from the analysis will necessarily have its maximum in the same direction as the maximum normal stress evaluated around the crack tip. Thus, it appears that this energy-based theory and the maximum normal stress theory correlate with one another.

1.1.3 Comparison of Mixed-Mode Theories

A number of researchers have attempted to compare the isotropic fracture theories outlined thus far with respect to their ability to predict both crack extension direction and critical stresses. A typical study is that by Swedlow [10] where the maximum normal stress and strain energy density theories are compared. In the study it is shown that, with respect to predicted direction of crack extension, both theories give similar predictions that compare reasonably well with experiment. Also, scatter is noted in the experimentally observed crack growth directions. The same type of results are generally found with respect to critical stress predictions. All of the prevalent mixed-mode fracture theories yield similar and reasonable values in isotropic materials, especially in light of experimental scatter. As a result, it currently appears that the study of fracture problems in isotropic materials does not provide a critical test to determine which theory and/or approach may be correct. This becomes especially important in attempting to extend one or more of these theories to the more complicated problem of crack extension in anisotropic materials.

1.2 Anisotropic Fracture Theories

A number of complexities present themselves in trying to extend current fracture analysis techniques, most originally developed for application to isotropic materials, to anisotropic materials such as composites. The directional dependence of stiffness and strength, for example, results in a number of complications. First, the cracked material stress solution must be able to account for stiffness anisotropy. Second, the direction of crack extension from an original flaw is strongly dependent on the directional dependence of strength. As a result, crack extension is typically not collinear with an original flaw regardless of applied far-field stress state. Not only does this result in the complications associated with mixed-mode fracture in isotropic materials, but the directional dependence of strength makes accurate prediction of crack extension direction essential in correctly predicting critical applied stresses. The high degree of composite material heterogeneity presents an even larger number of potential fracture analysis complications. As will be outlined in the subsequent section on micromechanical modelling, attempting to model composite material fracture behavior in a way that accounts for material heterogeneity has thus far resulted in complications and eventual limits on the types of problems that can be addressed.

Zweben [11] has outlined a number of approaches that have been taken to solve the problem of crack growth in composites. He divides these approaches into two groups, those that account for material heterogeneity by treating the problem on a micromechanical level, and those that assume that the material is homogeneous by treating it on a macroscopic level. The summary of approaches given in this report will roughly follow that of Zweben [11].

1.2.1 Micromechanical-Level Approaches

Faced with the highly heterogeneous nature of composite materials, a number of researchers have attempted to study the problem of a cracked composite on a micromechanical level, distinctly

modelling fiber, matrix, and interfacial regions. The most rigorous analyses of this type involve applying classical fracture mechanics principles to an elastic solution to the problem. Recent work by Wang and Choi [12,13] represents a good example of such efforts. Because of the complexity of the required analysis, various assumptions concerning material geometry must be made. Even with such assumptions, only a few, simple geometries can be analyzed. As a result, full elastic analyses on a micromechanical level are not readily applicable to real engineering problems. Because of this, most current micromechanical analyses apply an approach originally referred to by Zweben [11] as "material modelling." This approach involves making various assumptions concerning not only material geometry, but also material stress state, and, at times, failure mode. Recent work by Goree and Wolla [14] using a shear-lag crack growth model serves as a good example of the application of such an approach.

The attractiveness of micromechanical modelling of unidirectional composite crack growth is that it takes composite heterogeneity into account. The approach is not without a number of drawbacks, however. First, the complicated nature of the analysis currently limits its applicability to non-off-axis unidirectional or simple laminate [11] geometries. Even in analyzing unidirectional materials, with assumptions made concerning material behavior and geometry, the analysis is complicated. As a result, its potential flexibility in modelling generalized unidirectional composite crack problems is severely limited. This limit in the flexibility of the approach is more fully addressed in Section 2.1.1 of this report. There is also concern that the significant number of assumptions made to make the problem tractable sacrifices exactness to the point that the advantage of including fiber/matrix interactions is lost.

1.2.2 Macroscopic-Level Approaches

Because of the many complications and subsequent problems associated with analyzing composite fracture on a micromechanical level, many attempts have been made to solve the problem on a macroscopic level, neglecting material heterogeneity. A macroscopic approach to mod-

elling crack growth in composite materials treats the composite as a homogeneous anisotropic material, thus extending isotropic material fracture analysis techniques. Although composite crack extension is generally not collinear with an original flaw, in certain cases collinear crack extension does occur. As a result, the most straightforward macroscopic-level analysis uses a classical fracture mechanics stress intensity factor approach. Wu [15] has successfully employed this approach to model crack growth in unidirectional fiberglass. His work verifies that stress intensity factors can be used to predict failure in unidirectional composite specimens where the initial flaw or notch is oriented along the fiber direction. Except for problems having specific unidirectional geometries, however, stress intensity factors prove to be inadequate in predicting notched unidirectional composite strength. At best, the use of stress intensity factors is limited to problems where the orientation of the original notch with respect to the fibers remains constant. If their orientation with respect to one another is changed, a new set of critical stress intensity factors must be derived experimentally. Because of this substantial limitation, other fracture mechanics-based approaches have been proposed to model the problem. The most widely used approach involves evaluating local stresses at a specified distance from the crack tip using a homogeneous anisotropic elasticity solution. These stresses are then used within in a specific crack growth theory to determine critical stresses. This is analogous to the method used in applying fracture theories to mixed-mode problems in isotropic materials, where a circular core region shape is used. Three anisotropic fracture theories that use this approach are outlined below.

1.2.2.1 Tensor Polynomial Theory

The tensor polynomial failure criterion has been applied as a crack growth theory for anisotropic materials. It was originally derived, however, by Tsai and Wu [16] for application to uncracked composites. It is, therefore, a general failure theory that contains no hypotheses concerning what parameters may or may not contribute to crack extension. Its application as a crack growth theory on the border of a core region around a sharp crack tip represents a logical initial

attempt at crack growth analysis. The tensor polynomial failure criterion is based upon the existence of a failure surface in stress space of the form

$$f(\sigma_i) = F_i\sigma_i + F_{ij}\sigma_i\sigma_j \ , \tag{4}$$

where F_i and F_{ij} are strength tensors of second and fourth order, and σ_i is the contracted form of the stress tensor. In application of the tensor polynomial to fracture problems, it is assumed that crack extension occurs in the radial direction of maximum $f(\sigma_i)$, when $f(\sigma_i)$ reaches a value of 1.

1.2.2.2 Strain Energy Density Theory

The strain energy density theory has also been applied to the study of composite fracture [17]. The form and approach used to apply the theory are not modified from those used to study fracture in isotropic materials. Thus, the theory still hypothesizes that crack extension occurs in the direction of minimum S (Eq. 1), when S reaches a critical value. Because it has not been altered for application to composites, the strain energy density theory does not account for the directional dependence of material strength or resistance to crack extension. If the theory is indeed founded upon the assumption that a crack will extend in the direction of maximum potential energy density, it would seem logical that some account of the directional dependence of crack growth resistance would be necessary for its application to composites. If instead the theory represents an attempt at finding the direction having a large amount of volumetric strain energy density, then the directional dependence of strength would not affect the analysis and thus would not have to be accounted for.

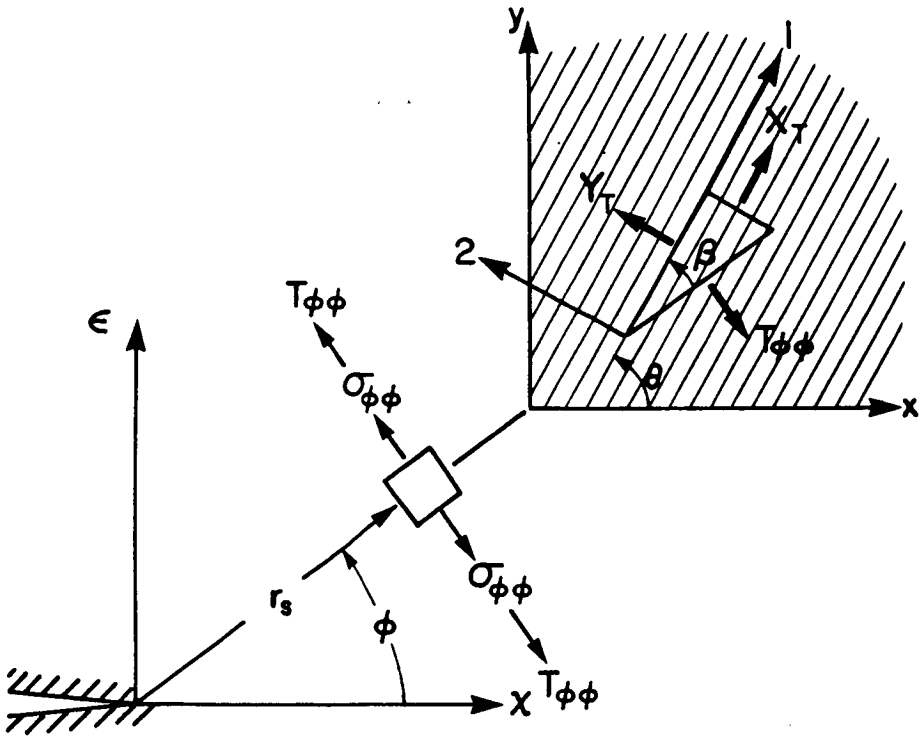

Figure 2. Normal Stress Ratio Theory Parameters

1.2.2.3 Normal Stress Ratio Theory

Buczek and Herakovich [18] have proposed the normal stress ratio as a crack growth direction criterion for composite materials. The theory is based upon work included in [19]. The normal stress ratio is defined as

$$R(r_s,\varphi) = \frac{\sigma_{\varphi\varphi}}{T_{\varphi\varphi}} \ . \tag{5}$$

In this expression, $\sigma_{\varphi\varphi}$ corresponds to the normal stress acting on the radial plane defined by φ, at a specified distance, r_s, from the crack tip. $T_{\varphi\varphi}$ is the tensile strength on the φ plane (Figure 2). The model assumes that the direction of crack extension corresponds to the radial direction having the maximum value of the normal stress ratio. In this study, the normal stress ratio theory will also be extended and used to predict critical applied far-field stresses. Critical stresses are defined as far-field stresses causing the value of the normal stress ratio along the predicted crack extension direction to equal 1. The normal stress ratio theory is clearly a direct extension of the maximum normal stress theory, formulated to make it applicable to anisotropic fracture problems. Like the maximum normal stress theory, it is based upon the assumption that mode I crack displacement controls crack extension. The difference between the two theories is that the normal stress ratio theory is able to account for a directional dependence of material strength through the strength parameter $T_{\varphi\varphi}$.

Because no experimental method currently exists for measuring the tensile strength on an arbitrary plane, $T_{\varphi\varphi}$ must be defined mathematically, in a manner consistent with tests that can be performed. Such tests require that $T_{\varphi\varphi}$ satisfy the following conditions:

1. for an isotropic material, $T_{\varphi\varphi}$ must not depend on φ;
2. for crack growth parallel to the fibers in a composite material, $T_{\varphi\varphi}$ must equal the transverse tensile strength, Y_t ;
3. for crack growth perpendicular to the fibers in a composite material, $T_{\varphi\varphi}$ must equal the longitudinal strength, X_t .

The definition of $T_{\varphi\varphi}$ used in [18] to satisfy these conditions is

$$T_{\varphi\varphi} = X_t \sin^2\beta + Y_t \cos^2\beta \ , \tag{6}$$

where β is the angle from the φ plane to the fiber axis (Figure 2).

Both the tensor polynomial and strain energy density theories have been compared extensively with experimental results from the persons who originally proposed them and from others. The tensor polynomial has been successfully applied to the fracture analysis of unidirectional fiberglass reinforced plastic [20] and also to multidirectional composite laminates [21], [22]. The strain energy density theory has been successfully applied to model crack extension in unidirectional fiberglass reinforced plastic, stainless steel reinforced aluminum, and graphite-epoxy composites [17]. Because it was more recently proposed, the normal stress ratio theory has had limited comparison with experiment and other theories. Three papers by this and other authors compare all three of the theories outlined in this report with experimentally observed crack extension directions. These results, detailed in Section 2.1.2 of this report, indicate a distinct difference in the ability of each of the three theories to correctly predict crack extension direction.

From the outline of anisotropic fracture theories just given, it is obvious that a great deal of effort has been made to extend, with or without modification, mixed-mode isotropic theories to the analysis of anisotropic materials. At this point, however, it appears that this practice cannot be significantly furthered. The only two major isotropic fracture theories yet to be modified and applied to anisotropic fracture problems are the maximum dilational strain energy density and maximum energy release rate theories. It does not appear possible, however, for either of these theories to be extended to application to anisotropic materials. For the maximum dilatational strain energy density theory to be applied to any material, closed-form expressions for the distortional and dilatational portions of the strain energy per unit volume must be deriveable. This does not appear possible for anisotropic materials. For the maximum strain energy release rate theory to be applied to a given type of material, a closed-form expression for the strain energy release rate for a crack propagating in its own plane, analogous to that given in Eq. 3, must be deriveable. Such an expression is not readily obtainable for an anisotropic material of arbitrary notch and fiber orientation.

2.0 Choosing an Analytical Approach

2.1 Choosing a Fracture Theory

2.1.1 Micromechanical vs. Macroscopic Approaches

As previously mentioned, application of a micromechanical-level approach to composite fracture results in a severe limit in flexibility in the type of problems that can be studied. The results of the aforementioned investigation by Goree and Wolla [14] illustrate this. In their study, a series of experiments on unidirectional AS4/3501-6 graphite-epoxy tensile coupons are performed in order to compare observed crack growth behavior to that predicted by their micromechanical shear-lag analysis. Their analysis assumes that the material fibers carry all extensional stresses, while the matrix carries all shear stresses. As illustrated in Figure 3, a crack is modelled as a number of consecutive broken fibers in an infinite two-dimensional material. It is also assumed that crack extension occurs along the fiber direction. In application of their model, a single baseline test must be performed in order to determine a value for G_m/h, where G_m is the matrix shear modulus and h

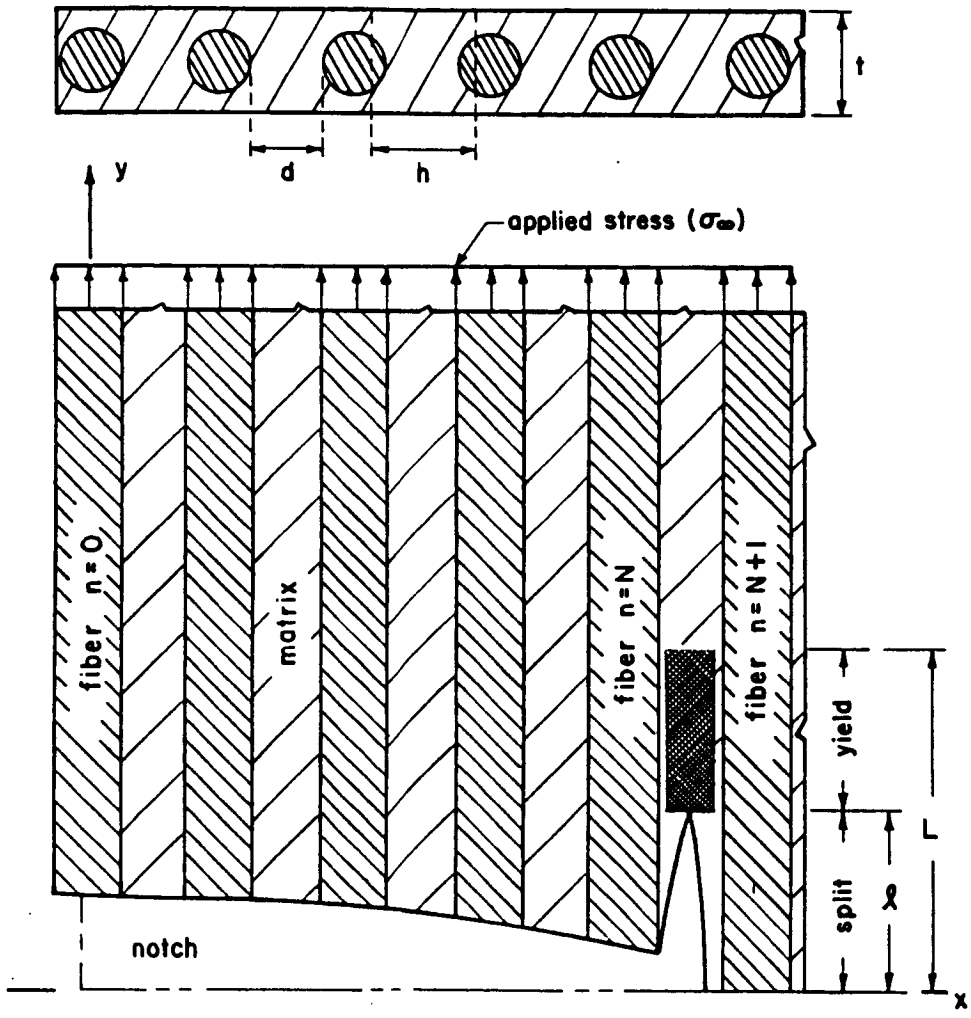

Figure 3. Problem Modelled Using the Shear-Lag Analysis of Goree and Wolla [14]: Figure Taken Directly from [14]

is related to the distance between fibers. The experimentally derived value of G_m/h is then treated as a material constant and used to predict critical stresses for other tests.

The experiments performed in [14] consisted of a series of tests on unidirectional tensile coupons with center notches of varying lengths. In all of the tests, the fiber and notch orientations were identical, with fibers oriented along the specimen loading axis and notches oriented at 90° to the loading axis (Figure 4). A combination of acoustic emission monitoring, brittle coating, x-ray radiography, and incremental loading was used to determine the applied axial stress at which crack initiation occurred. Comparisons were then made between observed critical stresses and those predicted by the analysis. Columns 1-3 of Table 1 present a short summary of the results of the experimental and analytical study. Values for number of broken fibers are proportional to the notch length. The test with a value for number of broken fibers of 19 was the baseline test. As a result, for this case experiment and theory match exactly. Comparison of the other experimental stress values with their corresponding theoretical predictions indicates that, for the cases studied, the shear-lag analysis presented in [14] appears to predict critical stresses well.

Although the application of the shear-lag theory as given in [14] illustrates the potential of using a micromechanical approach, this potential is limited. At this stage of micromechanical-level research on unidirectional materials, only the problem of a center-notched tensile coupon with fibers oriented along the loading axis and notch oriented at 90° to the loading axis can be analyzed. This presents two basic problems. Obviously, it presents a problem concerning how the theory might eventually be applied to general engineering applications. More importantly, however, it presents severe problems in attempting to verify the theory itself. For example, the agreement with experiment noted in [14] does not provide a full test of the validity of the shear-lag theory. Because only the length of the crack cut in each specimen was changed, only one type of crack growth test was really performed. In fact, predictions essentially identical to those of Goree and Wolla [14] can be obtained by assuming that crack initiation stresses are a function of the square root of the crack length. This macroscopic-level stress intensity factor-type approach is, as shown in [15], potentially applicable whenever the orientation of the crack with respect to the fibers is not changed from test to test. If, as in the shear-lag analysis, the test with 19 broken fibers is used as a baseline test (de-

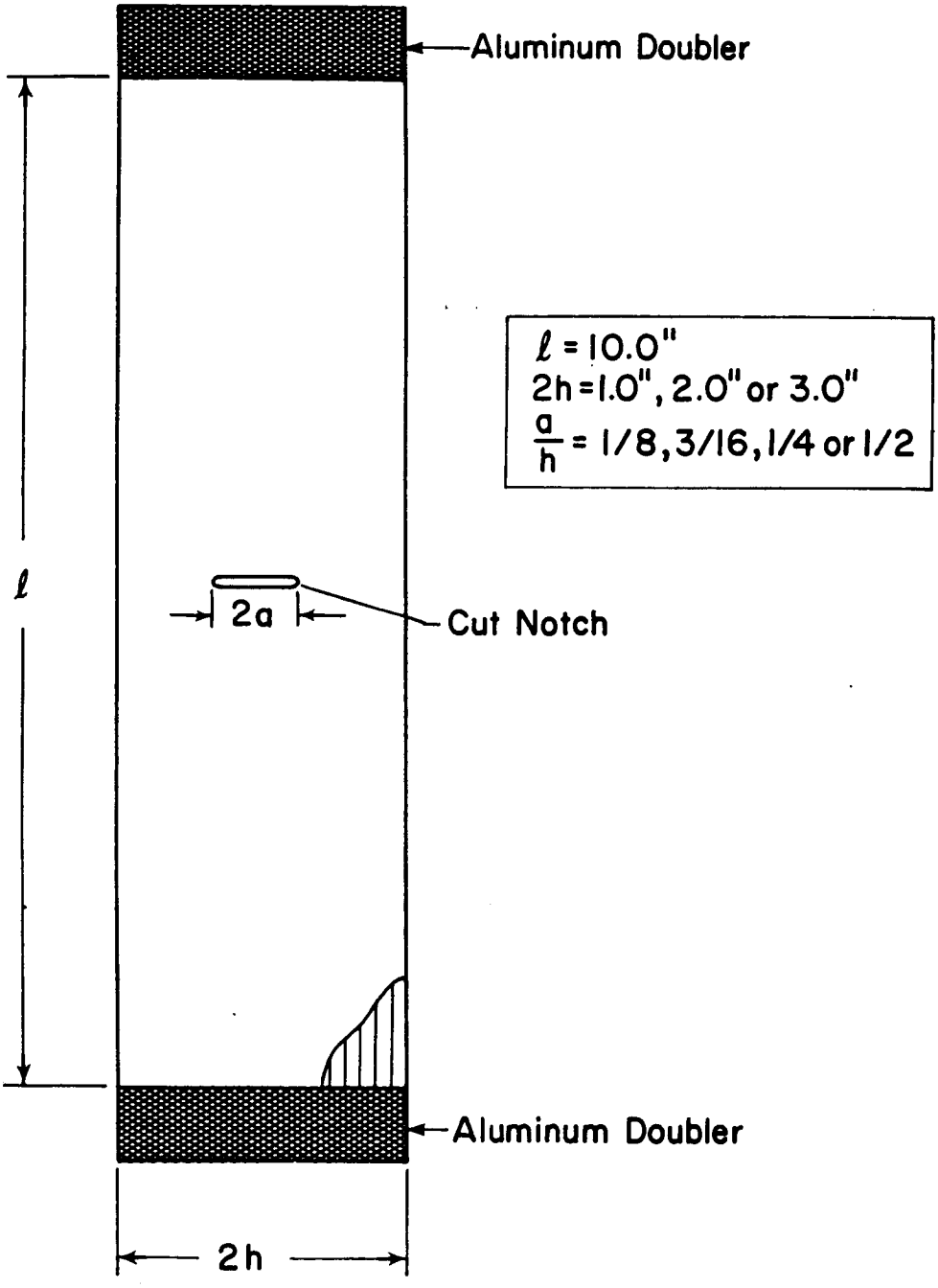

Figure 4. 0° Center-Notched Tensile Coupons Tested and Analyzed in [14]

Table 1. Micromechanical vs. Microscopic Composite Fracture Approaches

Comparison of Micromechanical and Macroscopic Critical Stress Predictions

Results from Goree and Wolla [14]			
Number of Broken Fibers (notch length)	Average Experimental Crack Initiation Stress ksi (MPa)	Shear Lag Analysis Predictions ksi (MPa)	Macroscopic Analysis Predictions ksi (MPa)
19	32.63 (225.0)	32.63 (225.0)	32.63 (225.0)
27	27.70 (191.0)	27.33 (188.4)	27.37 (188.7)
37	24.66 (170.0)	23.31 (160.7)	23.38 (161.2)
55	20.06 (138.3)	19.10 (131.7)	19.17 (132.2)
71	16.58 (114.3)	16.80 (115.8)	16.88 (116.4)
81	15.74 (108.5)	15.72 (108.4)	15.81 (109.0)
107	11.89 (82.0)	13.68 (94.3)	13.75 (94.8)
143	12.04 (83.0)	11.82 (81.5)	11.89 (82.0)
215	10.05 (69.3)	9.65 (66.5)	9.70 (66.9)

termining K_{IC}), accurate critical stresses can be predicted by simply normalizing its critical stress value of 32.63 ksi by the square root of the notch length (number of broken fibers). Thus, to predict a critical stress for the second test (having 27 broken fibers), a calculation of

$$\{32.63\}\ \sqrt{\frac{19}{27}} = 27.37 \tag{7}$$

is made. Comparison of the results of this very simple approach (column 4) with that of Goree and Wolla indicate that the predictions of each are essentially identical.

The fact that two very different crack growth modelling approaches can provide accurate and essentially identical predictions suggests that both approaches are reasonable. It is obvious, however, that the substantial effort expended in [14] to analyze the composite on a micromechanical level has resulted in an analysis that can only be applied to and tested against a single crack growth problem. In addition, the same problem can be dealt with in an almost trivial manner using a macroscopic-level approach. The advantage of applying a macroscopic-level analysis to crack growth problems becomes even greater when tests having different notch and fiber orientations are

modelled. A macroscopic-level analysis is applied by rotating the applied far-field stresses into the coordinate system associated with the crack. An existing elasticity solution, detailed in Section 3.3.2 of this report, can then be used to obtain the near-crack stresses for use within a particular crack growth theory. Although later research may yield micromechanical-level methods applicable to other types of problems, it does not appear that a micromechanical-level analysis will ever offer this level of flexibility in modelling problems with arbitrary notch and fiber orientations and applied far-field loads. This type of flexibility is essential if any fracture theory is to be tested fully.

The obvious disadvantage of using any macroscopic-level analysis and failure theory for predicting composite crack growth phenomena is that it ignores the significant degree of heterogeneity inherent in composites. The important question is whether composite heterogeneity must be accounted for, and if so, under what circumstances. The noted success of the application of a stress intensity factor approach to composites with an original flaw along the fiber direction indicates that in at least some cases composite heterogeneity can be neglected. Also, as previously mentioned, some successes have been noted in applying homogeneous anisotropic solutions with the three anisotropic fracture theories outlined in this study. Because of the current limits in applying a micromechanical-level analysis, and because of the flexibility, previous successes, and potential for application to real engineering problems associated with macroscopic-level analyses, only such analyses were considered for application in this study.

2.1.2 Comparison of Macroscopic-Level Theories

In papers by this and other authors [23-25], the tensor polynomial, strain energy density, and normal stress ratio theories have been compared with respect to their ability to predict observed directions of crack extension in unidirectional composites. The results provided in these publications are used as a basis for determining which macroscopic-level theory to emphasize in this study. Because it is the most recent of the three, and because it contains the most detailed description of the experiments involved, the paper by Beuth, Gregory, and Herakovich [25] will be referenced from

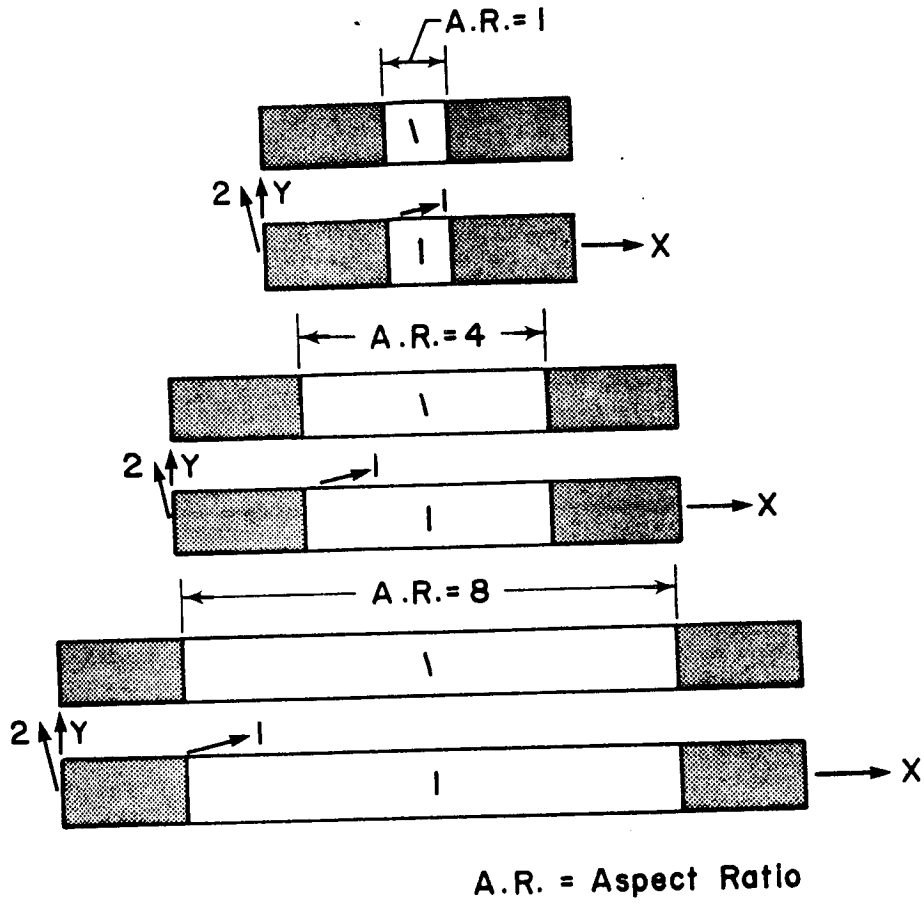

Figure 5. Center-Notched 15° Off-Axis Tensile Coupons Tested and Analyzed in [23-25]

this point on in this report. The experimental portion of the investigation consisted of tension tests on 15° off-axis specimens with constrained ends (Figure 5). Specimens with aspect ratios of one, four, and eight were tested with a center notch having one of two orientations. Notch orientations are measured with respect to the tensile axis (x axis). Thus, specimens designated as having 105° notches had their cut notches oriented perpendicular to the material fiber axis. Specimens designated as having 90° notches had their cut notches oriented perpendicular to the specimen loading axis. All of the twelve specimens tested (two of each aspect ratio/notch angle configuration) were made of 16-ply AS4/3501-6 graphite-epoxy. Each specimen had a total width of 1.00 in. (25.4 mm) and each specimen notch was 0.200 in. (5.1 mm) in length and 0.005 in. (0.127 mm) wide. Each specimen was loaded incrementally and monitored visually through a microscope for evidence of initial crack growth. From each test, the direction of initial crack growth, the stress causing initial crack growth, and the stress causing fracture were obtained. In each of the experiments, crack extension was observed to occur along the fiber direction, toward the nearest free edge. Further details concerning the experiments can be found in [25].

The three macroscopic crack growth theories presented in this paper are compared in [25] for their ability to predict observed crack growth directions for the experiments detailed above. Table 2 outlines this comparison. From the table, it is obvious that only the crack growth direction predictions made by the normal stress ratio theory show any correlation with the observed crack growth directions. For each of the test cases studied, the maximum difference between the experimentally observed crack direction and that predicted by the normal stress ratio theory is no more than 3°. In contrast, neither the tensor polynomial nor the strain energy density theories were able to achieve this level of accuracy for any of the test cases. The accuracy of the normal stress ratio theory in predicting crack extension direction for these cases becomes even more evident when it and the other theories are plotted as a function of angle about the crack tip (see Figure 6, Figure 7, and Figure 8). Unlike the other theories, the normal stress ratio consistently exhibits a very strong local maximum at the angle of observed crack growth. This tendency of the normal stress ratio theory is also important, considering the fracture behavior of the material it is modelling. Notched unidirectional graphite-epoxy exhibits a strong tendency to experience crack extension

Table 2. Comparison of Macroscopic-Level Crack Growth Direction Theories

Comparison of Theoretical and Experimental
Crack Growth Directions Provided in [25]
Fifteen Degree Off-Axis Tests

Aspect Ratio	Experimental Direction of Crack Extension[1]	Predicted Directions of Crack Extension[1]		
		Normal Stress Ratio	Tensor Polynomial	Strain Energy Density
		90° Notches		
1	-75°	-72°	14°	3°
4	-75°	-73°	-85°	43°
8	-75°	-74°	-87°	54°
		105° Notches		
1	-90°	-88°	-8°	-19°
4	-90°	-88°	-101°	30°
8	-90°	-88°	-103°	40°

[1]All angles are measured with respect to the cut notch, with an extension direction of 0° corresponding to crack growth collinear to the notch. See the angle φ in Figure 9.

along its fiber direction. Any theory used to model its crack growth behavior should also model this tendency. Clearly the normal stress ratio theory does this through its strong peaks along the material fiber direction.

This work represents the only direct comparison between the three most prominent macroscopic-level fracture theories to a single set of experiments. The tests analyzed yielded somewhat trivial results with respect to the direction of crack extension. Obviously, however, the tensor polynomial and strain energy density theories could not model this behavior. In contrast, the normal stress ratio theory was not only able to correctly predict crack extension directions, but it also was able to model the strong tendency for crack extension to occur along the fiber direction. Based on these facts, and the fact that direction of crack extension is an essential composite fracture parameter to predict, the normal stress ratio theory was chosen as the theory to emphasize in this study. A portion of the work performed as part of this study can be found in [26] and [27].

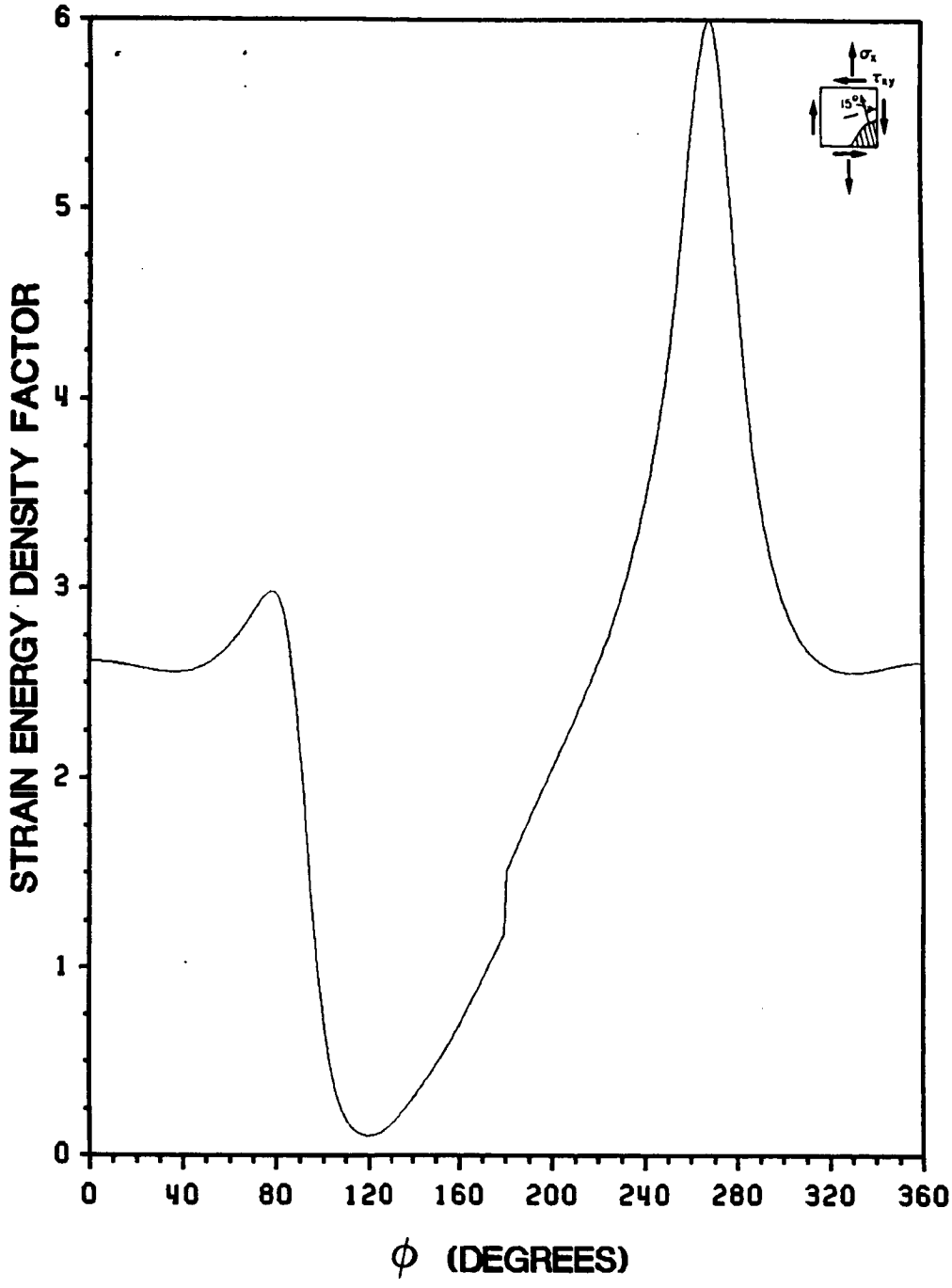

Figure 6. Strain Energy Density Factor vs. φ: 15° Off-Axis Tensile Coupon, AS4/3501-6 Graphite-Epoxy, Aspect Ratio = 8, 105° Notch

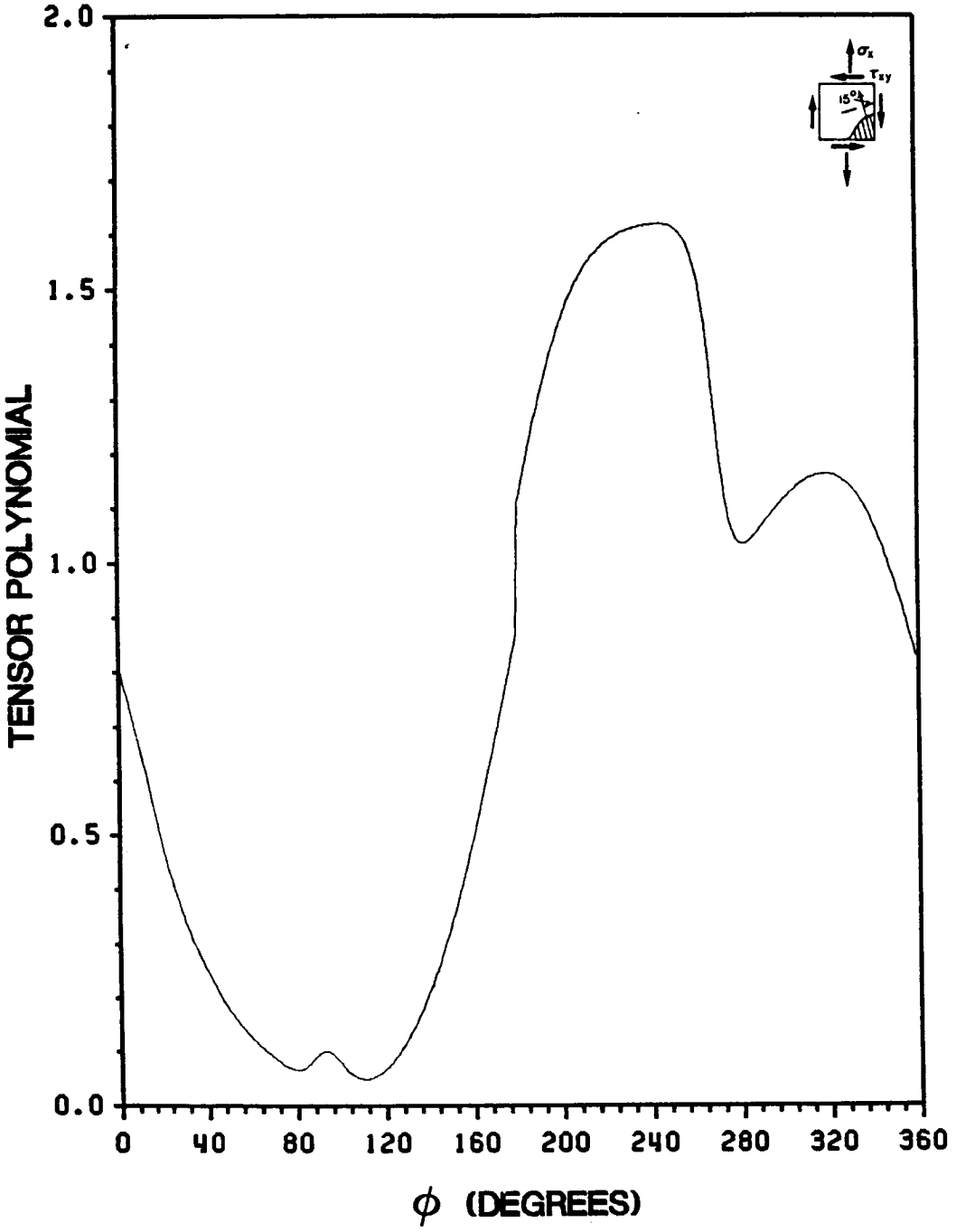

Figure 7. Tensor Polynomial vs. φ: 15° Off-Axis Tensile Coupon, AS4/3501-6 Graphite-Epoxy, Aspect Ratio = 8, 105° Notch

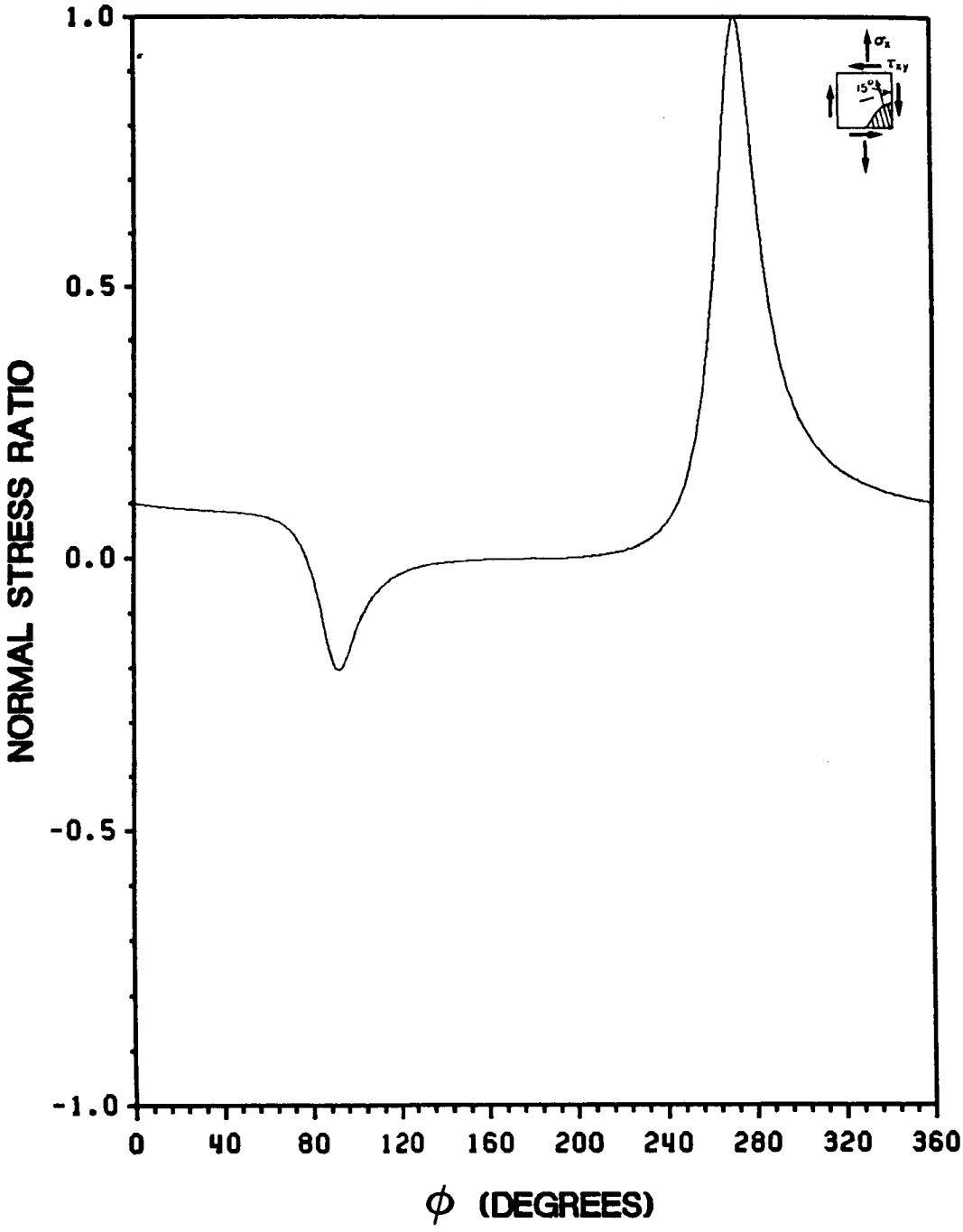

Figure 8. Normal Stress Ratio vs. φ: 15° Off-Axis Tensile Coupon, AS4/3501-6 Graphite-Epoxy, Aspect Ratio = 8, 105° Notch

2.2 *Defining the Class of Problems*

2.2.1 Single Flaws

Although composites often contain multiple flaws that interact with one another, the fundamental problem to address is that of predicting the crack growth behavior of a composite containing a single flaw. Specifically, it is desirable to be able to predict how a single flaw of arbitrary orientation will affect the strength of a composite subjected to generalized loading conditions. As a result, this study will treat only the problem of a single flaw in a composite material. Also, in order to keep the study well-defined in scope, only the through-the-thickness center-crack problem will be addressed.

2.2.2 Unidirectional Materials

Prediction of the strength behavior of a notched composite can be divided into two parts or steps, namely, application of a stress solution to approximate the material stress state and formulation and implementation of a crack growth theory within the chosen stress solution. Each of these parts necessarily contains a number of assumptions and/or simplifications that must be tested and proven. Also, in any crack growth experiment, a number of factors that are dependent on the type of material tested affect observed crack growth behavior. Obviously, in any experimental study it is desirable to limit the number of extraneous experimental factors that can affect results. Because the purpose of this study is specifically to present and attempt to verify a particular crack growth theory and its method of implementation, it is also important to limit the number of assumptions and simplifications made in approximating the material stress state. In this way, the assumptions associated with the crack growth theory itself can be better scrutinized. Because of these concerns,

the problem of a crack in a multidirectional composite laminate will not be addressed directly in this study, even though from an engineering standpoint fracture analysis on a laminate level is the ultimate goal.

The study of multidirectional materials is not desirable for this study from both an experimental and theoretical standpoint. Experimentally, crack growth behavior in multidirectional composites is very complex and typically a strong function of laminate lay-up geometry. As a result, for a given set of composite laminate experiments, it is difficult to separate the effects of the flaw from the effects of different lay-up geometries on material strength. From a theoretical standpoint, it is even more important that multidirectional composites not be addressed directly in this study. This is true for two reasons. First, at this time, no reliable analytical or numerical method exists for approximating the complicated three-dimensional stress state that exists at the notch tip in a multidirectional composite laminate. Use of a three-dimensional finite element model appears to be the most reasonable approach to the problem. Currently, however, mesh generation, memory requirements, and other aspects of this approach present enough problems that its application appears almost intractable. Second, nonlinear constitutive behavior effects can be significant in multidirectional laminates. As with the problem of modelling three-dimensional stress states, modelling nonlinear material behavior presents numerous complications.

Until a reliable three-dimensional analysis technique is available, more established two-dimensional analyses must be used. This necessarily precludes analysis of the vast number of three-dimensional notched laminate failures. Despite this, other researchers have applied two-dimensional fracture analyses to multidirectional composite laminate problems. Until a consistent rationale is developed for determining which laminate configurations can or cannot be treated using two-dimensional analyses, however, the use of such an approach can yield only marginal insight into the verification of a particular fracture theory. As a result, from both experimental and theoretical standpoints, trying to verify a crack growth model on a laminate level presents so many complications that they will tend to obscure problems with any crack growth theory used.

Because of the aforementioned problems in dealing with multidirectional laminates, the approach taken in this study for verifying the normal stress ratio crack growth theory is to work on

a unidirectional lamina level. By working exclusively with unidirectional materials, the experimental complications of accounting for the effects of different laminate geometries are eliminated. Also, because the state of stress in a unidirectional composite is primarily two-dimensional in nature and nonlinear constitutive behavior is typically not severe, linear, two-dimensional closed-form elasticity solutions and finite element models provide reasonable approximations of notched lamina stress states.

2.2.3 Arbitrary Flaw Orientation

This study will concern itself with an arbitrarily oriented flaw in a unidirectional material. Due to the anisotropic nature of unidirectional composites, naturally occurring flaws in it are almost always oriented along the fiber direction. It is important, however to look at flaws of arbitrary orientation in verifying a crack growth theory. As will be detailed later in this report, the crack growth behavior of unidirectional composites varies significantly with applied stress state and the orientation of the crack with respect to the principal material axis. As a result, crack growth behavior in unidirectional composites can be made significantly complicated for them to act as an appropriate experimental proving ground for verifying a composite crack growth theory. In using the lamina as a proving ground for testing a composite crack growth theory, it is assumed that whatever theory is used and whatever parameters are found to control crack extension on a lamina level will be applicable to the analysis of multidirectional composite crack extension problems.

3.0 Analytical Approach

3.1 Problem Analyzed

The problem studied analytically is depicted in Figure 9. The figure shows an infinite, two-dimensional, center-cracked, unidirectional composite plate, subjected to arbitrary far-field loading, with arbitrary crack and principal material axis orientations. Because crack extension in a composite is typically not collinear with an original flaw, this represents a model of original flaw geometry only. For most composite fracture problems, it becomes invalid as soon as any crack extension takes place. The problem diagrammed in Figure 9 is used in this study specifically because its near-crack-tip stress state can be solved for using a closed-form elasticity solution. This provides a great deal of flexibility in addressing a broad range of problems with different far-field applied stress states and notch and fiber orientations.

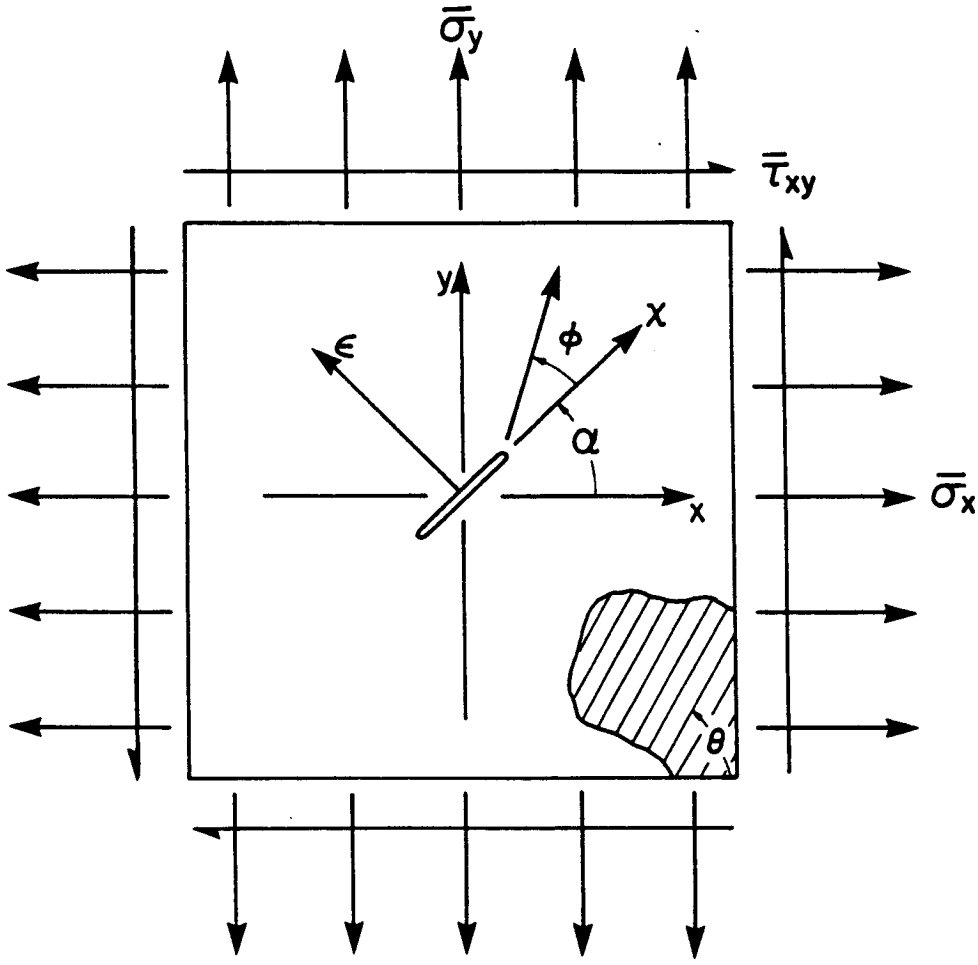

Figure 9. Problem to be Modelled Analytically: Infinite, Two-Dimensional, Center-Cracked Anisotropic Plate with Arbitrary Far-Field Loading, Fiber Orientation, and Crack Orientation

3.2 *Predictions Provided by the Analysis*

In this study, it is desired to use an analytical model to predict the direction of crack extension from an original notch and critical applied far-field stresses. A supplementary analysis will also provide predictions of the location of crack extension along the periphery of a rounded notch tip. Two experimentally determined critical stresses, the far-field stress causing crack extension and the far-field stress causing specimen failure, are potentially predictable from the analysis. For specimens experiencing only unstable crack extension, these two critical stresses are one in the same. Thus, in such cases, both critical stresses can be related to the appropriate critical stress prediction. A dilemma exists, however, concerning which critical stress should be predictable by theory for specimens exhibiting stable crack extension. In specimens exhibiting stable crack extension not collinear with the original flaw, the stress causing crack initiation should be the predictable quantity. This is because the original flaw geometry analysis becomes invalid as soon as the flaw geometry changes at the onset of crack extension. In specimens exhibiting stable crack extension collinear with the original flaw, however, crack geometry at failure is identical to the original crack geometry, implying that the specimen failure stress may be predictable by theory. Because of this dilemma, for all tests in this study that experience stable crack extension, theoretical critical stress predictions based on original crack geometry are compared to both crack initiation and failure stresses.

Another crack growth phenomenon that would be desirable to predict using a model of the problem depicted in Figure 9 is the stability of crack extension. In other words, it would be useful to know whether crack initiation will immediately lead to failure, or whether a significantly greater stress must be applied to the specimen for it to fail. Unfortunately, the problem modelled in this study is incapable of providing such predictions for most composite fracture problems, again because the problem geometry becomes invalid as soon as crack initiation occurs. An analysis of crack stability requires a theoretical model that is valid both before and after crack growth takes place.

3.3 *Analytical Procedure*

The analytical problem just outlined is used in this study to investigate the overall behavior of the normal stress ratio theory, designate certain critical tests in formulating the experimental test matrix, and compare predictions from the analysis with observed crack growth behavior. A three-step analytical procedure is used to accomplish these goals. The initial step involves determining appropriate far-field applied stresses for each specimen and testing configuration that is to be modelled. Step two involves using the appropriate far-field stresses within an elasticity solution for the near-crack-tip stresses in an infinite anisotropic plate with a sharp center crack. Step three consists of using the stresses near the crack tip within the normal stress ratio crack growth theory.

3.3.1 Step 1: Far-Field Applied Stresses

As will be outlined in the section on experimental methods, three types of experiments were performed as part of this study. On-axis tension, off-axis tension, and Iosipescu shear tests were performed in order to observe crack growth behavior in specimens subjected to a wide range of applied far-field stress states. In analyzing these tests, values for far-field stresses must be used that approximate those applied to actual specimens. The methods used to obtain appropriate far-field stress values for each type of test are detailed below.

3.3.1.1 On-Axis Tension Tests

An on-axis tension test is defined in this study as a tension test on a composite material with one of its principal material axes oriented along the tensile axis (see Figure 10). An on-axis tension test with the fibers along the tensile axis is designated as a 0° test. One with the fibers perpendicular

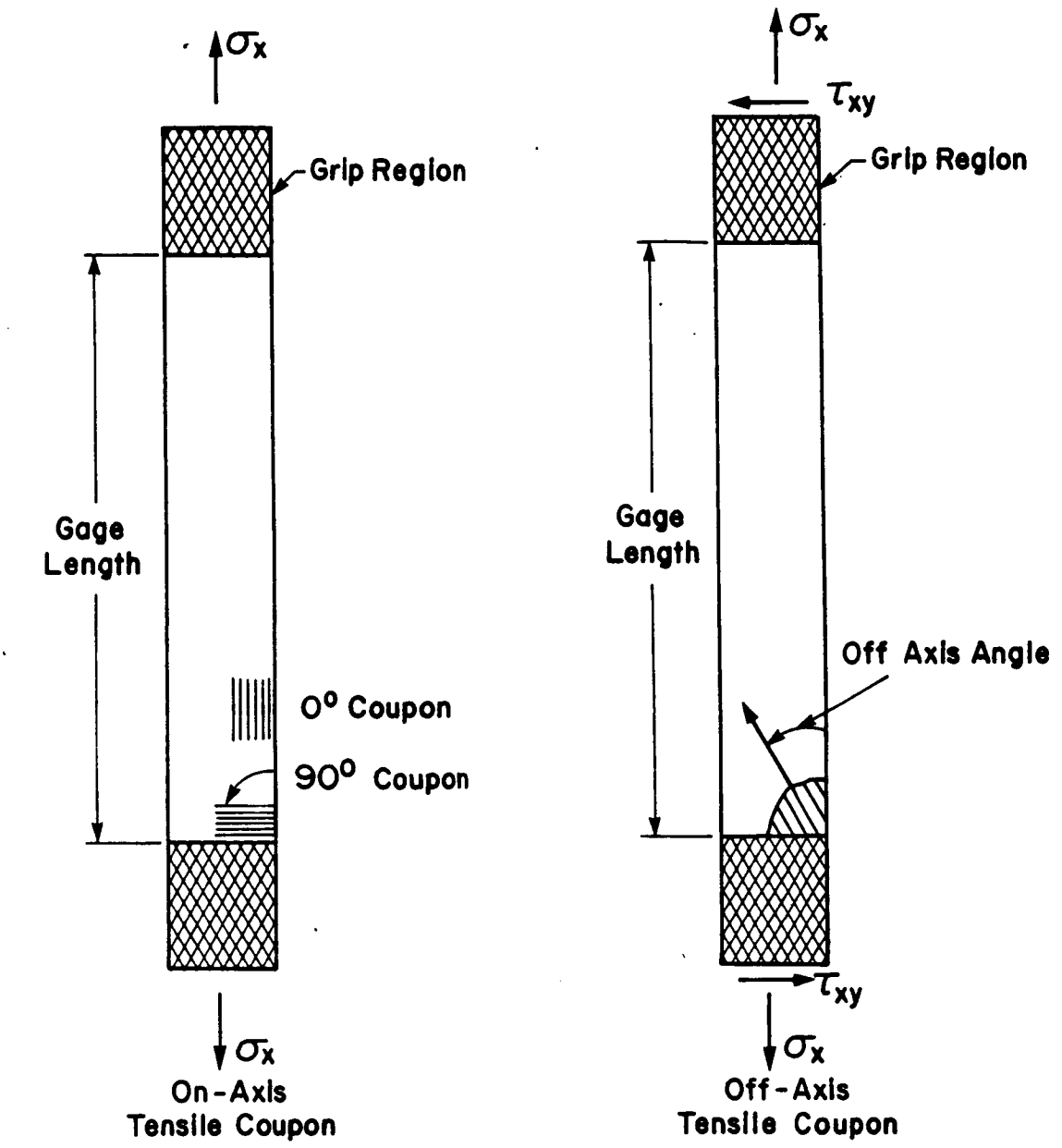

Figure 10. Unidirectional Tensile Coupons

to the tensile axis is designated as a 90° test. For such tests, a composite behaves as a macroscopically orthotropic material, meaning that the compliance coupling terms S_{16} and S_{26} are equal to zero. It is assumed in this study that for such tests the transverse normal stress caused by the coupling term S_{12} and the grip constraint on the specimen ends is negligible. Because of their relatively large aspect ratio, this is a reasonable assumption for the on-axis specimens tested and analyzed in this study. As a result, for these tests, the applied tensile stress is used as the far-field stress in the analysis.

3.3.1.2 Off-Axis Tension Tests

An off-axis tension test is defined in this study as a tension test on a composite material with one of the principal material axes oriented at an angle to the tensile axis (see Figure 10). Specimens are designated by the orientation of the fibers with respect to the tensile axis (x axis). Thus, a 15° off-axis tensile test has its fibers oriented 15° from the tensile axis. For these tests, the composite behaves macroscopically as a fully anisotropic material, with nonzero values of the compliance terms S_{16} and S_{26}. The effect of these terms on the specimen stress state can be significant, depending on the type of test and the specimen geometry. The effect of nonzero shear coupling compliance terms is illustrated in Figure 11, for an off-axis tensile specimen subjected to uniform axial stress and a uniform axial end displacement. If an off-axis specimen is subjected to uniform axial stress, allowing its ends to rotate, the S_{16} and S_{26} compliance terms cause the specimen to deform as shown. A different effect results if the specimen is subjected to a unform axial end displacement with no rotation of the specimen ends allowed. In such cases, a shear stress and bending moment are applied to the specimen in addition to the applied axial stress. This type of loading resembles the type applied to an actual off-axis specimen by grips attached to its ends. Obviously, simply using the applied axial stress as the far-field stress is incorrect in analyzing such tests. Some method of accounting for the shear stress applied to such specimens must be used. The method

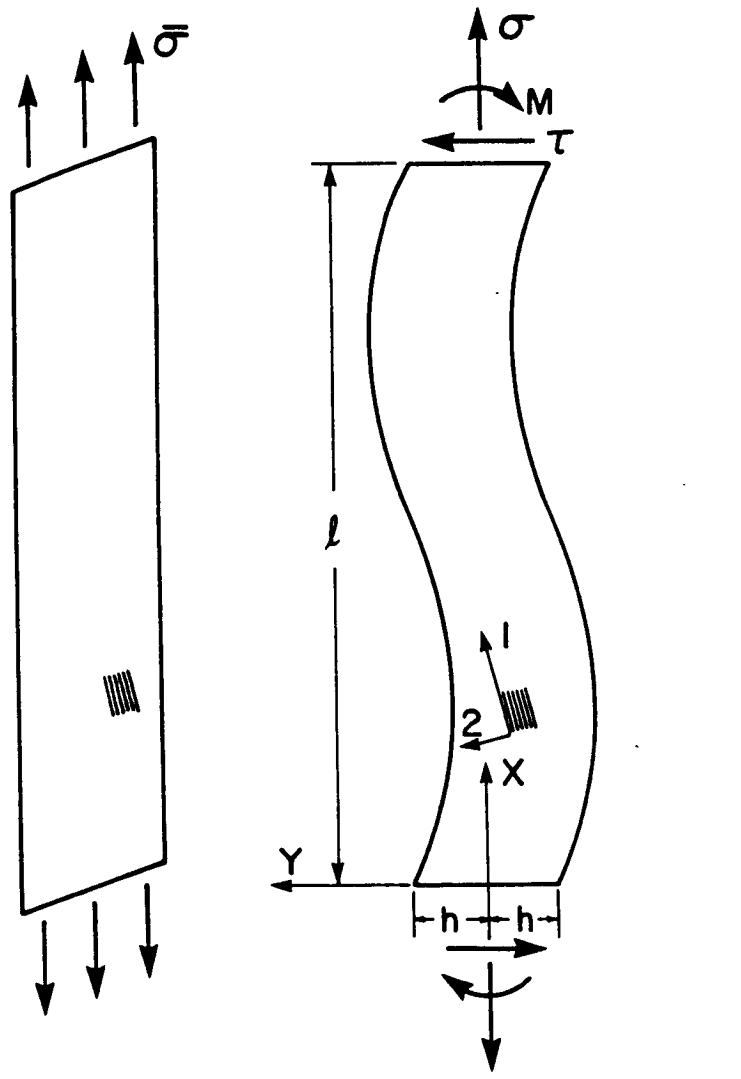

Figure 11. Effect of Nonzero Shear Coupling Compliance Terms in Tensile Coupons

chosen in this study makes use of a two-dimensional elasticity solution applied to the problem of an unnotched off-axis coupon.

A plane stress elasticity formulation by Pagano and Halpin [28] has yielded a closed-form solution approximating the stress state for the unnotched off-axis tensile coupon problem. In addition to satisfying the plane stress elasticity equations, their solution satisfies the following boundary conditions:

$$u(0,0) = 0 \quad v(0,0) = 0 \quad u(\ell,0) = \varepsilon_o \ell \quad v(\ell,0) = 0$$

$$\tau_{xy}(x,h) = 0 \quad \sigma_y(x,h) = 0 \quad \tau_{xy}(x, -h) = 0 \quad \sigma_y(x, -h) = 0 \tag{8}$$

$$\frac{\partial u}{\partial y}(0,0) = 0 \quad \frac{\partial u}{\partial y}(\ell,0) = 0 \ ,$$

where u is the displacement in the x direction and v is the displacement in the y direction. The x axis is along the specimen length, l, and the y axis is along the specimen width, $2h$ (Figure 11). These boundary conditions are based upon the realistic assumption that although the specimen ends are in rigid grips, they will tend to pull out of them near the specimen edges. As a result, the displacement boundary conditions given above are applied along the specimen centerline instead of across the entire specimen width. The stresses for an unnotched off-axis coupon that result from the analysis are of the form

$$\sigma_x = -2C_0xy - 2\frac{S_{16}}{S_{11}}C_0y^2 + C_1y + C_2$$

$$\sigma_y = 0 \tag{9}$$

$$\tau_{xy} = C_0(y^2 - h^2) \ ,$$

where

$$C_0 = \frac{6S_{16}\varepsilon_o}{6h^2(S_{11}S_{66} - S_{16}^2) + S_{11}^2\ell^2}$$

$$C_1 = C_0\ell$$

$$C_2 = \frac{C_0}{6S_{16}}\,(6S_{66}h^2 + S_{11}\ell^2)\ .$$

The S_{ij} are the plane stress lamina compliance coefficients in the x-y coordinate system. It is important to point out that this solution predicts that the transverse normal stress, σ_y, is equal to zero throughout the specimen. This is a direct consequence of the displacement boundary conditions, which specify that no constraint is applied to the specimen in the y direction. As in on-axis tests, actual off-axis tensile specimens have such a constraint imparted to the specimen ends by the grips. As in the analysis of the on-axis tensile tests, all off-axis test transverse normal stress effects will be assumed to be negligible in this study. Again, such an assumption is justifiable for large aspect ratio specimens, where the amount of normal stress that intrudes into the test region due to end constraints is relatively small. Some of the off-axis specimens analyzed as a part of this study are of small aspect ratio, however. In analyzing such specimens, neglecting transverse normal stresses represents a source of error in the stress distribution predicted by the Pagano and Halpin solution. As will be shown in the next section describing the sharp crack analytical model, if the transverse normal stress is other than along the axis of the crack, neglecting such stresses represents a source of error in the crack growth predictions given in this study.

The goal of using the stresses in Eq. (9) is to obtain a reasonable value of applied far-field shear stress for a given applied axial stress. This was done in this study by first integrating the stresses σ_x and τ_{xy} across the specimen thickness to obtain normal and shear force resultants applied to the specimen. The normal stress resultant, designated as P, that results is

$$P = t\int_{-h}^{h}\sigma_x\,dy = 2th\,(C_2 - \frac{2S_{16}C_0h^2}{3S_{11}})\ . \qquad (10)$$

The corresponding shear force resultant, designated as T, is given by

$$T = t \int_{-h}^{h} \tau_{xy}\, dy = -2t \left(\frac{2C_0 h^3}{3}\right) . \tag{11}$$

If the applied shear force is divided by the applied normal force, the expression that results simplifies to

$$\frac{T}{P} = \frac{1}{\frac{S_{16}}{S_{11}} - \frac{3S_{66}}{2S_{16}} - \frac{S_{11}\ell^2}{4S_{16}h^2}} , \tag{12}$$

where the definition of C_2 has been taken from Eq. 9. In this study, it is assumed that this ratio also defines the ratio of applied far-field shear stress to applied far-field axial stress. The applied far-field shear stress is therefore obtained by multiplying the applied axial stress by the ratio of $\frac{T}{P}$, resulting in the expression

$$\tau^{\infty} = \sigma^{\infty}\frac{T}{P} = \frac{\sigma^{\infty}}{\frac{S_{16}}{S_{11}} - \frac{3S_{66}}{2S_{16}} - \frac{S_{11}\ell^2}{4S_{16}h^2}} . \tag{13}$$

The value of τ^{∞} for a given value of σ^{∞} is a function of the compliance coefficients in the x-y coordinate system and $(\frac{l}{2h})$, the specimen aspect ratio. It is interesting to note the values that τ^{∞} assumes for two special cases of the off-axis problem. For cases where S_{16} is equal to zero (on-axis tensile tests), the value of the constant C_0 (Eq. 9) becomes zero. This causes T to equal zero, while P becomes equal to $\frac{2th\,\varepsilon_0}{S_{11}}$. As a result, $\sigma^{\infty} = \frac{\varepsilon_0}{E_1}$, and Eq. (13) gives $\tau^{\infty} = 0$, agreeing with the method used in this study of using the applied axial stress as the far-field stress for on-axis tests. Another interesting case is when the aspect ratio of the specimen is very large. From Eq. (13) it is obvious that the value of τ^{∞} approaches zero for large values of $(\frac{l}{2h})$. Thus, the effect of the end constraint is less significant for larger aspect ratio specimens.

3.3.1.3 *Iosipescu Tests*

The Iosipescu shear test is detailed in the section on experimental methods. The test was originally developed as a method for the determination of isotropic material shear properties using a flat specimen [29]. It has more recently been applied to determine composite material shear properties [30-33]. In this study it is used not only as a test for determining material shear properties, but also as a crack growth test. Figure 12 provides force, shear load, and moment diagrams for the specimen. These diagrams show that, as a result of idealized loads applied to the specimen, the center of the specimen is subjected to a zero bending moment. Also, the specimen center is under a state of pure shear stress equal to $\frac{P}{A}$, where P equals the downward force applied to the specimen and A equals the crossectional area of the specimen at its center.

Determination of appropriate far-field stresses to use in analyzing the center-notched version of the Iosipescu test is not a simple task. This is because, despite the fact that the resultant stress applied to the specimen is predominantly shear, edge effects and the method of loading the specimen result in a state of stress in the middle of the specimen that is not pure shear. Fortunately, a significant amount of finite element analysis has been performed to characterize the stress state in both unnotched [31] and notched [34] versions of this specimen. In [31], it is shown that, in the center section of the unnotched specimen, normal stresses do exist. By far the most significant of the normal stresses in the test section is a compressive stress along the vertical axis. As detailed in Section 4.2, the notched version of the specimen has its notch oriented along the vertical axis. As will be shown in next section detailing the sharp crack analysis, a normal far-field stress along the axis of the crack does not contribute to the near-crack-tip stress state. This at least suggests that normal stresses in the center of the specimen may not significantly affect crack growth results. As part of the work done in preparing [34], a preliminary comparison was made between the results from application of the normal stress ratio theory within a notched specimen finite element analysis and its application within the center-cracked infinite plate analysis detailed in the next section. In applying the infinite plate solution, the resultant shear stress applied to the Iosipescu specimen was used as the applied far-field stress. The comparison, which was not included in the final version

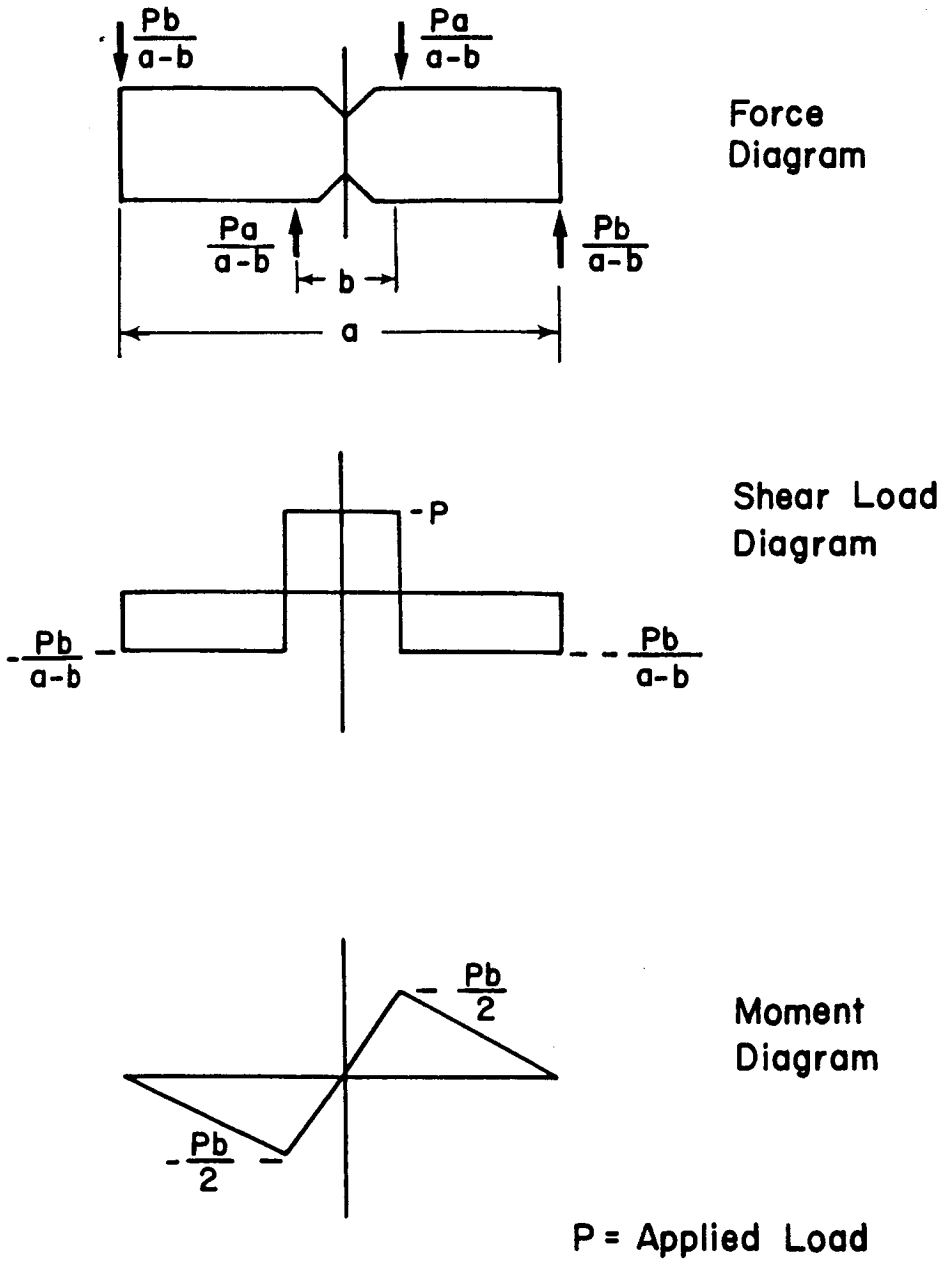

Figure 12. Iosipescu Shear Specimen

of [34], indicates that the two approaches yielded essentially identical results. Based on these results for unnotched and notched Iosipescu specimens, the resultant shear stress applied to the specimen was used as the applied far-field stress in the analytical portion of this study.

3.3.2 Step 2: Analysis of an Infinite Plate with a Sharp Crack

Lekhnitskii [35] has outlined a complex variable plane elasticity solution for an infinite homogenous anisotropic plate with an elliptical hole at its center. By reducing the minor axis dimension to zero and evaluating the stress potential functions in the neighborhood of the crack tip, the solution can be used to analyze the center-cracked infinite homogeneous anisotropic plate model used in this study. Wu [15] provides a detailed description of this procedure, which models a crack in an actual material as a line crack with an infinitely sharp tip. The analysis yields expressions for the stresses of the form

$$\sigma_{\chi\chi} = \frac{\sigma^{\infty}\sqrt{a}}{\sqrt{2r}} Re\{\frac{S_1 S_2}{(S_1 - S_2)}[\frac{S_2}{\psi_2^{1/2}} - \frac{S_1}{\psi_1^{1/2}}]\} + \frac{\tau^{\infty}\sqrt{a}}{\sqrt{2r}} Re\{\frac{1}{(S_1 - S_2)}[\frac{S_2^2}{\psi_2^{1/2}} - \frac{S_1^2}{\psi_1^{1/2}}]\}$$

$$\sigma_{\varepsilon\varepsilon} = \frac{\sigma^{\infty}\sqrt{a}}{\sqrt{2r}} Re\{\frac{1}{(S_1 - S_2)}[\frac{S_1}{\psi_2^{1/2}} - \frac{S_2}{\psi_1^{1/2}}]\} + \frac{\tau^{\infty}\sqrt{a}}{\sqrt{2r}} Re\{\frac{1}{(S_1 - S_2)}[\frac{1}{\psi_2^{1/2}} - \frac{1}{\psi_1^{1/2}}]\} \quad (14)$$

$$\tau_{\chi\varepsilon} = \frac{\sigma^{\infty}\sqrt{a}}{\sqrt{2r}} Re\{\frac{S_1 S_2}{(S_1 - S_2)}[\frac{1}{\psi_1^{1/2}} - \frac{1}{\psi_2^{1/2}}]\} + \frac{\tau^{\infty}\sqrt{a}}{\sqrt{2r}} Re\{\frac{1}{(S_1 - S_2)}[\frac{S_1}{\psi_1^{1/2}} - \frac{S_2}{\psi_2^{1/2}}]\},$$

where σ^{∞} and τ^{∞} are the applied far-field stresses in the crack coordinate system, a is one half of the crack length (Figure 13), S_1 and S_2 are the roots of the characteristic equation for a plane linear elastic anisotropic material, and

$$\psi_1 = \cos\varphi + S_1 \sin\varphi\,; \quad \psi_2 = \cos\varphi + S_2 \sin\varphi\,.$$

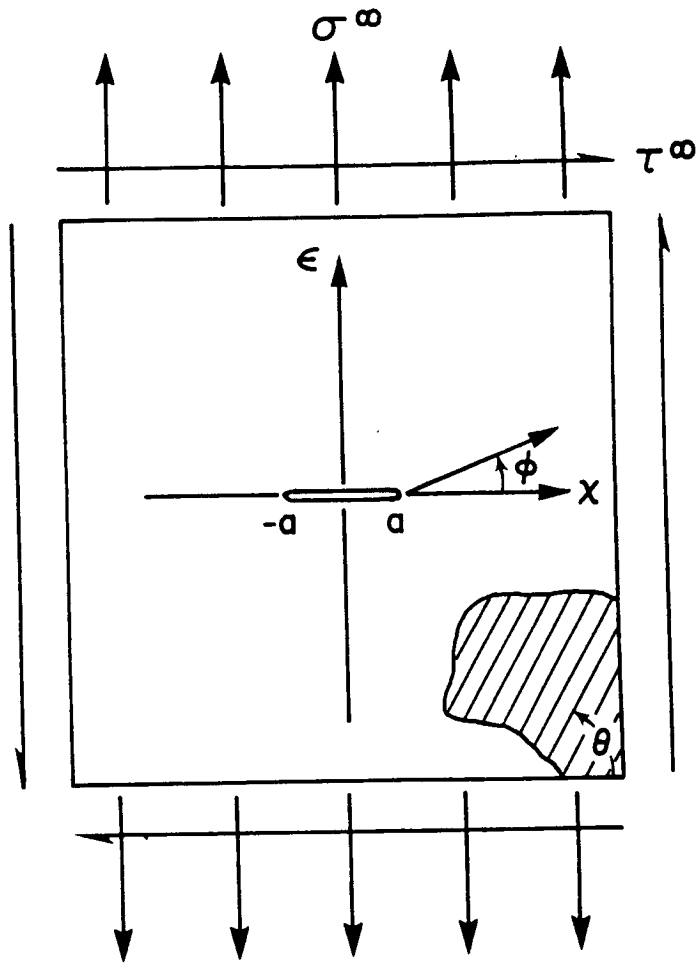

Figure 13. Problem Modelled by the Near-Crack-Tip Stress Solution of Lekhnitskii [35]

The angle φ is measured with respect to the crack. The problem modelled by the Lekhnitskii stresses illustrated in Figure 13 is not identical to the arbitrary notch angle problem modelled in this study (Figure 9). The discrepancy is easily resolved, however, by rotating the far-field stresses from the model in Figure 9 into the crack coordinate system, using the crack angle, α. Once this is done, the stresses given in Eq. (14) can be used directly.

The near-crack-tip stresses given in Eq. (14) possess a number of characteristics worth noting. First, only the far-field stresses σ^{∞} and τ^{∞} contribute to the stresses near the crack tip. The normal stress along the axis of the crack does not contribute to the near-crack-tip stress state. Second, the radial and angular variations of the stresses are decoupled. The angular dependency of the stresses is expressed through the terms ψ_1 and ψ_2. The radial dependency is expressed entirely by the $\frac{1}{\sqrt{r}}$ term that multiplies each stress expression. Thus, as in isotropic materials, a $\sqrt{r}$ stress singularity is predicted for center-cracked anisotropic materials. Third, unlike the stresses in an isotropic material, the stresses in an anisotropic material are a function of the material properties and the orientation of the crack with respect to the principal material axes. This dependency is expressed through the values of S_1 and S_2. Finally, as in isotropic materials, the stresses are predicted to be proportional to the square root of the half crack length, a. This is the basis of the stress intensity factor approach for anisotropic materials detailed in Section 1.2.2 of this report. For a given material and orientation of the crack with respect to the material fibers, S_1 and S_2 are constant and the magnitude of the stress distribution for the original crack geometry is controlled entirely by the original crack length.

3.3.3 Step 3: Application of the Normal Stress Ratio Theory

The normal stress ratio theory is detailed in Section 1.2.2.3 of this report. It is applied in this study by using the stresses obtained from the infinite homogeneous anisotropic plate solution just detailed. The FORTRAN program that calculates the Lekhnitskii stresses and applies the normal stress ratio theory was programmed as part of a previous Master's-level study [36]. The first step

of the analysis is to determine the direction of crack extension predicted by the theory. In accordance with the theory's formulation, the normal stress around the crack tip is evaluated at a constant radial distance from the crack tip. Fortunately, in using the stresses given in Eq. (14), the value of distance from the crack tip used is not important. This is because, as just noted, the radial and angular variations of the Lekhnitskii stresses are decoupled. Changing the distance from the crack tip that the stresses are evaluated at changes only the magnitude of the stresses, not the relative values of the stresses at various angles about the crack tip. The predictions provided by a linear theory such as the normal stress ratio are not dependent upon stress field magnitude.

The second step of the analysis is the determination of critical applied far-field stresses predicted by the normal stress ratio theory. Predicting critical stresses is based on not only finding the direction having the maximum normal stress ratio, but also on finding the maximum value. Because of this, predicted critical stress values are dependent on r_s , the specified distance from the crack tip at which the stresses are evaluated. As is outlined in the section on obtaining predicted critical stresses, the correct value of r_s, designated in this study by the nondimensionalized parameter $r_o = \frac{r_s}{a}$, cannot be determined analytically. In this study it is determined from a "baseline" crack growth experiment and then assumed to be a material constant. The experimentally determined value of r_o is then used to analyze subsequent notched material tests.

3.4 *Analytical Approach Assumptions*

In using the crack growth analysis and theory outlined above, a number of assumptions are made. Both the Pagano and Halpin and Lekhnitskii stress solutions assume that a state of plane stress exists in the composite plate. This is a reasonable assumption for the unidirectional materials addressed in this study. Both stress solutions also assume that the composite is a homogeneous, linear, elastic, anisotropic material with identical moduli in compression and tension. Again, for unidirectional graphite-epoxy the assumption of linear elastic behavior is reasonable. As noted in

the section on material property test results, however, some nonlinear behavior is exhibited in the material shear stress vs. shear strain response. Although no compression tests were performed on the graphite-epoxy used in this study, the material is known to exhibit little or no bimodularity. Perhaps the most important assumption made by the Lekhnitskii and Pagano and Halpin stress solutions is that the composite is a homogeneous material. It is important because composite crack extension may be controlled by the interaction of fibers and matrix near the crack tip and because graphite-epoxy is a highly heterogeneous material.

The near-crack-tip stress solution of Lekhnitskii makes two additional assumptions that have already been mentioned in its description. The first is its infinite plate assumption. This assumption represents the biggest disadvantage in using the Lekhnitskii solution compared to using numerical techniques, such as finite element modelling. Careful choice of appropriate far-field stresses to use in the analysis is a cumbersome yet essential step that must be taken to limit errors due to the infinite plate assumption. In the way that it is applied in this study, the Lekhnitskii solution also assumes that the stress state near the tip of a notch in a real material can be accurately represented by a stress solution for the near-tip region of an infinitely sharp line crack. There is evidence that a sharp crack model may not be applicable to some composite crack growth problems, and that a rounded notch tip model is more accurate in modelling observed crack extension behavior. This issue is addressed more fully in the section on analytical results.

In addition to the assumptions made by the stress solutions used in this study, the normal stress ratio theory also uses two principal assumptions in its formulation and application. The basic assumption of the theory is that mode I crack opening controls crack extension. Because of this assumption, no account is made of shear stress in the material or the material shear strength. Although it is reasonable to assume that mode I crack opening controls crack extension, it has never been rigorously compared with experimental observations. The other principal assumption made by the normal stress ratio theory is its assumed directional dependency of material normal strength. This assumption is necessary specifically because no experimental technique currently exists to determine the normal strength on a given plane in an anisotropic material. Although the expression

used for $T_{\varphi\varphi}$ is plausible and agrees with workable tests, any error in its values has the potential to produce substantial errors in crack growth direction and/or critical stress predictions.

It is important to note that a significant simplification in the analysis results as a consequence of assuming linear material behavior. This assumption and the fact that the normal stress ratio is a linear theory cause the entire crack growth analysis to be linear. In all of the analytical work performed as a part of this study, a single computer run is made using a unit value of far-field normal or shear stress. The predicted critical stress is then obtained by taking the reciprocal of the maximum normal stress ratio evaluated at the distance, r_o, from the crack tip. For example, if the maximum normal stress ratio value obtained at r_o for a 1.00 ksi far-field tensile stress were equal to 0.250, then the critical tensile stress predicted by the theory would be $\frac{1}{0.250} = 4.00$ ksi. In contrast to this simple procedure, use of a nonlinear stress analysis and/or a nonlinear crack growth theory typically requires numerous computer runs using different far-field stresses to obtain a single critical stress prediction.

4.0 Experimental Methods

All of the experiments outlined in this study were performed at Virginia Polytechnic Institute and State University in Blacksburg, Va., using a displacement-controlled screw-driven United Testing Systems model FM-20-A-E 20 kip capacity tension/compression machine. The data acquisition system consisted of a Measurements Group 2100 System amplifier in conjunction with a Digital MINC-23 computer, allowing real-time stress vs. strain plotting and data acquisition at a rate of approximately one data sweep per second (Figure 14). All modulus and Poisson ratio values were calculated on the computer using a straight-line least squares fit through the data. As a rule, these values were obtained from the point of initial loading to roughly 25% of the averaged ultimate specimen stress.

Almost all of the tests performed as a part of this study were on unidirectional composite specimens. A small number of preliminary tests, however, were performed on specimens made of aluminum. The composite material used in this study was 16-ply unidirectional AS4/3501-6 graphite-epoxy. Specimens were made from 12 in. x 12 in. plates cut from a single 7.5 ft. x 2.5 ft. material panel. Each of the plates was c-scanned at Hercules, Inc. and shown to have no voids or delaminations. The aluminum used in this study was from standard 0.125 in. thick 6061-T6 aluminum stock.

Figure 14. Experimental Load Frame and Data Acquisition System

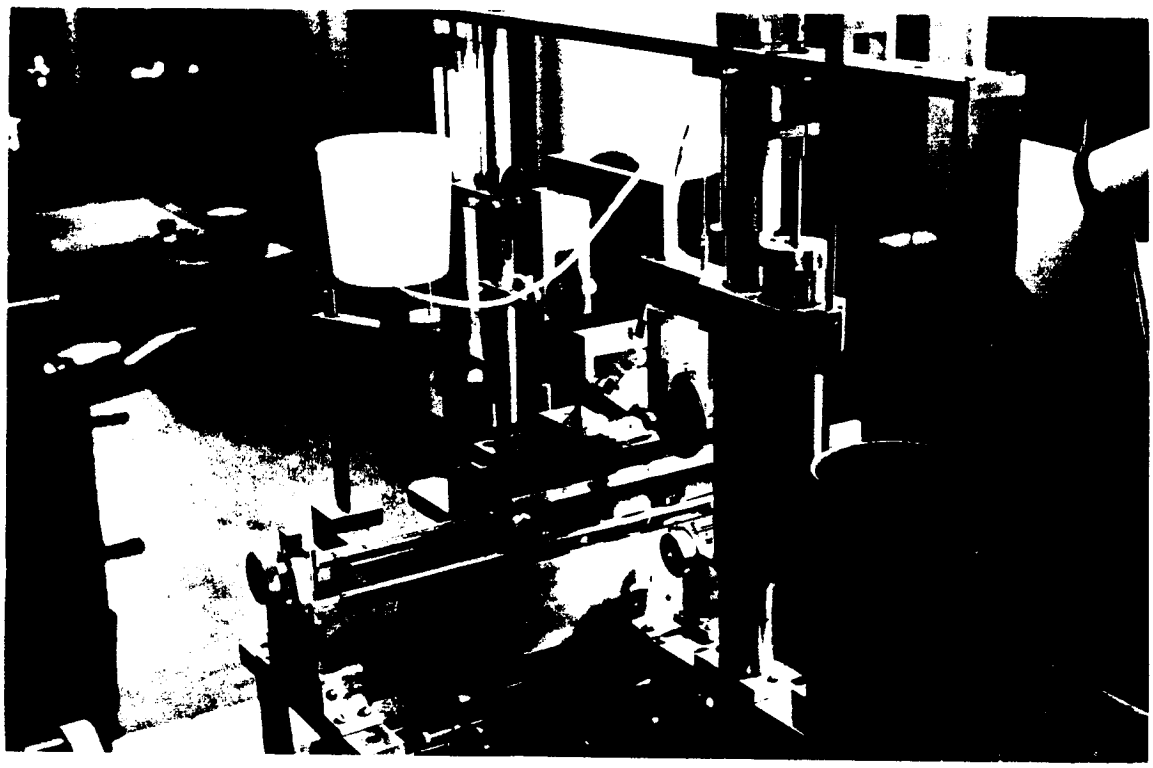

Figure 15. Wire Saw Used to Cut Center Notches in Specimens

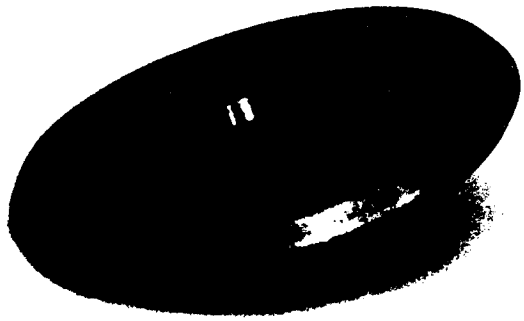

Figure 16. Diamond-Impregnated V-Notch Cutting Wheel for Graphite-Epoxy Iosipescu Specimens

All specimen preparation was performed at Virginia Tech. Graphite-epoxy specimens were cut from each plate using a diamond-impregnated circular saw blade. For the notched graphite-epoxy specimens, center notches were cut by first drilling a 0.037 in. diameter hole in the specimen center with a carbide-tipped drill bit. The hole was needed to allow a 0.005 in. diameter diamond-impregnated cutting wire to be threaded through the specimen. It also allowed the insertion of a crack opening displacement gage to monitor crack opening during testing. A wire saw was used to cut center notches in each specimen with the diamond-impregnated wire (Figure 15). V-notches were cut into the Aluminum Iosipescu specimens using a rotary cutting tool with a 90° included angle cutting wedge. V-notches were ground into the graphite-epoxy Iosipescu specimens with a 110° included angle diamond-impregnated wheel (Figure 16). All graphite-epoxy specimens with center and/or v-notches were x-rayed for possible damage imparted to them during the notch cutting operations. Before x-raying, specimen notched areas were soaked overnight in a zinc iodide-based x-ray opaque penetrant to allow the penetrant to soak into any damaged regions. After x-raying, the specimens were washed thoroughly to remove the penetrant.

Before testing, all graphite-epoxy specimens used in this study were oven-dried to eliminate moisture. Two types of drying ovens were used, a conventional oven and a vacuum oven. Specimens dried in the conventional oven were kept at approximately 110° F. Specimens were kept in the vacuum oven at approximately 110° F., at a vacuum of 28 mm Hg. In order to monitor moisture weight loss, specimens were weighed on a daily basis using a closed-door balance accurate to 0.0001 g. Specimens dried in the conventional oven typically took two weeks to attain a constant weight, indicating that all moisture had been driven off. Specimens dried in the vacuum oven typically took only two or three days to reach a constant weight. The total weight loss varied significantly from specimen to specimen. Results indicated that differences in weight loss were related to the fact that graphite-epoxy absorbs moisture primarily through its free edges. Specimens cut from the edge of a plate, or specimens that are allowed to sit out for weeks or months after being cut have an opportunity to absorb moisture from the air and thus exhibited weight loss during drying. In this study, specimens cut away from the edges of a plate and soon thereafter placed in

a drying oven did not, as a rule, exhibit significant moisture weight loss. Maximum specimen weight loss was on the order of 0.5 percent of the total specimen weight.

4.1 Tension Tests

Tension tests were used in this study as both material property tests and crack extension tests. Specimens of 1.0, 0.5, and 0.3 in. widths were used. For the crack growth specimens, center notches were 0.100 in. in length and 0.005 in. wide. Complete dimensions for individual tests are given in the sections describing each test. End tabbing was not used in any of the tension tests performed as a part of this study. In order to decrease end grip stress concentrations and to increase gripping hold on the graphite-epoxy specimens, however, one layer of medium grit emery cloth was placed between each specimen and the grip surfaces. Two types of specimen grips were were used for the tension tests. Standard Instron grips (Figure 17) were used in all tests on 1.0 in. wide specimens and in material property tests on specimens experiencing high ultimate loads (0° graphite-epoxy specimens). A rotating grip assembly (Figure 18) was used in all off-axis and 90° graphite-epoxy material property tests. These grips were used for their superior alignment capabilities, their reduction of the near-grip stress concentrations in off-axis specimens, and an optional holding bracket feature that allows fragile specimens to be handled carefully.

4.2 Iosipescu Shear Tests

As will be shown in the portion of this report outlining analytical results, the normal stress ratio theory applied as a crack growth direction criterion to the problem of a sharp crack subjected

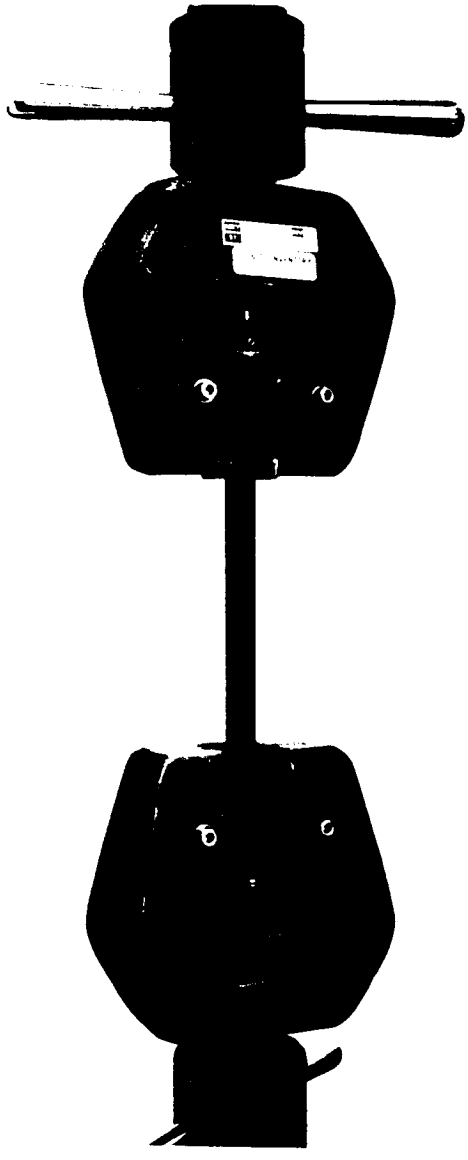

Figure 17. Instron Grips Used for Tensile Testing

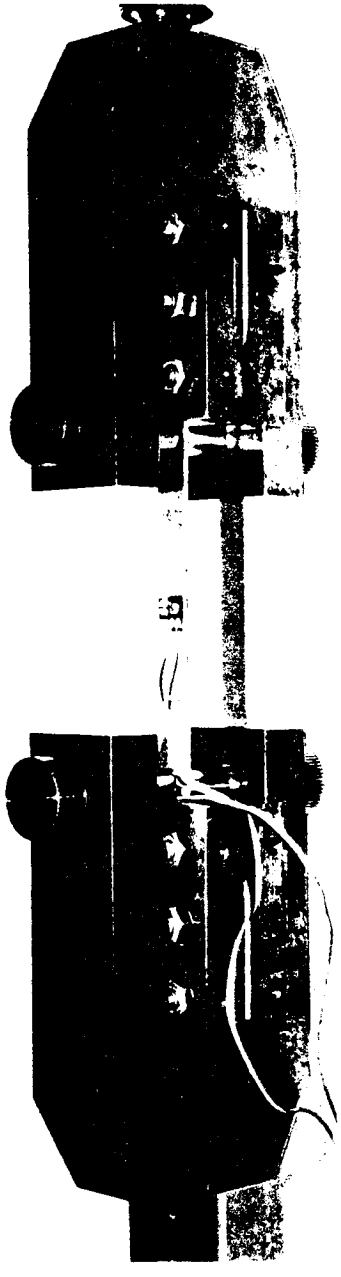

Figure 18. Rotating Grip Assembly Used for Tensile Testing

to pure shear far-field stresses appears to predict crack growth to include fiber breakage. Experimental verification of such predictions represents a critical test of the normal stress ratio theory. Also, because the theory is ignorant of global shear strength, comparison of theoretical and experimental critical stresses for cases of far-field shear loading represents a strong test of the theory and its method of application. These facts pointed to the need for a series of far-field shear crack growth experiments. The shear test chosen for use in this study was the Iosipescu test originally proposed in [29] for use in determining isotropic material shear properties. It was chosen for its simplicity in comparison to symmetric rail shear and thin-walled tube tests.

The Iosipescu tests performed in this study are based on similar tests performed as part of a series of investigations by Walrath and Adams at the University of Wyoming [30-32]. Their work concentrated on using the test to determine material shear properties. Figure 19 provides a photograph of the fixture used in all of the Iosipescu tests for this study, which was designed and built at the University of Wyoming. The specimen is clamped in the center of the fixture using sliding wedge grips located in each fixture side. During testing, the left-hand side of the fixture remains fixed while the right-hand side is displaced downward. The resultant applied shear stress is defined as the downward force applied to the right hand side of the fixture divided by the crossectional area at the specimen center, between the roots of its v-notches. Figure 20 provides the dimensions and configuration used for all of the Iosipescu specimens tested as part of this study. As in the Wyoming studies, specimens measured 3.00 in. in length and 0.75 in. in width. V-shaped notches with a notch root radius of 0.050 in. were ground into the sides of each specimen to a depth of 0.15 in. For the isotropic material tests, the v-notch included angle was 90°. For the graphite-epoxy tests, an included angle of 110° was used. These follow the included angle sizes suggested in [31] to achieve the largest area of uniform shear stress in the specimen center and the smallest amount of stress concentration at the v-notch roots, based on finite element models of the specimen. As indicated in Figure 19, the fiber orientation for composite Iosipescu specimens will be referenced in this study with respect to the horizontal. In the work by Walrath and Adams, aluminum, 0° unidirectional, and some woven composite specimens were tested and analyzed in determining material shear properties. In this study the test was extended by using graphite-epoxy specimens

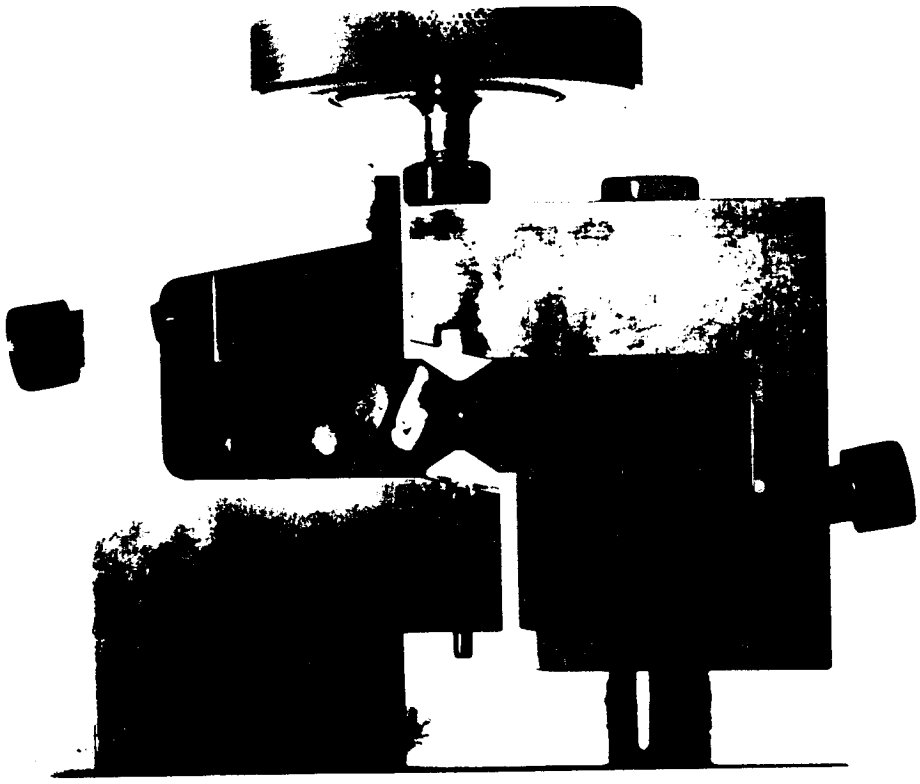

Figure 19. Iosipescu Shear Test Fixture

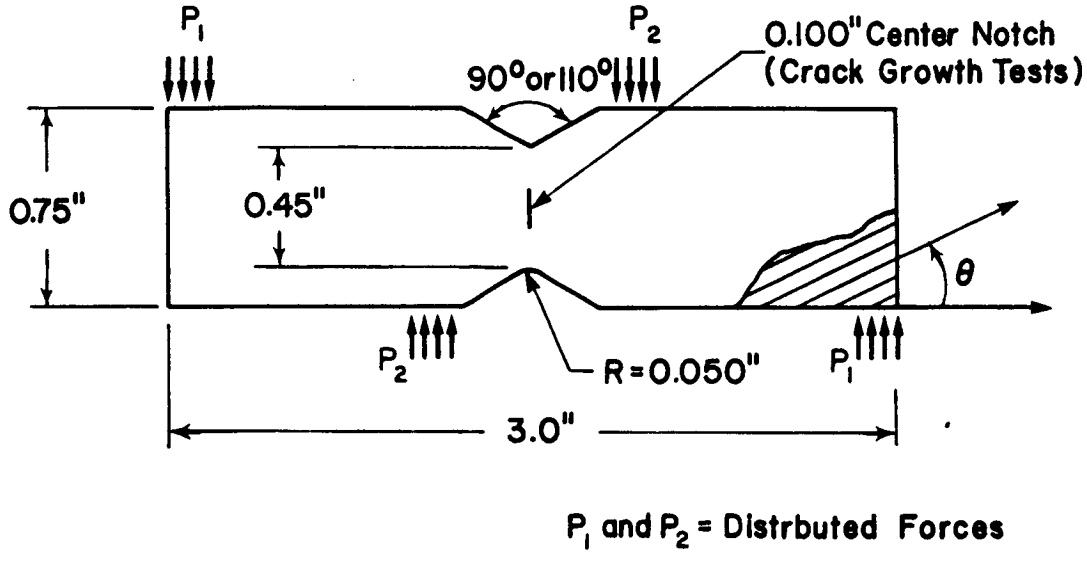

Figure 20. Iosipescu Specimen Dimensions and Configuration

of both 0° and 90° fiber orientations to determine shear properties. Also, the test was extended for use as a composite crack growth shear test by locating a cut notch in the center of the specimen oriented at 90° (vertical), and allowing an arbitrary fiber orientation. As in the notched tensile tests, Iosipescu specimen notches were 0.100 in. long and 0.005 in. in width.

5.0 Preliminary Experiments

A number of preliminary experiments were performed to aid in both the analytical and experimental portions of this study. The first preliminary tests were material property tensile coupon tests. As mentioned in the section describing the Lekhnitskii solution for the stresses near the tip of a center crack in an infinite anisotropic plate, the stresses themselves are a function of the material elastic properties. The predictions made by the normal stress ratio theory are thus dependent upon these elastic properties and the strengths X_t and Y_t. As a result, it is essential that accurate values of these properties be obtained in order to accurately apply the theory. The material property tensile coupon tests were used in this study to obtain these properties and the shear strength, S. The second type of preliminary tests consisted of unnotched Iosipescu tests on aluminum and graphite-epoxy. These were performed in order to get a feel for the accuracy of the Iosipescu test in determining shear properties in both isotropic and anisotropic materials and to note any difficulties in applying the test. Values for G and τ_{ult} from the aluminum Iosipescu tests were compared to values in the literature and from a single aluminum tension test. Values for G_{12} and τ_{max} from the graphite-epoxy Iosipescu tests were compared to values from the graphite-epoxy material property tensile coupon tests.

5.1 *Material Property Tensile Coupon Tests*

A summary of all individual material property tensile coupon tests and their results is provided in Appendix A. The final material property values obtained from all of the tests are given in Table 3. Briefly, 0°, 10°, 45°, and 90° specimens were tested to obtain values for E_1, E_2, ν_{12}, G_{12}, X_t, Y_t, and S for the AS4/3501-6 graphite-epoxy used in this study. For each type of material property test, four specimens were originally designated for testing. As a group, the material property tensile coupon tests yielded consistent, reliable results. For a small number of specimens, however, accurate modulus and/or strength values could not be obtained. In particular, accurate strength values were difficult to obtain for the 0° and 90° specimens, due to their tendency to experience failure in their grip regions. In order to obtain good average strength values for these tests, one supplemental test of each type was run to obtain another strength value only. The 10° and 45° tests each yielded values of G_{12} and τ_{max}. Because the 45° test experiences only a small amount of shear coupling due to grip end constraint, its value of G_{12} was used. The value of τ_{max} from the 10° off-axis test was originally designated to be used as the material shear strength, S, because, compared to the 45° test, the 10° test experiences a more shear dominant failure. Subsequent tests on 0° Iosipescu tests, however, yielded significantly higher maximum shear stress values than were obtained for the 10° off-axis tests. As outlined in the next section, because its test section stress state is predominantly shear, the 0° Iosipescu test appears to provide a much better value for composite shear strength than the 10° off-axis test, which has significant tensile normal stresses perpendicular to its fibers. Because of this, the value of S provided in Table 3 is taken from the 0° Iosipescu shear tests.

Table 3. Material Property Tensile Coupon Tests

Summary of Strength and Stiffness Properties
Material Property Coupon Tests
AS4/3501-6 Graphite-Epoxy

Stiffness Properties			Strength Properties		
E_1	=	18.3 msi (126. GPa)	X_t	=	210. ksi (1.45 GPa)
E_2	=	1.45 msi (10.0 GPa)	Y_t	=	7.75 ksi (53.4 MPa)
G_{12}	=	0.814 msi (5.61 GPa)	S	=	14.4 ksi (99.3 MPa)
ν_{12}	=	0.305			

5.2 *Unnotched Iosipescu Tests*

Before it was applied as a crack growth test, the Iosipescu test was used in a preliminary manner to determine material shear properties. It was used to verify shear properties in both 6061-T6 aluminum and AS4/3501-6 graphite-epoxy. A detailed outline of the results and observations from the individual tests is provided in Appendix B with numerical test results given in tables B1 and B2. A total of two Iosipescu tests were performed on 6061-T6 aluminum to obtain values for G and τ_{ult}. The values obtained from these tests were subsequently compared to the value of G obtained from a single tension test and a value of τ_{ult} obtained from the literature. These comparisons and observations made from the tests led to a number of conclusions. First, the linear initial shear stress vs. shear strain behavior of the aluminum and its ductile nature made the material easy to test. The material's ductile nature reduced compressive stress concentrations imparted to the specimen by the Iosipescu fixture. This allowed each specimen to experience a true shear-dominated failure. The material's initial linear shear stress vs. shear strain behavior increased the ease in which the initial shear modulus was calculated. The second conclusion from the tests was that, due in part to the ease in which the 6061-T6 aluminum could be tested, highly consistent values for shear modulus and shear strength could be obtained. Finally, the averaged values from

the tests appeared accurate, agreeing very well with the results from the tensile test and the literature. In summary, the Iosipescu test yielded highly favorable results for 6061-T6 aluminum.

Iosipescu tests were also used to obtain values for G_{12} and τ_{max} for the unidirectional AS4/3501-6 graphite-epoxy material used in this study. Four 0° and four 90° specimens were tested. Their results were then compared to one another and to the results from the off-axis coupon tests already outlined. The test results lead to a number of conclusions concerning the use of the test as both a test for determining composite material shear properties and as a composite far-field shear crack growth test. In determining values for τ_{max} , normal stresses imparted to the test specimen caused failure before the material shear strength could be reached in 90° specimens. As a result, this specimen could not yield reliable shear strength values. In 0° specimens, stress concentrations caused two types of failures to occur in specimens before a true shear-dominated test section failure occured. Stress concentrations at the v-notch roots caused specimen cracking to occur. As more load was applied after cracking, compressive stress concentrations caused a final crushing failure in the specimen before a shear failure could be achieved. Despite these problems, the value of applied shear stress causing each of these failure events in 0° Iosipescu test tests was significantly higher than the value of τ_{max} obtained from a typical 10° off-axis tension test. Also, the results noted with aluminum, where the material ductility helped reduce compressive stress concentrations, suggest that other composite materials may not experience crushing failures at all. Thus, despite the problems noted in the tests in this study, it appears that the 0° Iosipescu test offers significant potential over the 10° off-axis tensile coupon test for determining composite material shear strength.

The values for G_{12} obtained from the unnotched Iosipescu tests were discouraging for a number of reasons. First, 0° and 90° tests yielded significantly different average shear modulus values. Comparison with the G_{12} value obtained from the 45° off-axis tensile tests indicates that the true shear modulus for AS4/3501-6 graphite-epoxy lies somewhere inbetween the values obtained from 0° and 90° Iosipescu tests. This occurs because the state of stress in the specimen gage section is dependent on the specimen fiber orientation. This effect can be accounted for by finite element modelling of the specimen [33], but this procedure is a cumbersome one to follow in obtaining material shear properties. In addition to this problem, the Iosipescu tests showed significant scatter

in shear modulus values within each of the two types of tests. As a result, it appears that the 45° off-axis tension test is better suited for obtaining values for G_{12} .

With respect to applying the Iosipescu test as a crack growth test, the results from the unnotched Iosipescu tests suggest some potential problems. First, because of the difficulties noted in obtaining high applied shear stress values in the 90° specimens, it is likely that crack growth specimens with fiber orientations equal or close to 90° are difficult to perform. Second, the problems of specimen cracking and eventual crushing pose a potential problem, but should not present themselves in crack growth tests. This is because both premature failure events occurred only at high applied shear stresses in the unnotched tests. Notch-tip stress concentrations should cause crack growth and failure to occur well before specimen crushing. Perhaps the most significant potential problem indicated in using the Iosipescu test as a crack growth test is the apparent dependence of gage section stress state on specimen fiber orientation. Because the analytical procedure specifies that pure shear far-field stresses be used in modelling Iosipescu crack growth tests, changes in specimen stress state with fiber orientation represent a potential source of error in comparing experiment and theory for different tests.

6.0 Analytical Results

6.1 Role of Normal Stress in Material Fracture

As outlined in the section describing the normal stress ratio theory, and in Section 3.4, the theory's fundamental assumption is that mode I crack opening controls crack extension. Because of this assumption, the theory only takes into account local normal stresses that can contribute to mode I crack growth, ignoring other stress components and failure modes. In this way, the normal stress ratio theory is fundamentally different from general anisotropic material failure criteria such as the tensor polynomial and Tsai-Hill theories. Such theories take into account all stress components and numerous failure modes. In analyzing crack extension problems in notched materials, it is reasonable to use an approach that assumes a single failure mode related to crack geometry is dominant. It remains to be determined, however, if such an approach is correct, and if so, whether the ratio of local normal stress to normal strength is the specific quantity acting to control notched material fracture.

6.1.1 Problems Studied

The issue of what if any single failure mode controls notched material crack extension is investigated in this section by addressing two problems, uncracked and cracked infinite homogeneous anisotropic composite plates subjected to a uniformly applied far-field tensile stress (Figure 21). The material studied is AS4/3501-6 graphite-epoxy. Both types of plates have an arbitrary fiber orientation. The cracked plate contains a single macroscopic center crack oriented along the horizontal axis (at 90°). The uncracked problem is analyzed assuming a homogeneous state of pure tensile stress, using the normal stress ratio theory on a global level to predict specimen fracture angles. The cracked problem is analyzed using both the normal stress ratio and the tensor polynomial as crack growth theories on a local near-crack-tip level to predict fracture angles (see Sections 1.2.2.1 and 1.2.2.3). The uniform stress problem is studied for its simplicity. Also, a uniform applied tensile stress approximates the far-field applied state of stress in unidirectional tensile coupons of large aspect ratio. The fracture angle predictions for both problems are thus compared to known experimental behavior for notched and unnotched unidirectional graphite-epoxy tensile coupons.

6.1.2 Known Experimental Behavior

Although the approaches used to analyze notched and unnotched tensile coupons are very different, the experimental fracture direction behavior for the two types of problems is essentially identical for unidirectional graphite-epoxy. For both center-notched and unnotched unidirectional graphite-epoxy coupons, failure occurs along the fiber direction. The only exception to this rule is the unnotched 0° coupon, which typically experiences a failure that is roughly perpendicular to the fiber direction. This failure behavior is not always observed, however. Such specimens are known to, in some cases, experience a series of failures throughout the specimen thickness, some of which

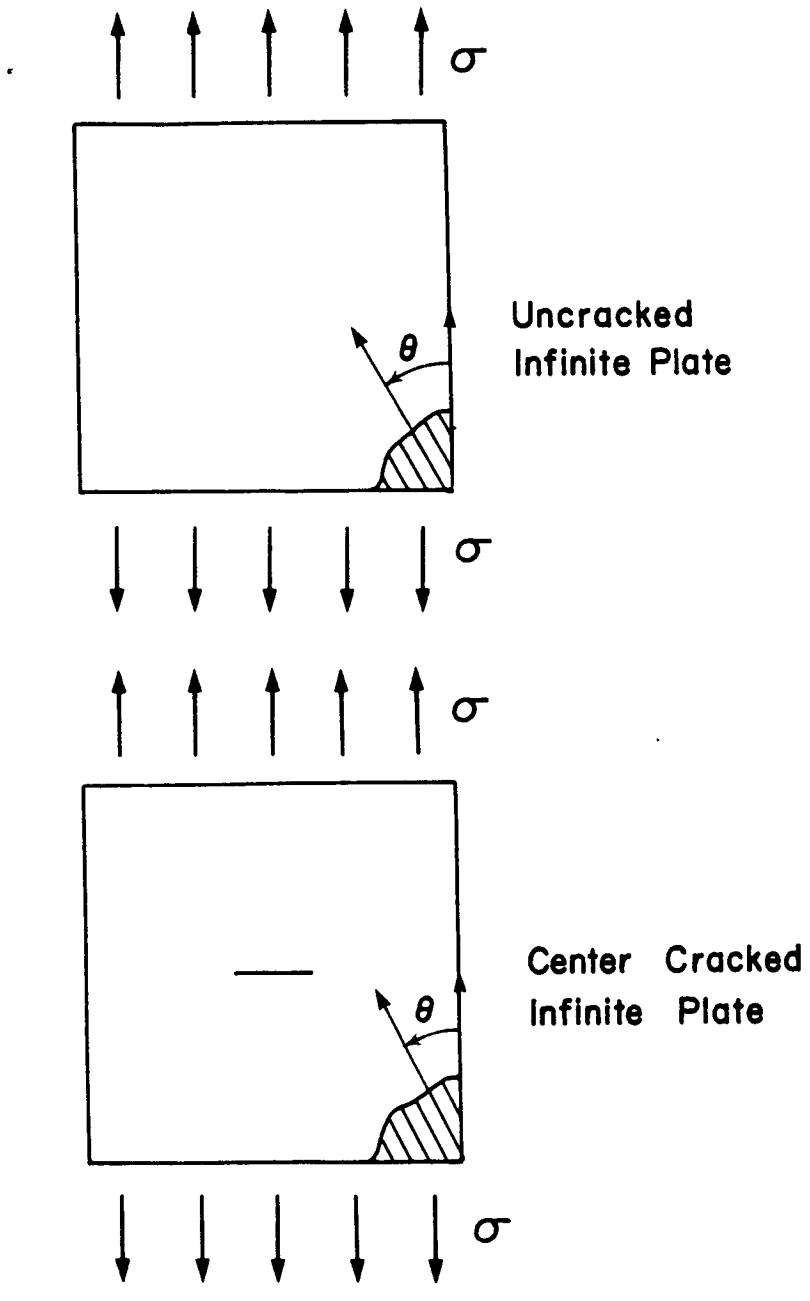

Figure 21. Problems Modelled as Large Aspect Ratio Tensile Coupons

are along the fiber direction and others which are perpendicular to the fiber direction. The failed specimen that results has a broomstick type of appearance. In such cases, the fracture angle is not well defined. Also, such failures are likely caused by the interaction of the applied axial normal stress and the transverse tensile stresses induced in the specimen due to grip end constraints and specimen Poisson contraction. This type of interaction is not accounted for by an analysis using only an applied axial stress. Because of these facts, for this analysis the experimentally observed fracture angle for an unnotched 0° coupon is best characterized as always being perpendicular to the fibers.

6.1.3 Predicted Behavior

Fracture angles predicted by the normal stress ratio theory for the unnotched tensile coupon problem are plotted in Figure 22 against specimen off-axis angle, over a range of 0° to 90°. The fracture angle predicted by the normal stress ratio theory was designated as the angle having the maximum ratio of global normal stress to normal strength. Fracture angles are measured with respect to the fibers, with an angle other than 0° corresponding to fracture predicted to occur other than along the fiber direction. As indicated in Figure 22, the normal stress ratio theory performs well for only a portion of unnotched tensile coupon problems. The theory works well for specimens having large off-axis angle values. As the off-axis angle is decreased, however, the theory begins to predict fracture angles that diverge from the fiber direction by increasingly larger amounts, until, for a 0° coupon, the theory correctly predicts crack extension to occur at 90° to the fiber direction. Although many of the predictions of the normal stress ratio are incorrect for this problem, such inaccuracies are not unexpected. Unnotched tensile coupons with fibers oriented close to the tensile axis fail predominantly due to the influence of far-field shear stresses acting along the fiber direction. This provides the basis for using the 10° off-axis test for estimating material shear strength. When applied on a global level, the normal stress ratio theory clearly cannot account for and predict such global shear-dominated failures. This explanation of the theory's behavior also

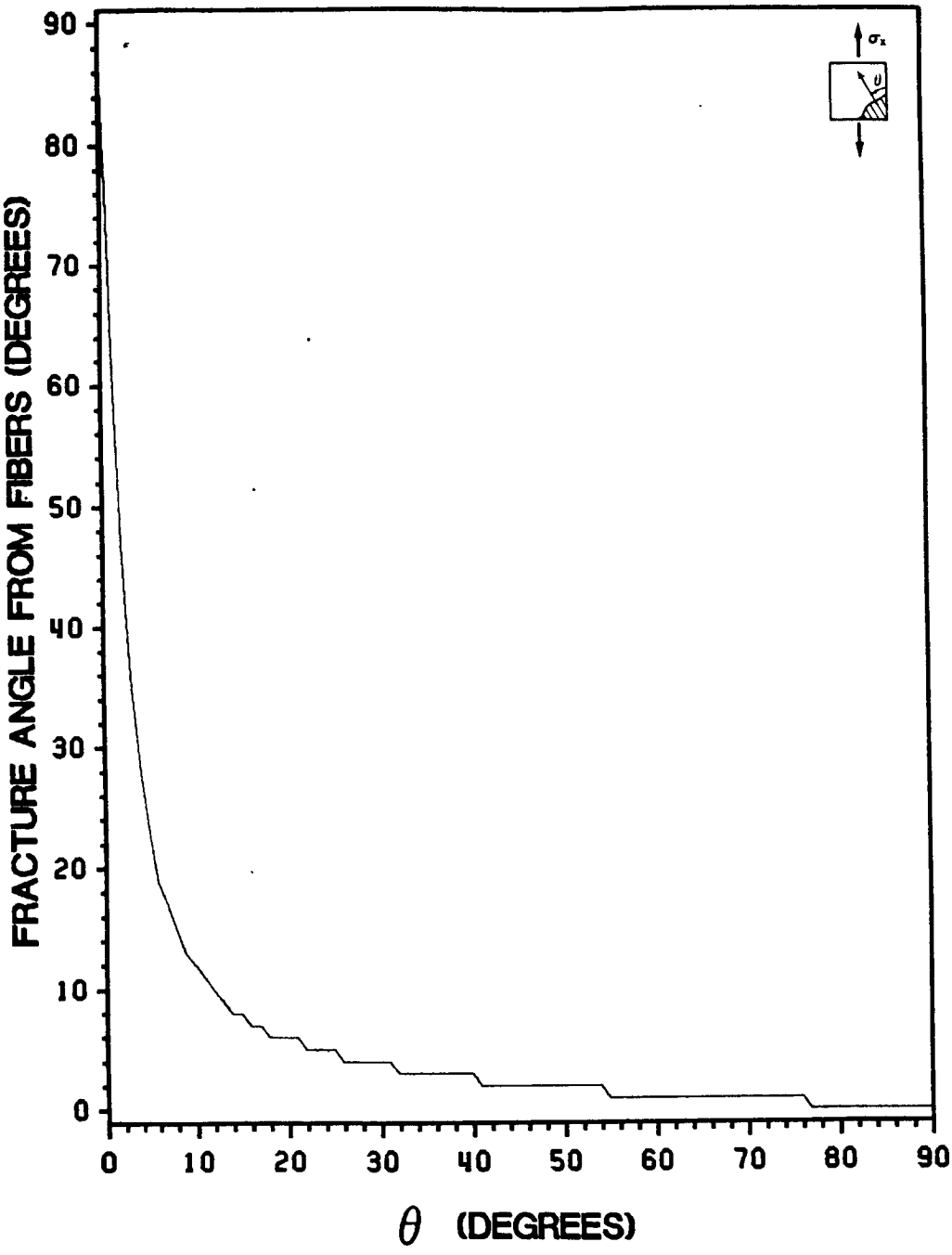

Figure 22. **Normal Stress Ratio Predictions for Unnotched Off-Axis Tensile Coupons:** Fracture Angle Predictions vs. Fiber Angle for Specimens of AS4/3501-6 Graphite-Epoxy Subjected to Uniform Applied Far-Field Axial Stress

accounts for the fact that even though the fracture angle predictions for small off-axis angles are incorrect, the theory does predict the correct fracture angle for the normal-stress-dominated 0° coupon.

Figure 23 and Figure 24 provide plots similar to that provided in Figure 22, except the problem that is analyzed is a tensile coupon with a horizontal center notch. In determining the fracture angles for this problem, both tensor polynomial and normal stress ratio theories are applied to the local stress field predicted by the Lekhnitskii stress solution (Eq. 14), at a specified distance from the analytically modelled sharp crack tip. The ratio of distance from the crack tip to half crack length used was 0.001. As noted in Section 3.3.2, however, the angular variation of the stresses in Eq. 14 is not a function of the radial distance, r. Because of this, crack growth direction predictions made by a linear theory such as the normal stress ratio using the Lekhnitskii solution stresses are independent of the distance from the crack tip used. In applying the tensor polynomial theory, crack growth direction predictions are, in general, dependent upon the magnitude of the stress field, and thus the distance from the crack tip used in the analysis. This is because the tensor polynomial contains both linear and quadratic terms. At different load levels, different terms may dominate the tensor polynomial value. In this study, however, it is assumed that compressive and tensile material strengths are equal. This causes the tensor polynomial to become a purely quadratic theory which will provide crack growth direction predictions that are independent of stress field magnitude and thus distance from the crack tip used in the analysis. The direction of crack extension predicted by each theory is designated as the predicted specimen fracture angle. As indicated in Figure 23, the tensor polynomial theory provides very erratic predictions of fracture angles, none of which are correctly at 0° regardless of the off-axis angle. In contrast, Figure 24 shows that the normal stress ratio theory now provides essentially accurate fracture angle predictions of 0° (along the fibers) for all off-axis angle values.

An important characteristic of the plots provided in Figure 22, Figure 23, and Figure 24 is their apparent lack of smoothness. This is not necessarily caused by the theories themselves, but is instead a consequence of the method in which they are applied. In applying any of the crack growth theories presented in this study using the Lekhnitskii solution, all parameters are evaluated

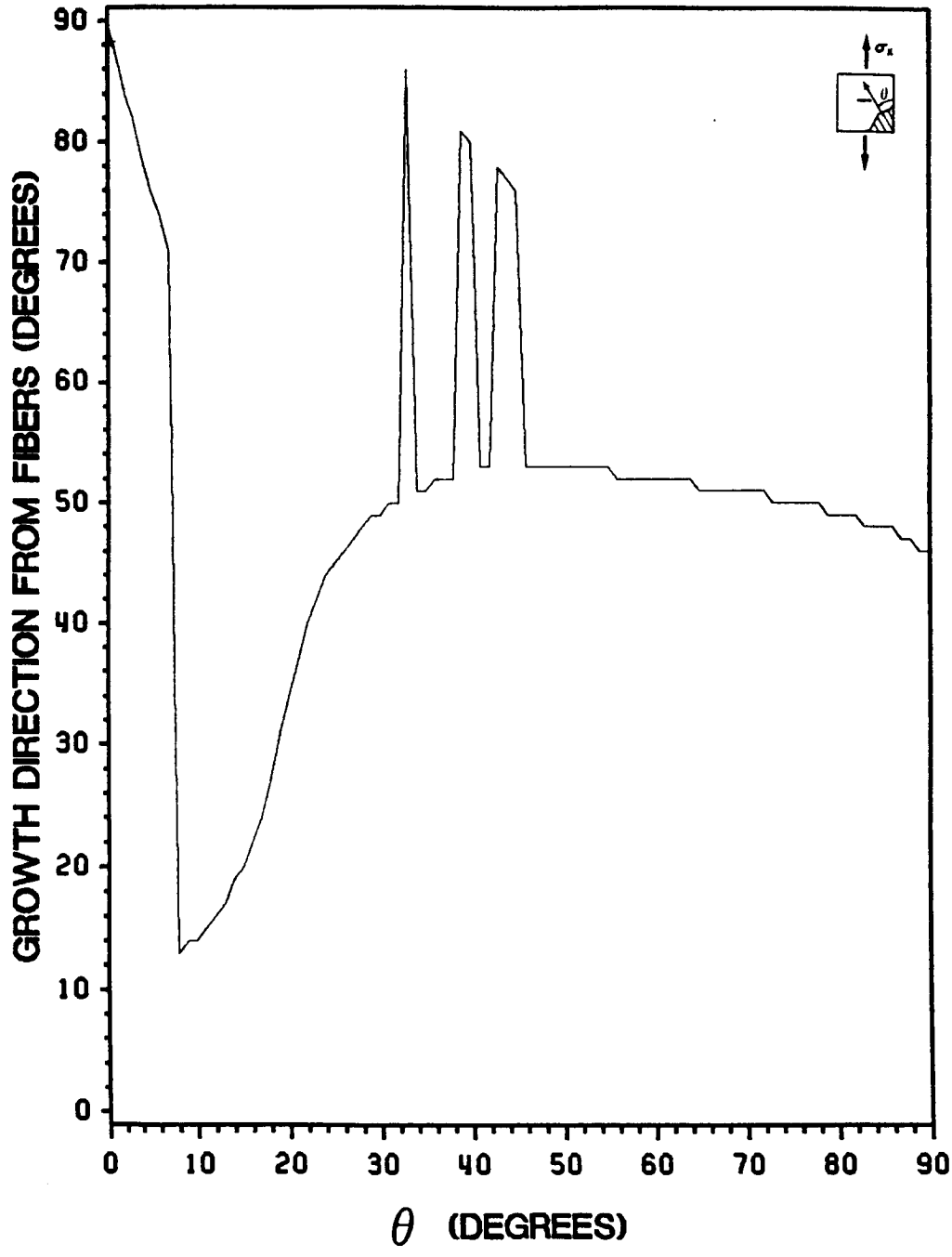

Figure 23. Tensor Polynomial Predictions for Center-Notched Off-Axis Tensile Coupons: Crack Growth Direction Predictions vs. Fiber Angle for Specimens of AS4/3501-6 Graphite-Epoxy Subjected to Uniform Applied Far-Field Axial Stress

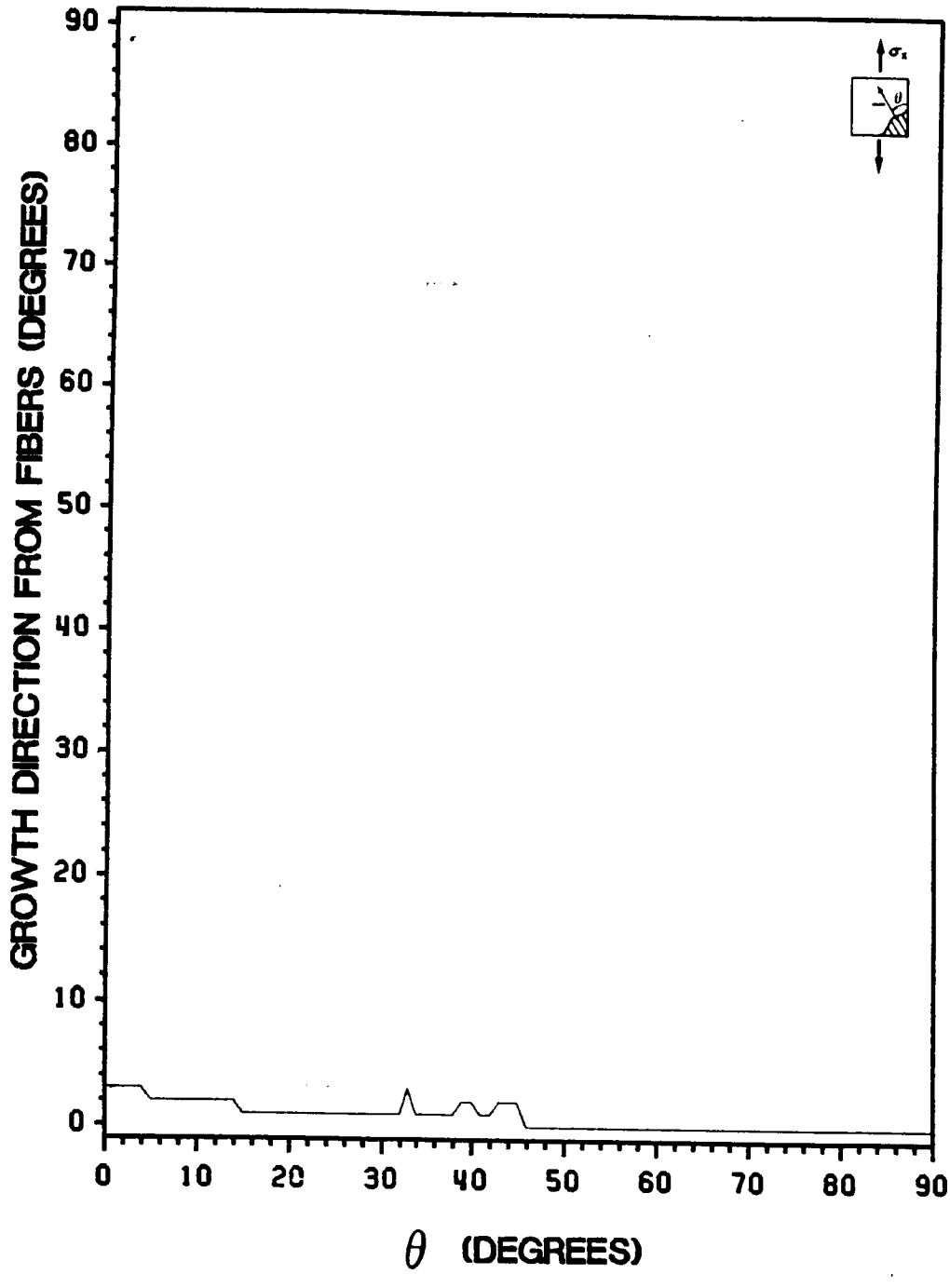

Figure 24. Normal Stress Ratio Predictions for Center-Notched Off-Axis Tensile Coupons: Crack Growth Direction Predictions vs. Fiber Angle for Specimens of AS4/3501-6 Graphite-Epoxy Subjected to Uniform Applied Far-Field Axial Stress

in 1° increments. This necessarily results in a step-wise appearance to criteria prediction plots, which are made by connecting individual data points. All of the plots included in this report were created by a piecewise joining of individual data points. No smoothing or curve-fitting plotting routines have been used.

6.1.4 Implications and Conclusions

The comparisons just made between the fracture angle predictions made by the tensor polynomial and normal stress ratio theories and known experimental fracture angle behavior suggest a number of important conclusions. It has been demonstrated that, for an unnotched material, a theory based solely on normal stresses and strengths can predict correct fracture angles only if specimen fracture is normal stress dominated. It is reasonable to assume that an analogous condition exists for the analysis of notched material problems on a local level. If crack extension in a notched material is not normal stress controlled, then an analysis based solely on normal stress should be applicable only to a small class of notched material problems. In contrast to the normal stress ratio theory, the tensor polynomial theory accounts for all stress components. It is thus reasonable to assume that the tensor polynomial can therefore account for non-normal stress dominated failure modes in notched material problems. The predictions that result from the application of the normal stress ratio and tensor polynomial theories to the prediction of fracture angles for center-notched off-axis tensile coupons thus imply two things. First, in accounting for numerous failure modes, the tensor polynomial provides predicted crack extension behavior that is incorrect. It appears that the theory takes into account stresses and/or failure modes that are not important in notched material fracture behavior. Second, by accounting only for the balance of local normal stress and strength as defined in the normal stress ratio theory, correct crack extension direction values can be obtained even in cases exhibiting global shear-type failures.

The results of this short analytical study suggest that the balance of normal stress and strength indeed acts as a controlling parameter on a local near-crack-tip level for materials with macroscopic

notches. This implication may not be limited to the analysis of materials with macroscopic-sized notches, however. In this section the normal stress ratio theory was used to analyze a material without a macroscopic flaw by assuming it to be free of flaws entirely. Although this type of approach is commonly used in global strength analyses, it is recognized that even macroscopically uncracked materials do contain microscopic flaws. These flaws strongly influence material global strength and failure. If the stress state near such flaws can be approximated, it is possible that local normal stress can be shown to control fracture even in macroscopically unflawed materials. The identification of possible local controlling fracture mechanisms in materials having vanishingly small flaws is a topic that, although not addressed in this study, offers potential for unifying current global and local fracture analysis approaches.

6.2 *A Critical Test of the Analysis*

A substantial amount of effort has been expended by this and other researchers in attempting to identify critical tests of the normal stress ratio theory and its proposed method of application. Because it was originally proposed exclusively as a criterion for the prediction of crack growth direction, and because there is a strong tendency for crack extension in graphite-epoxy to be along the fiber direction, efforts have centered around identifying theoretical cases for which the theory predicts crack extension other than along the fibers. A number of potential cases have been identified. One specific case, however, provides the greatest insight into the possible limitations of the theory and its application. This case is illustrated in Figure 25. An infinite unidirectional graphite-epoxy plate with a center crack along the fiber direction is subjected to pure shear loading in the coordinate system of the crack. For the positive shear case illustrated in Figure 25, the direction of crack extension measured with respect to the crack predicted by the normal stress ratio theory is -12°. Symmetry conditions result in a prediction of $\varphi_c = 12°$ for a negative applied shear stress.

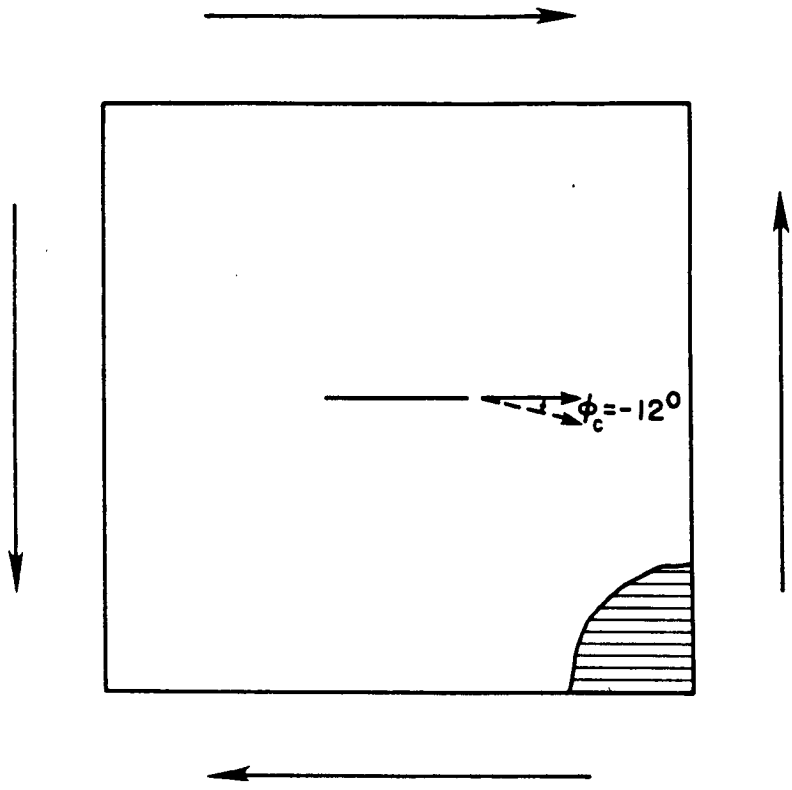

Figure 25. Infinite Anisotropic Plate with a Crack Along the Principal Material Axis Under Pure Shear Far-Field Stress

The normal stress ratio theory prediction of crack extension at 12° from the fibers for this case does not appear to offer a severe contradiction with expected experimental crack extension behavior. Within potential errors in the theory and analysis, a discrepancy of 12° between theory and experiment is almost reasonable. The criticality of this case with respect to the ability of the normal stress ratio theory to predict crack extension direction does not have to do with the magnitude of the apparent error in its prediction. It is instead the reason why the theory does not predict crack extension along the fibers that is important. For all cases of pure shear far-field loading in the crack coordinate system, the Lekhnitskii solution predicts that $\sigma_{\varepsilon\varepsilon}$, the normal stress along the $\varphi = 0$ axis (see Figure 13), will equal zero. This occurs due to the fact that at $\varphi = 0$, $\psi_1 = \psi_2 = 1$ (see Eq. 14). For the particular case of a crack along the fiber direction, the angle $\varphi = 0$ corresponds to the fiber direction. Thus, no local normal stresses exist perpendicular to the fibers. The normal stress ratio theory, as it is applied in this study, is therefore incapable of predicting crack extension along the fibers for this case. This result is not limited to the analysis of graphite-epoxy, but is instead valid for any notched anisotropic material analyzed using the Lekhnitskii solution, regardless of its elastic and/or strength properties. As a result, crack extension along the fiber direction cannot be predicted, even for an idealized material with an infinitesimal value of normal strength, Y_t, and a large value of normal strength, X_t. Thus, the error in the theory's prediction for this case is not simply due to potential inaccuracies, but is instead due to a fundamental error either in the theory itself or in the way in which is applied and interpreted.

It is important to note that the type of critical case illustrated in Figure 25 is directly the result of the extension of macroscopic-level fracture techniques to anisotropic materials. As mentioned in Sections 1.1.3 and 1.2.2, a number of theories proposed for the analysis of mixed-mode fracture in isotropic materials have been extended to the analysis of anisotropic materials. The normal stress ratio theory is one of these. Unfortunately, the study of isotropic material fracture does not appear to produce critical tests for evaluating the validity of any of these theories. For example, for a center-cracked isotropic plate subjected to pure shear loading in the crack coordinate system, there is also no local normal stress along the $\varphi = 0$ plane. This does not result in a critical test of a normal stress-based theory, however, because the $\varphi = 0$ plane is not the experimental direction of crack

extension. For the anisotropic material problem, the orientation of the principal material axes can act to constrain expected experimental behavior to that exhibiting crack extension along the fiber direction. This constraint can thus be exploited to obtain critical crack growth direction cases by aligning the material fibers along directions experiencing little or no normal stress. As a result, studying the problem of crack extension in anisotropic materials can provide fundamental insight in determining an appropriate analytical approach for predicting crack extension behavior in all materials.

The most apparent explanation for the reason why the normal stress ratio appears to break down for the case illustrated in Figure 25 is that this is a theoretical case where a theory based solely on local normal stress cannot yield correct results. This suggests the possible need for the inclusion of stress components other than the normal stress defined with respect to the crack within a crack growth theory. A more subtle explanation for the discrepancy between theory and expected behavior is that the use of the stress solution by Lekhnitskii is incorrect. The Lekhnitskii stress solution models an actual notch as a line crack with an infinitely sharp tip. The practice of modelling a notch in this manner originated with the work of Irwin [2] in formulating classical fracture mechanics principles. Clearly, however, a discrepancy exists between the geometry of an actual rounded notch tip and that of the sharp crack model. For a crack growth theory such as the normal stress ratio, which is formulated to depend entirely upon near-crack-tip stresses, it is possible that this discrepancy is highly significant. In the next two sections, this possibility and the possible need for the inclusion of other stress components in a crack growth analysis are investigated.

6.3 Use of a Rounded Notch Tip Model

In an attempt to more accurately model the shape of real notch tip regions, and to help determine the influence of notch tip shape on the analysis, the normal stress ratio theory has been applied in [37] within the stress solution presented in [38] for an elliptical hole in the center of an

infinite anisotropic plate. In [37], the rounded shape of a notch cut in unidirectional graphite-epoxy is modelled by specifying the ratio of major to minor axis dimensions so that the radius of curvature of the tip of the ellipse equals the cut notch tip radius. This method is used to specifically analyze some of the tests performed as a part of this study, where the radius of the cut notch tip is 0.0025 in. In this section, only the results from application of the analysis to the critical pure shear case outlined in Section 6.2 will be addressed. Further comparisons are made with experimental results in Section 8.3.

The stress solution for an ellipse with a non-vanishing minor axis dimension does not exhibit stress singularities at the ellipse tips. As a result, in [37] the normal stress ratio is not applied at a specified distance from the modelled notch tip, as it is for the sharp crack analysis presented in this study. Instead, the stresses used within the normal stress ratio theory are evaluated along the elliptical boundary itself. Figure 26 illustrates the procedure used in [37]. At each point on the boundary of the elliptical hole, defined by the angle Ω, the normal stress ratio is evaluated over a range of radial directions, defined by the angle φ. The angle φ is varied over a 180° range bounded by the tangent to the elliptical boundary. Crack extension is predicted to occur in the direction of maximum normal stress ratio, at the point on the ellipse defined by the corresponding value of Ω. In this way, not only a direction of crack extension, but also a point of origin of crack extension along the elliptical boundary is obtained from the analysis. This method is used in this section to determine if, when the rounded shape of a notch tip is approximately modelled, the normal stress ratio theory will predict crack extension along the fiber direction for the pure shear case outlined in Section 6.2 and illustrated in Figure 25.

An illustration of the results of the analysis is provided in Figure 27. In the figure, the ellipse used to model the rounded shape of the notch tip is indicated by a solid line. The solid line extending from the elliptical boundary represents the predicted location and direction of crack extension. The figure shows that, when this stress solution and application procedure are used to model this case, the normal stress ratio theory predicts crack extension along the fiber direction. The location of crack extension is also important to note. Instead of predicting crack extension from the tip of the rounded notch, crack extension is predicted to occur just away from the tip of the notch.

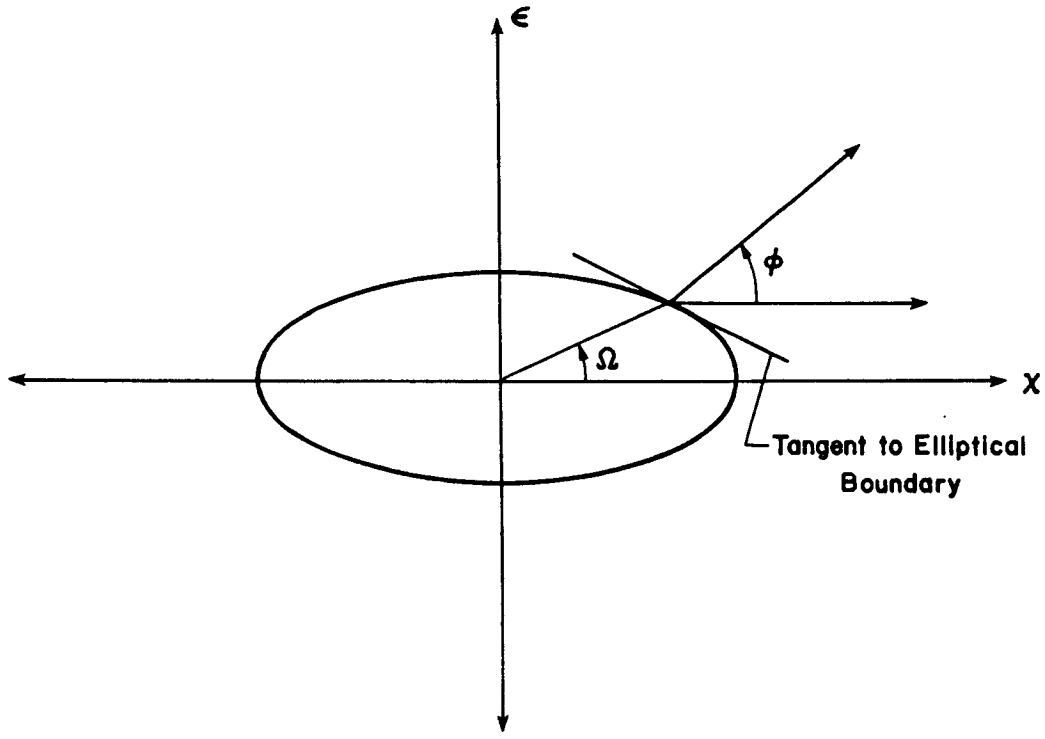

Figure 26. Elliptical Hole Crack Growth Analysis Approach Used in [37]

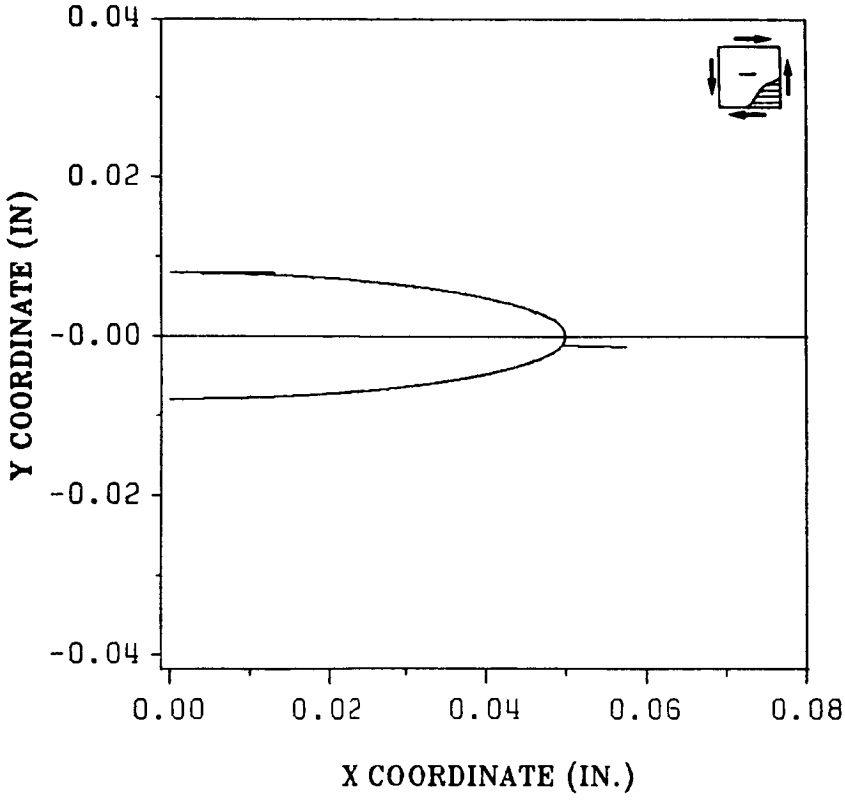

Figure 27. Result of the Elliptical Hole Analysis for the Case of a Crack Subjected to Pure Shear Far-Field Stress: see Figure 25

In using a sharp crack solution, it is assumed a priori that crack extension will occur from the notch tip. For this case, a sharp crack analysis therefore acts to constrain the predicted crack extension location so that crack growth must occur from a notch tip location that has no normal stress acting along the fiber direction. It appears that in using a rounded notch tip solution and by allowing crack extension to occur away from the tip of the notch, a more realistic crack growth direction prediction can be obtained for this case. Thus, this approach indicates that a crack extension direction criterion based solely on local normal stress can provide accurate crack extension predictions if real notch tip geometry is more accurately modelled.

6.4 Strain Energy Balance Theory

6.4.1 Fundamental Principles

Although it is reasonable to assume that normal stress alone controls crack extension behavior, an argument based on energy considerations can be made that indicates that a local shear stress component should also be included in the formulation. Figure 28 illustrates the configuration of a flawed material before and after crack extension. Energy principles demand that crack extension can occur only if it allows the material to achieve a lower energy state than it possesses before crack extension. The energy-based argument for the inclusion of shear stress in a crack growth theory presented in this study is based upon the simple observation that a crack is a free surface embedded within a material. Because it is a free surface, the stresses normal to the crack boundary are equal to zero. As illustrated in Figure 28, then, along the surface of a crack embedded in a material, the boundary stresses $\sigma_{\xi\xi}$ and $\tau_{\chi\xi}$ are equal to zero, leaving the stress $\sigma_{\chi\chi}$ as the only nonzero stress. At any point in the material not on the crack boundary, all three stresses are, in general, nonzero. As Figure 28 illustrates, when crack extension occurs, the free surface of the crack extends into the

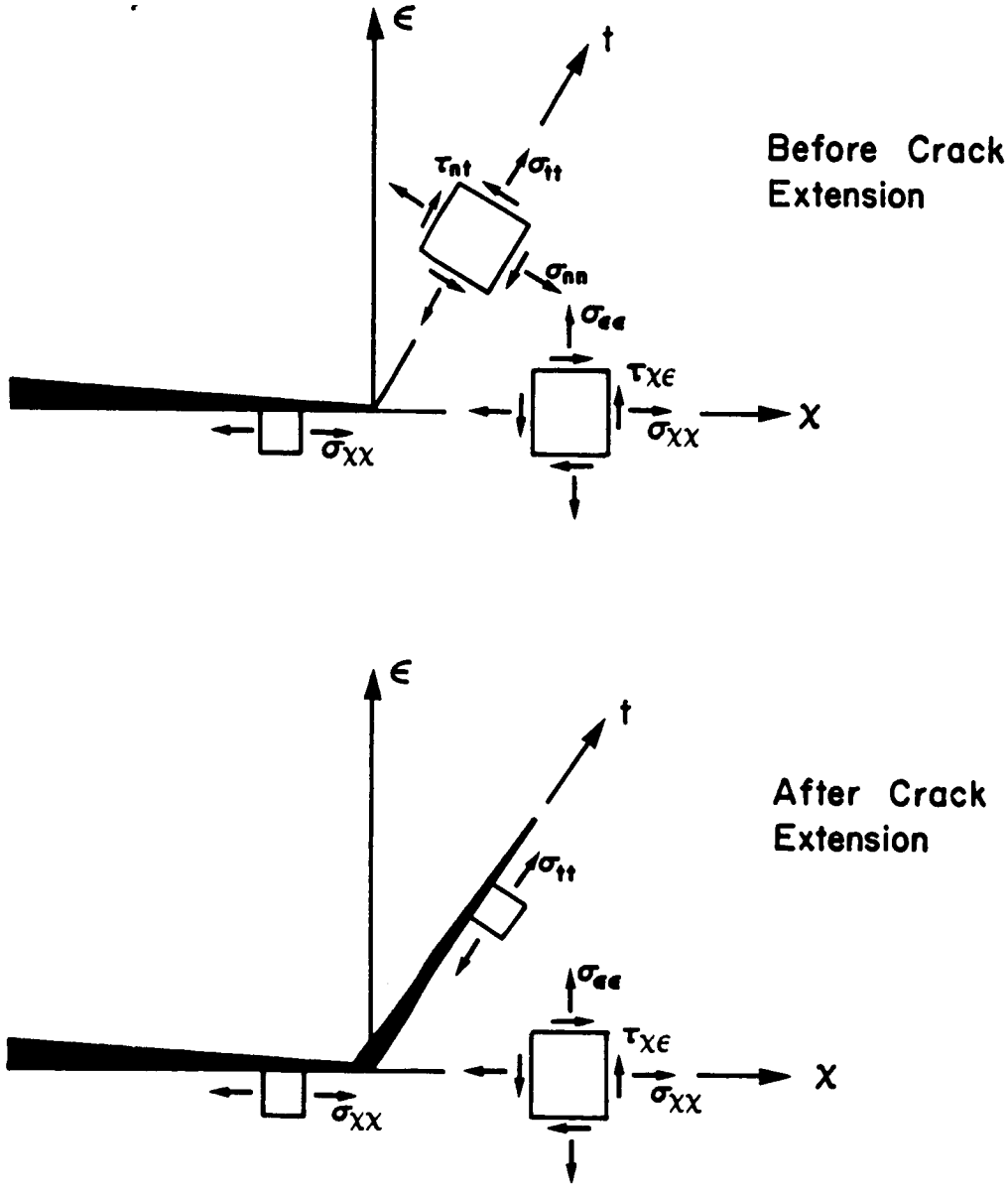

Figure 28. Stresses in a Cracked Plate

C-2

material. As this extension occurs, the stresses normal to the new crack boundary, σ_{nn} and τ_{nt} , must become zero to satisfy the new free surface boundary conditions. Elimination of these boundary stresses during crack extension represents a release of strain energy that allows the flawed material to relax. From this viewpoint , it appears that not only the normal stress, σ_{nn}, but also the shear stress, τ_{nt} contributes to crack extension, because the creation of new free crack boundaries forces both stresses to become equal to zero as the crack extends into the material. The strain energy balance theory presented in this section assumes that the reduction in strain energy caused by the elimination of these stresses acts as the driving force behind crack extension.

6.4.2 Strain Energy Balance Theory Statement

The strain energy balance theory assumes that crack extension is controlled by the balance of two strain energy density parameters. The first strain energy density parameter, designated as E_r, represents the aforementioned strain energy per unit volume released as the result of relaxation of the material during crack extension. The second strain energy density parameter, designated as E_s , represents the surface energy per unit volume that must be supplied to the system in order to break material bonds during crack extension. This term is included in the theory because although crack extension allows a flawed material to relax, some amount of energy must be supplied to the system in order to break material bonds and extend the crack surface. This energy serving to resist crack extension must be dependent on the material strength. In an isotropic material, material strength, and thus the energy required to separate the material are independent of direction. In an anisotropic material such as a composite, however, material strength and the energy required to separate the material are directionally dependent. In order for an energy-based crack extension theory to be applicable to both isotropic and anisotropic materials, it must take into account any directional dependence of the resistance to crack extension.

If released energy is assumed positive, the strain energy balance theory can be expressed by stating that

$$E_r \geq E_s. \tag{15}$$

is a necessary condition for crack extension. For crack extension to occur, it is necessary that the parameter representing the strain energy per unit volume released during crack extension be greater than or equal to the parameter representing the surface energy per unit volume that must be supplied to separate the material and extend the crack. The radial direction of crack extension is defined as the direction having the largest value of $(E_r - E_s)$.

6.4.3 Strain Energy Release Parameter

The parameter representing the strain energy per unit volume acting to drive crack extension is defined as equalling the strain energy density that is released when the stresses σ_{nn} and τ_{nt} become zero. In Section 1.1.2.2, the total strain energy per unit volume under plane stress conditions was given. Because the strain energy per unit volume is an invariant quantity, it can be expressed in the $n - t$ (extended crack) coordinate system as

$$\frac{\partial W}{\partial V} = \frac{1}{2}\left(\sigma_{nn}\varepsilon_{nn} + \sigma_{tt}\varepsilon_{tt} + \tau_{nt}\gamma_{nt}\right). \tag{16}$$

This can be expanded in terms of only stress and compliance terms to the form

$$\frac{\partial W}{\partial V} = \frac{1}{2}\left(S_{11}\sigma_{tt}^2 + 2S_{12}\sigma_{nn}\sigma_{tt} + 2S_{16}\sigma_{tt}\tau_{nt} + S_{22}\sigma_{nn}^2 + 2S_{26}\sigma_{nn}\tau_{nt} + S_{66}\tau_{nt}^2\right), \tag{17}$$

where the S_{ij} terms are the material compliances in the $n - t$ coordinate system. If only the strain energy density terms containing σ_{nn} and τ_{nt} are assumed to contribute to energy release during crack extension, then the term $S_{11}\sigma_{tt}^2$ should be eliminated from the total strain energy density expression to obtain E_r. As a result, the parameter E_r is defined by the equation

$$E_r = \frac{\partial W}{\partial V} - \frac{1}{2}S_{11}\sigma_{tt}^2 = \frac{1}{2}\left(\sigma_{nn}\varepsilon_{nn} + \sigma_{tt}\varepsilon_{tt} + \tau_{nt}\gamma_{nt} - S_{11}\sigma_{tt}^2\right). \tag{18}$$

As in the strain energy density theory, the stresses and strains are evaluated at a specified radius, r_s, from the original crack tip using an elastic solution to the original crack geometry problem.

6.4.4 Surface Energy Parameter

The strain energy balance theory defines a parameter representing the surface energy per unit volume acting to resist crack extension, designated as E_s, by considering the problem of an uncracked isotropic or anisotropic material under uniaxial far-field loading (Figure 29). If the material is anisotropic, its principal material axis is defined by the angle θ measured with respect to to the x axis. When the uniaxial stress, σ_x, reaches the ultimate strength of the material in the x direction, fracture occurs. Energy balance requires that, at the point of fracture, the strain energy in the material equals the energy required to break the material bonds along the x direction. As a result, the energy per unit volume required to break the material bonds along the x direction can be represented by the equation,

$$E_S = \frac{1}{2} (T_{xx} e_{xx}) , \tag{19}$$

where T_{xx} and e_{xx} are, respectively, the ultimate tensile strength and ultimate tensile strain in the x direction. As noted in the formulation of the normal stress ratio theory, the tensile strength on an arbitrary plane in an anisotropic material must be defined mathematically. Thus, the strain energy balance theory uses the expression for theoretical normal strength, $T_{\varphi\varphi}$, already developed in deriving the normal stress ratio theory (Eq. 6) as the expression for T_{xx}.

Noting that, when σ_x is the only nonzero stress, e_{xx} equals T_{xx} multiplied by the material compliance in the x direction, and substituting $T_{\varphi\varphi}$ for T_{xx}, Eq. (19) can be rewritten as

$$E_S = \frac{1}{2} (T_{\varphi\varphi}^2 S_{\varphi\varphi}) , \tag{20}$$

where $S_{\varphi\varphi}$ is the material compliance perpendicular to the φ plane.

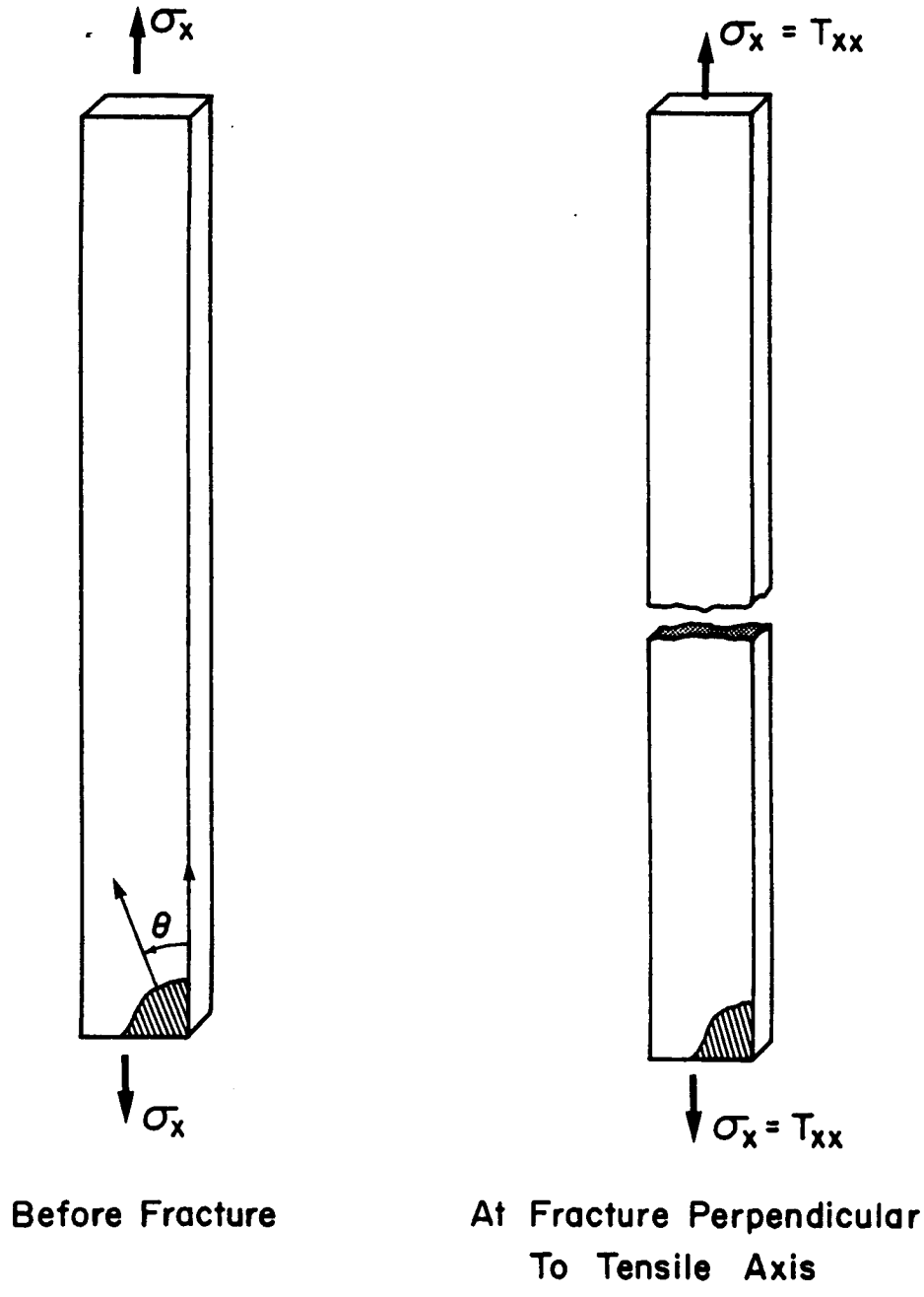

Figure 29. Anisotropic Material Under Uniaxial Tension

6.4.5 Explicit Expression of the Strain Energy Balance Theory

In order to make the strain energy balance theory more directly comparable to other theories, it will be expressed in the form of a ratio. If both sides of Eq. (15) are divided by E_s, the expression that results is

$$\frac{E_r}{E_s} \geq 1. \tag{21}$$

Substituting the expressions from eqns. (18) and (20) and cancelling $\frac{1}{2}$ from the numerator and the denominator results in the explicit form of the theory used in this study. Crack extension is predicted to occur when

$$\frac{(\sigma_{nn}\varepsilon_{nn} + \sigma_{tt}\varepsilon_{tt} + \tau_{nt}\gamma_{nt} - S_{11}\sigma_{tt}^2)}{(T_{\varphi\varphi}^2 S_{\varphi\varphi})} \geq 1 \tag{22}$$

along the predicted direction of crack extension. The predicted direction of crack extension corresponds to the direction having the maximum value of the above ratio.

6.4.6 Comparison with the Normal Stress Ratio Theory

The strain energy balance theory is most easily compared to the normal stress ratio theory by expressing E_r in its expanded form, in terms of stresses and compliances only. If this is done, and if it is recognized that $S_{\varphi\varphi} = S_{22}$, the expression that results is

$$\frac{(2S_{12}\sigma_{nn}\sigma_{tt} + 2S_{16}\sigma_{tt}\tau_{nt} + S_{22}\sigma_{nn}^2 + 2S_{26}\sigma_{nn}\tau_{nt} + S_{66}\tau_{nt}^2)}{(T_{\varphi\varphi}^2 S_{22})} \geq 1. \tag{23}$$

This can be rewritten in the form

$$\frac{\sigma_{nn}^2}{T_{\varphi\varphi}^2} + \frac{(2S_{12}\sigma_{nn}\sigma_{tt} + 2S_{16}\sigma_{tt}\tau_{nt} + 2S_{26}\sigma_{nn}\tau_{nt} + S_{66}\tau_{nt}^2)}{(T_{\varphi\varphi}^2 S_{22})} \geq 1. \quad (24)$$

From Eq. 24, it is clear that the strain energy balance theory parameter is equal to the normal stress ratio squared plus a term that is is a function of the stresses and compliances in the extended crack coordinate system. As in the normal stress ratio theory, the strain energy balance theory attempts to account for the directional dependence of material strength. Also, both theories hypothesize that crack extension occurs in the direction of a maximum in their respective crack extension parameters. Thus, the strain energy balance theory appears to be an extension of the normal stress ratio theory derived under energy-based assumptions.

6.4.7 Comparison with the Strain Energy Density Theory

As previously stated, the strain energy density theory hypothesizes that crack extension will occur along the radial direction having the minimum value of the strain energy density factor, S, when S reaches a critical value. If S is expressed in terms of stress and strain components in the $n - t$ coordinate system, it is given by the expression

$$S = \frac{r}{2}(\sigma_{nn}\varepsilon_{nn} + \sigma_{tt}\varepsilon_{tt} + \tau_{nt}\gamma_{nt}). \quad (25)$$

Comparison of eqns. (22) and (25) reveals that the strain energy balance theory parameter is similar to the strain energy density factor. The two theories differ in three essential respects, however. First, the strain energy balance theory hypothesizes that only a portion of the strain energy density functional acts as a parameter controlling crack extension. Specifically, it is hypothesized that the term $S_{11}\sigma_{tt}^2$ should be eliminated from the strain energy density factor expression, because σ_{tt} is not a boundary stress for the extended crack. Thus, it is assumed that the term $S_{11}\sigma_{tt}^2$ does not contribute to the release of strain energy acting to drive crack extension. The second difference

in the two theories is that the strain energy balance theory hypothesizes that crack extension will occur in the radial direction having a maximum (not a minimum) of the strain energy balance parameter. As with the first difference noted in the two theories, this arises because the strain energy balance theory assumes that the modified strain energy density factor represents the strain energy release that drives crack extension. The final difference in the two theories is that the strain energy balance theory attempts to balance its strain energy density expression with a surface energy density expression based on material strength ($T^2_{\varphi\varphi}S_{\varphi\varphi}$). In contrast, the strain energy density theory makes no attempt to account for the directional dependence of the resistance to crack extension.

6.4.8 Crack Extension Direction Predictions

6.4.8.1 Anisotropic Materials

Because the pure shear crack extension case illustrated in Figure 25 provided part of the motivation for investigating the inclusion of shear stress within a crack growth theory, its analysis using the strain energy balance theory is studied here. It is critical to determine if, when the term given in Eq. 24 is added to the normal stress ratio, the predicted direction of crack extension is changed from 12° away from the fiber direction to a direction along the fibers. In Figure 30, a plot is provided of the strain energy balance parameter as a function of the angle φ around the crack tip. As the figure illustrates, not only does the strain energy balance parameter exhibit a maximum along the angle $\varphi = 0$ for this case, but the peak is a very strong one.

The success of the strain energy balance theory for this case is significant. Similar successes are noted in applying the theory to the analysis of tensile coupon and Iosipescu shear specimen problems. Strong peaks are consistently exhibited along the fiber direction. This also occurs in cases where the normal stress ratio exhibits a slight error of perhaps 2° or 3°, again suggesting that

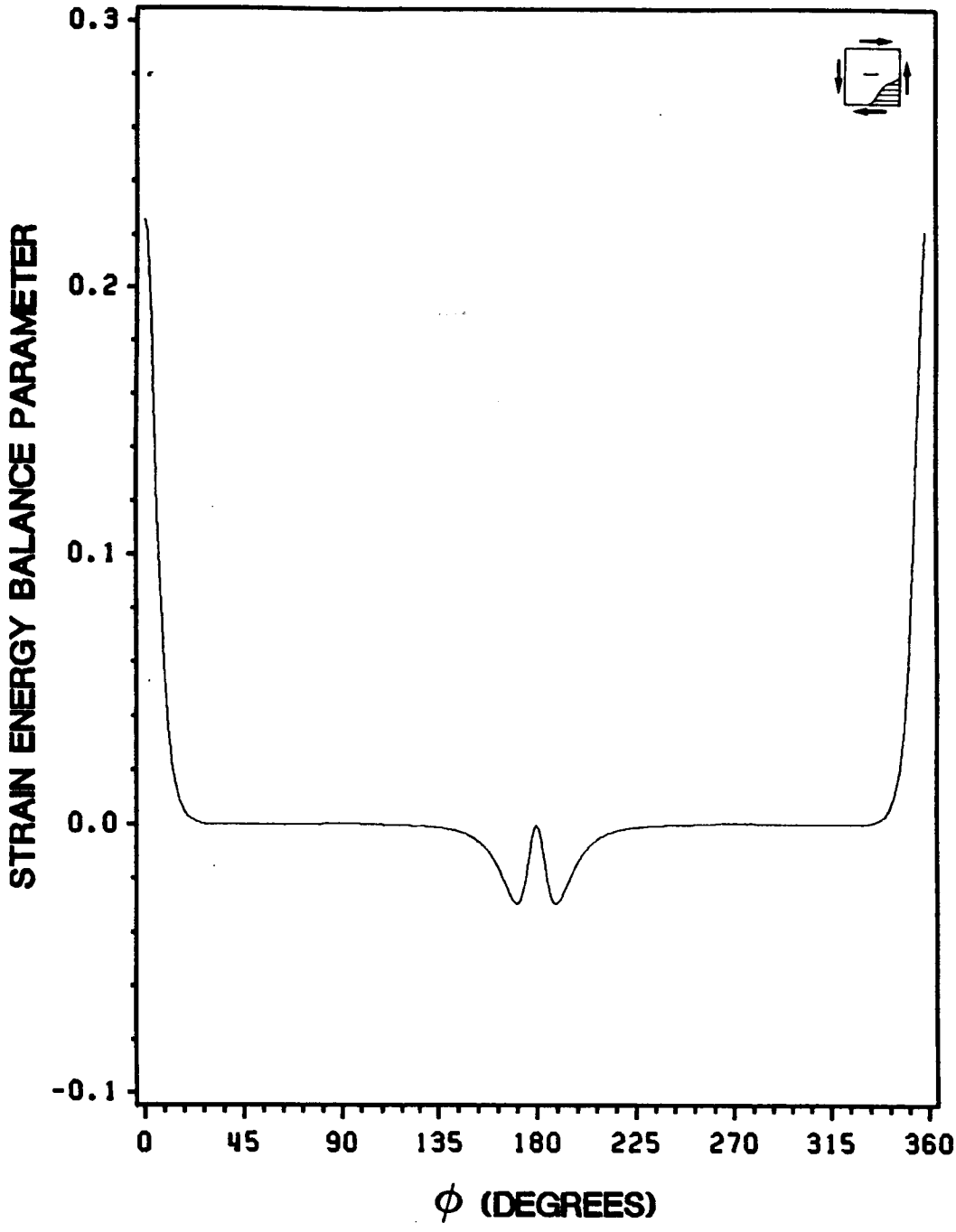

Figure 30. Strain Energy Balance Parameter vs. φ for a Center Crack Along the Fibers Under Pure Shear: See Figure 25

the inclusion of stress components other than the normal stress, as specified by the strain energy balance theory, acts to correct normal stress ratio predictions.

6.4.8.2 Isotropic materials

In isotropic materials, the material normal strength, and thus the resistance to crack extension are not directionally dependent. As a result, from an energy standpoint, only the strain energy acting to drive crack extension acts to control crack extension behavior. For isotropic materials, then, application of the the strain energy balance theory to predict crack growth direction simplifies from evaluating the expression in Eq. 22 to evaluating the parameter

$$(\sigma_{nn}\varepsilon_{nn} + \sigma_{tt}\varepsilon_{tt} + \tau_{nt}\gamma_{nt} - S_{11}\sigma_{tt}^2)\,. \tag{26}$$

Crack extension is predicted to occur in the direction having a maximum of this parameter, when the maximum reaches a critical value. Obviously, then, for predicting crack growth direction in isotropic materials, the strain energy balance theory parameter becomes equal to the strain energy density theory parameter divided by $\frac{r}{2}$, minus the term $S_{11}\sigma_{tt}^2$. While the strain energy balance theory hypothesizes that the direction of crack extension corresponds to a maximum in this parameter, the strain energy density theory hypothesizes that it corresponds to a minimum in the full strain energy density parameter. One critical test of the strain energy balance theory is therefore to determine whether subtraction of the $S_{11}\sigma_{tt}^2$ term acts to change the values of the strain energy density functional as a function of φ so that the correct direction of crack extension corresponds to a maximum, not a minimum in the functional.

In this study, mode I and mode II isotropic fracture problems are investigated using material properties for 6061-T6 aluminum as given in [39]. In analyzing an isotropic material, the Lekhnitskii solution cannot be used. Plugging isotropic material properties into the Lekhnitskii solution stresses (Eq. 14) causes the roots of the characteristic equation, S_1 and S_2, to equal one another. This causes the stresses, each of which are given by equations with the term $(S_1 - S_2)$ in

their denominator, to be divided by zero and thus be invalid. Instead of using these equations, specific isotropic material near-crack-tip stress equations must be used. The equations used in this study were developed by Sneddon [40] and are given by

$$\sigma_{\chi\chi} = \frac{\sigma^{\infty}\sqrt{a}}{\sqrt{2r}}\cos(\frac{\theta}{2})[1 - \sin(\frac{\theta}{2})\sin(\frac{3\theta}{2})] - \frac{\tau^{\infty}\sqrt{a}}{\sqrt{2r}}\sin(\frac{\theta}{2})[2 + \cos(\frac{\theta}{2})\cos(\frac{3\theta}{2})]$$

$$\sigma_{\varepsilon\varepsilon} = \frac{\sigma^{\infty}\sqrt{a}}{\sqrt{2r}}\cos(\frac{\theta}{2})[1 + \sin(\frac{\theta}{2})\sin(\frac{3\theta}{2})] + \frac{\tau^{\infty}\sqrt{a}}{\sqrt{2r}}\cos(\frac{\theta}{2})\sin(\frac{\theta}{2})\cos(\frac{3\theta}{2}) \qquad (27)$$

$$\tau_{\chi\varepsilon} = \frac{\sigma^{\infty}\sqrt{a}}{\sqrt{2r}}\sin(\frac{\theta}{2})\cos(\frac{\theta}{2})\cos(\frac{3\theta}{2}) + \frac{\tau^{\infty}\sqrt{a}}{\sqrt{2r}}\cos(\frac{\theta}{2})[1 - \sin(\frac{\theta}{2})\sin(\frac{3\theta}{2})]$$

Interestingly enough, due to the way in which the particular computer program used to calculate the Lekhnitskii stresses for this study was created, use of isotropic material properties within the Lekhnitskii stress solution results in stress values that are very close to those obtained from the equations above. This is because the complex roots calculated in the program are single precision variables, causing the routine used to calculate them to never yield roots that are exactly equal. The stresses that result in applying the Lekhnitskii solution are for a very mildly anisotropic material and are close to those that result from the equations above. It is also important to note that the stresses given in Eq. 27 are not a function of the isotropic material properties. As a result, the stresses calculated this study for 6061-T6 aluminum are valid for any isotropic material.

Experimentally, for an isotropic material subjected to pure mode I far-field loading, crack extension is collinear with an original notch (along $\varphi = 0°$). Figure 31 provides a plot of the variation of the strain energy density factor as a function of φ for the isotropic material mode I problem. The plot indicates that the strain energy density functional exhibits two minima. The primary minimum occurs at $\varphi = 180°$, corresponding to the crack free surface behind the crack tip. If this minimum is ignored, the strain energy density functional does indeed predict crack extension collinear with the original notch, exhibiting a minimum along the direction $\varphi = 0$. Figure 32 provides a plot of the strain energy balance theory parameter vs. φ for the identical case of isotropic material mode I loading. The magnitude of the y axis values is significantly less than that of the y

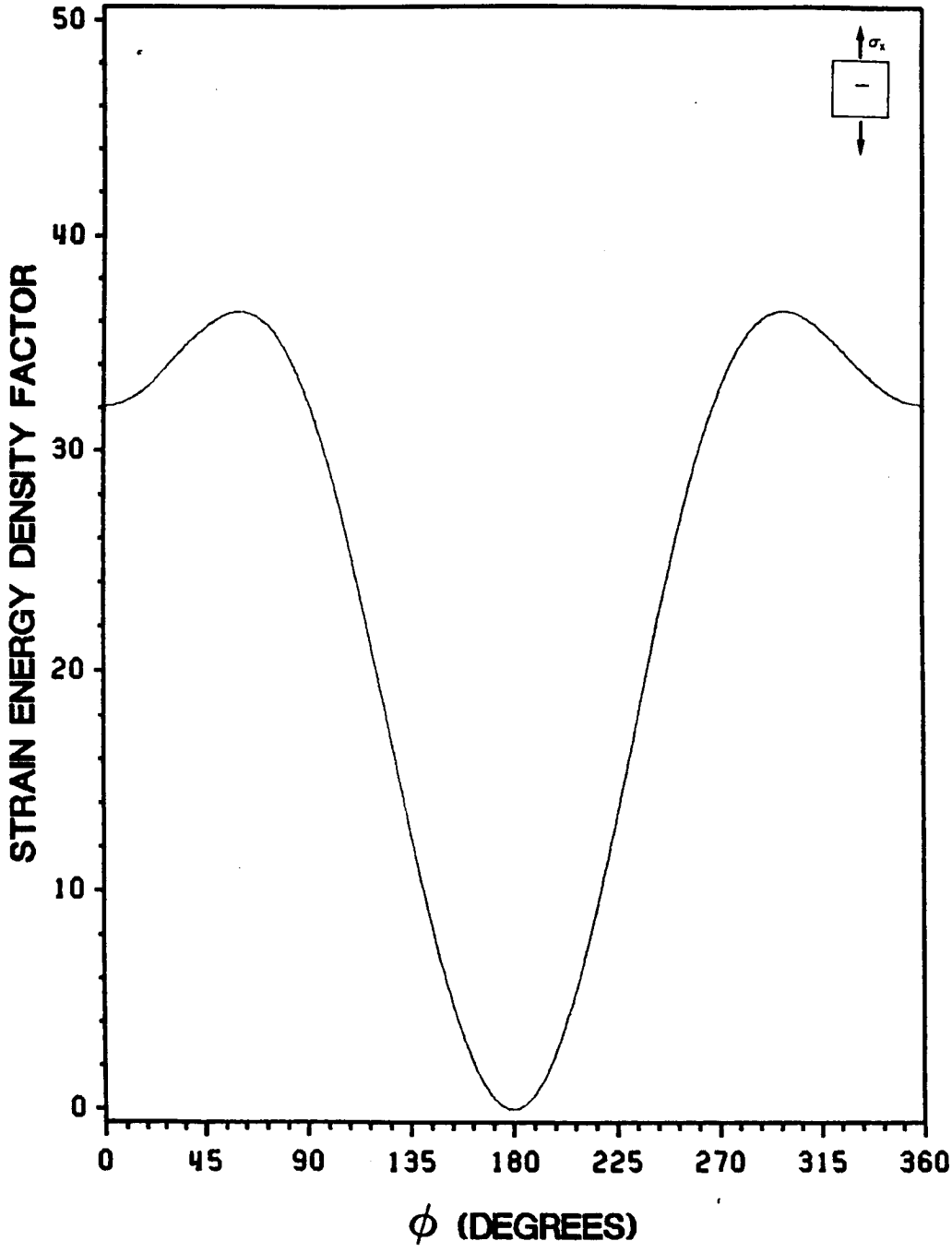

Figure 31. Strain Energy Density Factor vs. φ for Mode I Isotropic Fracture: Center-Notched Infinite Plate of 6061-T6 Aluminum

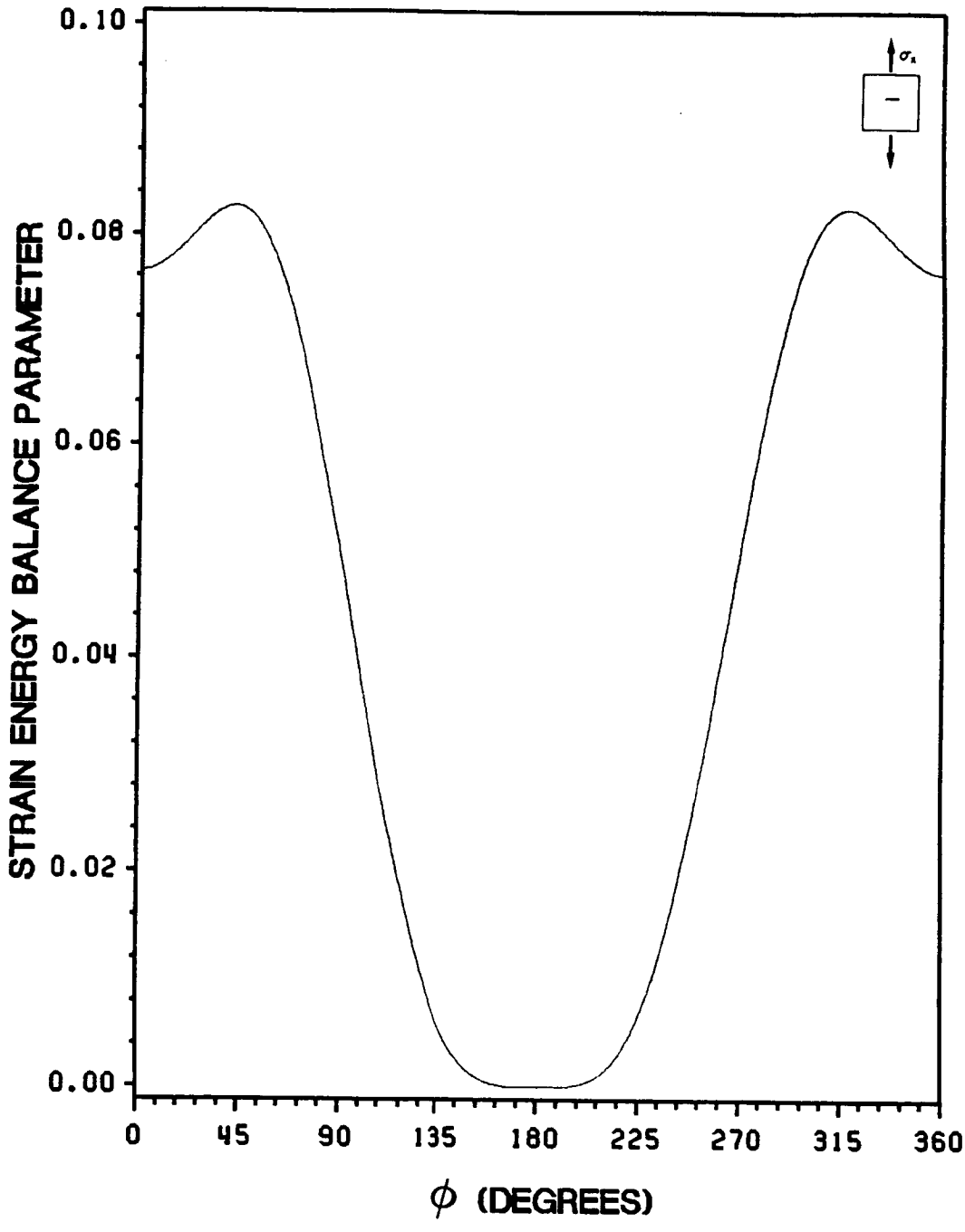

Figure 32. Strain Energy Balance Parameter vs. φ for Mode I Isotropic Fracture: Center-Notched Infinite Plate of 6061-T6 Aluminum

axis values for the strain energy density plot. This is primarily due to the fact that the strain energy balance parameter is divided by the crack growth resistance energy density parameter. The shape of the plot in Figure 32 is very similar to that in Figure 31. In comparison with the strain energy density plot, the strain energy balance parameter plot has its maxima shifted only slightly toward the location $\varphi = 0$. As a result, the strain energy balance theory does not predict crack extension collinear with the original notch for this case.

This application of the strain energy balance theory to the fundamental mode I isotropic material problem, and its comparison with strain energy density theory results suggests that the successes noted in applying the theory to anisotropic materials may not be realizable in its application to isotropic fracture problems. Under entirely different assumptions than the strain energy density theory, the strain energy balance theory hypothesizes that only a portion of the strain energy density expression contributes to crack extension in isotropic materials, and that a maximum, not a minimum of this expression corresponds to the direction of crack extension. For the case of isotropic mode I far-field loading it is clear that there is an inconsistency between the theory's assumptions and its ability to predict known behavior.

Because the strain energy balance theory appears to posses a weakness in analyzing isotropic material fracture problems, it has also been applied in this study to the problem of an isotropic material subjected to pure mode II far-field loading. Experimentally, the exact direction of crack extension is not well defined for this problem. It is known, however, that crack extension does occur in a direction other than collinear with the original notch. The results of the analysis are illustrated in Figure 33, again as a plot of the strain energy balance parameter vs. φ. As with the results from the mode I isotropic material case just detailed, the results for this case are disappointing. The theory clearly predicts crack extension collinear with the original notch, contradicting known isotropic material experimental behavior.

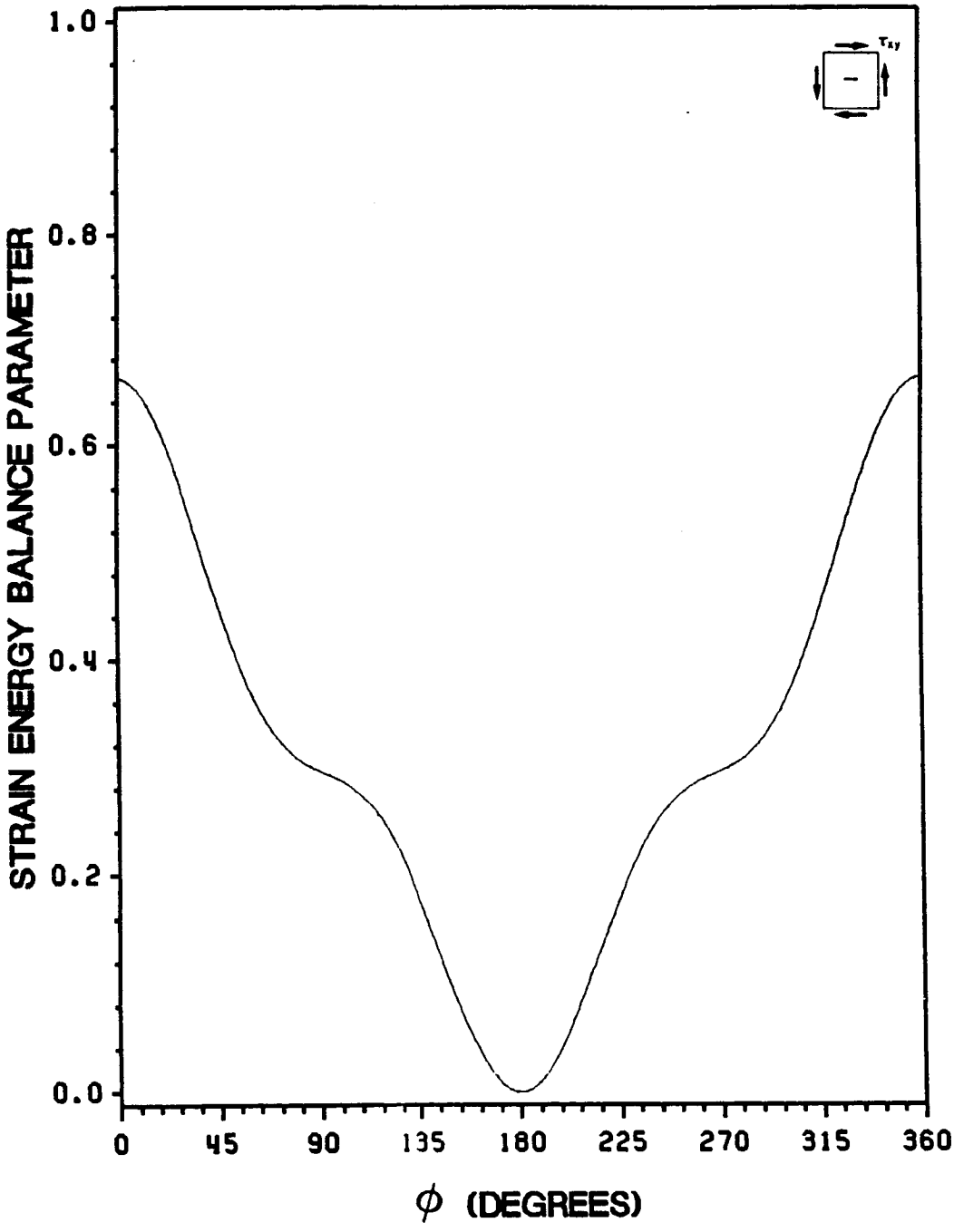

Figure 33. Strain Energy Balance Parameter vs. φ for Mode II Isotropic Fracture: Center-Notched Infinite Plate of 6061-T6 Aluminum

6.4.9 Conclusions

In general, the strain energy balance theory appears to perform well in modelling the behavior of unidirectional graphite-epoxy. Still, though, the theory's application to fundamental isotropic fracture problems has revealed strong inconsistencies in comparison to known experimental behavior. These inconsistencies suggest that the theory itself, though reasonable, is inadequate as an alternative crack extension theory that includes stress components other than the normal stress defined with respect to the crack in its formulation. It is important to note that work by this and other researchers at Virginia Tech, has indicated that, for center-cracked anisotropic materials, the strain energy density functional tends to exhibit a peak near or along the fiber direction. The plot provided in Figure 6 serves as a good example of this. This suggests some relationship between a maximum in the local strain energy per unit volume and the ability to predict crack growth direction. Whether such a relationship truly exists remains to be determined, however.

An energy-based formulation does not represent the only method for the inclusion of shear stress components in a crack growth theory. The alternative is a stress-based approach. In an energy-based approach, the contribution of all stress components are lumped together and compared to a single limiting parameter. In a stress-based approach, individual components are compared to individual strength limits. The theoretical basis for the point-wise application of a stress-based approach is much more sound than that for the point-wise application of an energy-based approach. In an energy-based formulation, energetic quantities should be integrated over the specimen volume, instead of evaluated at discrete points. A stress component exceeding the material strength at a point clearly corresponds to a failure event. On the other hand, the significance of an energy component exceeding an energy limit at a point is not clear. From this standpoint, it appears possible that a correct energy density-based theory cannot be formulated.

Work has previously been performed to formulate a stress-based theory to include shear stress components in the normal stress ratio formulation [41]. The traction ratio theory proposed as a result of this effort also showed some inconsistencies in comparison with experiment. Despite the

problems that have been noted in applying the strain energy balance and traction ratio theories, the issue of the inclusion of shear stress components in a crack extension theory is an important one that must be looked into in attempting to determine what if any parameters control crack extension.

6.5 *Formulation of the Test Matrix*

6.5.1 Test Methods

As previously mentioned, the tests chosen in this study for the experimental verification of normal stress ratio theory predictions are on and off-axis tensile coupon and Iosipescu shear tests. The tensile coupon test was chosen as a standard test, because of its extensive use in composite materials testing. As outlined below, tensile coupon tests do not appear to offer any critical tests of the theory's ability to predict crack extension direction in AS4/3501-6 graphite-epoxy. Use of on-axis and off-axis tensile coupon tests does, however, offer a simple method of testing theory predictions under tensile and combined tensile and shear far-field loading conditions. Also, tensile coupon tests potentially offer a wide range of strength values, unlike Iosipescu or other shear tests. The Iosipescu test was chosen for a number of reasons. First, as outlined in the next section, and as illustrated by the theoretical case detailed in Section 6.2, the normal stress ratio theory appears to predict crack extension other than along the material fibers for some cases of pure shear far-field applied stress. Second, because the normal stress ratio theory does not account for local shear stress or material shear strength, a comparison of its predicted critical stresses with those obtained from tests on specimens subjected to far-field applied shear stress also acts as a critical test of the theory. Determining whether or not the normal stress ratio theory can predict critical stresses in a notched specimen subjected to far-field shear stress provides a strong indication whether or not the ratio of local normal stress to material normal strength acts to control notched composite fracture. Com-

pared with other shear testing methods, the Iosipescu test is relatively simple, thus offering an easy way to test the normal stress ratio theory under nearly pure shear far-field loading conditions.

6.5.2 Critical Direction Prediction Tests

In formulating the test matrix for this study it was desired to include some experiments that can thoroughly test the theory's ability to predict crack extension direction. The kind of experiments that would best do this are those for which a normal stress ratio theory analysis appears to predict crack extension other than along the fibers. If such tests can be identified and performed, their results can yield information either verifying the theory's predictions or perhaps suggesting reasons why the theory apparently provides predictions that are incorrect. Critical crack growth direction tests are identified in this section by applying the normal stress ratio theory to the analysis of tensile coupons and Iosipescu specimens of numerous notch and fiber orientations.

For the notched coupon tests, both fiber and notch orientations are entirely arbitrary. Varying both orientations in 1° increments provides a total of 90 x 180 = 16,200 different fiber and notch orientation combinations that can be analyzed to identify potential critical tests for a single material. Also, for cases where the coupled shear stress exerts a strong influence on the results, the specimen aspect ratio can be varied. As a result, fully analyzing all potential tensile coupon crack extension cases is a highly cumbersome task. Extensive work has been performed in attempting to identify critical cases of predicted crack extension direction in tensile coupons of AS4/3501-6 graphite-epoxy without running every possible test case. This work has failed to identify any critical cases, however. The behavior of the normal stress ratio theory in predicting crack extension behavior in tensile coupons is illustrated in this section by looking at a typical case, a tensile coupon with a horizontal notch and arbitrary off-axis angle. In Figure 34, a plot of predicted direction of crack extension vs. off-axis angle is provided over the entire 0° to 90° off-axis angle range. The plot is very similar to the plot provided in Figure 24, except that in this analysis the shear stress from end constraints is included in the far-field applied stresses. All of the cases analyzed used the

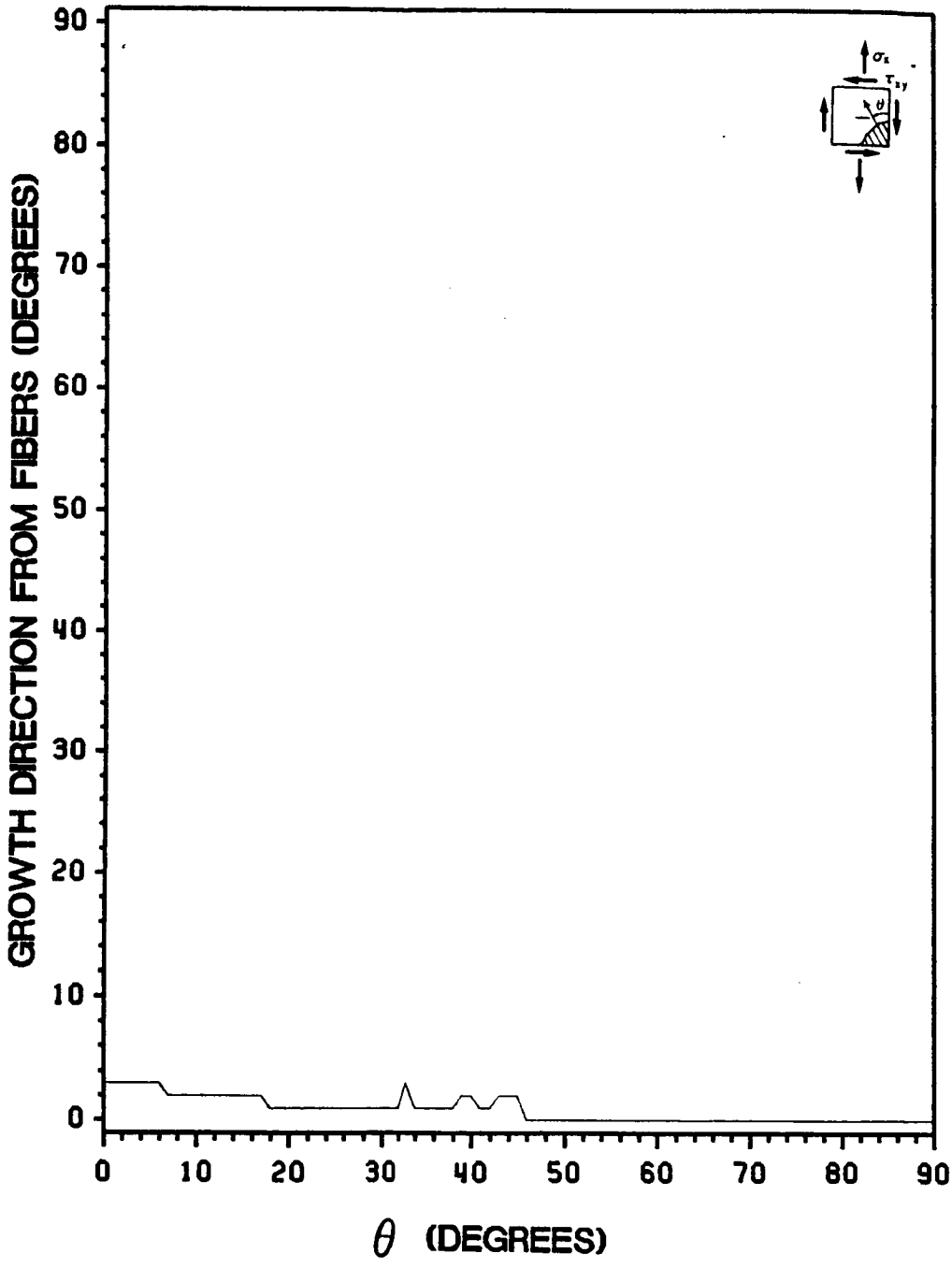

Figure 34. **Normal Stress Ratio Predictions for Center-Notched Tensile Coupons:** Horizontal Center Notches, Crack Growth Direction Predictions vs. Fiber Angle, AS4/3501-6 Graphite-Epoxy, Shear Coupling Effects Included

Pagano and Halpin shear stress value obtained from Eq. 13 for a specimen aspect ratio of 5. As the plot indicates, for graphite-epoxy the normal stress ratio theory predicts crack extension essentially along the fibers for all off-axis angles. In fact, this plot is almost identical to that provided in Figure 24, indicating that normal stress ratio crack extension direction predictions are not strongly affected by shear coupling effects. This agrees with the experiments detailed in [25] which indicate that crack extension direction in graphite-epoxy coupons is not altered by changes in aspect ratio. This behavior is typical of the analysis for all tensile coupon problems with this material. Apparently, in cases dominated by far-field tensile stress, the normal stress ratio works well as a predictor of crack extension direction in AS4/3501-6 graphite-epoxy.

A full analysis of the notched Iosipescu shear test does not present the large number of potential test cases that a full analysis of the notched tensile coupon test does. This is because the shape of the region of relatively uniform shear stress in the Iosipescu shear specimen requires that a notch cut in the specimen test section should be along the vertical axis or close to it. In [30] and [31], Walrath and Adams apply a finite element analysis to the problem that indicates that in AS4/3501-6 graphite-epoxy the area of relatively uniform shear stress in the test section is roughly elliptically shaped, with the major axis along the vertical direction. In performing a crack extension test using such a specimen, the cut notch should be within this region, thus constraining the notch orientation to being close to or along the vertical. Because of this constraint, the Iosipescu test can be analyzed as a crack test by looking at only 180 cases, using a vertical crack orientation and varying the fiber orientation in 1° increments over 180°. Figure 35 provides a plot of the results of such an analysis, similar to the plot provided in Figure 34. The plot indicates that, unlike the tensile coupon test, the Iosipescu shear test does appear to provide potential critical tests of the normal stress ratio theory. As indicated in the plot, for pure shear loading and fiber angles roughly between 85° and 110° there is a strong peak in the predicted angle of crack extension away from the fibers. Within this peak area, the maximum value of predicted direction of crack extension away from the fibers is 24°, occurring for a fiber angle of 97°. Thus, with respect crack extension direction predictions of the normal stress ratio theory, it appears that Iosipescu tests on specimens with fiber angles between 85° and 110° may offer critical theory tests.

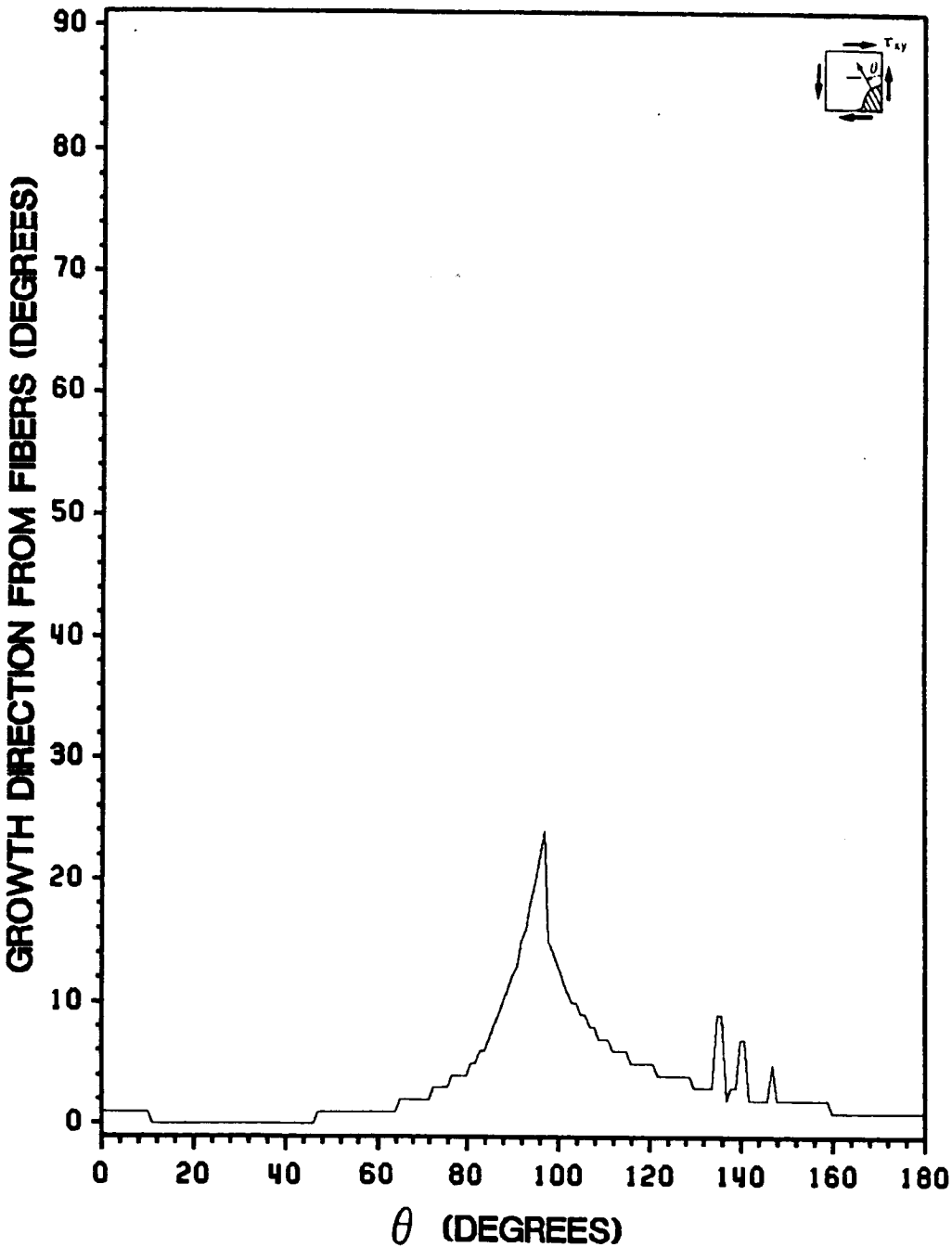

Figure 35. Normal Stress Ratio Predictions for Iosipescu Shear Specimens with Vertical Notches: Crack Growth Direction Predictions vs. Fiber Angle, Pure Shear Far-Field Loading, AS4/3501-6 Graphite-Epoxy

As illustrated in Figure 35, other peaks in normal stress ratio crack direction predictions occur close to fiber angle values of 135°, 140°, and 147°. From this single plot, it appears that these sharp peaks could designate possible critical direction prediction tests for the normal stress ratio theory. Comparison with similar plots for other types of specimens suggests, however, that these and other sharp peaks in normal stress ratio predictions are the consequence of something other than the application of the theory itself. The issue of the source of such peaks is more thoroughly investigated and discussed in Section 8.2.6. For the sake of identifying critical tests of the normal stress ratio theory, the three sharp peaks in Figure 35 are not highly important regardless of their source. This is for two reasons. First, the magnitudes of the peaks, which are 9°, 7°, and 5° are significantly smaller that the magnitude of the principal peak in the plot occurring at 97° Second, the peaks at 135°, 140°, and 147° are highly sensitive to changes in fiber orientation. Experimentally, a small error in notch and/or fiber orientation could result in a peak being "missed."

The requirement that the cut notch be oriented along the vertical direction in a notched Iosipescu specimen is not strict. As long as the notch is oriented close to the vertical, it should still be within the region of relatively uniform shear stress in the Iosipescu specimen. This fact, coupled with the fact that the critical tests identified in the above analysis all have fiber orientations that are close to the vertical axis has provided motivation for a supplementary analysis of the notched Iosipescu specimen. In this analysis, the crack is always oriented along the fiber direction, with the fiber direction varied over a $\pm 30°$ range around the vertical axis. The results of the analysis are plotted in Figure 36. This series of cases appears to offer even more critical tests of the normal stress ratio theory, with a maximum predicted direction of crack extension away from the fibers of 46°, occurring at a fiber and notch angle of 102°. These tests also offer an added experimental option. Because the crack is along the fiber direction, these specimens can be fatigue pre-cracked before shear testing is done in order to obtain sharp crack tips. In this way, the issue of the influence of notch tip sharpness, which is addressed in another portion of this section, can be investigated experimentally.

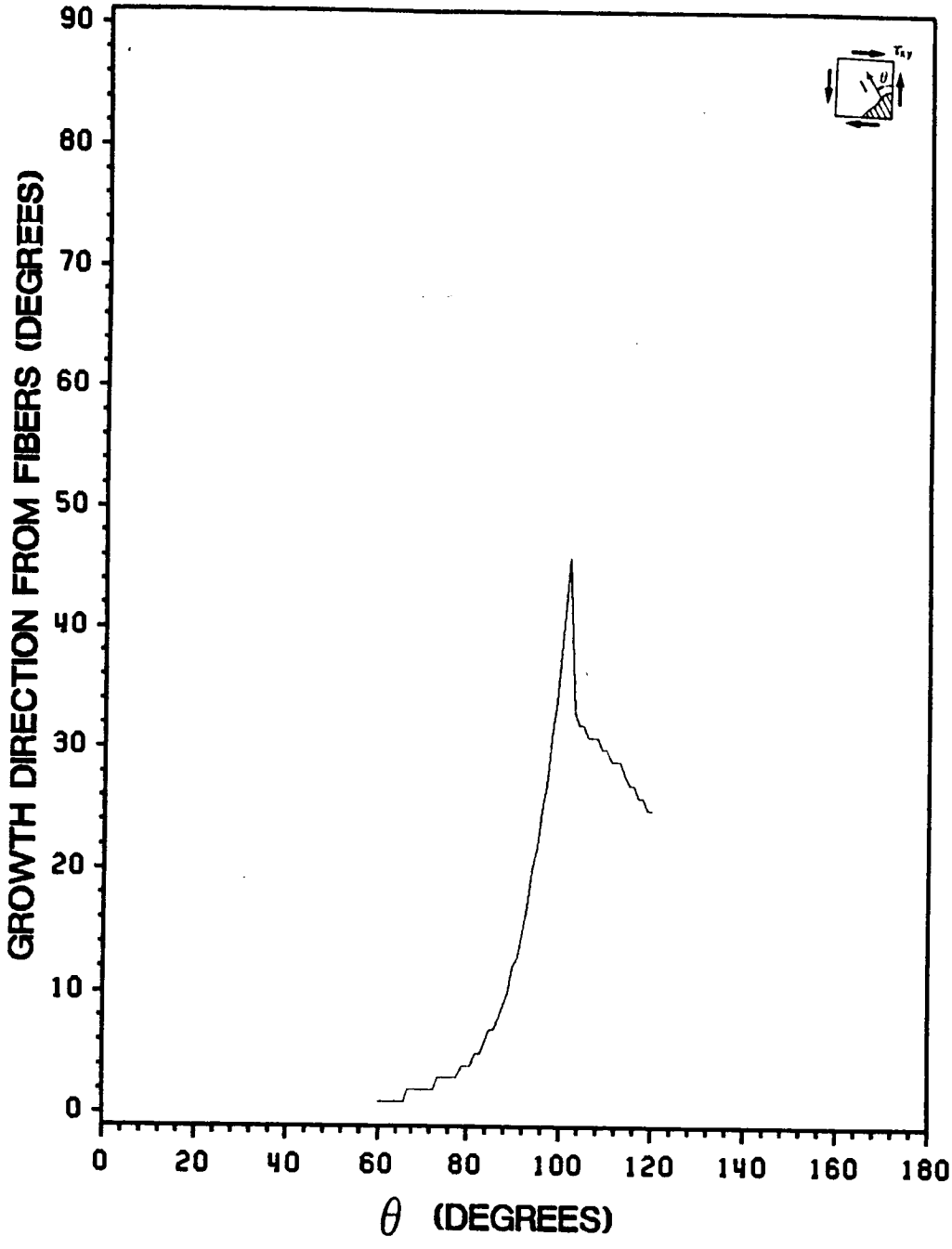

Figure 36. Normal Stress Ratio Predictions for Iosipescu Shear Specimens with Notches Along the Fibers: Crack Growth Direction Predictions vs. Fiber Angle, Pure Shear Far-Field Loading, AS4/3501-6 Graphite-Epoxy

6.5.3 Standard Tests

In addition to the critical direction prediction tests just outlined, a series of standard tests are included in the test matrix for this study. These tests are designated as standard because they do not appear to offer a critical test of the normal stress ratio theory's ability to predict crack extension direction. If properly chosen, however, they can offer an opportunity to test the theory as a predictor of critical stresses. This can best be accomplished by including notched tests on specimens having a broad range of unnotched strengths. Clearly, tests on tensile coupons of various off-axis angles including 0° and 90° specimens offer the best opportunity to do this.

The inclusion of these standard tests of the theory is important because it has already been observed in the preliminary Iosipescu tests that specimens with 90° fiber orientations fail at low applied shear stresses, due to normal stress concentrations and specimen weakness perpendicular to the fibers. Because all of the critical crack growth tests suggested by the plots in Figure 35 and Figure 36 have fiber orientations close to 90°, the problem of premature failure may make such tests difficult or impossible to perform. The critical parameter determining the workability of such tests is whether the stress concentration caused by the cut notch is great enough to cause a given specimen to experience crack extension before stress concentrations caused by the fixture cause it to fail. Because of this potential problem, the test matrix contains not only these potential critical direction Iosipescu tests, but also some Iosipescu tests to be used as tests of normal stress ratio critical stress predictions. These tests will not necessarily offer the range of critical stress values that tensile coupon tests can, but they will offer an opportunity to test the theory under far-field applied shear stress conditions. As pointed out previously, this is important in testing the theory, which is based entirely on local normal stress and normal strength.

7.0 Notched Specimen Experiments

7.1 Specimen Dimensions and Configurations

The test matrix used for this study contained tests for achieving two purposes. The first group of specimens was designed to test the normal stress ratio theory in general, as a predictor of crack extension direction and as a predictor of critical applied stresses. It was desirable to include specimens subjected to various ratios of far-field stress components and specimens that would experience a wide range of critical far-field stress values. These specimens provided the bulk of the experimental data acquired for this study. The second group of tests was designed specifically to test the ability of the normal stress ratio theory to predict crack extension direction. These tests were chosen on the basis of the analytical work detailed in the previous section. It was recognized that the tests suggested by the analysis may not be workable using the Iosipescu shear test. As a result, these tests were not heavily relied upon for results.

7.1.1 Standard Tests

The first group of standard tests chosen to be performed in this study were actually performed as part of a previous research effort, the results of which are published in [25]. These tests, illustrated in Figure 5, were on 15° off-axis tensile coupons having aspect ratios of 1, 4, and 8. Specimen dimensions are provided in Section 2.1.2. A total of twelve specimens were tested, two of each notch orientation/aspect ratio configuration. Each specimen was strain gaged, however the data from the gages was not used in this study. Also, a crack opening displacement gage, used in the other tests for this study, was not used in these tests.

Other tensile coupon tests chosen as standard tests in this study were center-notched 0°, 45° off-axis and 90° tests. All of these specimens had horizontal (90°) notch orientations and an aspect ratio of 5. This choice of aspect ratio value was based upon work by Nemeth, Herakovich, and Post in analyzing off-axis tensile coupons [42] In their study, they compare results from the aforementioned analytical solution of Pagano and Halpin [28] and a finite element model to moire′ results from tests on 15° off-axis coupons having aspect ratios of 5 and 15. They conclude that centerline displacements predicted by the analytical and numerical solution approaches agreed well with those obtained experimentally for specimens of both aspect ratios. This conclusion provides reasonable assurance that the application of the Pagano and Halpin solution to determine far-field applied stresses in notched off-axis coupons is accurate for specimens having aspect ratios as small as 5. As a result, all coupon tests for this study were chosen to have an aspect ratio of 5. As with the 15° off-axis specimens, each of these specimens had a total width of 1.0 inch.

The tensile coupon tests specified include far-field applied stresses of pure tension (0° and 90° tests), and combined tension and shear (15° and 45° tests). The amount of applied shear stress for 45° off-axis coupons is small because of the small influence of shear coupling effects in them. The amount of applied far-field shear stress for 15° off-axis coupons can be significant, however. Thus the entire group of tests allows both mode I and mixed-mode far-field loading conditions. By

specifying that both 0° and 90° coupon tests be run along with off-axis tests, the full range of potential critical stresses can be obtained.

In addition to the tensile coupon tests specified above, a series of standard Iosipescu tests were performed for this study. Iosipescu specimen dimensions are provided given in Section 4.2 and illustrated in Figure 20. Each specimen had a center notch cut in it, oriented along the vertical axis (at 90°). It was important that these tests be workable, because, as noted in the previous section, the critical direction prediction Iosipescu tests might not be. Thus, the specimens chosen for standard notched Iosipescu tests had fiber orientations along or close to the horizontal, at angles of 0°, 15°, 30°, and 45°. Even within this group it was realized that the 45° test might not be workable because of its weakness along the horizontal direction. Also, judging from unnotched strengths, this group of specimens is not likely to provide a broad range of critical stress values. In order to minimize error in obtaining subtle experimental critical stress trends, these experiments have to be done carefully.

7.1.2 Direction Prediction Tests

The tests proposed to specifically test the ability of the normal stress ratio to predict crack growth direction are summarized in Table 4. As the table indicates, two types of Iosipescu tests are proposed, those having a vertical notch and those having a notch along the fiber direction. For each type of test, specimens having fiber orientations from 85° to 110° are specified in 5° increments. The 90° tests of each specimen type are identical and also correspond to the critical test case illustrated in Figure 25. Table 4 also provides predicted directions of crack extension away from the fibers. The 100° specimen with it's notch along the fiber direction presents itself as the most critical test of the analysis. The dimensions for these specimens were identical to those used for all other Iosipescu specimens tested for this study.

Table 4. Direction Prediction Tests

Predicted Angles of Crack Extension
Normal Stress Ratio Theory
Potential Critical Iosipescu Shear Tests

Specimen Fiber Orientation (θ)	Predicted Angle of Crack Extension Away from Fibers
Specimens with Vertical Notches	
85°	7°
90°	12°
95°	20°
100°	13°
105°	9°
110°	7°
Specimens with Notches Along the Fibers	
85°	7°
90°	12°
95°	22°
100°	38°
105°	32°
110°	30°

7.1.3 All Tests

As is outlined in the section on experimental results, the 15° off-axis tests did not experience crack initiation from both notch tips at exactly the same time. The realization that each notch tip can have its own unique crack initiation stress led to a change in the way that subsequent tests were run. Smaller 0.100 in. length notches were used in the 0°, 45°, and 90° tensile coupon and all Iosipescu tests to allow both notch tips to be viewed at once during testing. The 0.100 in. notch length was chosen as the best notch size to allow simultaneous viewing of both notch tips, a magnification high enough to observe crack extension behavior, and a reasonable ratio of notch length to notch width (20 to 1). By viewing both notch tips during testing, it was possible to obtain two

values for the stress causing crack initiation, one for each notch tip. It is also pointed out in the section on experimental results that the critical stress values obtained from the tests on 15° off-axis specimens were not always consistent. This, coupled with the fact that only two tests were performed for each specimen type made obtaining subtle trends in the critical stresses difficult, if not impossible. Because of this, all subsequent experimental work included at least three tests on each specimen type and, depending on the difficulty in obtaining critical stress values, sometimes more.

The tests on 15° off-axis specimens also pointed out the need to have some method of monitoring the specimen behavior near the notch. Strain gages used in such tests offered little information concerning the specimen's crack extension behavior. In order to address this need, in all subsequent tests, a crack opening displacement (c.o.d.) gage was used during testing (Figure 37). In order to use the gage, a 0.037 in. diameter hole had to be drilled in the center of each cut notch. This allowed two semicircular prongs on the front of the gage to be inserted. Crack opening displacement was measured as a change of resistance in strain gages mounted on the back of the c.o.d. gage. The c.o.d. gage was calibrated by adjusting amplifier gain and excitation voltage so that a displacement of 0.0040 inches resulted in an amplifier output of 1.000 volts. This conversion factor was used by the computer data acquisition software to provide crack opening displacement data in inches during testing. In all of the tests in this study, the crack opening displacement gage was oriented so that it opened perpendicular to the cut notch, measuring the cut notch opening displacement. In addition to providing a method of measuring notch opening, it was hoped that data from the gage might provide a method other than visual monitoring for determining the onset of crack initiation during a test.

7.2 Experimental Procedures

A series of experimental procedures were developed specifically for this study by its author. The pre-testing procedure was designed to minimize the influence of extraneous experimental pa-

Figure 37. Crack Opening Displacement Gage Used in Notched Specimen Experiments

rameters such as slight variations in flaw size and specimen moisture content on test results. The testing procedure was developed in order to allow the most complete observation and record of crack growth events and test data possible. Specifically, a computerized data acquisition system coupled with a system for microscopic monitoring, videotaping, and photography of crack growth events was used to accomplish these tasks. The purpose of the post-testing procedure was to review recorded test data and crack growth events and to obtain stresses at crack initiation for those specimens exhibiting stable crack extension before fracture.

7.2.1 Pre-Testing Procedure

A four-step procedure was followed before the testing of each notched specimen in order to increase test data accuracy. The first step was to measure specimen notch length, width, and orientation and note any deviance from expected values. In particular, the total notch length, which varied slightly from specimen to specimen, needed to be measured and accounted for because of the theoretical proportional relationship between the square root of a crack's length and its near-crack-tip stress field intensity. After testing, measured notch lengths were used to normalize crack initiation stresses so that results from all specimens represented a notch length of 0.100 in. The second step taken before testing was to x-ray the notched area of each specimen for possible damage imparted to the material from the notch cutting operation. As mentioned in the section on experimental procedures, an x-ray opaque zinc iodide-based penetrant was allowed to soak into the notched area of each specimen overnight before x-raying. Typical x-ray radiographs for the specimens are provided in Figure 38. As outlined in [25], some of the 15° off-axis specimens did exhibit damage in their cut notch regions before testing. Of the specimens tested, though, only one had any damage near its notch tip and it provided consistent results. Near-notch damage was not a problem at all for subsequent tests performed for this study. X-ray radiographs of all subsequent specimens appeared as those illustrated in Figure 38, exhibiting no near-notch damage.

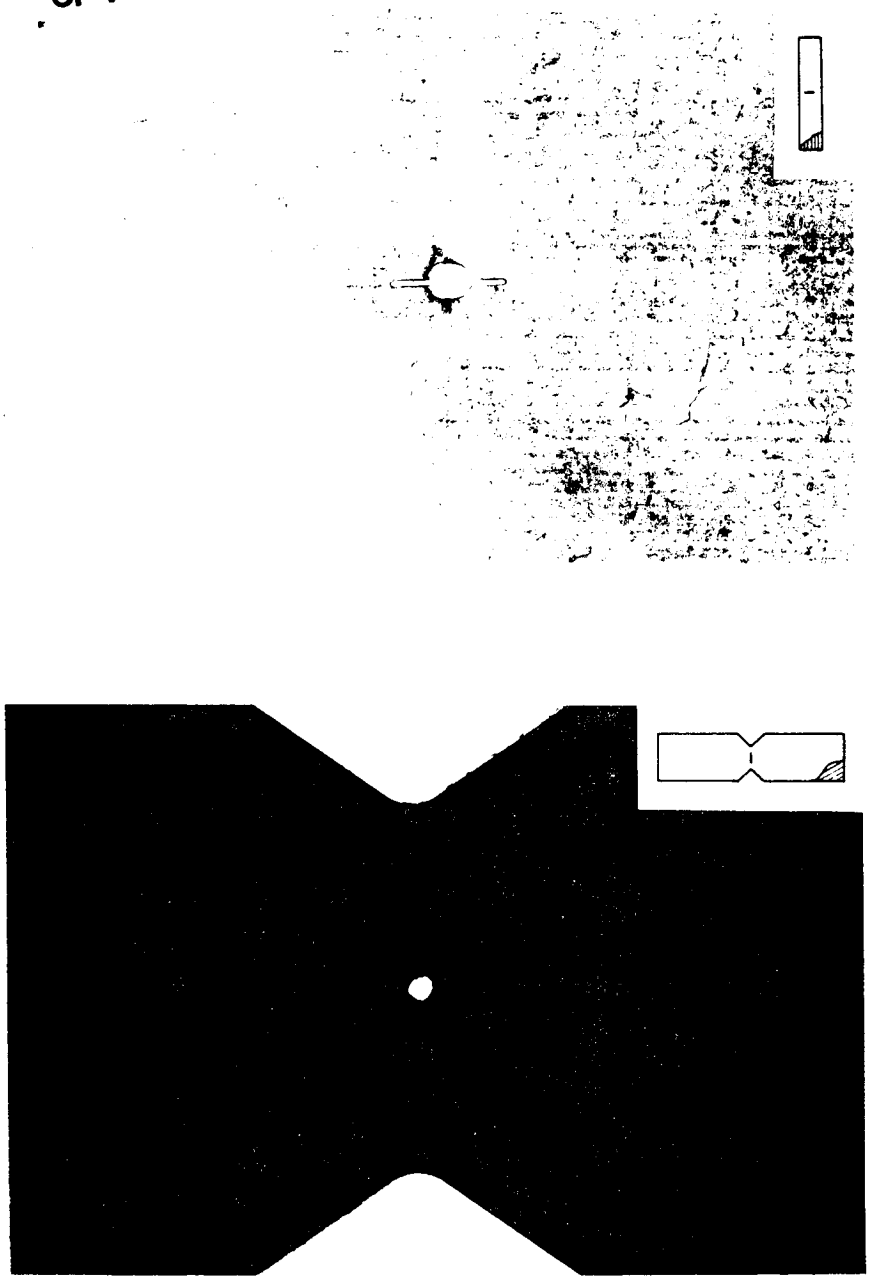

Figure 38. X-ray Radiographs

The third step taken before testing was to polish the specimen surface near its notched area. This was done only to some specimens, in an attempt to determine if polishing could aid in the visual observation of notch growth. The goal of polishing was to eliminate the cloth-type pattern that existed on unpolished specimen surfaces. This pattern came from the bleeder cloth pressed against the material during curing. This cloth pattern was a hinderance in observing small, thin cracks. Unfortunately, however, surface polishing proved to be of limited use. Although it eliminated the cloth pattern, it also acted to highlight the line pattern of the material fibers. Because crack extension occurred along the fiber direction, the fiber line pattern tended to interfere with the observation of extended cracks. Polishing also tended to increase light reflection from the specimen surface. This caused some problems with the intense lighting needed to observe notch tip areas microscopically. The final step taken before testing was the aforementioned drying procedure used for all specimens tested in this study. It was important that this step be taken after x-raying and polishing, both of which required washing of the specimen in water.

7.2.2 Testing Procedure

The testing procedure used for the 15° off-axis specimens consisted of observing the notched areas of each specimen through a microscope as the specimen was loaded in a slow, incremental manner. Careful notes were taken at each stop and the time of observed crack initiation was recorded during the test. Photographs could also be taken to record crack growth events. This method was adequate in determining crack initiation stresses for these tests, but it was highly cumbersome and time consuming to run each test slow enough to obtain a written record of all crack growth events. The need was recognized for a method that would provide a permanent, continuous record of all crack growth events for review after testing. This was especially important if a number of tests exhibiting highly varied crack extension behavior were to be performed.

During all subsequent experiments, a pre-determined procedure was followed to ensure that accurate crack initiation stress values could be obtained, along with a complete videotape and

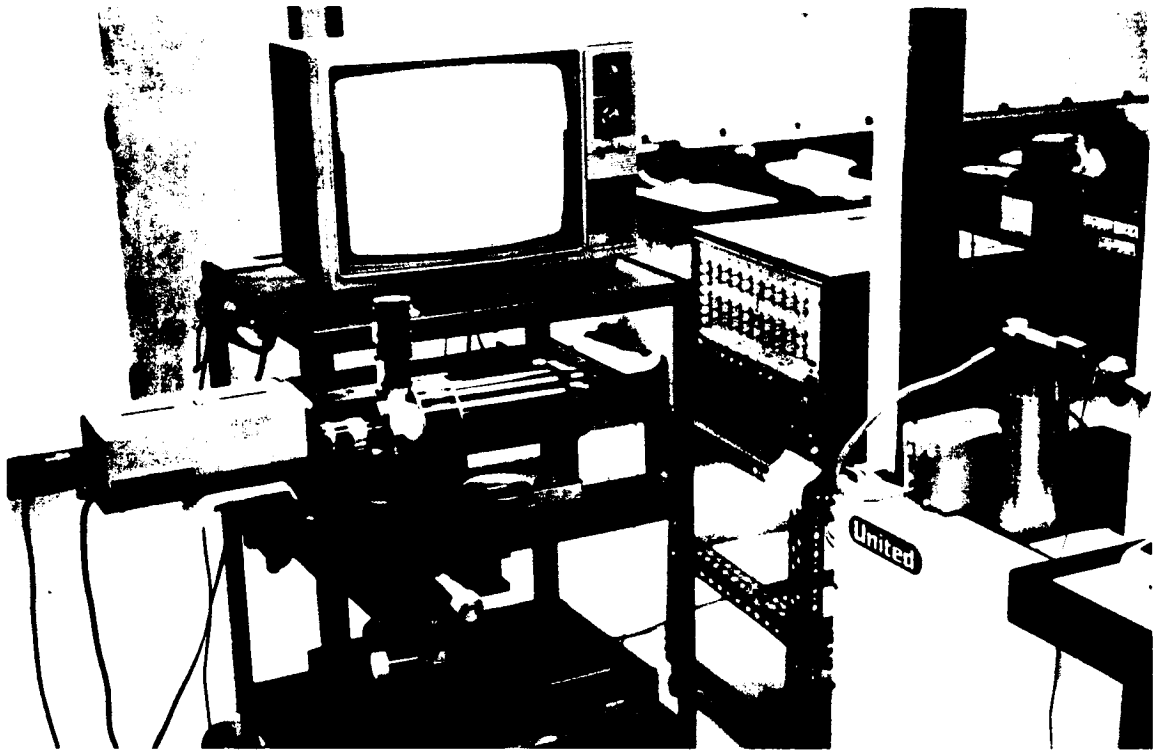

Figure 39. Videotape/Camera/Microscope Set-Up Used to Record Crack Growth Events in Notched Specimen Experiments

photographic record of specimen crack growth behavior. This procedure also had to include a method for linking videotaped events and computer data so that crack growth behavior could be correlated with a particular applied far-field stress. A photograph of the videotape/camera/microscope set-up used is provided in Figure 39. The equipment used included a Questar model QM-1 long distance microscope, a Nikon model FM-2 35mm camera, a Sony model AVF-3200 video camera, a Sony model VO-2611 video recorder, and a Videotek model RM-198 video monitor. As shown in Figure 39, the video camera was mounted on the back of the microscope. The 35mm camera was mounted on top of the microscope but it is not shown in the figure. Microscope magnification could be changed by inserting one of three lenses inbetween one of the cameras and the microscope, and by changing the distance between the microscope and the specimen. Also, for any given magnification level, a lever on the microscope allowed the 35mm camera magnification to be increased by approximately 60%. The microscope was specifically designed for testing type applications, having the ability to focus on a specimen from a distance of approximately 2 to 5 feet. This eliminated possible vibrations and failure events from disrupting visual monitoring. The design of the microscope required that a lever be flipped and the microscope re-focussed when switching from the video camera to the 35mm camera. This required that the test be stopped in order to take 35mm photographs.

Each crack growth test was run by first setting up the microscope/camera equipment to monitor the test on videotape. As illustrated in Figure 39, this allowed the specimen notched area to be displayed on the video monitor during testing. The microscope magnification was set to allow the entire notch to be visible on the screen. In addition to monitoring and storing test events visually, the tests were also monitored on the audio portion of the videotape, by placing a microphone next to the specimen and turning the videotape machine audio input level control to maximum. This allowed not only a record of possible audible cracking, but also a record of when the testing machine motor was running and applying a displacement to the specimen ends, and when it was off, holding the displacement. This was important because the computer data acquisition software also kept a record of what time during the test crosshead displacement was stopped. By making

frequent stops during each test, the time of a test event recorded on videotape could be correlated very accurately with computer data.

Tests were begun by manually starting the videotape machine at the same time that the computer began crosshead displacement. The sound that the testing machine motor made as it displaced the crosshead was audible on the videotape, thus providing a record of the starting time of the test. The computer also started timing the test as soon as it initiated crosshead displacement. As displacement was applied to the specimen, its notched area was observed on the video monitor. As soon as any possible crack growth event was observed on the monitor, crosshead displacement was stopped by pressing a single key on the computer. The stopping of the testing machine motor was audibly recorded on the videotape. The computer software recorded the stop by halting data acquisition and resetting the test time to zero. If no photographs were desired at this point in the test, crosshead displacement was restarted by pressing a key on the computer. If photographs were desired, the first step taken was to pause the videotape machine. On video playback, the pausing action was noticeable, thus providing a record of when photographs were taken. The next step was to rotate the lever on the microscope to enable viewing of the specimen through the 35mm camera. The microscope was then re-focussed and photographs were taken. The test was re-started after rotating the lever on the microscope, re-focussing the image on the video monitor, and re-starting the videotape. This incremental testing procedure was continued until specimen failure.

7.2.3 Post-Testing Procedure

The essential tasks to perform after testing were to acquire critical stress values and crack opening displacement data, and to review observed crack extension behavior. In reviewing crack growth behavior, notes taken during testing were compared with videotape replays and revised if necessary to note important crack growth events. The failure stress and crack opening displacement data were stored by the computer and easily retrieved. Applied stresses at crack initiation were acquired by first listing the times recorded on the computer as to when crosshead displacement was

halted. The videotape was then reviewed to determine during which displacement step crack initiation was observed at each notch tip. A stopwatch was then used during videotape playback to determine the time within the given displacement step when crack initiation began. This time value was then used to obtain the corresponding applied stress from in the computer data file. In this way, the applied stress at the time of any observed cracking event could be accurately obtained. The use of both audio and video test monitoring proved highly successful in obtaining accurate applied stress values. The final step taken after testing was to normalize all crack initiation stress values with the square root of the notch length measured before testing. Crack initiation stress values were normalized to represent a total notch length of 0.100 inches. As a result, crack initiation stresses were normalized using the equation

$$Initiation\ Stress = \{Experimental\ Value\} \sqrt{\frac{2a_m}{0.100}}, \tag{28}$$

where $2a_m$ is the measured total notch length.

7.3 *Tensile Coupon Test Results*

7.3.1 Fifteen Degree Off-Axis Tests

In all of the 15° off-axis notched coupon tests detailed in [25], crack extension occurred along the fiber direction, with cracks extending from the cut notch toward the nearest specimen free edge. This yielded experimental values of φ_c = -75° for the coupons with 90° notches and φ_c = -90° for the coupons with 105° notches. Figure 40 provides a photograph of the specimens after fracture. As detailed in [25] most of the specimens experienced stable crack extension before fracture. Only two of the twelve specimens tested experienced unstable crack growth. Figure 41 provides typical photographs of crack extension occurring during testing. Cracks appeared as dark lines extending

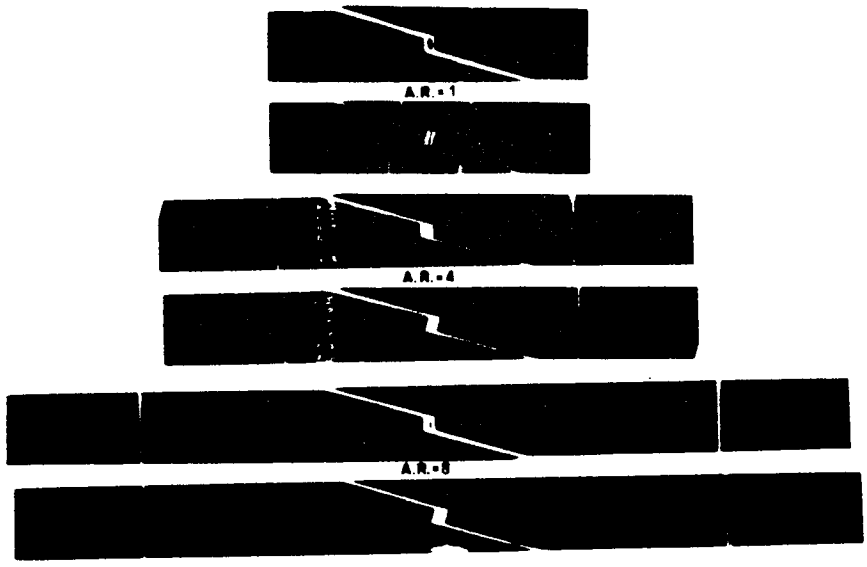

Figure 40. Fractured 15° Off-Axis Tensile Coupons

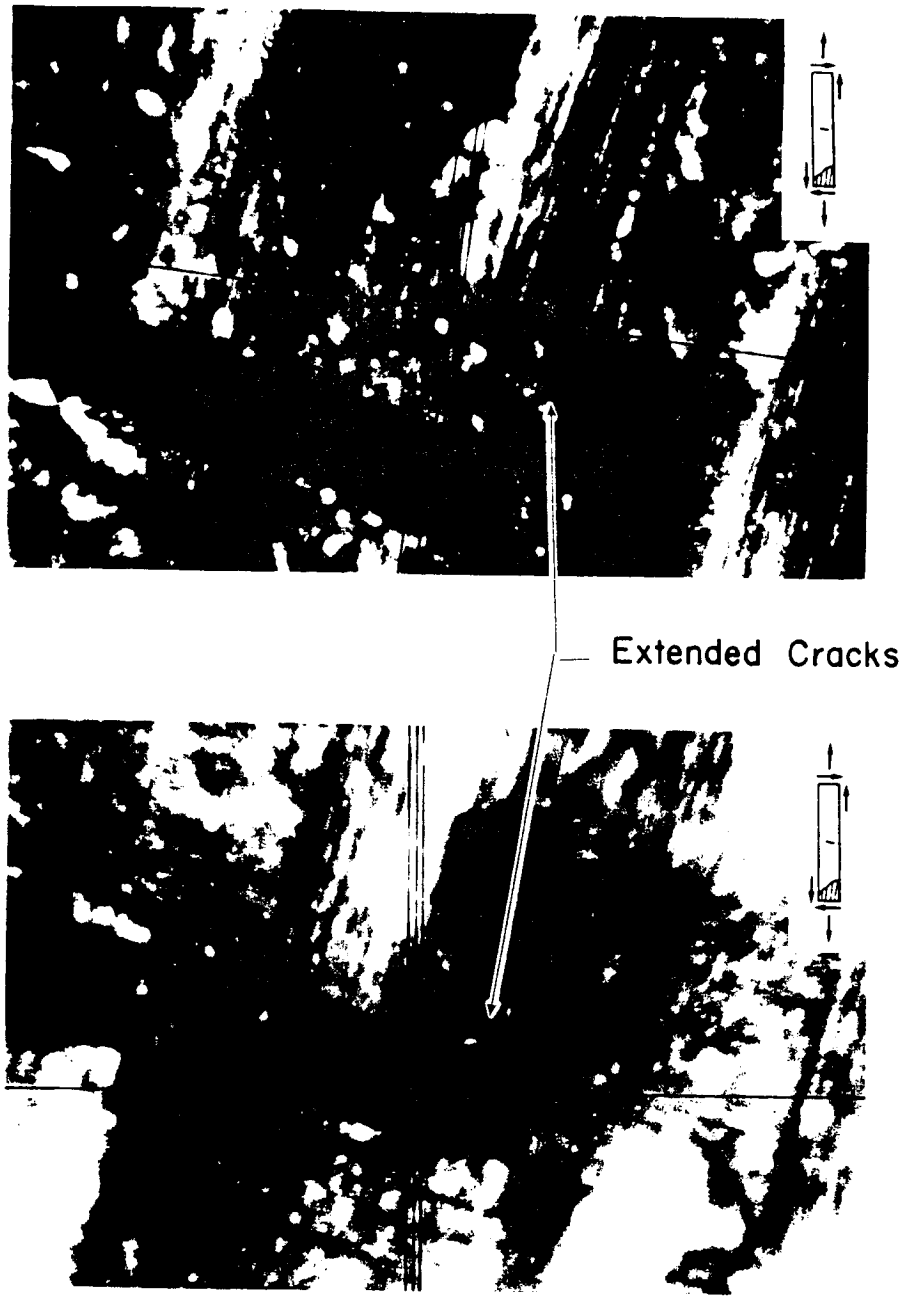

Figure 41. Microscopic Photographs of Crack Extension in 15° Off-Axis Tensile Coupons

from the cut notch. As with the stability behavior of the specimens, the location of crack extension along the cut notch boundary varied in the tests. In some specimens, cracks initiated form the tip of the notch. In other specimens, cracks clearly initiated away from the tip, near the point of tangency between the straight and semicircular notch tip regions. These two cases, each illustrated in Figure 41, represent extremes in behavior, with other specimens experiencing crack initiation at these locations and inbetween them. Crack initiation typically did not occur simultaneously at the two notch tips, although at this point in the research only the stress causing crack initiation at the first notch tip was obtained. After initiation, crack extension became roughly symmetric as extended crack lengths increased. Because the crack opening displacement gage was not used for these tests, the opening of the original cut notch was not monitored. In the specimens experiencing stable crack extension, however, it was clearly observed that extended cracks opened significantly during the tests. It was also observed that cracks in these specimens extended in a sporadic manner. As displacement was steadily applied to the specimen, cracks extended in jumps. For other specimen types tested for this study that experienced slow crack extension, this sporadic crack extension behavior was not clearly observed.

Table 5 provides a summary of the critical stresses obtained from the 15° off-axis tests. A number of characteristics of the results are important to note. First, some of the critical stress values obtained for specimens of the same type indicated scatter in the results. For the stresses causing crack initiation, the specimens with 90° notches and aspect ratios of 4 and 8 exhibited scatter. For the stresses causing fracture, the specimens with a 105° notch and aspect ratio of 1 and a 90° notch and aspect ratio of 4 exhibited scatter. As a group, however, the specimens with 105° notches provided highly consistent crack initiation stresses.

For these tests, the possibility exists for trends to be exhibited with respect to two test parameters, aspect ratio and notch orientation. Neither the crack initiation or fracture stresses exhibited any trends with respect to aspect ratio. Also, the fracture stresses did not indicate any apparent trend with respect to notch orientation. Crack orientation does appear, however, to correspond to a trend in the stresses causing crack initiation. From the table, it is apparent that the

Table 5. Fifteen Degree Off-Axis Tests

Comparison of Theoretical and Experimental
Critical Stresses
Fifteen Degree Off-Axis Tests

Specimen Number	Axial Stress at Initial Crack Extension ksi (MPa)	Averages ksi (MPa)	Axial Stress at Fracture ksi (MPa)	Averages ksi (MPa)	Predicted Critical Axial Stress ksi (MPa)
			90° Notch A.R. = 1		
1	8.49 (58.5)		8.49 (58.5)		
2	7.55 (52.1)	**8.02 (55.3)**	8.79 (60.6)	**8.64 (59.6)**	**12.2 (84.1)**
			105° Notch A.R. = 1		
1	7.88 (54.3)		11.7 (80.7)		
2	7.55 (52.1)	**7.72 (53.2)**	8.42 (58.1)	**10.0 (68.9)**	**10.3 (71.0)**
			90° Notch A.R. = 4		
1	10.1 (69.6)		12.8 (88.3)		
2	7.70 (53.1)	**8.91 (61.4)**	9.61 (66.3)	**11.2 (77.2)**	**7.17 (49.4)**
			105° Notch A.R. = 4		
1	6.76 (46.6)		10.3 (71.0)		
2	6.76 (46.6)	**6.76 (46.6)**	8.92 (61.5)	**9.59 (66.1)**	**6.64 (45.8)**
			90° Notch A.R. = 8		
1	10.1 (69.6)		10.1 (69.6)		
2	7.94 (54.7)	**9.00 (62.1)**	9.30 (64.1)	**9.68 (66.7)**	**6.06 (41.8)**
			105° Notch A.R. = 8		
1	7.59 (52.3)		9.32 (64.3)		
2	7.58 (52.3)	**7.59 (52.3)**	10.1 (69.6)	**9.73 (67.1)**	**5.74 (39.6)**

specimens having 90° center notches have consistently higher average crack initiation stresses than the specimens of the same aspect ratio having 105° notches.

7.3.2 Zero Degree Tests

In all of the 0° notched coupon tests, crack extension occurred along the fiber direction, yielding experimental values of $\varphi_c = \pm 90°$. Figure 42 provides a photograph of typical crack extension that occurred during testing. Cracks extended from the cut notch, forming an "H" shape, with crack extension occurring from the very tip of the notch in all cases. Of the experiments performed for this study, these were unique in that cracks extended in two directions from each notch tip. All of the specimens experienced slow and stable crack extension. Crack opening displacement gage results indicate that the original cut notch experienced significant opening displacement during the test. In contrast to the original cut notch, extended cracks did not open significantly during the tests. Because they did not open, extended cracks appeared as very thin white lines which were difficult to see. This made pinpointing the exact stress causing crack initiation difficult. In fact, of the tests performed in this study, these tests proved to be the most difficult to determine crack initiation stresses for. Without the use of videotape replays, the task would not have been possible. The sporadic crack growth behavior noted in the 15° off-axis tests also appeared to occur in these specimens. However, because extended cracks were difficult to see, especially near their tips, it could not be determined whether sporadic crack extension actually occurred.

In the notched 0° tensile coupons, crack extension typically occurred in an unsymmetric manner. Because each notch tip had cracks extending in two directions, this presented the possibility of obtaining four crack initiation stresses from each test. The difficulty in observing extended cracks made it essentially impossible to obtain all four initiation stress values from each test, however. Instead, two critical crack initiation stress values were obtained from each test, one for each notch tip. Extended cracks did not show a strong tendency to be equal in length at any point in the tests. As extended cracks grew in length, all of them eventually extended into the specimen grip

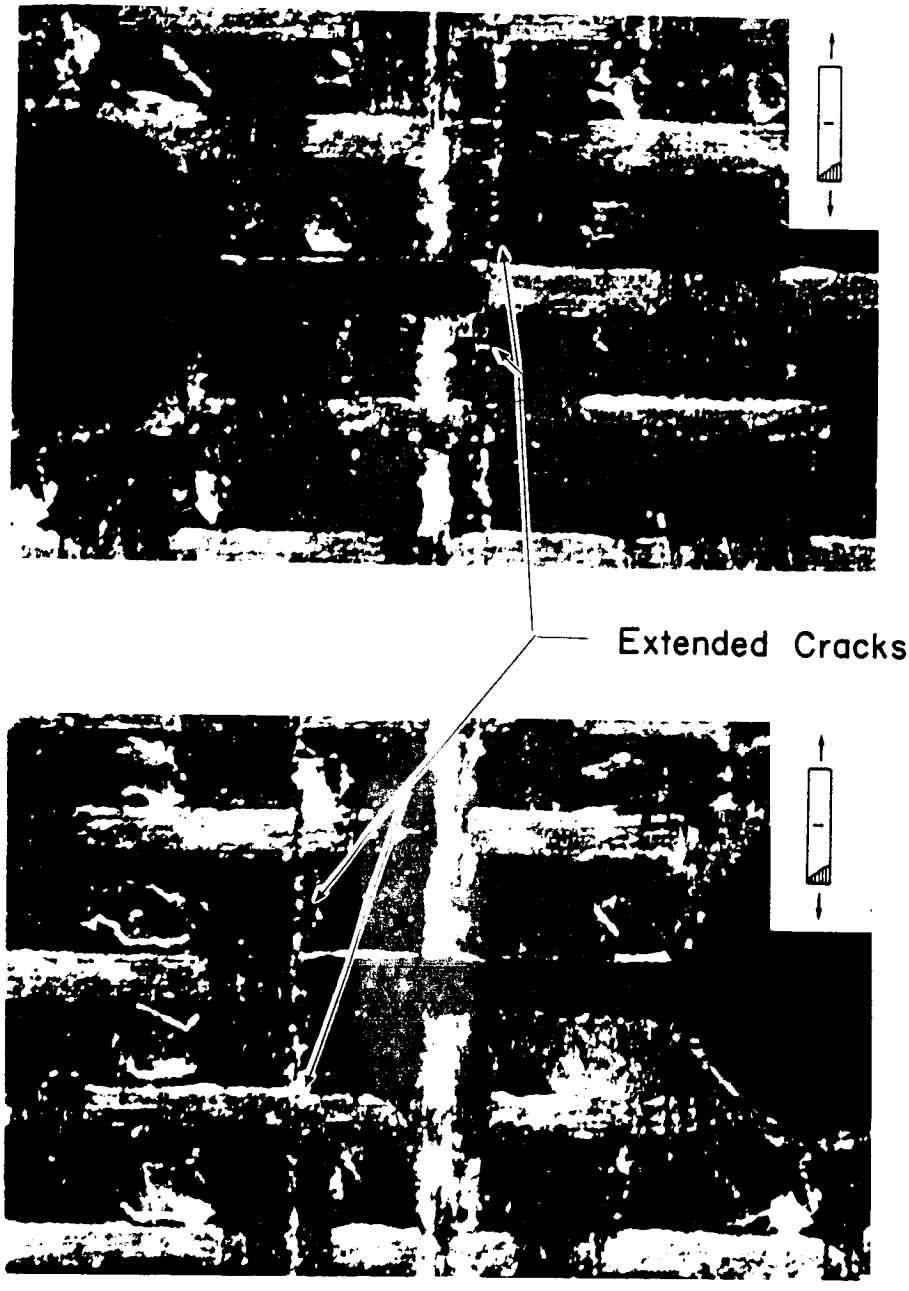

Figure 42. Microscopic Photographs of Crack Extension in a 0° Tensile Coupon

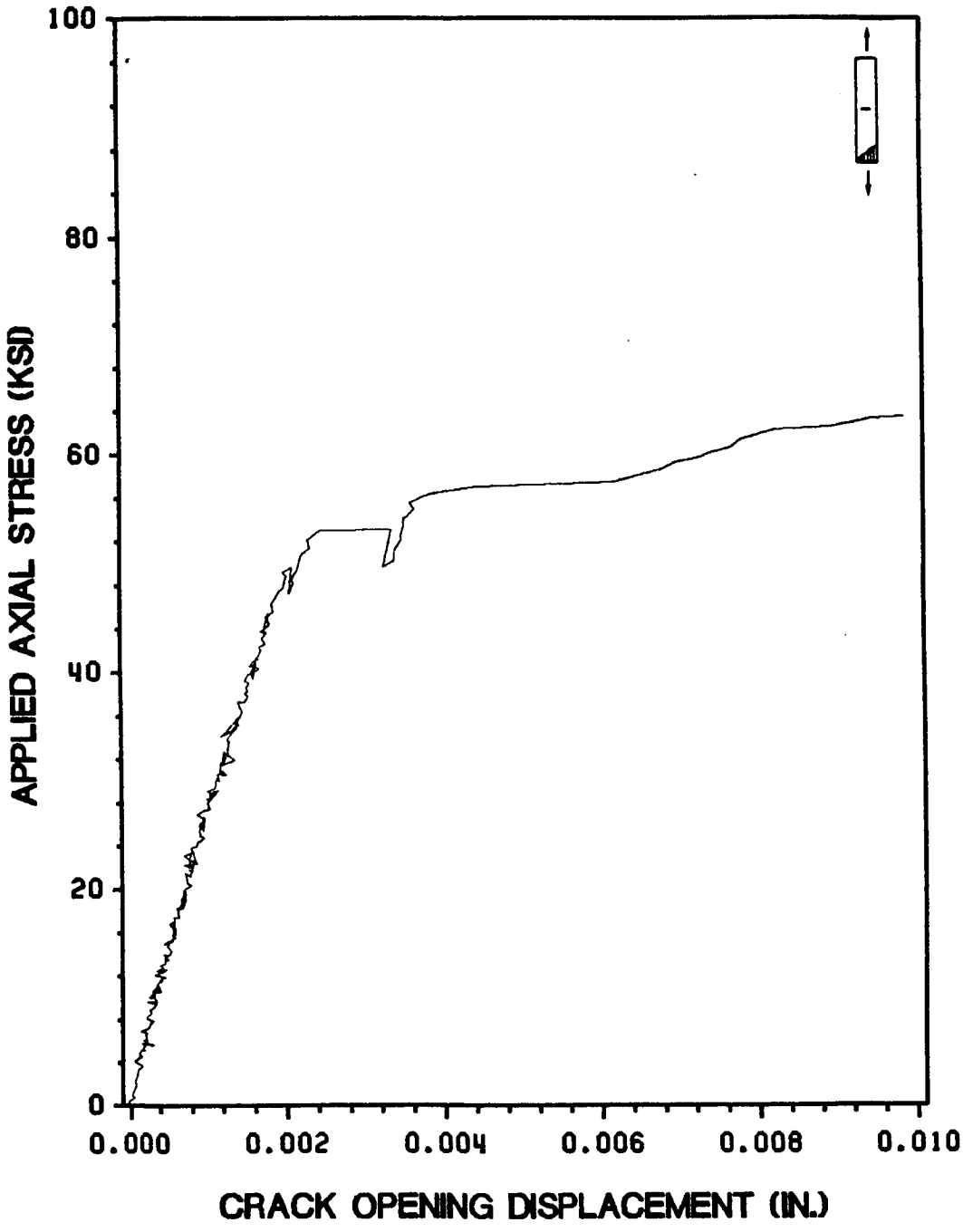

Figure 43. Applied Axial Stress vs. Crack Opening Displacement for a Typical Notched 0° Tensile Coupon Test

areas. At this point in the tests, the middle of the specimens became entirely separated from the specimen sides. This caused the specimen to behave essentially as two intact coupons with a single fractured coupon inbetween. As more displacement was applied to the specimen ends, the middle of the specimen continued to displace with respect to the specimen sides while the sides of the specimen carried essentially all of the load. Because of this, specimens did not experience true fractures, presenting the need to define specimen failure. Failure stress was defined as the axial stress causing the first noticeable displacement of the specimen center with respect to its sides. The weave pattern of the material surface, which became disrupted as soon as the center of the specimen displaced with respect to the sides, served to aid in obtaining failure stress values for these tests. Also, the white fiber line pattern revealed by polishing of some specimens tended to hide the thin white extended cracks. As a result, surface polishing tended to hinder crack extension observations in these specimens.

Figure 43 provides a typical plot of applied axial stress vs. crack opening displacement for a notched 0° coupon. As indicated in the figure, cut notch stress vs. crack opening displacement plots were linear to approximately 50. ksi. The deviation from linear behavior occurred well beyond the point of crack initiation from both notch tips in all of the specimens. As a result, the crack opening displacement gage did not act as a good indicator of crack initiation for these tests. The deviation from linear behavior did occur, however, at the applied stress causing the center of the specimen to initially displace with respect to its sides. Thus, the c.o.d. gage results acted as an excellent indicator of specimen failure as it was defined for this test.

Table 6 provides a summary of all of the critical stress values obtained from the notched 0° tensile coupon tests. The average crack initiation stress value was obtained by averaging all of the crack initiation stress values (from both tips) together. A total of five 0° tests were run because of the difficulty in obtaining crack initiation stress values and the scatter exhibited by the results. Two characteristics of the results are important to note. The first is the experimental scatter. The scatter in failure stress values is not too severe. The crack initiation stress value scatter is significant, however. A portion of this scatter is likely due to the difficulty in observing extended cracks. This difficulty can only explain a small amount of scatter, however, not the amount exhibited by these

tests. The second important characteristic of the results is the differences in the stresses causing crack initiation from each notch tip of a given specimen. In two of the five tests, crack initiation stress values for each notch tip differed greatly. Even in the other tests crack initiation stresses were never close to being equal. With respect to these two characteristics, the 0° notched coupon tests were highly similar to the 15° off-axis tensile coupon tests. As will be detailed later, no other notched specimen tests exhibited noticeable differences in stresses causing crack initiation from each notch tip or significant experimental scatter. It is possible that these characteristics are typical of tests on center-notched tensile coupon specimens with small off-axis angle values.

7.3.3 Forty-Five Degree Off-Axis Tests

In all of the 45° notched coupon tests, crack extension occurred along the fiber direction, yielding an experimental value of φ_c = -45° All of the specimens experienced unstable crack extension. Figure 44 provides a photograph of the notched region of a typical specimen after fracture. As the figure indicates, crack extension occurred away from the notch tip in all cases. The location of crack initiation along the cut notch is best characterized as occurring at an angle of -45° measured along the semi-circular notch tip. This location of crack initiation was very consistent throughout the tests. A plot of applied axial stress vs. cut notch opening displacement for a typical test is provided in Figure 45. The plotted results indicate that the original cut notch experienced little or no opening displacement during the test. The critical stresses obtained from the 45° off-axis tensile coupon tests are given in Table 6. Because only unstable crack extension was exhibited in these tests, the stresses at crack initiation and failure are identical for each specimen. The values obtained from the tests are highly consistent, exhibiting little experimental scatter.

7.3.4 Ninety Degree Tests

Table 6. Zero, Forty-Five and Ninety Degree Notched Coupon Tests

Comparison of Theoretical and Experimental
Critical Stresses
0°, 45°, and 90° Notched Coupon Tests

Specimen Number[1]	Axial Stress at Initial Crack Extension ksi (MPa)		Averages ksi (MPa)	Axial Stress at Failure ksi (MPa)	Averages ksi (MPa)	Predicted Critical Axial Stress ksi (MPa)
	(first tip)	(second tip)				
			0° Tests			
1	38.6 (266.)	48.0 (330.)		64.0 (441.)		
2	37.8 (261.)	41.6 (287.)		67.9 (468.)		
3	42.4 (292.)	45.8 (316.)		55.1 (380.)		
4	29.7 (205.)	33.3 (230.)		53.0 (365.)		
5	28.1 (194.)	36.9 (254.)	**38.2 (263.)**	54.1 (373.)	**58.8 (405.)**	**20.9 (144.)**
			45° Tests			
1	3.85 (26.5)			3.85 (26.5)		
2	4.19 (28.9)			4.19 (28.9)		
3	4.24 (29.2)			4.24 (29.2)		
4	4.19 (28.9)		**4.12 (28.4)**	4.19 (28.9)	**4.12 (28.4)**	**5.02 (34.6)**
			90° Tests			
1	2.72 (18.8)			2.72 (18.8)		
2	2.95 (20.3)			2.95 (20.3)		
3	2.75 (19.0)		**2.81 (19.4)**	2.75 (19.0)	**2.81 (19.4)**	**(baseline test)**

[1]All 0°, 45°, and 90° coupons had notches at 90° to the specimen loading axis (horizontal).

In all of the 90° notched coupon tests, crack extension occurred along the fiber direction, yielding an experimental value of $\varphi_e = 0°$ All of the specimens experienced unstable crack extension. Figure 46 provides a photograph of the notched region of a typical specimen after fracture. As the figure indicates, crack initiation occurred at the very tips of the notches in these specimens. Figure 47 provides a plot of applied axial stress vs. crack opening displacement for a typical test. As indicated by the plot, the original cut notch did experience opening displacement during the test.

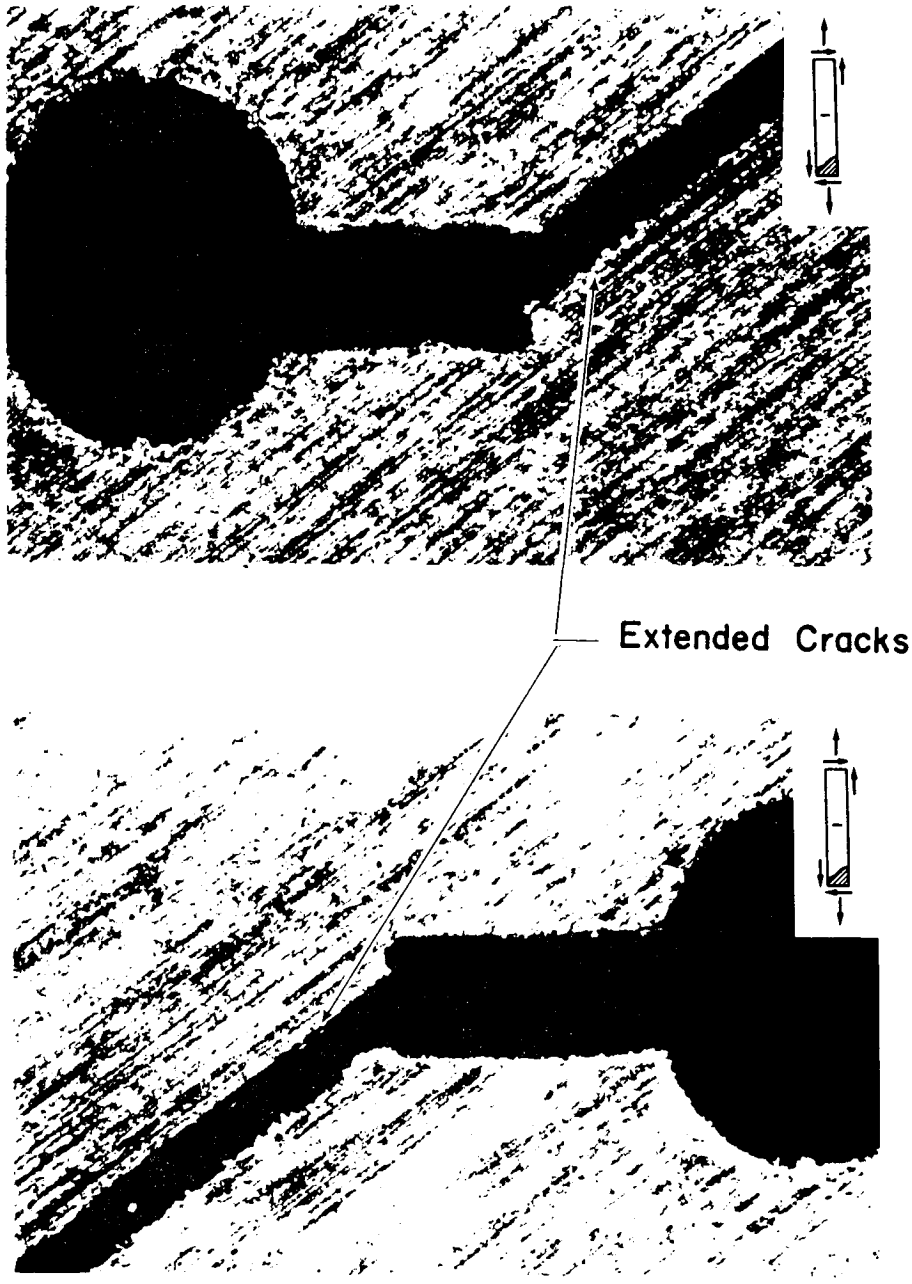

Figure 44. Microscopic Photographs of the Near-Notch Region in a 45° Off-Axis Tensile Coupon After Fracture

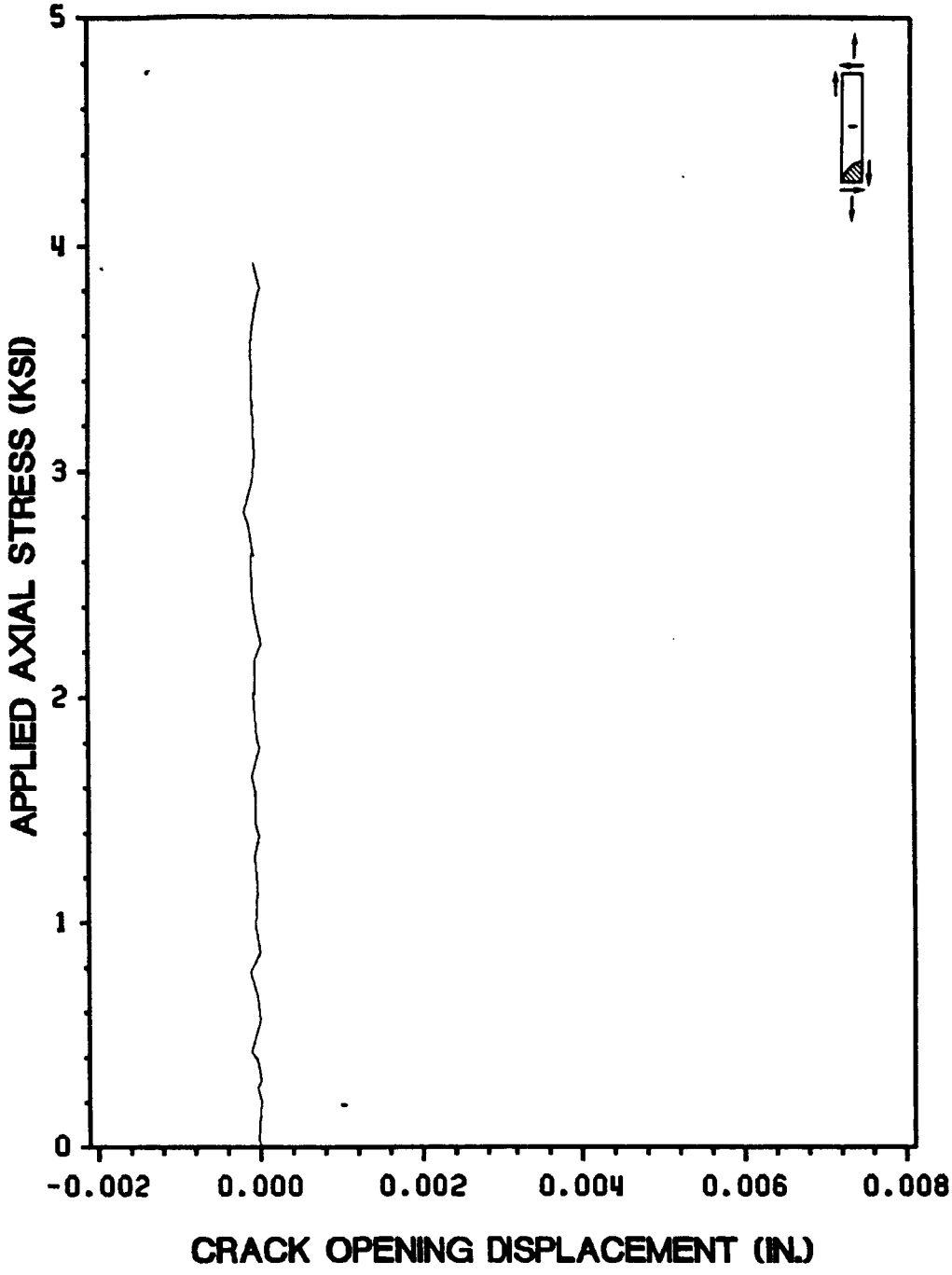

Figure 45. Applied Axial Stress vs. Crack Opening Displacement for a Typical Notched 45° Off-Axis Tensile Coupon Test

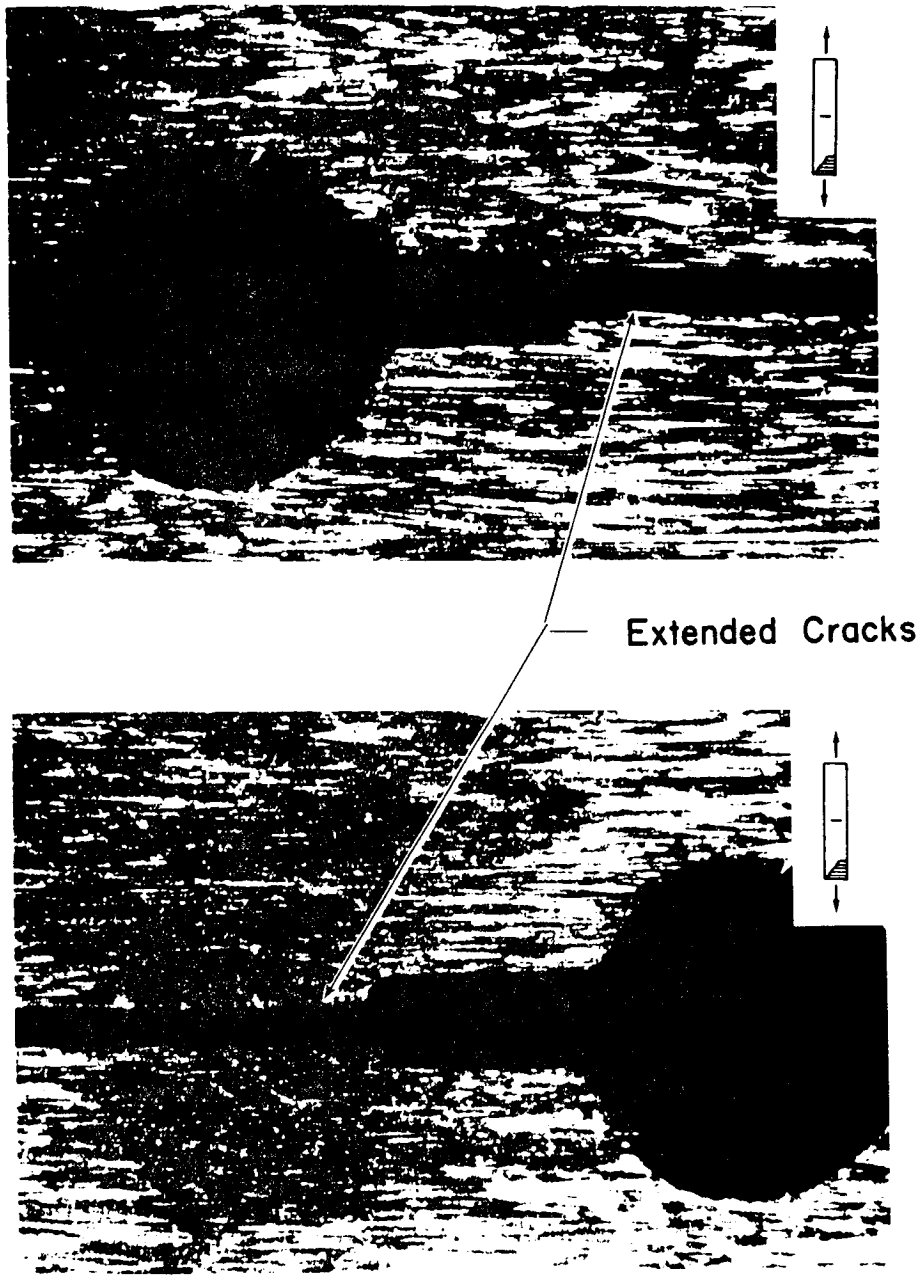

Figure 46. Microscopic Photographs of the Near-Notch Region in a 90° Tensile Coupon After Fracture

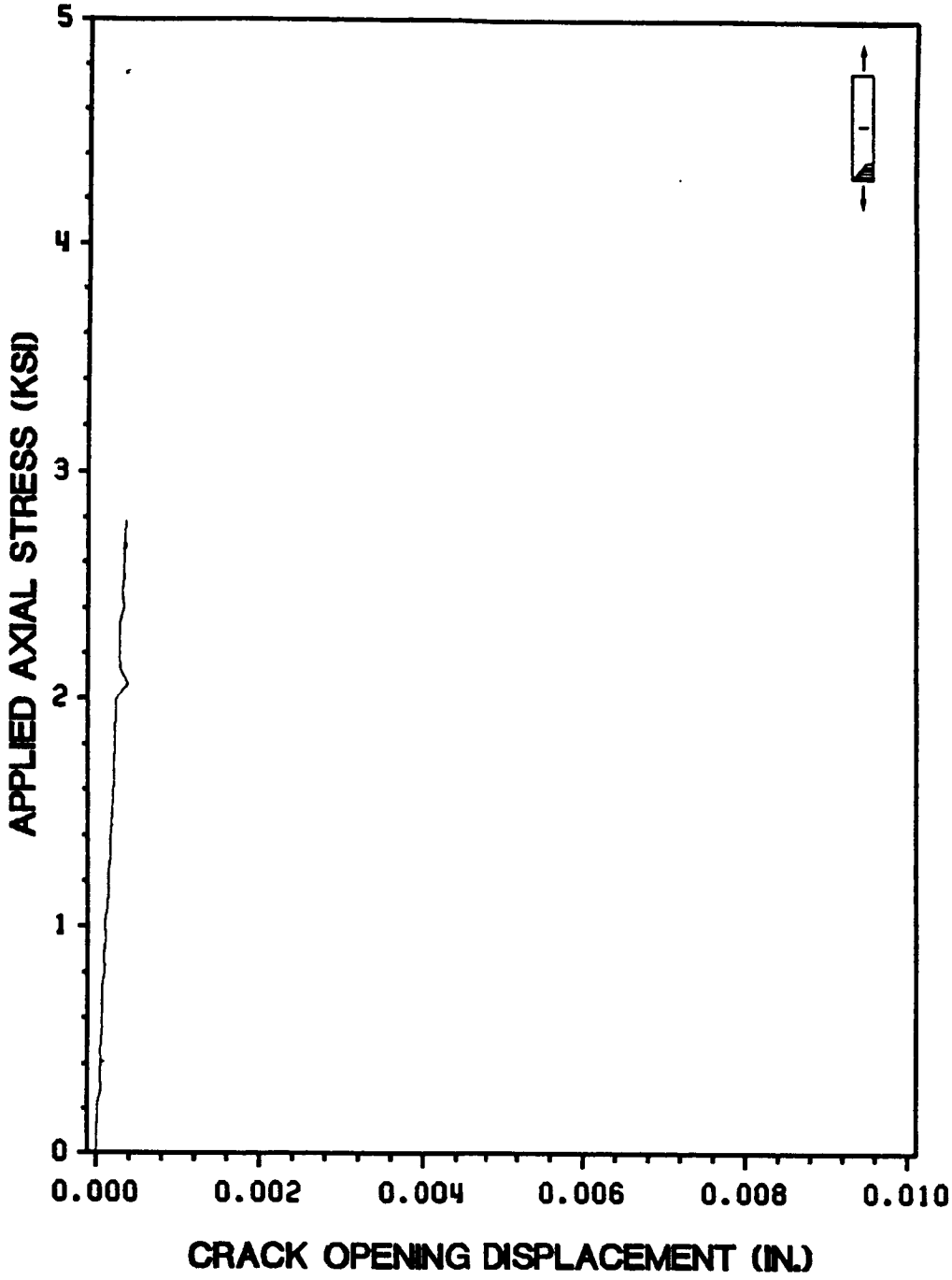

Figure 47. Applied Axial Stress vs. Crack Opening Displacement for a Typical Notched 90° Tensile Coupon Test

All cut notch stress vs. crack opening displacement plots were essentially linear to failure. The critical stresses obtained from the 90° tensile coupon tests are given in Table 6. Because only unstable crack extension was exhibited in these tests, the stresses at crack initiation and failure are identical for each specimen. As with the 45° off-axis tests, the fracture stress values obtained from the tests are highly consistent.

7.4 Iosipescu Specimen Test Results

7.4.1 Critical Direction Prediction Iosipescu Tests

Because it was realized that the critical direction prediction tests given in Table 4 might not be workable using the Iosipescu test, two preliminary experiments were performed in order to judge the value of subsequent testing. The tests performed were on one 90° specimen and one 105° specimen, each with vertical notch orientations. Of these two specimens, it was reasoned that the 105° specimen would be most likely to experience crack extension before failure because of its slightly higher tensile strength along the horizontal direction. A photograph of the failed specimens is provided in Figure 48.

The 90° specimen was loaded to an applied shear stress of 4.03 ksi. At that point, the specimen fractured near the cut notch. During the test, the original notch exhibited no crack opening displacement. Specimen fracture took place so rapidly that it could not be determined whether or not the fracture was the result of any type of crack extension or simply failure of the material due to normal stresses near the v-notch roots. Examination of the failed specimen indicated that the latter of the two events occurred. Fracture did occur near one of the cut notch tips, but clearly occurred along the boundary of the cut center hole on the other side of the notch. This suggests that the stress concentration caused by the cut notch tips was not high, and that fracture actually

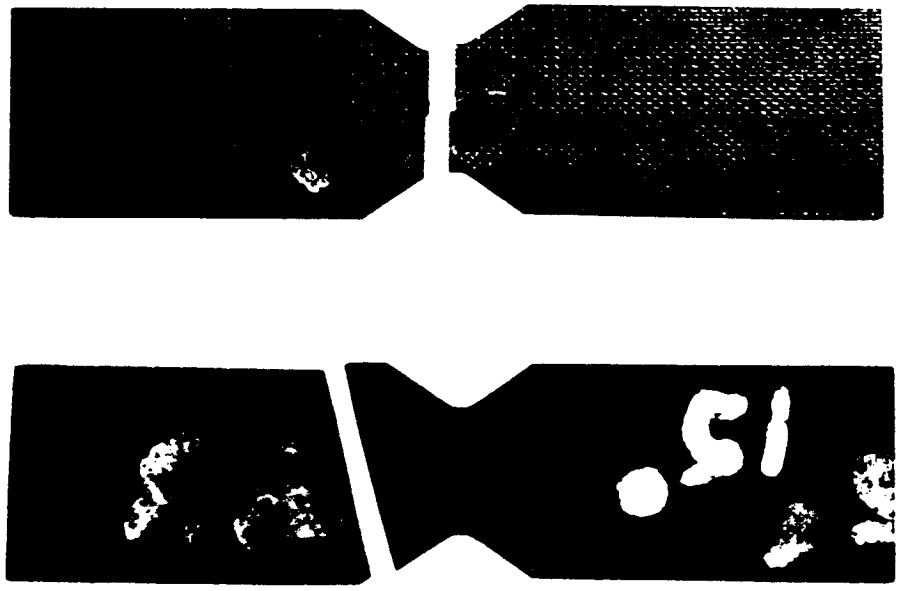

Figure 48. Failed Critical Direction Prediction Iosipescu Specimens

initiated at the v-notch roots and then propagated through the center of the specimen. The shear stress at fracture, which is close to the value obtained from unnotched specimens that fractured due to cracking near the v-notch roots, also suggests that normal stress concentrations at the v-notch roots caused premature fracture in this specimen.

The 105° specimen was loaded to an applied shear stress of 4.57 ksi, where it failed along the fiber direction just outside of the test section. During this test, the original cut notch exhibited slight crack closure. As indicated by the photograph in Figure 48, this specimen definitely did not experience crack extension before gross specimen failure occurred. Failure occurred outside of the test section and away from the cut center notch. Neither of these two tests appeared to work as crack extension tests. Apparently the stress concentration caused by the cut notch was not great enough to cause crack extension before the specimen itself failed due stress concentrations induced by the specimen geometry and the fixture. Because of these results, no additional critical direction prediction tests were attempted as a part of this study. Another shear test method, such as a thin tube torsion test would be more applicable to running these tests.

7.4.2 Zero Degree Iosipescu Tests

In all of the 0° notched Iosipescu tests, crack extension occurred along the fiber direction, yielding an experimental value of φ_c = -90° All of the specimens experienced stable crack extension. Figure 49 provides a photograph of typical crack extension that occurred during testing. Crack extension occurred far from the notch tip in all cases. Crack extension always occurred in a symmetric manner, yielding a single critical crack initiation stress value for each test. Videotape replays of each test clearly showed that, at the point of crack initiation, cracks extended from both notch tip regions as part of a single cracking event. This event was also clearly audible on videotape playbacks. The observed symmetric crack extension behavior suggests two things. First, it suggests that, as indicated by the x-ray radiographs taken before testing, no damage was imparted to the specimen during notch cutting that might cause one crack tip to experience crack extension before

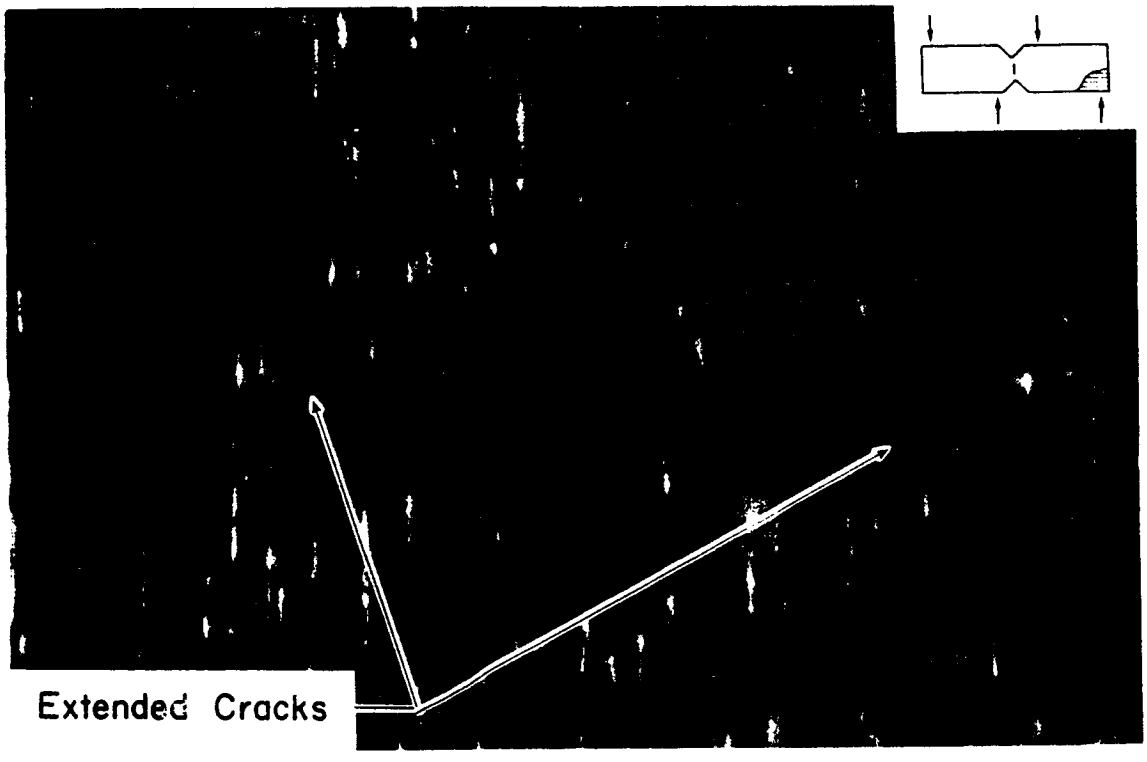

Figure 49. Microscopic Photograph of Crack Extension in a 0° Iosipescu Shear Specimen

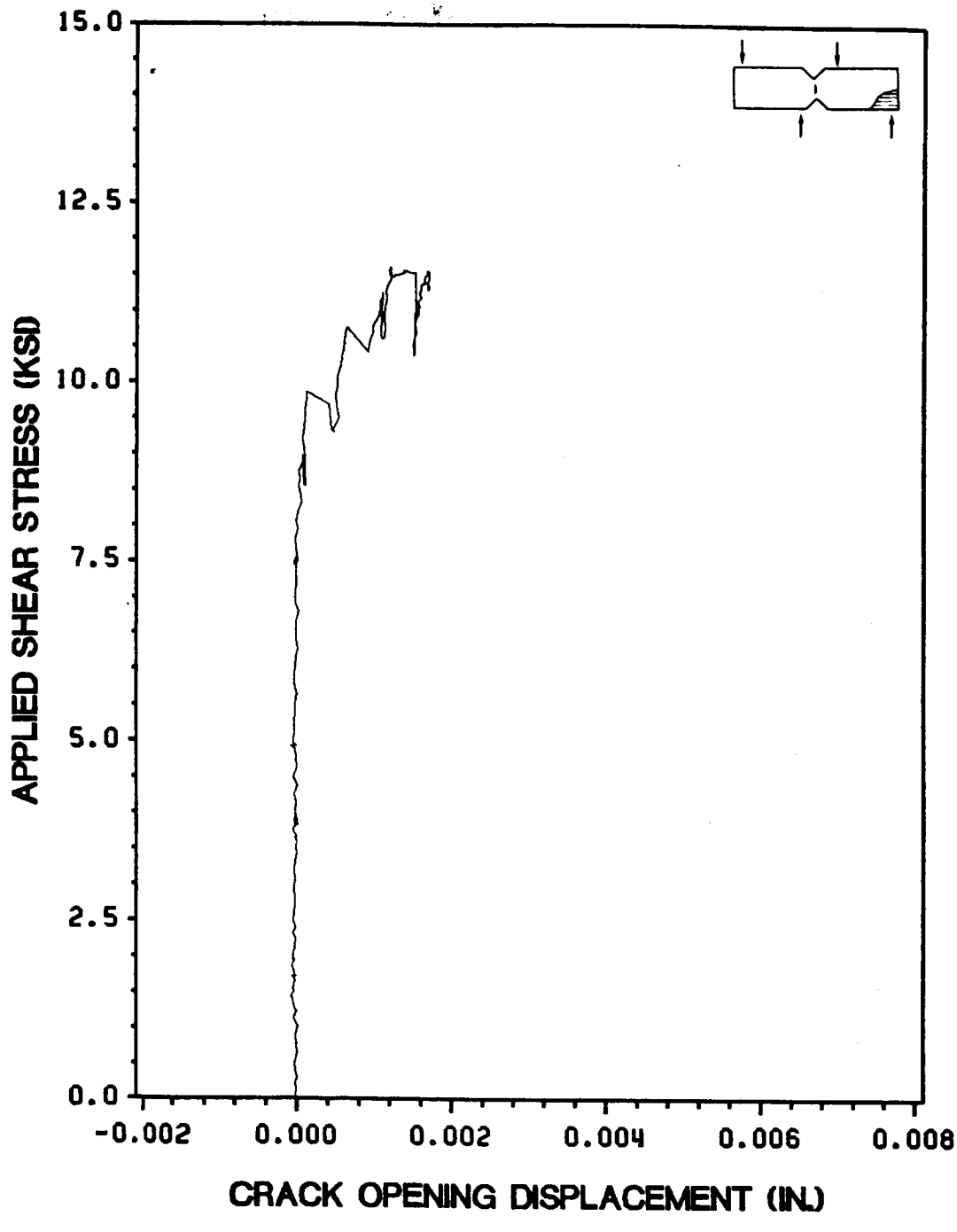

Figure 50. Applied Shear Stress vs. Crack Opening Displacement for a Typical Notched 0° Iosipescu Test

the other. Second, it suggests that the stress state in the specimen is symmetric with respect to the cut notch. V-notch cracking, which occurred at approximately 12 ksi, took place significantly beyond the stress causing crack initiation from the cut center notch (average value of 4.03 ksi). The direction of v-notch cracking was opposite of that occurring at the cut center notch. A plot of applied shear stress vs. cut notch opening displacement is provided in Figure 50. As the plot indicates, the original cut notch did not experience opening displacement during the test until after cracking occurred at the specimen v-notch roots. Thus, the c.o.d. gage results did not act aid in determining stresses at crack initiation. Unlike the original cut notch, extended cracks did open significantly during the tests, making them appear as dark lines. Extended cracks did not continue to grow throughout the tests. Instead, extended cracks stopped growing at a distance of approximately one half of the total notch length (0.050 in.) from the original notch tip. As more displacement was applied to the specimen, extended cracks continued to open without extending.

After cracking occurred at the v-notch roots, the material near the original notch tip started to appear as if it were yielding. This behavior, which almost appeared to be some type of collinear crack extension, was likely a result of the entire specimen beginning to experience global shear stress failure, as such effects began to dominate the test. These specimens did not experience final fracture. They also did not experience the crushing failure exhibited by the unnotched 0° Iosipescu specimens. Specimen failure stress was defined as the maximum shear stress applied to the specimen. The critical stresses obtained from the 0° Iosipescu tests are given in Table 7. The highly stable crack extension exhibited by these specimens is reflected in the significant difference between crack initiation and failure stresses in all of the tests. Both the crack initiation and failure stresses exhibited very little experimental scatter.

7.4.3 Fifteen Degree Iosipescu Tests

In all of the 15° notched Iosipescu tests, crack extension occurred along the fiber direction, yielding an experimental value of φ_e = -75° All of the specimens experienced highly stable crack

Table 7. Iosipescu Shear Tests

Comparison of Theoretical and Experimental Critical Stresses
Iosipescu Shear Tests

Specimen Number[1]	Shear Stress at Initial Crack Extension ksi (MPa)	Averages ksi (MPa)	Shear Stress at Failure ksi (MPa)	Averages ksi (MPa)	Predicted Critical Shear Stress ksi (MPa)
			0° Tests		
1	4.32 (29.8)		12.3 (84.9)		
2	3.92 (27.0)		12.4 (85.8)		
3	3.94 (27.2)		12.1 (83.3)		
4	3.95 (27.2)	**4.03 (27.8)**	11.7 (80.5)	**12.1 (83.6)**	**3.10 (21.4)**
			15° Tests		
1	3.69 (25.4)		9.89 (68.2)		
2	3.34 (23.0)		10.2 (70.3)		
3	3.46 (23.9)	**3.50 (24.1)**	9.45 (65.2)	**9.85 (67.9)**	**2.88 (19.9)**
			30° Tests		
1	4.17 (28.8)		7.18 (49.5)		
2	4.02 (27.7)		7.67 (52.9)		
3	4.19 (28.9)	**4.13 (28.5)**	7.70 (53.1)	**7.52 (51.8)**	**3.01 (20.8)**
			45° Tests		
1	3.96 (27.3)		3.96 (27.3)		
2	4.01 (27.6)		4.01 (27.6)		
3	4.28 (29.5)	**4.08 (28.1)**	4.28 (29.5)	**4.08 (28.1)**	**3.80 (26.2)**

[1] Each Iosipescu test specimen had a cut notch at 90° (vertical).

extension before failure. Figure 51 provides a photograph of typical crack extension that occurred during testing. As the figure indicates, crack extension occurred away from the notch tip in all cases. The location of crack extension was not as far from the notch tip as it was for the 0° notched Iosipescu tests, however. Crack extension consistently occurred in a highly symmetric manner,

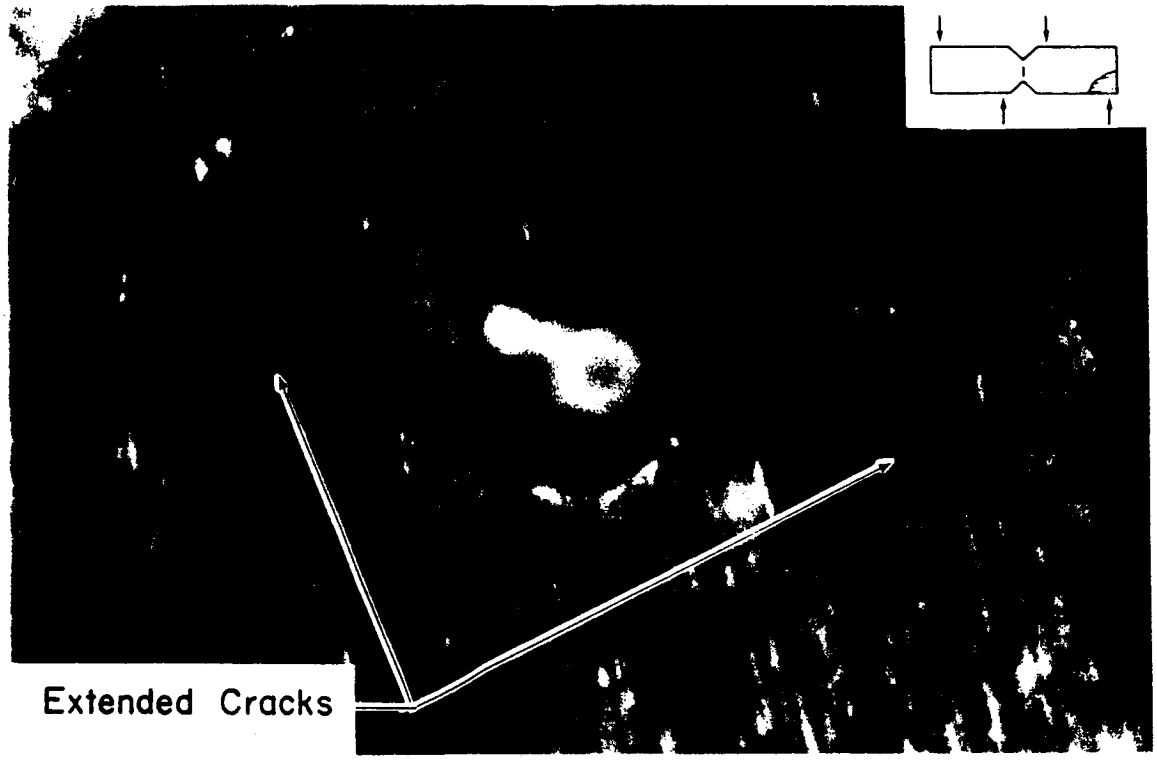

Figure 51. Microscopic Photograph of Crack Extension in a 15° Iosipescu Shear Specimen

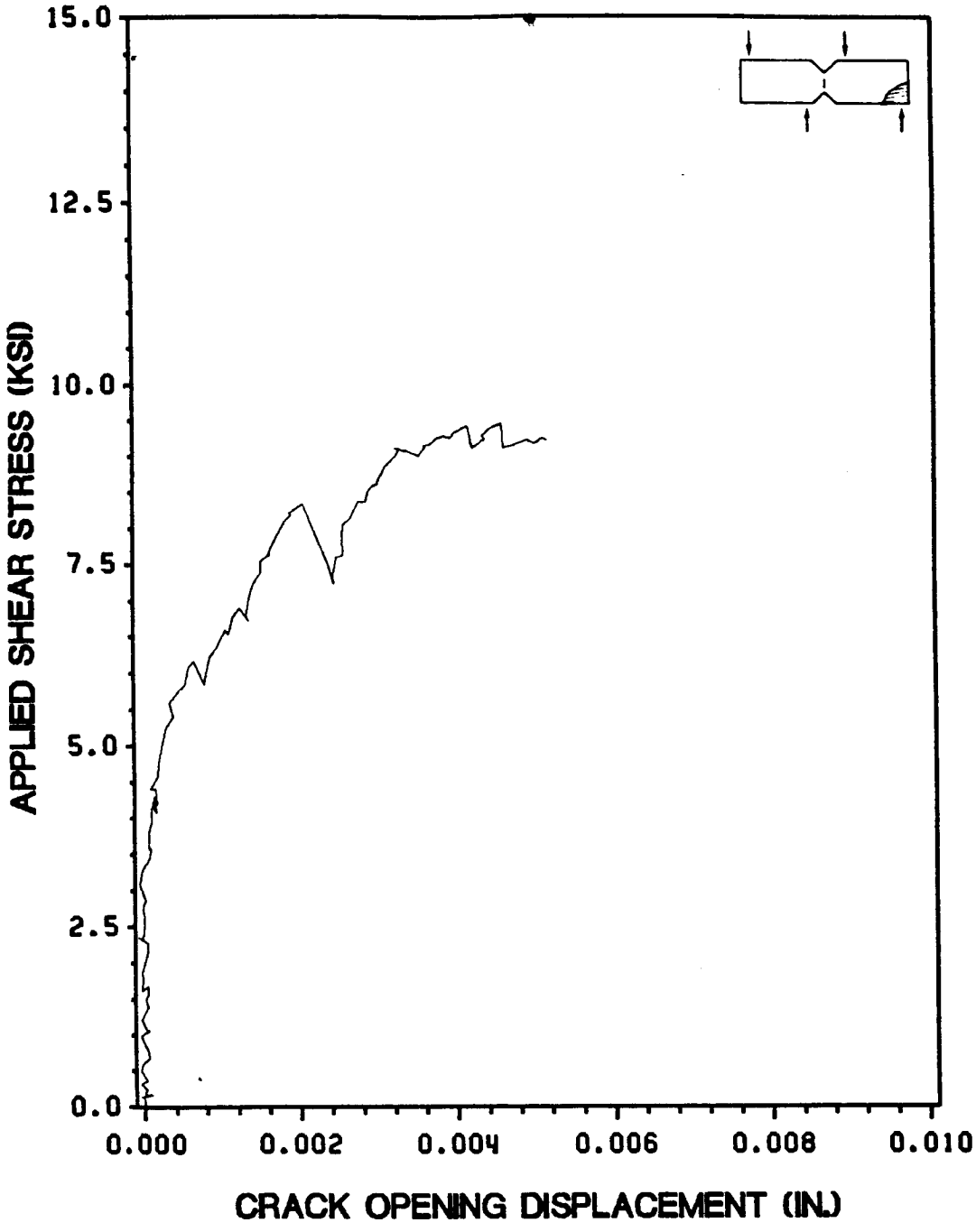

Figure 52. Applied Shear Stress vs. Crack Opening Displacement for a Typical Notched 15° Iosipescu Test

yielding a single critical crack initiation stress value for each test. Again, as in the 0° tests, crack initiation occurred as a single event that was audible on video playback. In these tests, however, the event was significantly more noticeable than it was in the 0° tests. A plot of applied shear stress vs. original cut notch opening displacement is provided in Figure 52. As the plot indicates, the original cut notch did not exhibit opening displacement until after crack initiation occurred. At initiation, the shear stress vs. crack opening displacement plot began to curve gradually. This gradual increase in crack opening displacement continued until v-notch cracking occurred, which resulted in the drop in applied load and increase in crack opening displacement exhibited in the stress vs. c.o.d. plot. Because crack initiation did not cause a sudden increase in measured crack opening displacement, its use in pinpointing the exact crack initiation stress was limited. As in the 0° tests, extended cracks did open significantly during the tests, making them appear as dark lines. The extended cracks also did not continue to grow throughout these tests, instead stopping after reaching a length of approximately 1.5 original notch lengths (0.150 in.) and then opening as more displacement was applied to the specimen.

Table 7 provides a summary of the critical stresses obtained from the 15° Iosipescu tests. As in the 0° tests, these specimens did not experience a true failure event. Therefore, as with the 0° tests, specimen failure stress was defined as the maximum shear stress applied to the specimen. As Table 7 indicates, specimens continued to acquire a significant amount of applied shear stress beyond that causing crack initiation. The difference between crack initiation and failure stress levels is clearly less than it was for the 0° tests however. Both critical stress values obtained from these tests exhibited little experimental scatter. Both the average stress causing crack initiation and that causing failure were significantly less than those obtained from the 0° Iosipescu tests.

7.4.4 Thirty Degree Iosipescu Tests

In all of the 30° notched Iosipescu tests, crack extension occurred along the fiber direction, yielding an experimental value of φ_c = -60° All of the specimens experienced stable crack exten-

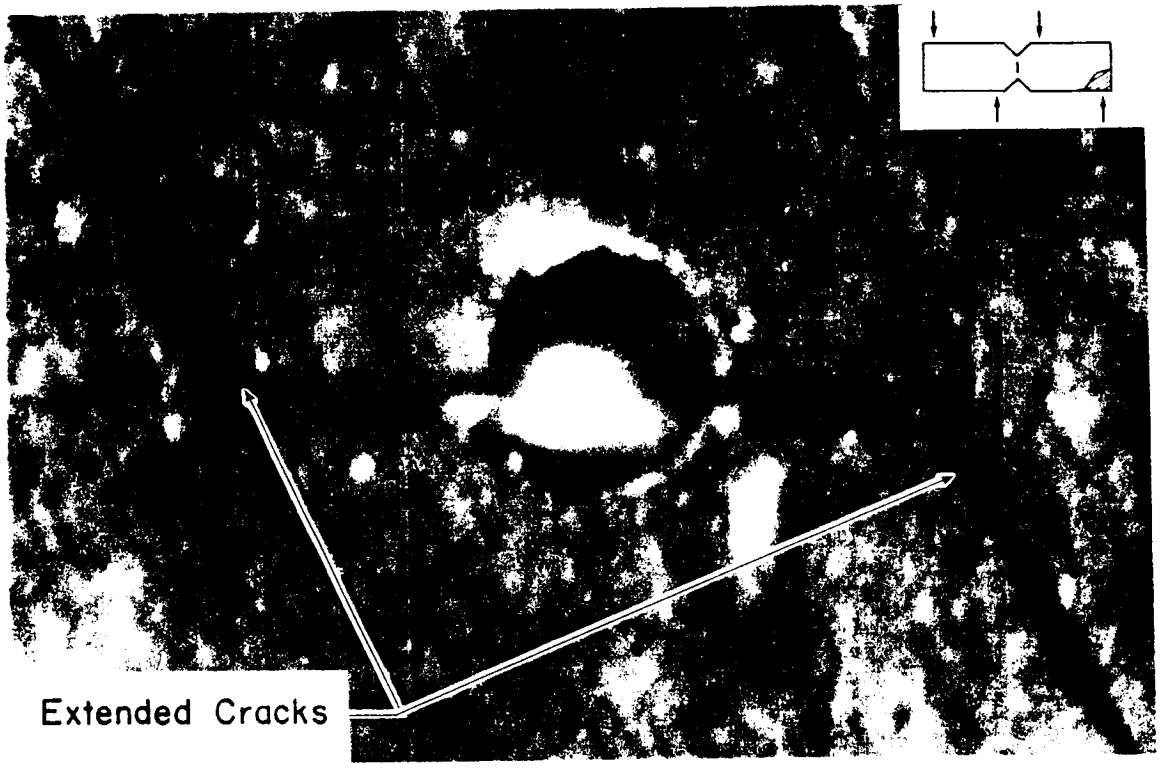

Figure 53. Microscopic Photograph of Crack Extension in a 30° Iosipescu Shear Specimen

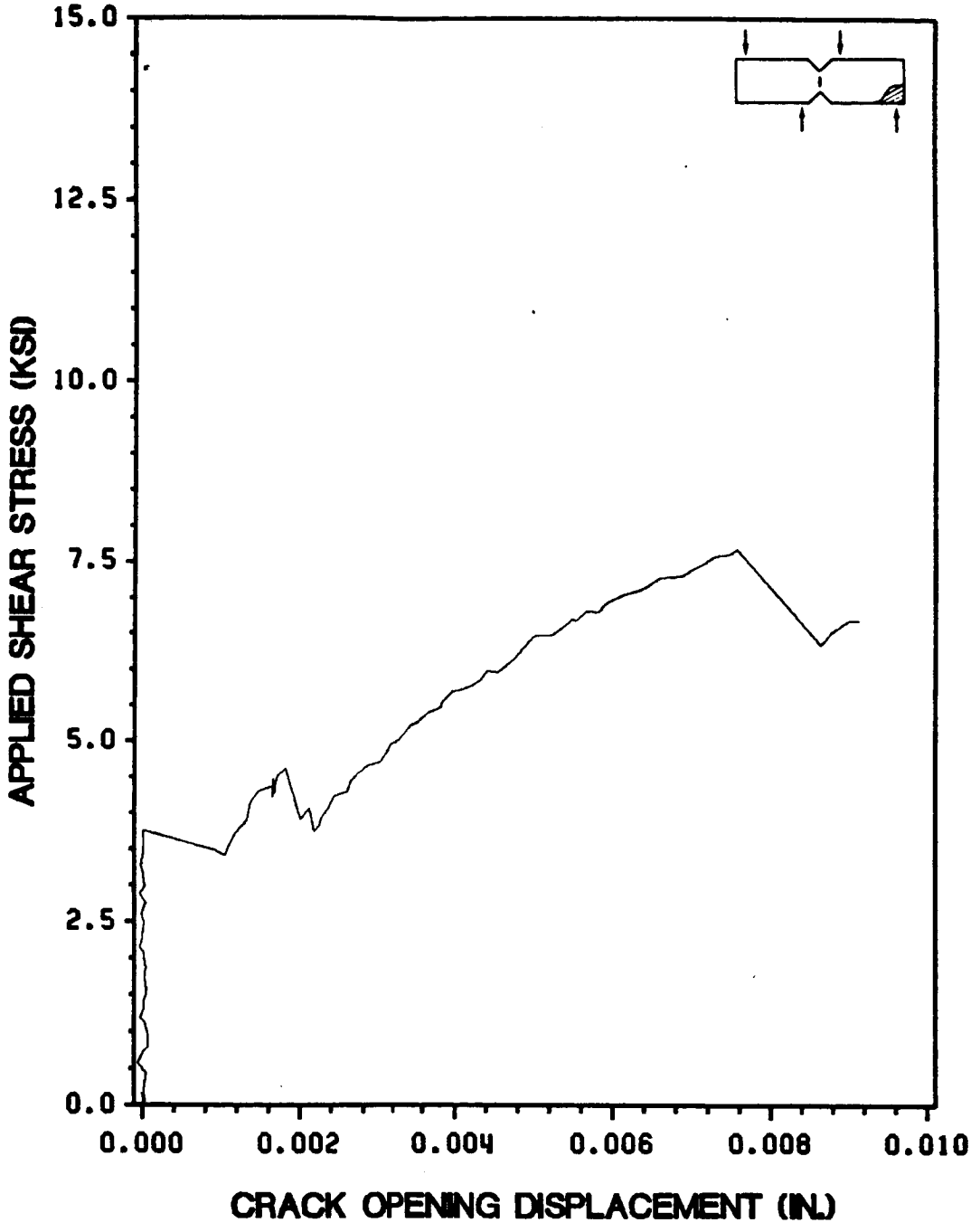

Figure 54. Applied Shear Stress vs. Crack Opening Displacement for a Typical Notched 30° Iosipescu Test

sion. Figure 53 provides a photograph of typical crack extension that occurred during testing. Crack extension occurred away from the notch tip in all cases. The distance away from the notch tip at which crack initiation occurred was less than that observed for the 15° Iosipescu tests. Crack extension typically occurred in a highly symmetric manner, yielding a single crack initiation stress value for each test. Again, as in the 0° and 15° notched Iosipescu tests, crack initiation occurred as a single event that was audible on video playback. The event was even more noticeable in these tests, however. Figure 54 provides a plot of applied shear stress vs. original notch opening displacement. As indicated by the plot, the original cut notch did not exhibit opening displacement until crack initiation occurred. At the stress causing crack initiation, however, the original cut notch experienced immediate, significant crack opening displacement. Subsequent v-notch cracking also resulted in in immediate, significant crack opening displacement. Because crack initiation caused a sudden increase in measured crack opening displacement, c.o.d. gage results were very useful in pinpointing the stress at crack initiation. Crack initiation was highly noticeable visually and audibly and also caused a significant decrease in the shear stress applied to the specimen, however. As a result, the added indication of crack initiation provided by the c.o.d. gage results was not really needed. As in the other notched Iosipescu tests, extended cracks opened significantly during the tests, giving them the appearance of dark lines. The extended cracks also did not continue to grow throughout these tests, instead stopping after reaching a length of approximately 2 original notch lengths (0.200 in.) and then opening as more displacement was applied to the specimen.

Table 7 provides a summary of the critical stresses obtained from the 30° Iosipescu tests. Unlike the notched Iosipescu specimens described, thus far, these specimens did experience a fracture type failure event. Therefore, specimen failure stress was simply the stress at specimen fracture. As Table 7 indicates, specimens continued to acquire a significant amount of applied shear stress beyond that causing crack initiation. The difference between crack initiation and failure stress levels is clearly less than it was for the 0° and 15° notched Iosipescu tests however. Both critical stress values obtained from these tests exhibited little experimental scatter. Although the failure stress continued the decreasing trend exhibited in going from the 0° to the 15° fiber orientations, the av-

erage stress at crack initiation was clearly higher than that observed from either the 0° or the 15° notched Iosipescu tests.

7.4.5 Forty-Five Degree Iosipescu Tests

In all of the 45° notched Iosipescu tests, crack extension occurred along the fiber direction, yielding an experimental value of φ_c = -45°. All of the specimens experienced stable crack extension. Crack initiation caused a significant drop in the shear stress applied to the specimen. As more displacement was applied to the specimen after crack initiation, the specimen acquired more stress, however, the stress the specimen could withstand never reached the value that caused crack initiation from the original cut center notch. As a result, crack initiation occurred at the maximum stress that the specimen could withstand, and the stress causing crack initiation was also designated as the failure stress for each specimen. Figure 55 provides a photograph of typical crack extension that occurred during testing. Crack extension occurred away from the notch tip in all cases, at a location close to -45° around the rounded notch tip. In this way the location of crack extension was essentially identical to that observed for the 45° off-axis tension tests. Compared to the other notched Iosipescu tests performed as a part of this study, this test experienced a location of crack initiation that was the closest to the notch tip. As in the other notched Iosipescu tests, crack extension occurred in a highly symmetric manner, yielding a single crack initiation stress value for each test. Again, crack initiation occurred as a single event that was audible on video playback. Of all of the Iosipescu specimen tests, crack initiation for these tests was the most visually and audibly noticeable.

A plot of applied shear stress vs. original notch opening displacement for a typical 45° Iosipescu test is provided in Figure 56. As the plot indicates, the original cut notch did not exhibit opening displacement until crack initiation occurred. At the stress causing crack initiation, however, the original cut notch experienced immediate, significant crack opening displacement. As with the 30° Iosipescu tests, because crack initiation caused a sudden increase in measured crack opening

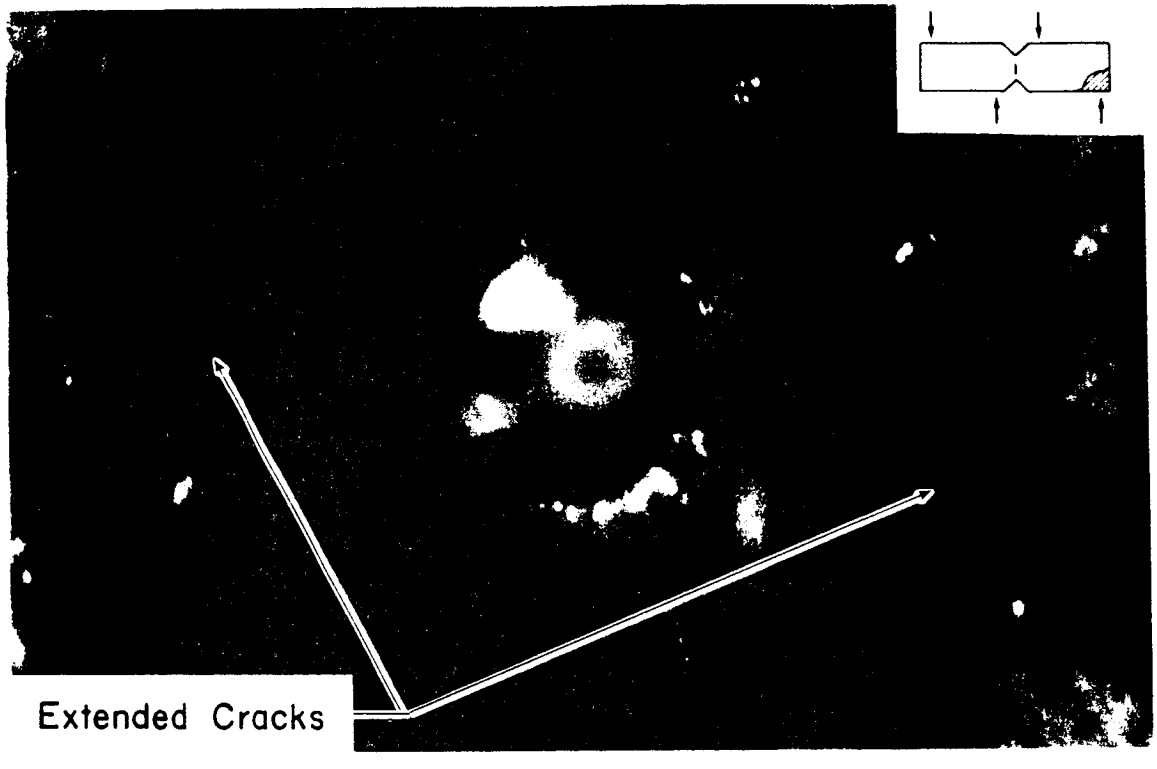

Figure 55. Microscopic Photograph of Crack Extension in a 45° Iosipescu Shear Specimen

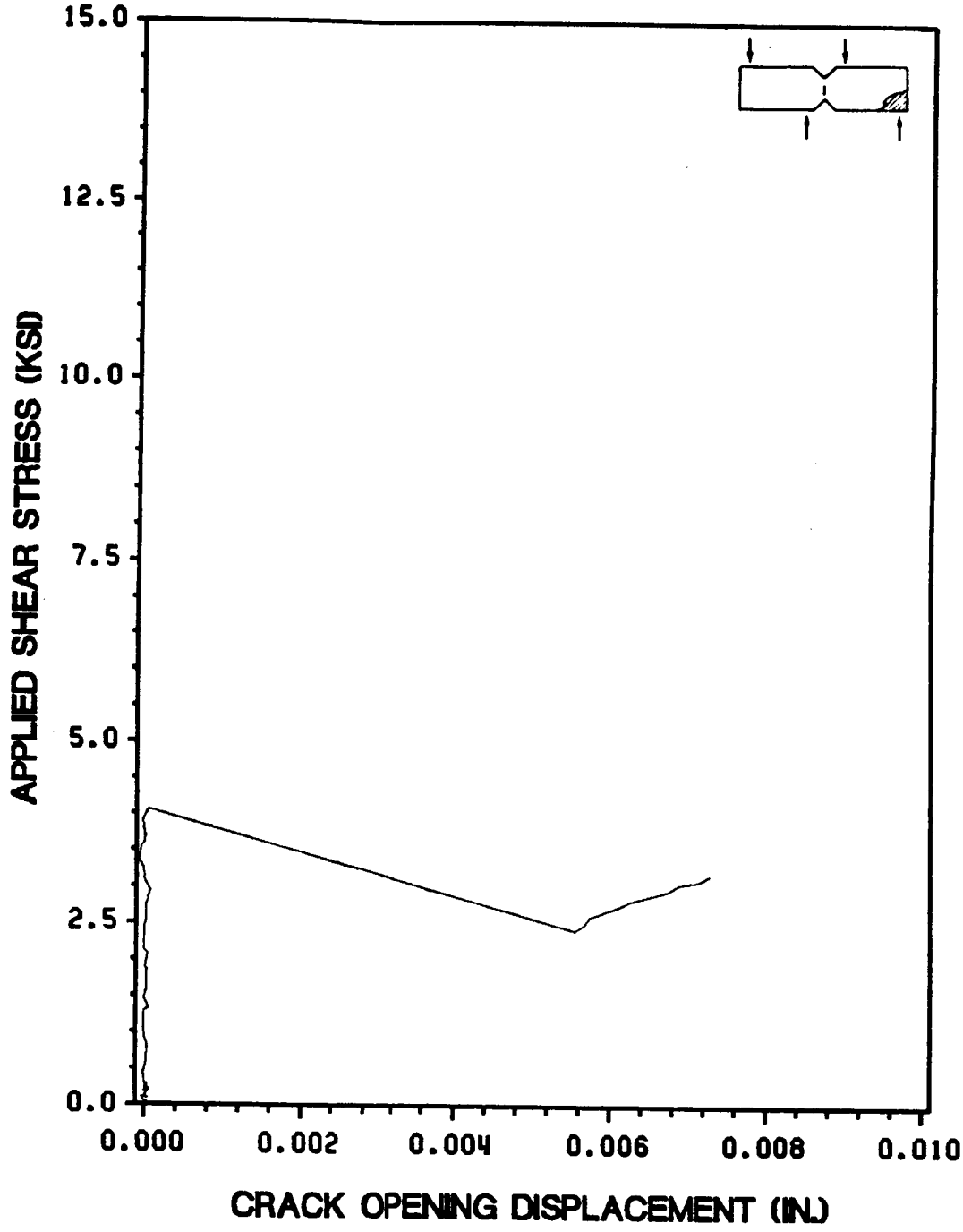

Figure 56. Applied Shear Stress vs. Crack Opening Displacement for a Typical Notched 45° Iosipescu Test

displacement, c.o.d. gage results were very useful in pinpointing the stress at crack initiation. Again, however, crack initiation was so noticeable, and caused such a significant decrease in the shear stress applied to the specimen that the added indication of crack initiation provided by the c.o.d. gage results was not really needed. As in the other notched Iosipescu tests, extended cracks opened significantly during the tests, giving them the appearance of dark lines. As with the other notched Iosipescu specimens, extended cracks did not continue to grow throughout the tests on the 45° specimens. In fact, almost all of the crack extension occurred at crack initiation. At initiation, cracks immediately extended almost to the specimen edges. Crack extension essentially ceased after crack initiation. After testing, each specimen was either in two pieces or close to it. This contrasted significantly with other notched Iosipescu specimens, which remained intact throughout their tests.

Table 7 provides a summary of the critical stresses obtained from the 45° Iosipescu tests. As already noted, the specimen crack initiation and failure stresses are identical for these tests. Obviously, these tests exhibited the smallest difference between crack initiation and failure stress levels of all of the Iosipescu tests. The critical stress values obtained from these tests exhibited little experimental scatter. The failure stress continued the decreasing trend exhibited in going from the 0° to the 15° and 30° fiber orientations. The average stress at crack initiation was essentially the same as that obtained from the 30° tests.

7.4.6 Overall Standard Notched Iosipescu Test Characteristics

The standard notched Iosipescu tests exhibited a number of common characteristics. First, for all of the standard (0°, 15°, 30°, and 45°) tests, crack extension occurred from the cut center notch before cracking occurred at the v-notch roots. Cracking at the v-notch roots appears to be a common trait of all Iosipescu tests on unidirectional composites. It presents problems because it is not entirely clear what the specimen stress state is after v-notch cracking occurs. As mentioned in Section B2.1, a very rough finite element analysis by Walrath and Adams [31] has indicated that for 0° specimens without a center notch the formation of v-notch cracks does not significantly alter

test section stress state, other than to possibly decrease the v-notch root stress concentration. Whether this is completely true and whether it is true for specimens of other fiber orientations is not clear. The fact that each notched Iosipescu specimen was able to achieve crack initiation before v-notch cracking occurred is encouraging because it indicates that the crack initiation stress values are not influenced by extraneous factors related to the specimen and its geometry. Another common characteristic of the standard notched Iosipescu tests is that all specimens exhibited extended cracks that reached a certain length and then stopped growing. It is not apparent exactly what caused this behavior, but it is likely related to the geometry of the Iosipescu specimen. In other types of far-field applied shear tests, such as the torsion of cylindrical tubes, similar crack growth behavior would probably not be observed. Finally, all of the standard Iosipescu shear specimens exhibited crack initiation away from their notch tips. The location of crack initiation was highly consistent for specimens having the same fiber angle.

The standard notched Iosipescu tests also exhibited a number of obvious trends that were a function of their fiber orientation. One of these trends was the length of the extended cracks when they stopped growing. As the fiber orientation was increased, the final length of the extended cracks increased, until, for the 45° specimens, cracks extended almost to the edges of the specimen. Another obvious trend in the tests was that of location of crack initiation along the cut notch border as a function of fiber angle. Clearly, as the specimen fiber orientation was increased, the location of crack initiation became closer to the notch tip. The Iosipescu specimens also exhibited a distinct trend in the visual appearance of their crack growth behavior. After crack initiation, extended cracks in the 0° Iosipescu specimens extended only a short distance, and then stopped. From that point on the 0° specimens would continue to withstand a significant increase in applied load before reaching an ultimate applied load value. Visually, crack extension in the 0° Iosipescu specimens most resembled what might be observed in a very ductile material. As specimen fiber angle was increased, this behavior changed dramatically, to something that resembled what might be observed in a highly brittle material. This trend is substantiated in the decreasing difference between crack initiation and failure stresses as a function of Iosipescu specimen fiber angle. For the 45° specimens, the crack initiation stress was the ultimate stress the specimen could withstand.

It is also important to note the observed trends in the averaged critical stresses that were obtained from the standard Iosipescu tests. The averaged failure stresses consistently and steadily decreased as specimen fiber orientation was increased. The average crack initiation stresses, however, showed a distinct decrease in going from fiber orientations of 0° to 15°, but then increased in going from 15° to 30°. The crack initiation stresses for the 30° and 45° specimens were essentially equal. This trend in the crack initiation stresses intuitively seems peculiar. Whether or not it can be predicted analytically will act as an important test of the normal stress ratio theory.

7.5 Overall Notched Specimen Experimental Results

The results just detailed for all of the notched specimen tests exhibit a number of notable characteristics. The first is that the tests themselves and their crack extension behavior were highly diverse. Specimens were subjected to a wide range of ratios of applied far-field normal and shear stresses. Also, the magnitudes of the critical stresses obtained from the tests covered a wide range. Some of the specimens experienced only highly unstable crack extension, fracturing in a brittle manner. Other specimens exhibited only stable crack extension with no final fracture event occurring at all. Still others exhibited behavior inbetween these two extremes. The locations of crack initiation along the periphery of the cut notches varied from the notch tip to very far away from it. Specimens exhibited varied amounts of symmetry with respect to the stress causing crack initiation from each tip. Finally, the opening displacement of the original cut notch and the extended cracks were each found to vary greatly from test to test. The difficulty of finding an analytical technique and theory that can describe the crack growth behavior for tests exhibiting such diverse crack extension behavior cannot be overemphasized. Despite the diverse crack extension behavior exhibited by all of the tests performed in this study, one obvious consistency existed. In all of the tests, crack extension clearly occurred along the fiber direction. This reflects the strong tendency for crack extension to occur along the fiber direction in graphite-epoxy.

The crack opening displacement gage proved to be a an almost indispensable tool in characterizing crack extension behavior, and in identifying or defining specimen failure events. Its usefulness was especially significant in that no other simple method is available for monitoring crack opening or extension. Applied stress vs. c.o.d. plots provided a means of monitoring specimen crack growth behavior in a way similar to the way stress vs. strain plots are used in unnotched material testing. In some cases, data from the c.o.d. gage also acted as a good indicator of crack initiation. In these cases, however, the crack initiation was also easily identifyable either visually and/or by a decrease in applied load. This was most likely a consequence of the tests that were run for this study. Clearly, a crack opening displacement gage is only able to provide an indication of crack initiation if it results in an opening of the original notch. This suggests that initiation of crack extension along or close to the axis of the original notch ($\varphi = 0$) will be most detectable by a c.o.d. gage. Except for the 90° tensile coupon tests, the notched specimen tests in this study had cracks extend at an angle of at least 45° from the original notch axis. Despite this, the c.o.d. gage was still able to indicate crack initiation in the 30° and 45° Iosipescu specimens. In these cases the problem of crack extension away from the original notch axis was compensated for by the fact that cracks extended a significant distance at initiation as part of a single sudden event. Again, however, in these tests this crack initiation event was easily observable anyway.

It is the author's opinion that a crack opening displacement gage can be of even greater use than it was in this study if a test matrix is chosen so as to exploit its use. Certainly, choosing tests with predicted directions of crack extension closer to the axis of the original notch would be a first step. Another idea is to experiment with orienting the gage other than perpendicular to the original cut notch axis. Orienting the gage so that it is perpendicular to the expected direction of crack extension could aid in detecting crack initiation. Another possibility is to use two gages oriented at 90° to each other or to have a single biaxial gage fabricated. If crack opening displacement were measured in two directions at once, a complete measure of cut notch displacement could be obtained in all directions through the use of simple vector transformations.

8.0 Comparison of Theory and Experiment

8.1 Crack Extension Directions

Table 8 provides a direct comparison between the directions of crack extension observed in the experiments of this study and those predicted by the normal stress ratio. A comparison between experiment and analysis for the 15° off-axis coupon tests has already been provided in Table 2. The values provided in Table 2 are taken from the analysis performed in [25]. That analysis used AS4/3501-6 graphite-epoxy material property values other than those given in Table 3 and a different method of accounting for the influence of aspect ratio on the applied stress state. In [25], the amount of applied shear stress for a given applied axial stress is based upon the stress state predicted by the elasticity solution Pagano and Halpin [28] at the location of the crack. This method predicts higher shear stress values than the method used in this study does. A comparison between the predictions provided in Table 2 and those provided in Table 8 show that the crack growth direction predictions of the normal stress ratio theory are only slightly altered by the change in material properties and applied stress state.

A comparison of the experimental and analytical values provided in Table 8 show a strong agreement between theory and experiment. In some cases, the predictions of the normal stress ratio

Table 8. Crack Extension Directions

Comparison of Theoretical and Experimental
Crack Growth Directions
All Tests

Specimen Type[1]	Experimental Direction of Crack Extension[2]	Direction of Crack Extension Predicted by Normal Stress Ratio[1]
	0°, 45°, and 90° Notched Coupon Tests	
0° Specimens	±90°	±87°
45° Specimens	-45°	-43°
90° Specimens	0°	0°
	15° Off-Axis Notched Coupon Tests	
	90° Notch	
A.R.= 1	-75°	-72°
A.R.= 4	-75°	-73°
A.R.= 8	-75°	-73°
	105° Notch	
A.R.= 1	-90°	-87°
A.R.= 4	-90°	-88°
A.R.= 8	-90°	-88°
	Notched Iosipescu Shear Tests	
0° Specimens	-90°	-89°
15° Specimens	-75°	-75°
30° Specimens	-60°	-60°
45° Specimens	-45°	-45°

[1]All 0°, 45°, and 90° coupons had notches at 90° to the specimen loading axis (horizontal). Each Iosipescu test specimen had a cut notch at 90° (vertical).

[2]All angles are measured with respect to the cut notch, with an extension direction of 0° corresponding to crack growth collinear to the notch. See the angle φ in Figure 9.

theory are exact. The maximum disagreement between theory and experiment is 3°. As pointed out in Section 2.1.2, this type of predictive behavior may seem somewhat trivial, considering the strong tendency for graphite-epoxy to exhibit crack extension along the fiber direction. The com-

parison provided in Section 2.1.2 clearly indicates, however, that the ability to consistently predict crack extension direction in graphite-epoxy is not shared by other approaches and theories.

8.2 *Critical Stresses*

8.2.1 Baseline Test

As previously mentioned, in order to predict critical stresses, the normal stress ratio theory must be applied at a specific radial distance from the crack tip. For clarity, in this study the distance from the crack tip will be nondimensionalized with respect to the half-crack length in the form of the fraction $\frac{r}{a}$. The nondimensionalized specified distance from the crack tip will thus be referred to as $r_o = \frac{r_{(specified)}}{a}$. In order to apply the theory to predict critical stresses, a value for r_o must be found experimentally from a baseline test. Once a value for r_o is found, it is treated as a material constant. The theory can then be applied to obtain a critical stress prediction for a test with any fiber or notch orientation or applied stress state. Because all predictions are dependent on the value of r_o calculated from the baseline test, it is important to use a baseline test for which the critical stress is not ambiguous and can be consistently determined experimentally. Thus, specimens experiencing no stable crack extension and consistent fracture stress values are desirable.

In this study, the 90° coupon test was chosen as the baseline test. This test was chosen for a number of reasons. First, by orienting the notch along the fiber direction, crack extension was made to be collinear with the original cut notch (along $\varphi = 0°$). For such crack extension in a composite, a macroscopic stress analysis (one using stress intensity factors [15]) has been shown to be applicable. Second, the test is clearly normal stress dominated, therefore application of the normal stress ratio theory should be valid for this test even if it is not for others. Third, experimentally, no slow crack extension was observed for this test. As a result, the critical stress was not

ambiguous and easily determined as the fracture stress. Finally, the tests themselves yielded consistent fracture stress values.

Using the average value of fracture stress for the three baseline tests (2.81 ksi) as the applied far-field stress (σ^{∞}) , the normal stress ratio theory was applied along the predicted direction of crack extension (φ = 0°). Along this direction, the normal stress ratio equalled 1 at a value of r_o = 0.06573. The theory was then applied to the tensile coupon and Iosipescu tests presented in this study to obtain the applied far-field stresses to provide a normal stress ratio value of 1 at r_o = 0.06573, along the predicted direction of crack growth. Because the notches in the 15° off-axis specimens were twice as long as those in the baseline test specimens, the predictions for those tests were normalized with respect to the square root of the notch lengths. The predicted critical stress values are given in Table 5, Table 6, and Table 7.

8.2.2 Fifteen Degree Off-Axis Tests.

Based on the values given in Table 5, a number of comparisons can be made between the experimentally observed 15° off-axis specimen critical stresses and those predicted by the normal stress ratio. First, the overall magnitudes of the critical stress predictions provided by the normal stress ratio theory agree well with experimental values. Second, the theory provides highly accurate critical stress predictions for the specimens with an aspect ratio of 4. For each of the two specimen configurations having an aspect ratio of 4, the predicted critical stress is very close to the average observed stress at crack initiation. Third, the theory provides critical stress predictions for the specimens of aspect ratio 8 that are lower than those observed experimentally. Why this occurs is not readily apparent, however the discrepancy between theory and experiment is not severe. Finally, the theory appears to predict higher critical stresses than were observed experimentally for the two specimen configurations having an aspect ratio of 1. The prediction for the specimens with 105° notches corresponds best with the average experimental fracture stress, while the prediction for the specimens with 90° notches is higher than both the averaged experimental critical stresses. At

this point in the research, the most suspect portion of the analysis of the specimens of aspect ratio 1 is the use of the off-axis coupon solution by Pagano and Halpin to provide appropriate far-field stresses. In accounting for the different aspect ratios of the tested specimens, the only variable that was altered was the value of applied shear stress relative to the applied axial stress, as specified by the Pagano and Halpin analysis. This shear stress acts to increase critical stress values. It is not believed that the applied shear stress predicted by the solution for an aspect ratio of 1 corresponds well with the actual stress state. Some concern also exists for the role that end effects may play in the problem, for small aspect ratio specimens. In actual tests, a far-field displacement is applied to the specimen instead of a far-field stress. In using the infinite plate solution of Lekhnitskii, it is assumed that end effects are negligible, and that far-field displacement boundary conditions can be represented by carefully chosen far-field stresses. For small aspect ratio notched specimens, this may not be the case. Current efforts by other researchers in the ESM department at Virginia Tech involves modelling the off-axis problem using a finite element solution and various displacement boundary conditions to determine how the results of such an analysis compare with those from the analysis used in this study.

Two distinct trends are noticeable in the predicted critical stresses for the 15° off-axis tests given in Table 5. The most obvious is an increase in predicted critical stress with a decrease in aspect ratio. This trend was not apparent in the experiments. With respect to this trend, it will be noted again that the changes in predicted critical stresses with aspect ratio, and thus this observed trend, are dependent entirely upon the far-field stresses predicted by the Pagano and Halpin solution. Also, the predicted trend is by far most pronounced in going from specimens of aspect ratio 4 to those of aspect ratio 1. Because of these facts, it is likely that the strength of the trend in the predictions is exaggerated by the aforementioned possible limit in the applicability of the Pagano and Halpin solution for specimens of small aspect ratio. Thus it is possible that the scatter in the experimental values has acted to obscure a subtle trend in the results with respect to aspect ratio. Still, however, this lack of agreement between theory and experiment is significant. Further investigation into the influence of aspect ratio on predicted and experimental critical stresses is warranted.

The second trend apparent in the 15° off-axis test predictions in Table 5 is that the predicted critical stress for each specimen with a 90° notch is higher than that for the 105° notched specimen having the same aspect ratio. As outlined in the section on experimental results, this trend was observed experimentally, with the stresses at crack initiation in some of the specimens with 90° notches actually being higher than the stresses at fracture in the 105° notched specimens of the same aspect ratio. Because this trend in the predictions is independent of aspect ratio, it is independent of the possible limits of the Pagano and Halpin analysis for specimens of small aspect ratio. As a result, this predicted trend appears to be a consequence of application of the normal stress ratio theory only.

8.2.3 Zero, Forty-Five, and Ninety Degree Tensile Coupon Tests

Table 6 provides comparisons of predicted and experimentally obtained critical stress values for the 0°, 45°, and 90° tensile coupon tests. Obviously, because the 90° test has been used as the baseline test for this study, a comparison between prediction and experiment cannot be made for it. The normal stress ratio theory prediction of 5.02 ksi for the 45° off-axis test is higher than the average critical stress value of 4.12 ksi obtained from experiment, however the agreement is reasonable. For the 0° tests, the normal stress ratio prediction of 20.9 ksi agrees best with the crack initiation stresses obtained from the experiment, however, it is clearly overly conservative. The difficulty noted in observing extended cracks in the 0° tensile coupon specimens could have contributed to the discrepancy between theory and experiment. It is possible that some type of crack initiation event occurred before extended cracks were observed. As a result, any error in obtaining the experimentally observed stresses at crack initiation would likely cause higher values. This potential source of error in the experiments cannot account for the magnitude of the discrepancy between the theoretical and experimental critical stress values provided in Table 6, however. The normal stress ratio theory does appear to pick up critical stress trends for the coupon tests. Further

comparisons between theory and experiment for a range of off-axis angles are needed to help pinpoint the source of any inaccuracies in the theory for these tests.

8.2.4 Iosipescu Tests

Table 7 gives comparisons of the predicted and experimental critical stresses from the Iosipescu tests. The critical stresses of 3.10, 2.88, 3.01, and 3.80 ksi predicted by the normal stress ratio are slightly lower than observed average stresses at crack initiation of 4.03, 3.50, 4.13, and 4.08 ksi, but agree well in general. The agreement between theory and experiment is even more striking with respect to their trends with respect to specimen fiber orientation. Both experiment and theory provide critical stresses that decrease in going from 0° to 15° fiber orientations and then increase in going from 15° to 30° orientations. The theory predicts a subsequent increase in critical stress values in going from 30° to 45° fiber orientations that is not exhibited in the crack initiation stress results, however. The approximations made in analyzing the Iosipescu test, especially the assumption of a pure shear far-field stress state, suggest that this single disagreement between theory and experiment may not be significant. Because of their weakness in the horizontal direction, the presense of tensile stresses along this direction in the 45° Iosipescu specimens could easily lower experimental crack initiation stress values. It is also important to note that the normal stress ratio critical stress predictions do not agree with the experimentally observed failure stresses in magnitude or with respect to the trends exhibited as a result of changing specimen fiber angle. As a result, stresses at crack initiation appear to be the critical stresses predictable by theory for these tests.

The agreement between critical stress values from the Iosipescu tests and theory is especially significant in that the normal stress ratio is entirely ignorant of the shear strength of the material. As equation (4) indicates, only the longitudinal and transverse tensile strengths of the material are included in the theoretical formulation. The agreement of the theory with shear test results suggests that the strength of a notched specimen under far-field shear loading can be predicted using an analysis based solely on normal stress and normal strength.

8.2.5 Overall Stress Prediction Results

The comparisons between theoretical and experimental critical stresses values for all of the tests in this study indicate that, for an analysis based on original flaw geometry, stresses causing crack initiation are most comparable to theory. This is most strongly indicated in the the comparison between analysis and experiment for the Iosipescu specimens. For the tests analyzed in this study, there was generally good agreement in critical stress value magnitudes and trends. The most significant exception to the relatively good experimental and theoretical correlation was the lack of an observed trend in crack initiation stresses with respect to aspect ratio for the 15° off-axis specimens. The normal stress ratio theory clearly predicts an increase in critical stress values with a decrease in aspect ratio. Also, the overly conservative prediction of the theory for the 0° tensile coupon test warrants further investigation. The most impressive correlation between theory and experiment occurred for the Iosipescu shear tests.

It is important to recognize that a large number of variables and assumptions that can affect critical stress predictions are involved in the analysis presented in this study. The assumptions of the analysis, which are outlined in Section 3.4, include an idealized crack geometry, approximate far-field stresses, and an infinite plate assumption. The most significant variable in the analysis is the parameter, r_o, which is obtained from a single test and hence forth assumed to be a material constant. The number of individual sources of error in predicted critical stress values highlights the significance of the agreement with experiment observed in this study.

8.2.6 Test Specimen Critical Stress Analyses

8.2.6.1 Tensile Coupon Tests

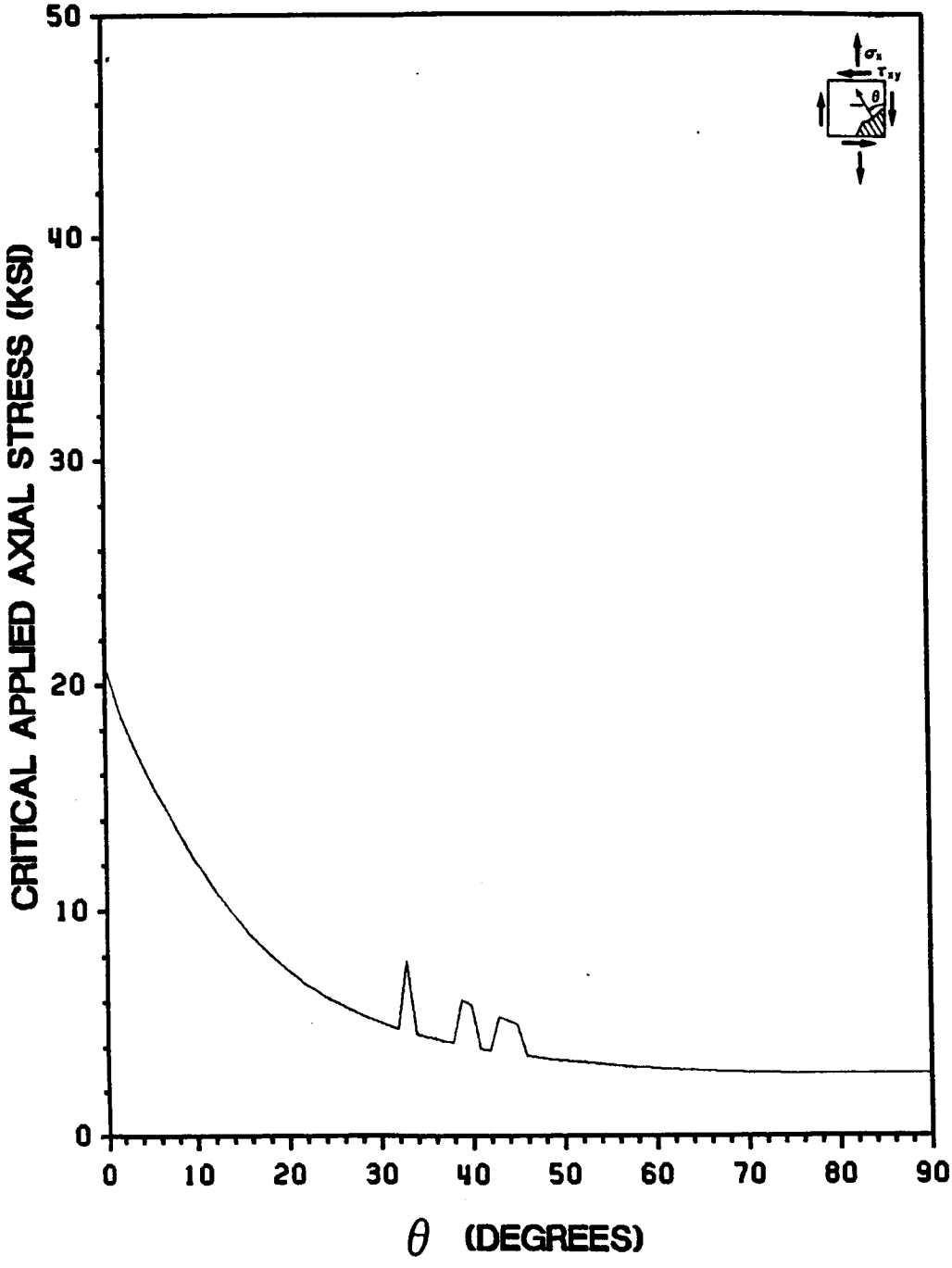

Figure 57. Predicted Critical Axial Stresses vs. Fiber Angle for Tensile Coupons with Horizontal Center Notches: Shear Coupling Effects Included, AS4/3501-6 Graphite-Epoxy

Because a value has been obtained for r_o from the 90° tensile coupon tests, any of the previous cases studied for the predicted direction of crack extension can now also be analyzed for predicted critical stresses. This has been done for the tensile coupon and Iosipescu specimen analyses outlined earlier in this study, with interesting results. Figure 57 provides a plot of predicted critical axial stress vs. off-axis angle for tensile coupon specimens, over the entire 0° to 90° off-axis angle range. The plot indicates a relatively smooth increase in predicted critical stress values from 2.81 ksi for a 90° coupon to 20.9 ksi for a 0° coupon, with most of the increase in critical stress values occurring at small off-axis angle values. This corresponds well with expected behavior.

Three peaks in the critical stress values are exhibited in the plot for fiber angle values between 30° and 50°. The strength of these peaks is significant, the largest of which, at 33°, has a predicted critical stress value of 7.81 ksi. This is approximately 3 ksi above nearby critical stress values. These peaks are disturbing in that they do not correspond to expected critical stress behavior. One of the peaks includes a fiber angle value of 45°. This explains why the normal stress ratio theory provides a critical stress value for the 45° off-axis test that is slightly higher than experiment. The 45° tensile coupon predicted critical stress value is slightly distorted by one of these three unexpected peaks in critical stress values.

It is important to observe that the peaks in critical stress values in Figure 57 correspond in location and shape to the three peaks in predicted direction of crack extension away from the fibers exhibited in the plot in Figure 34. An almost identical set of peaks is also exhibited in the crack growth direction plot for a tensile coupon without shear coupling effects included in Figure 24. In the direction prediction analyses accompanying Figure 24 and Figure 34 the problem of these peaks was not addressed because of their magnitude. In these plots, the largest deviation in the predicted direction of crack extension from the fibers is 3°. In looking at the magnitude of the normal stress ratio value, and hence the critical stress values it predicts, however, the peaks are of significant magnitude to warrant concern.

Because the peaks in the critical stress plots in Figure 57 are significant, it is important to determine their nature and source. The source of the peaks can be found by examining the plot of the directions of crack extension predicted by the tensor polynomial provided in Figure 23. That

plot exhibits sharp peaks at the same locations between 30° and 50° that the normal stress ratio plots in Figure 24 and Figure 34 do. As a result, it appears that the source of the peaks in normal stress ratio predictions is an error in the method used to program the Lekhnitskii solution. The solution program used in this study has been used extensively by this researcher and others at Virginia Tech without any errors becoming apparent. The plots provided in this study, however, particularly the critical stress plots, suggest a problem in the program's applicability to problems having certain orientations of the fibers with respect to the crack. It is believed that this is also the source of the sharp peaks in the Iosipescu specimen normal stress ratio direction predictions noted in Section 6.5.2 and the corresponding sharp peaks in critical stress predictions noted in the next section of this report.

8.2.6.2 Iosipescu Shear Specimen Tests

Figure 58 and Figure 59 provide plots similar to that in Figure 57 for the Iosipescu specimen with a notch oriented along the vertical axis and the fiber direction respectively. These plots show a significant resemblance to those provided in Figure 35 and Figure 36 of predicted directions of crack extension away from the fibers as a function of fiber orientation. The exception to this resemblance occurs in the plots for Iosipescu specimens with notches along the fibers, for fiber angles greater than 102°. In the crack growth direction plots, the values reach a peak of 46° at a fiber angle of 102°. In the critical stress plots, values continue to increase for fiber angles larger than 102°, reaching a predicted value of 99.0 ksi at 120°, the largest fiber angle analyzed. The critical stress plots also appear smoother than the crack growth direction plots because they are not as strongly affected by the use of 1° increments in the analysis.

The critical stress plot for an Iosipescu specimen with a vertical notch (Figure 58) exhibits the same type of sharp peaks noted in the direction prediction plot for the same specimen (Figure 35). An investigation into application of the tensor polynomial to this problem has shown that similar types of peaks are exhibited in a plot of its critical stress predictions as a function of

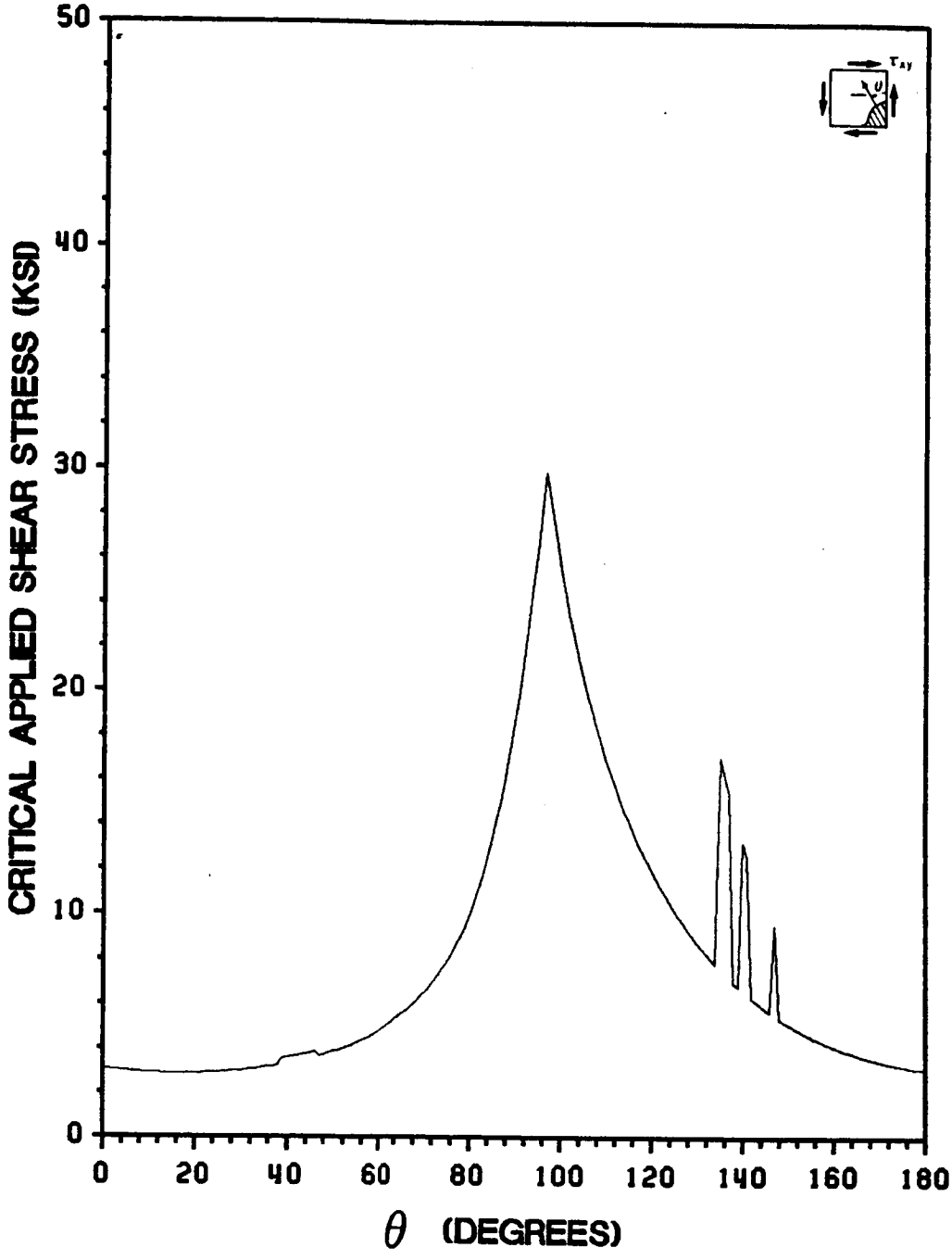

Figure 58. Predicted Critical Applied Shear Stress vs. Fiber Angle for Iosipescu Shear Specimens with Vertical Notches: Pure Shear Far-Field Loading, AS4/3501-6 Graphite-Epoxy

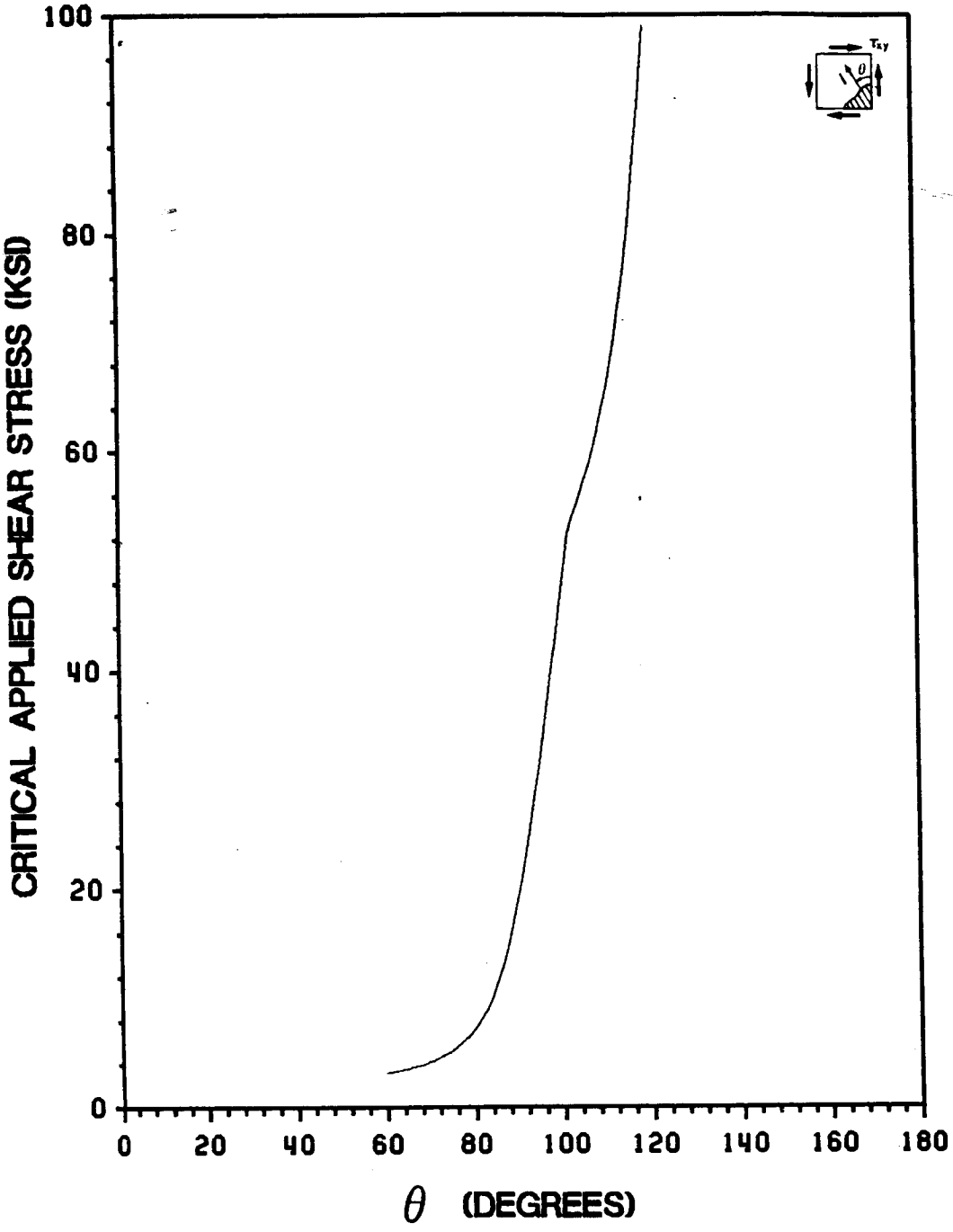

Figure 59. Predicted Critical Applied Shear Stress vs Fiber Angle for Iosipescu Shear Specimens with Notches Along the Fibers: Pure Shear Far-Field Loading, AS4/3501-6 Graphite-Epoxy

specimen fiber angle. As a result, the sharp peaks in predictions for this problem appear independent of the crack growth theory used. Also, these peaks occur at the same values of fiber orientation with respect to the notch that the peaks in the tensile coupon plot do. As a result, these peaks are likely related to the error in the method used to program the Lekhnitskii solution noted in the results for tensile coupons.

The apparent resemblance between critical stress and crack growth direction plots indicates that, as for the tensile coupon analysis, the predicted direction of crack extension exerts a strong influence on predicted critical stresses. For the Iosipescu test, this influence is so strong that for fiber orientations near 90° the theory actually predicts critical stress values that are higher than the ultimate shear strength on the principal material plane. For these cases, application of the normal stress ratio theory as a crack growth direction criterion only, as it was originally proposed, suggests that the theory is predicting crack extension across fibers. In applying it more fully as a predictor of critical stresses, it appears to be indicating that the far-field loading and orientation of the crack with respect to the fibers cause such a small normal stress ratio concentration that crack growth will not occur. The material is predicted to fail in pure shear before normal stress can cause a crack at the notch tip to open up and grow.

8.2.6.3 Re-evaluation of Crack Growth Direction Predictions

The Iosipescu specimen critical stress plots, and their corresponding plots of predicted direction of crack extension indicate that the use of the normal stress ratio theory solely as a predictor of crack extension direction may be incorrect. Instead, the crack growth direction predictions of the normal stress ratio theory may have to be used in conjunction with its critical stress predictions. At least some heretofore designated critical tests of the theory's ability to predict crack extension direction may instead be cases for which the theory is predicting that no crack extension will occur. Such cases do not represent critical tests of the ability of the normal stress ratio theory to predict crack growth direction because a crack growth theory cannot be expected to predict material be-

havior unless an existing crack dominates its behavior. Also, the normal stress ratio theory appears to actually be predicting no crack growth, instead of predicting crack growth across the fibers. It seems reasonable that an additional requirement of the theory be that if the predicted critical stress is above the strength of an unnotched material, then crack growth is predicted not to occur. Normal stress ratio critical stress predictions should therefore be compared to unnotched material strength predictions from an appropriate unnotched material theory, such as the tensor polynomial.

Although the critical crack growth direction cases identified in this study may not be tests of the normal stress ratio's ability to predict crack extension direction, they are still very important tests to run. If anything, their criticality has been heightened. Such tests would determine whether or not crack extension does occur in such cases. In the past, expected behavior has always been defined as crack extension along the fiber direction. Instead, expected behavior may be gross material failure without any crack extension. Performance of these tests may help determine exactly what expected behavior really is.

8.3 Locations of Crack Extension

One of the most notable characteristics of the notched specimen tests performed as a part of this study is that the location of crack extension along the periphery of the cut notch varied, depending on the far-field stress state and the orientation of the notch with respect to the fibers. The possible problems associated with using a sharp crack tip analysis to model an actual cut notch with a rounded tip have already been detailed in Sections 6.2 and 6.3. These observations and concerns provided motivation to compare the locations of crack initiation predicted by the rounded notch tip analysis procedure of Gurdal and Herakovich [37] to those observed in the tests of this study. This was done by simply substituting the elliptical notch solution of Savin [38] for the sharp crack analysis of Lekhnitskii [35] into the three-step analytical procedure used thus far in this study. The locations of crack extension for each of the experiments are detailed in the individual sections de-

scribing each test. Briefly, for the notched tensile coupon tests, the 0° and 90° specimens experienced crack initiation at the very tips of their notches. The 45° specimens experienced crack initiation at approximately -45° around the rounded notch tip. The 15° off-axis specimens exhibited varied locations of crack extension that appeared to be independent of notch orientation and aspect ratio. Because the 15° off-axis specimens did not exhibit a consistent location of crack extension, it appears that such specimens possess only a weak tendency for crack extension away from their notch tips. For the Iosipescu specimens, the locations of crack initiation steadily changed from being very far from the notch tip in the 0° specimens to being roughly at -45° around the rounded notch tip for the 45° specimens. The rounded notch analysis is applied here to see if it predicts in a qualitative way these same trends in crack initiation locations, while continuing to predict the correct directions of crack extension.

The results of the rounded notch analysis of the tests performed for this study are illustrated in Figure 60 through Figure 63. As in Figure 27, the results are represented graphically, with the location and direction of crack initiation designated by a solid line extending from the ellipse boundary. Because there was not an apparent crack initiation location trend with respect to the different 15° off-axis specimen configurations, only one configuration, that having a horizontal notch and an aspect ratio of 8, was analyzed in this section. As a group. the figures indicate that application of the normal stress ratio theory within an elliptical notch solution results in predicted directions of crack extension that are essentially correct for all of the cases studied, while allowing crack initiation to occur away from the tip of the ellipse. The magnitude of the largest error in the predictions is 4°. Furthermore, the crack initiation location predictions of the analysis appear to provide excellent qualitative correlation with those observed experimentally.

Both of the graphical representations provided in Figure 60 indicate crack initiation from the tip of the notch, as observed in the 0° and 90° tensile coupon specimens. Note that the line indicating crack extension from the notch tip in the 90° specimen coincides exactly with the horizontal reference line of the plot. In Figure 61, both modelled test cases show crack initiation away from the notch tip, as observed experimentally in the 15° and 45° off-axis tensile specimens. Figure 62 and Figure 63 provide graphical representations of the predicted locations of crack initiation for the

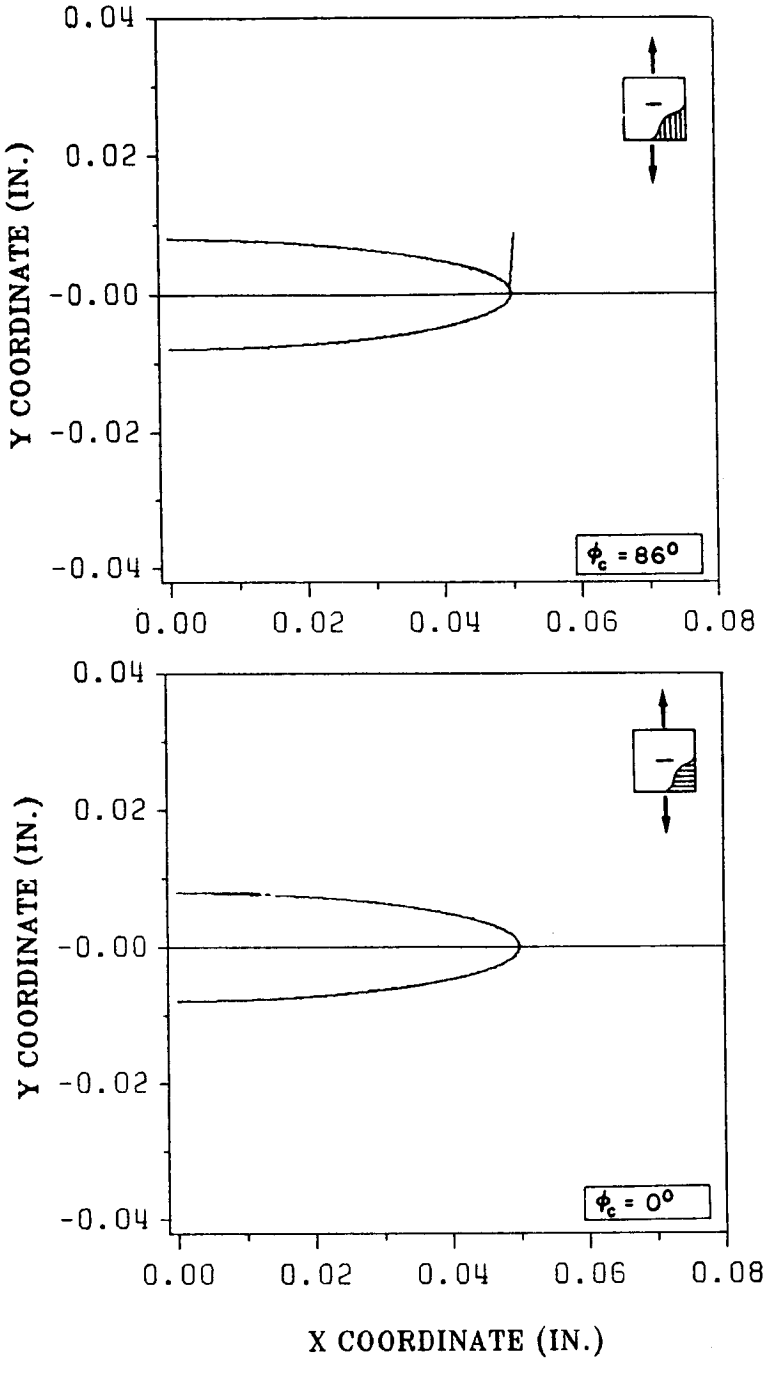

Figure 60. Predicted Locations of Crack Initiation for 0° and 90° Tensile Coupons

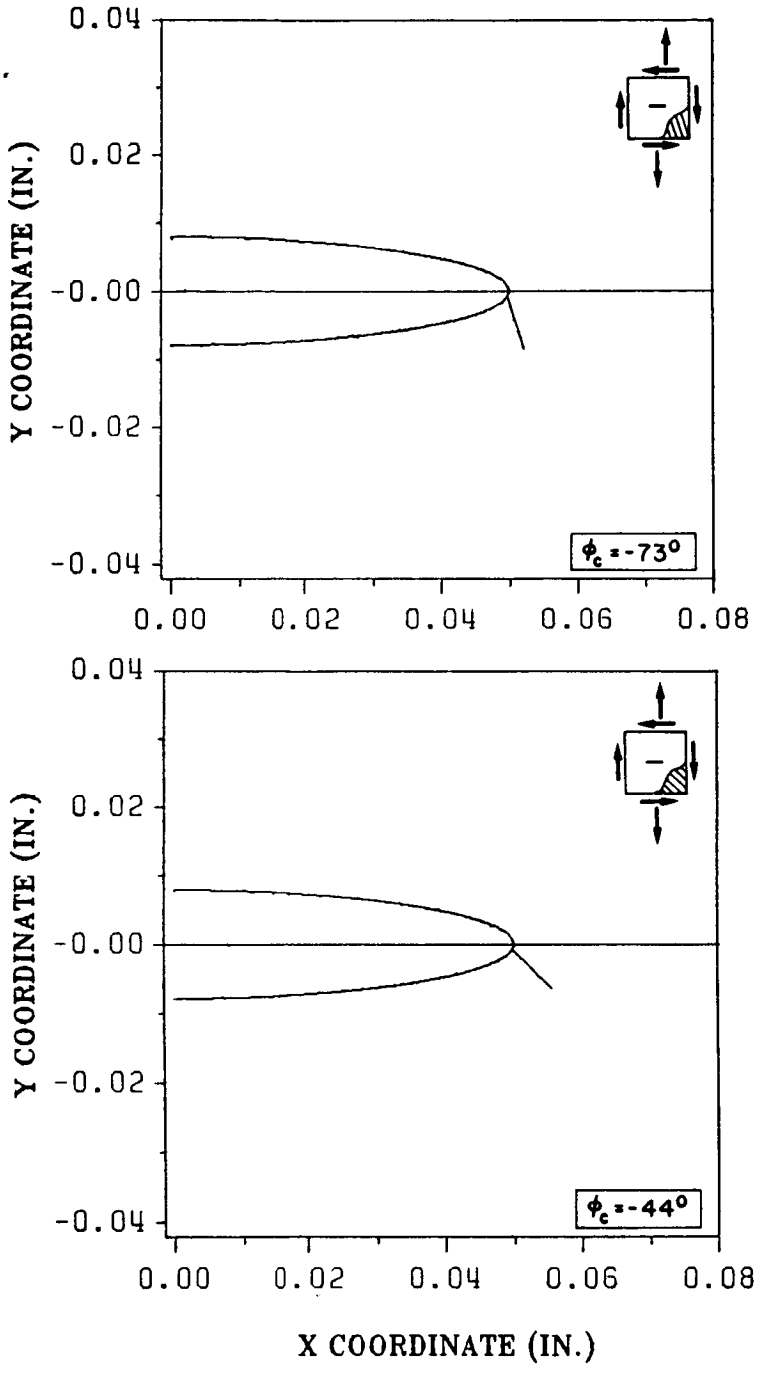

Figure 61. Predicted Locations of Crack Initiation for 15° and 45° Off-Axis Tensile Coupons

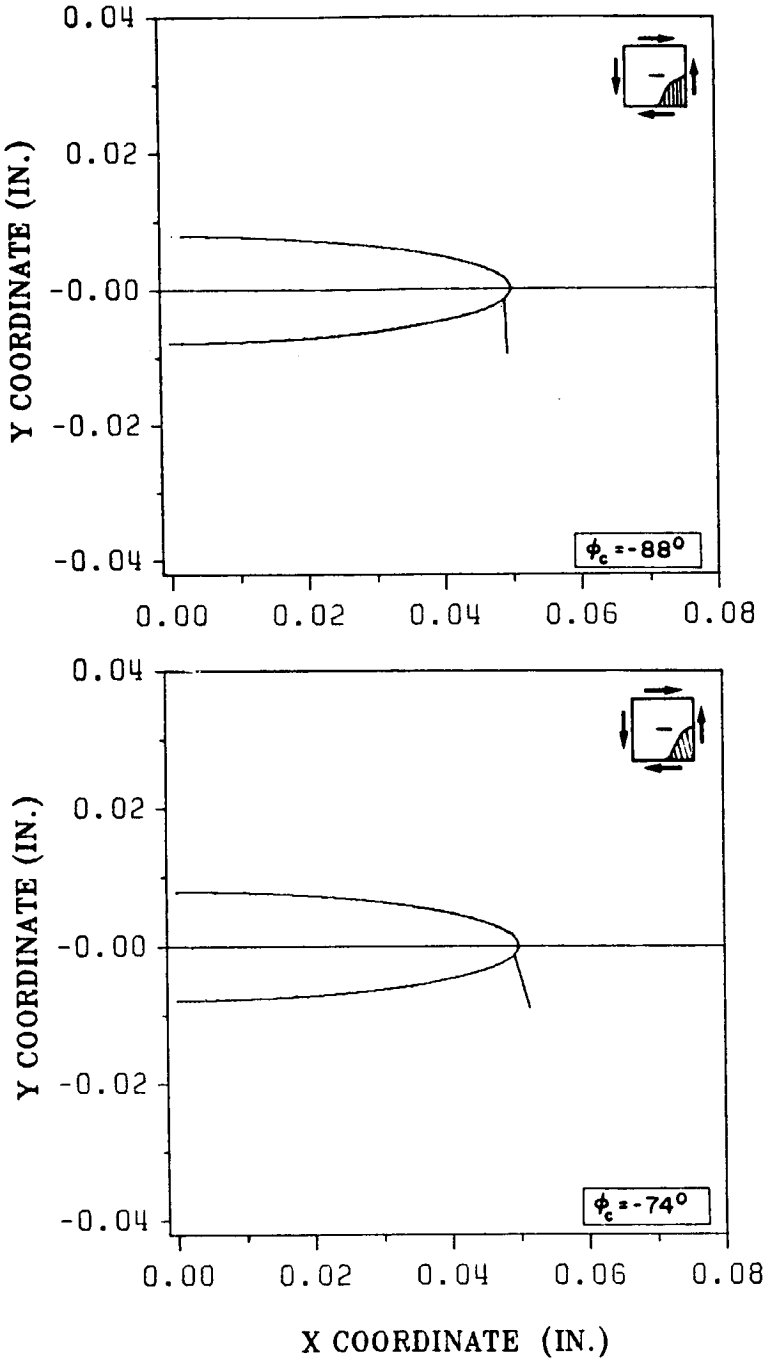

Figure 62. Predicted Locations of Crack Initiation for 0° and 15° Iosipescu Shear Specimens

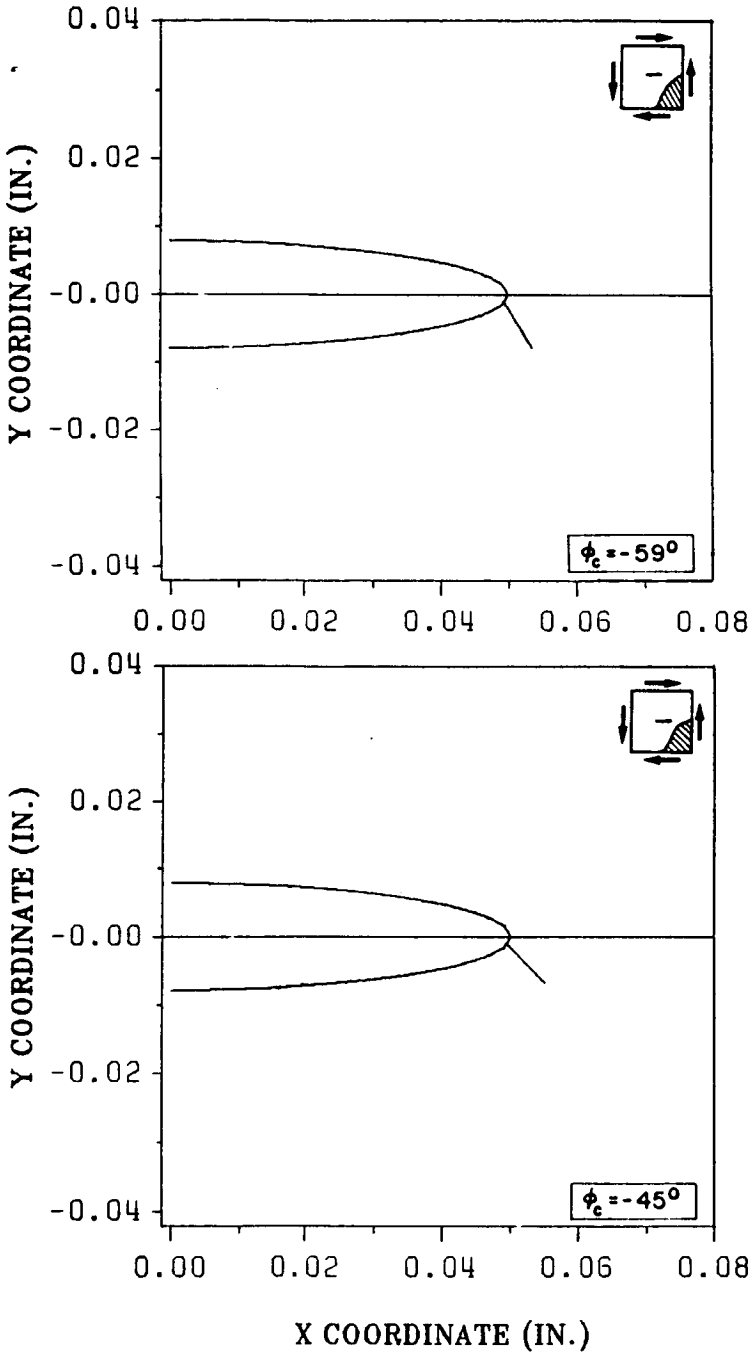

Figure 63. Predicted Locations of Crack Initiation for 30° and 45° Iosipescu Shear Specimens

Iosipescu tests. As observed experimentally, the predicted location of crack initiation is away from the notch tip for all of these tests. The observed trend in location of crack extension with respect to fiber orientation is also well represented in the analysis predictions. The analysis predicts that the location of crack initiation will move closer to the notch tip with an increase in fiber angle, up to a fiber angle value of 30°. An identical location of crack initiation is predicted for the 30° and 45° Iosipescu specimens.

9.0 Conclusions and Comments

A large number conclusions have been made based upon the analytical and experimental work of this study. The most significant of them are as follows:

- Application of the normal stress ratio theory within a macroscopic-level sharp crack analysis shows significant potential for analyzing the problem of a through-the-thickness center notch in a unidirectional fibrous composite.

- Through its application within a rounded notch tip analysis, the normal stress ratio theory has also demonstrated a qualitative ability to relate problem parameters and notch tip shape to observed locations of crack initiation along actual rounded notch tip borders.

- Extension of the normal stress ratio theory to predict critical stresses has provided a significant number of added opportunities to test its validity.

- The critical tests that could not be performed in this study using the Iosipescu shear specimen should be attempted using another shear test method.

Application of the normal stress ratio theory within a sharp crack stress solution has provided reasonable predictions for the experiments performed. As has been noted in previous work, the

theory has exhibited a strong ability to correctly predict crack extension direction. The theory's correlation with experimental stresses at crack initiation was also good. The theory provided reasonable estimates of the magnitude of the stress at crack initiation for individual tests and was also able to follow observed crack initiation stress trends. The most notable exceptions to this were the normal stress ratio theory's critical stress prediction for the 0° tensile coupon and its prediction of an increase in crack initiation stress with a decrease in aspect ratio in the 15° off-axis specimens. Each of these predictions did not correspond well with experiment. The comparison of predicted and observed critical stresses suggests strongly that although crack initiation stresses may be predictable by an analysis based on original geometry, failure stresses generally are not.

Through its application within an elliptical notch stress solution, the theory was also able to qualitatively predict the location of crack initiation along the boundary of an actual rounded notch tip. This was done while still providing predicted directions of crack extension that were essentially as accurate as those provided through application of the theory within the sharp crack solution. This suggests that future efforts should include a more thorough application of a rounded notch tip model. In particular, use of such a model to predict crack initiation stresses is suggested. As a group, the results from this study indicate that positive steps have been taken in relating quantitative and qualitative experimental crack growth behavior with theoretical predictions. The predictive abilities of the normal stress ratio theory have been evaluated using results from specimens subjected to varied ratios of far-field applied stresses.

Extension of the normal stress ratio theory to predict critical stresses offered a strong test of the theory's validity. The normal stress ratio theory was most strongly tested in analyzing the notched Iosipescu shear tests. The ability of the theory to provide reasonable critical stress predictions for notched shear specimens is especially significant in that the theory does not include local shear stresses or material shear strengths in its formulation. Because of the potential added opportunities it offers to test the theory, future analytical efforts should include use of the normal stress ratio theory as a predictor of critical stresses.

The critical shear tests outlined in Table 4, which include the critical test case illustrated in Figure 25, could not be performed using the Iosipescu shear test because of the weakness of the

specimens along the horizontal axis. It is important that these tests be performed using another shear test method in order to determine correct experimental behavior. Application of the normal stress ratio theory within a sharp crack model to the analysis of these tests results in the prediction of either crack extension other than along the fiber direction or specimen shear failure before the critical stress causing crack initiation can be reached. By applying the theory to these cases within an elliptical notch analysis, it appears that crack extension along the fiber direction may be predicted. The determination of which, if any, of these events does occur for these tests can provide significant insight into the validity of the normal stress ratio theory and its method of application.

A number of other supplementary experimental research efforts are suggested by the work of this study. Further work in attempting to correlate theory with experiment clearly remains to be done. A more thorough testing of the theory's critical stress predictions for notched tensile coupons of AS4/3501-6 graphite-epoxy is needed, the results of which could be compared to the plot of Figure 57. A cause for the lower than observed critical stress predictions of the theory for the 0° coupons of this study could probably be obtained from such an effort. An investigation of the influence of aspect ratio on observed and predicted critical stresses for off-axis coupons could also be performed. Investigations paralleling this one using a different material system are also suggested as supplemental research efforts. A less anisotropic material with more likelihood for observed and/or predicted crack extension across fibers would likely provide more critical tests of the theory's ability to predict crack growth direction.

Based on the results of this study, at least one important analytical investigation should be performed as a part of future research. That task is to identify the cause of and perhaps remedy the observed peaks in the normal stress ratio predictions due to an apparent error in the computer formulation of the Lekhnitskii solution. Again, the solution has provided reasonable results in past work and the problems noted in this study appear to occur only for certain values of fiber orientation with respect to the notch. Finally, a number of other research topics not directly suggested by the results of this study could provide significant insight into the problem of the applicability of the normal stress ratio theory. Appendix C contains a summary of three experimental methods for the testing of individual assumptions of the normal stress ratio theory. It is the author's opinion

that further composite crack growth research along these and other avenues will allow the determination of whether the balance of local normal stress with a reasonable estimate of normal strength does indeed act as a principal controlling parameter in flawed composite fracture.

References

1. Griffith, A. A., "The Phenomena of Rupture and Flow in Solids," *Phil. Trans. Roy. Soc. of London*, A 221, 1921, pp. 163-197.

2. Irwin, G. R., "Analysis of Stresses and Strains Near the End of a Crack Traversing a Plate," Trans. ASME, *Journal of Applied Mechanics*, Vol. 24, 1957, pp. 361-364.

3. Erdogan, F., and Sih, G. C., "On the Crack Extension in Plates Under Plane Loading and Transverse Shear," ASME, *Journal of Basic Engineering*, Vol. 85, 1963, pp. 519-527.

4. Sih, G. C., "A Special Theory of Crack Propagation," *Method of Analysis and Solutions to Crack Problems*, edited by G. C. Sih, Wolters-Noordhoff, 1972, pp. XXI-XLV.

5. Sih, G. C., and MacDonald, B., "Fracture Mechanics Applied to Engineering Problems - Strain Energy Density Fracture Criterion," *Engineering Fracture Mechanics*, Vol. 6, 1974, pp. 361-386.

6. Theocaris, P. S., Kardomateas, G. A., and Adrianopoulos, N. P., "Experimental Study of the T-Criterion in Ductile Fractures," *Engineering Fracture Mechanics*, Vol. 17, 1982, pp. 439-447.

7. Theocaris, P. S., and Adrianopoulos, N. P., "The T-Criterion Applied to Ductile Fracture," *International Journal of Fracture*, Vol. 20, 1982, pp. R125-R130.

8. Yehia, N. A.B., "On the Use of the T-Criterion in Fracture Mechanics," to be published in *Engineering Fracture Mechanics*.

9. Nuismer, R. J., "An Energy Release Rate Criterion for Mixed Mode Fracture," *International Journal of Fracture*, Vol. 11, 1975, pp. 245-250.

10. Swedlow, J. L., "Criteria for Growth of the Angled Crack," *Cracks and Fracture*, ASTM STP 601, American Society for Testing and Materials, 1976, pp. 506-521.

11. Zweben, C., "Fracture Mechanics and Composite Materials: A Critical Analysis," *Analysis of the Test Methods for High Modulus Fibers and Composites*, ASTM STP 521, American Society for Testing and Materials, 1973, pp. 64-67.

12. Wang, S. S., and Choi, I., "The Interface Crack Between Dissimilar Anisotropic Materials," Trans. ASME, *Journal of Applied Mechanics*,Vol. 50, March, 1983, pp. 169-178.

13. Wang, S. S., and Choi, I., "The Interface Crack Behavior in Dissimilar Anisotropic Materials Under Mixed-Mode Loading," Trans. ASME, *Journal of Applied Mechanics*,Vol. 50, March, 1983, pp. 179-183.

14. Goree, J. G., and Wolla, J. M., "Longitudinal Splitting in Unidirectional Composites, Analysis and Experiments," NASA CR-3881, April, 1985.

15. Wu, E. M., "Fracture Mechanics of Anisotropic Plates," *Composite Materials Workshop*, edited by S. W. Tsai, J. C. Halpin, and N. J. Pagano, Technomic Press, Stamford, CT, 1968, pp. 20-43.

C - 3

16. Tsai, S. W., and Wu, E. M., "A General Theory of Strength for Anisotropic Materials," *Journal of Composite Materials*, Vol. 5, 1971, pp. 58-80.

17. Sih, G. C., Chen, E. P., Huang, S. L., and McQuillen, E. J., "Material Characterization of the Fracture of Filament-Reinforced Composite," *Journal of Composite Materials*, Vol. 9, 1975, pp. 167-186.

18. Buczek M. B., and Herakovich, C. T., "A Normal Stress Criterion for Crack Extension Direction in Orthotropic Composite Materials," *Journal of Composite Materials*, Vol. 19, 1985, pp. 544-578.

19. Buczek, M. B., and Herakovich, C. T., "Finite Element Models for Predicting Crack Growth Characteristics in Composite Materials," VPI-E-82-29, Virginia Tech, Oct., 1982.

20. Wu, E. M., "Strength and Fracture of Composites," *Composite Materials*, Vol. 5, edited by L. J. Broutman, Academic Press, New York, 1974, pp. 191-247.

21. Wu, E. M. "Failure Criteria to Fracture Mode Analysis of Composite Laminates," Advisory Group for Aerospace Research and Development Conference Proceedings, AGARD-CP-163, North Atlantic Treaty Organization, 1974.

22. Lo, K. H., Wu, E. M., and Konishi, D. Y., "Failure Strength of Notched Composite Laminates," *Journal of Composite Materials*, Vol. 17, 1983, pp. 384-398.

23. Herakovich, C. T., Gregory, M. A., and Beuth, Jr., J. L., "Crack Growth Direction in Unidirectional Off-Axis Graphite-Epoxy," in *Mechanical Characterization of Load Bearing Fibre Composite Laminates*, (Cardon and Verchery, eds.), Elsevier Applied Science Publishers, New York, 1985, pp. 97-114, also available as CCMS-84-17, VPI-E-84-34, Virginia Tech, Oct., 1984.

24. Gregory, M. A., Beuth, Jr., J. L., Barbe, A., and Herakovich, C. T., "Application of the Normal Stress Ratio Theory for Predicting the Direction of Crack Growth in Unidirectional Composites," *Fracture of Fibrous Composites*, (Herakovich, C. T., editor), ASME, AMD Vol. G00294, New York, 1985, pp. 33-42.

25. Beuth, Jr., J. L., Gregory, M. A., and Herakovich, C. T., "Crack Growth in Unidirectional Graphite-Epoxy Under Biaxial Loading," *Experimental Mechanics*, Vol. 24, No. 3, Sept., 1986, pp. 245-253.

26. Beuth, Jr., J. L., and Herakovich, C. T., "On Fracture of Fibrous Composites," *Composites '86: Recent Advances in Japan and the United States*, (S. Kawata, S. Umekawa, and A. Kobayashi, eds.), Proc. Japan-U.S. CCM-III, Tokyo, 1986, pp. 267-277.

27. Beuth, Jr., J. L., Gurdal, Z., and Herakovich, C. T., "Composite Fracture Using the Normal Stress Ratio Theory," Proceedings, ASME Winter Annual Meeting, 1986, (in press).

28. Pagano, N. J., and Halpin, J. C., "Influence of End Constraints in the Testing of Anisotropic Bodies," *Journal of Composite Materials*, Vol. 2, 1968, pp. 18-31.

29. Iosipescu, N., "New Accurate Procedure for Single Shear Testing of Metals," *Journal of Materials*, Vol. 2, No. 3, Sept., 1967, pp. 537-666.

30. Walrath, D. E., and Adams, D. F., "Analysis of the Stress State in an Iosipescu Shear Test Specimen," UWME-DR-301-102-1, University of Wyoming, June, 1983.

31. Walrath, D. E., and Adams, D. F., "Verification and Application of the Iosipescu Shear Test Method," UWME-DR-401-103-1, University of Wyoming, June, 1984.

32. Walrath, D. E., and Adams, D. F., "Iosipescu Shear Properties of Graphite Fabric/Epoxy Composite Laminates," UWME-DR-501-103-1, University of Wyoming, June, 1985.

33. Pindera, M. J., Choksi, G. N., Hidde, J. S., and Herakovich, C. T., "A Methodology for Accurate Shear Characterization of Unidirectional Composites," to be published.

34. Choksi, G. N., and Herakovich, C. T., "Fracture of Composites Using Singular Finite Elements," *Numerical Methods in Fracture Mechanics*, (A. R. Luxmoore, D. R. J. Owen, Y. P. S. Rajapakse, and M. F. Kanninen, eds.), Proc., Fourth International Conference on Numerical Methods in Fracture Mechanics, San Antonio, 1986, pp. 551-564.

35. Lekhnitskii, S. G., *Theory of Elasticity of an Anisotropic Body*, English translation by Brandstatton, Holden-Day Inc., San Francisco, 1963.

36. Gregory, M. A., and Herakovich, C. T., "Prediction of Crack Extension Direction in Unidirectional Composites," CCMS-84-11, VPI-E-84-27, Virginia Tech, Aug., 1984.

37. Gurdal, Z., and Herakovich, C. T., "Effect of Initial Flaw Shape on Crack Extension in Orthotropic Composite Materials," (to be published).

38. Savin, G. N., *Stress Concentrations Around Holes*, Pergamon Press, Oxford, 1961.

39. *Metals Handbook*, Desk Edition, (H. E. Boyer and T. L. Gall, eds.), American Society for Metals, 1985.

40. Sneddon, I. N., "The Distribution of Stress in the Neighbourhood of a Crack in an Elastic Solid," *Proc. R. Soc.*, London, Vol. 187, 1946, pp. 229-260.

41. Barbe, A., and Herakovich, C. T., "A Critical Assessment of Crack Growth Criteria in Unidirectional Composites," CCMS-85-09 VPI-E-85-09, Virginia Tech, Sept., 1985.

42. Nemeth, M. P., Herakovich, C. T., and Post, D., "On the Off-Axis Tension Test for Unidirectional Composites," *Composites Technology Review*, Vol. 5, No. 2, Summer, 1983, pp. 61-68.

43. Pindera, M. J., and Herakovich, C. T., "Shear Characterization of Unidirectional Composites with the Off-Axis Tension Test," *Experimental Mechanics*, Vol. 26, No. 1, March, 1986, pp. 103-112.

44. Peters, Piet, "Fracture Mechanical Investigations on Unidirectional Boron-Aluminum and Boron-Epoxy Composites," *Journal of Composite Materials*, Vol. 12, 1978, pp. 250-261.

45. Beaumont, P. W. R., and Phillips, D. C., "Tensile Strength of Notched Composites," *Journal of Composite Materials*, Vol. 6, 1972, pp. 32-47.

Appendix A. Material Property Tensile Coupon Test Results

A.1 0° Tension Tests

Tension tests on 0° coupons were performed in order to obtain the material properties E_1, X_t, and ν_{12} . Specimens measured 0.30 in. in width and had a gage section length of 6.0 in., providing an aspect ratio of 20. Each specimen had a Micro-Measurements type CEA-06-062WT-120 0.062 in. gage length stacked two-way gage attached to its center, oriented to measure axial and transverse strains. A typical plot of axial stress vs. axial strain is provided in Figure 64. As outlined in Table 9, tests 1 through 4 yielded average values of E_1 = 18.3 msi and ν_{12} = 0.305. Of the four specimens originally tested, specimens 1 and 4 experienced failure in their grip regions at a stress significantly below the ultimate stress exhibited by tests 2 and 3. Because of this, the ultimate stress values from tests 1 and 4 were not used and a supplementary test was run to obtain an ultimate stress value only. Thus, tests 2, 3, and 5 yielded an average value of X_t = 210. ksi.

Table 9. Summary of Material Property Tensile Coupon Test Results

Results of Material Property Tensile Coupon Tests
AS4/3501-6 Graphite-Epoxy

0° Tests

Test Number	E_1 (msi)	ν_{12}	X_t (ksi)
1	18.1	0.330	---
2	17.5	0.310	208.
3	18.5	0.270	216.
4	18.9	0.311	---
*5	n/a	n/a	207.
Averages	**18.3**	**0.305**	**210.**

10° Off-Axis Tests

Test Number	Fracture Angle	*Experimental Values* G_{12} (msi)	τ_{max} (ksi)	Correction Factor	*Corrected Values* G_{12} (msi)	τ_{max} (ksi)
1	11.5°	0.816	9.27	0.9335	0.762	8.65
2	11.5°	0.829	9.98	0.9335	0.774	9.32
3	12.0°	0.824	10.4	0.9376	0.773	9.75
4	12.0°	0.820	10.6	0.9376	0.769	9.94
Averages		**0.822**	**10.1**		**0.770**	**9.42**

45° Off-Axis Tests

Test Number	Fracture Angle	*Experimental Values* G_{12} (msi)	τ_{max} (ksi)	Correction Factor	*Corrected Values* G_{12} (msi)	τ_{max} (ksi)
1	45.0°	-----	6.07	1.003	-----	6.09
2	44.75°	0.828	6.55	1.003	0.830	6.57
3	45.5°	0.810	7.72	1.003	0.812	7.74
4	46.0°	0.798	6.35	1.003	0.800	6.37
Averages		**0.812**	**6.67**		**0.814**	**6.69**

90° Tests

Test Number	E_2 (msi)	Y_t (ksi)
1	1.59	----
2	1.43	7.92
3	----	----
4	1.34	7.34
*5	n/a	7.98
Averages	**1.45**	**7.75**

* Supplemental Strength Tests

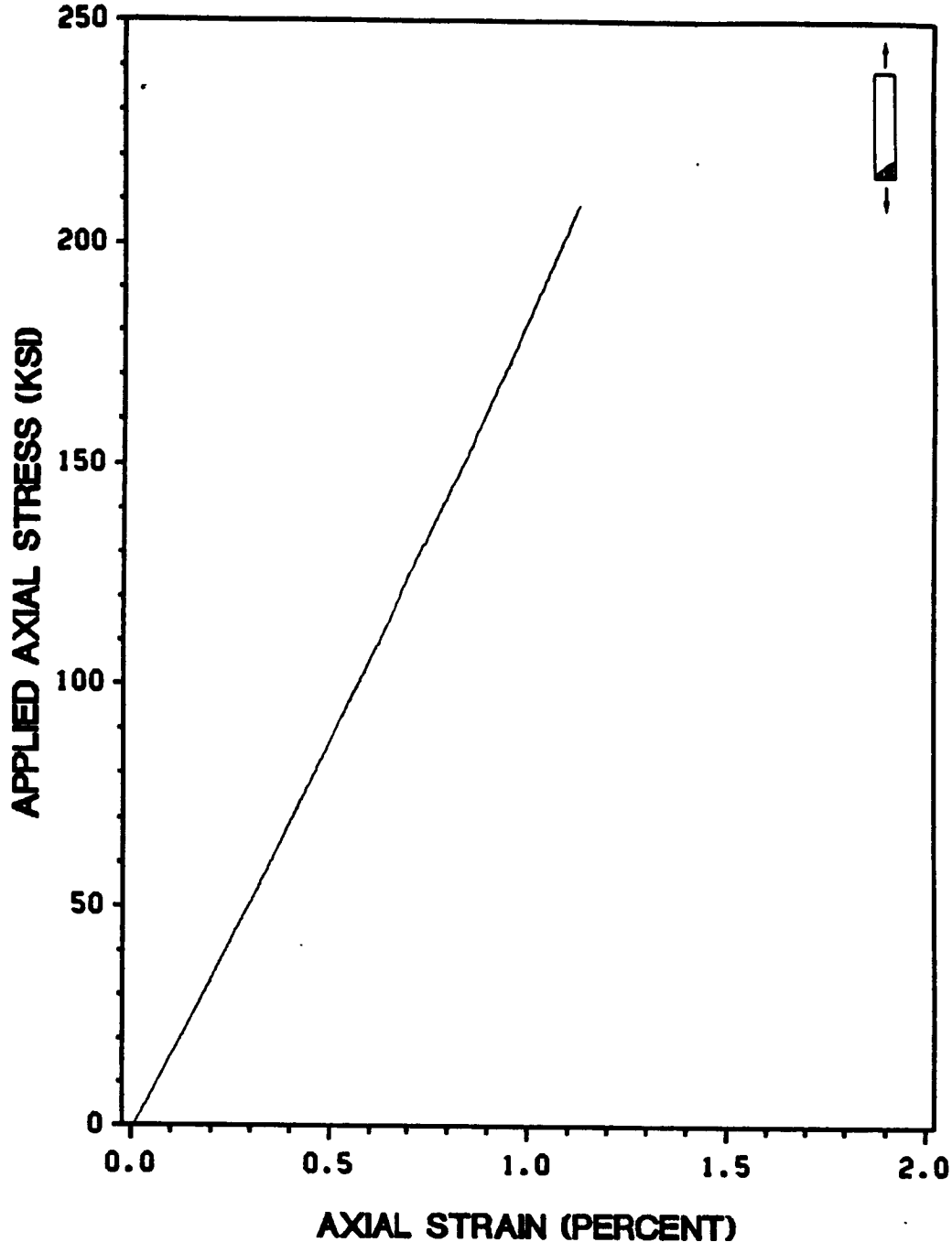

Figure 64. Axial Stress vs. Axial Strain for a Typical 0° Tension Test: AS4/3501-6 Graphite-Epoxy

A.2 10° Off-Axis Tests

Tension tests on 10° off-axis coupons were performed to obtain values for G_{12} and τ_{max}. Specimens were 0.50 in. in width with a gage section length of 6.0 in., providing an aspect ratio of 12. Each specimen had a Micro-Measurements type WK-06-120WR-120 0.120 in. gage length stacked 45° strain gage rosette attached to its center. Each gage was oriented on the specimen to measure axial and transverse strains, with the 45° gage oriented away from the fibers (Figure 65). This resulted in more accurate strain readings by allowing the 45° gage to experience higher strains. After testing, specimen off-axis angles were determined by measuring each specimen fracture angle. Accurate measurement of specimen off-axis angles is essential to achieve accurate results for small angle off-axis tensile tests. In this study, angles were measured to the nearest 0.25°. As indicated in Table 9, this angle was not equal to 10° for any of the specimens tested. Experimental values of G_{12} and τ_{max} were obtained by transforming stresses and strains to the principal material coordinate system using the measured off-axis angle. In obtaining the experimental quantities, it was assumed that the axial stress reading from each test was the stress applied to the specimen, with no account made of shear coupling effects caused by end grip constraints. Figure 66 provides a typical plot of shear stress vs. shear strain in the principal material coordinate system, with shear coupling effects neglected. As Table 9 indicates, tests 1 through 4 yielded average experimental values of G_{12} = 0.822 msi. and τ_{max} = 10.1 ksi. As will be outlined in Section A.5, on determining final shear property values from the 10° tests, shear coupling effects were accounted for using a correction factor from the literature.

A.3 45° Off-Axis Tests

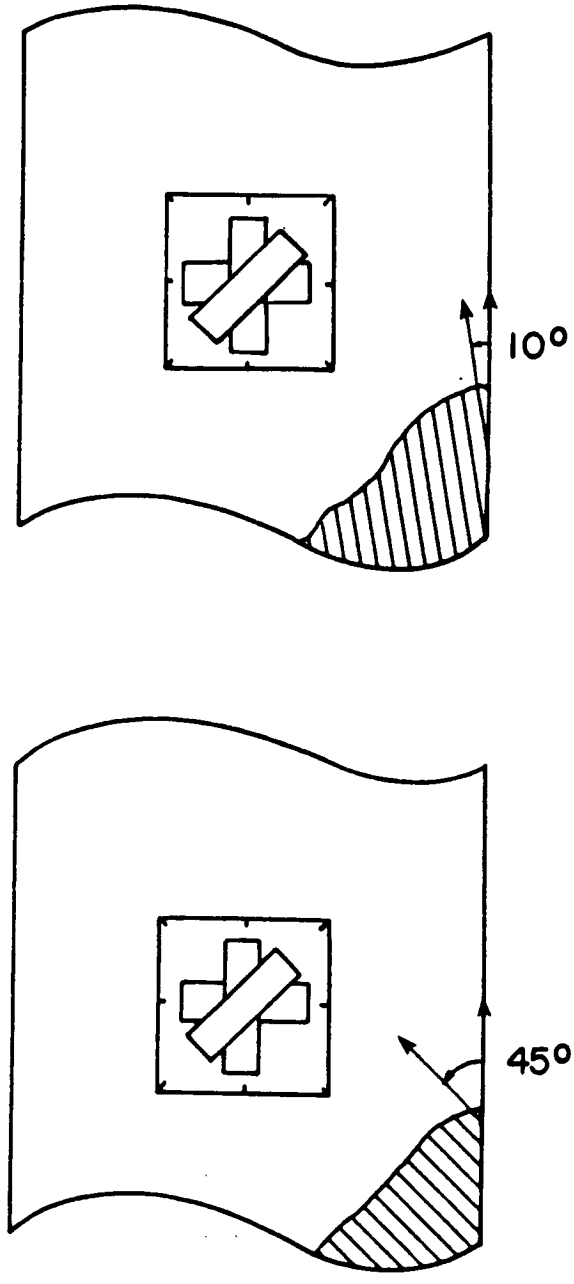

Figure 65. Off-Axis Tensile Coupon Strain Gage Rosette Orientations

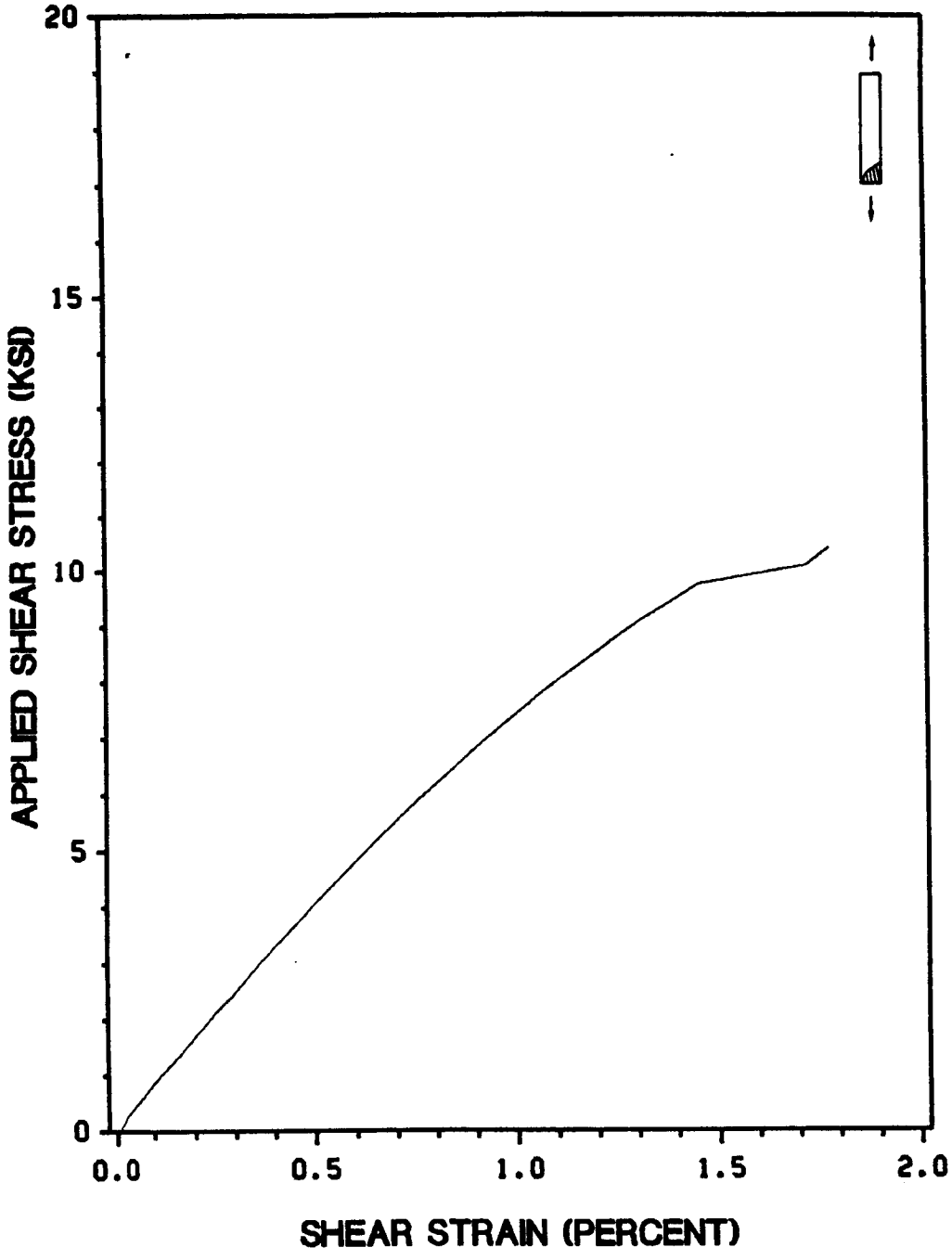

Figure 66. Shear Stress vs. Shear Strain for a Typical 10° Off-Axis Tensile Test: AS4/3501-6 Graphite-Epoxy, Shear Coupling Effects Not Included

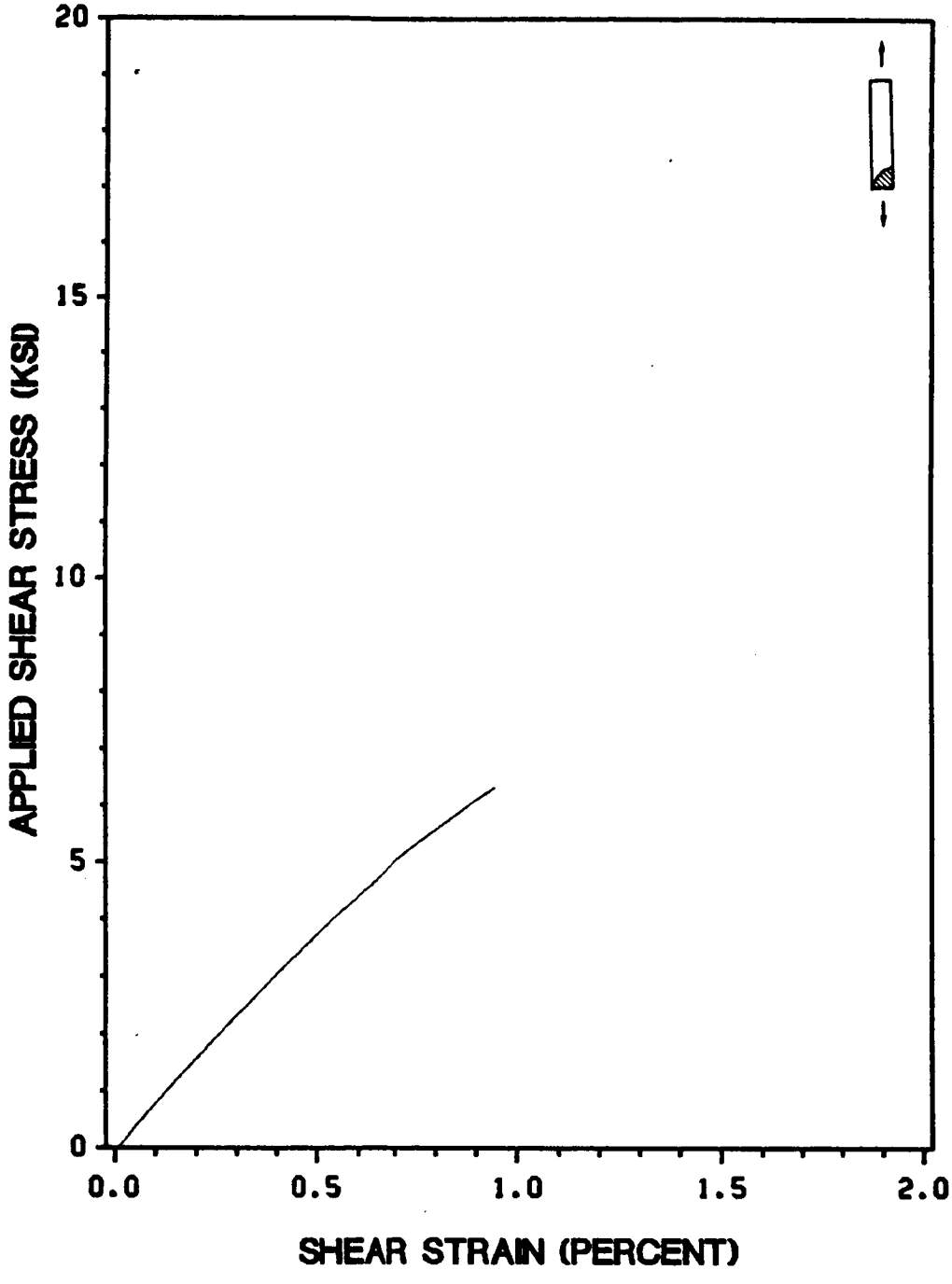

Figure 67. Shear Stress vs. Shear Strain for a Typical 45° Off-Axis Tensile Test: AS4/3501-6 Graphite-Epoxy, Shear Coupling Effects Not Included

Tension tests on 45° off-axis coupons were also performed to obtain values for G_{12} and τ_{max}. Specimens were 0.50 in. in width with a gage section length of 6.0 in., providing an aspect ratio of 12. Each specimen had a Micro-Measurements type WK-06-120WR-120 0.120 in. gage length stacked 45° strain gage rosette attached to its center. The gage orientation was similar to that used for the 10° specimens, with the 45° gage oriented perpendicular to the fibers (Figure 65). As with the 10° tests, this increased the accuracy of the strain readings by allowing the 45° gage to experience higher strains. Fracture angles were measured for each specimen after testing and these angles were used in transforming the stresses and strains to the material principal coordinate system. As in the 10° off-axis tests, experimental values for G_{12} and S were obtained using the measured axial stress, thus ignoring shear coupling effects. Figure 67 provides a typical plot of shear stress vs. shear strain in the principal material coordinate system, with shear coupling effects neglected. As outlined in Table 9, tests 2 through 4 yielded an average experimental value of G_{12} = 0.812 msi. Test 1 experienced strain gage problems during testing and thus did not yield a reliable value for G_{12}. All tests provided reasonable ultimate stress values, however, yielding an average measured value of τ_{max} = 6.67 ksi. As with the 10° off-axis tests, the 45° off-axis test shear property values are corrected in Section A.5 for shear coupling effects. It will be demonstrated, however, that these effects do not exert a strong influence on shear property values obtained from 45° off-axis coupons of relatively large aspect ratio.

A.4 90° Tension Tests

Tension tests on 90° coupons were performed to obtain the material properties of E_2 and Y_t. Values of ν_{21} proved to be inconsistent due to the small transverse strain magnitude, and were thus not obtained from these tests. Specimens were 0.50 in. in width with a gage section length of 8.0 in., providing an aspect ratio of 16. Each specimen had a Micro-Measurements type CEA-06-062-WT-120 0.062 in. gage length stacked two-way gage attached to its center, oriented to

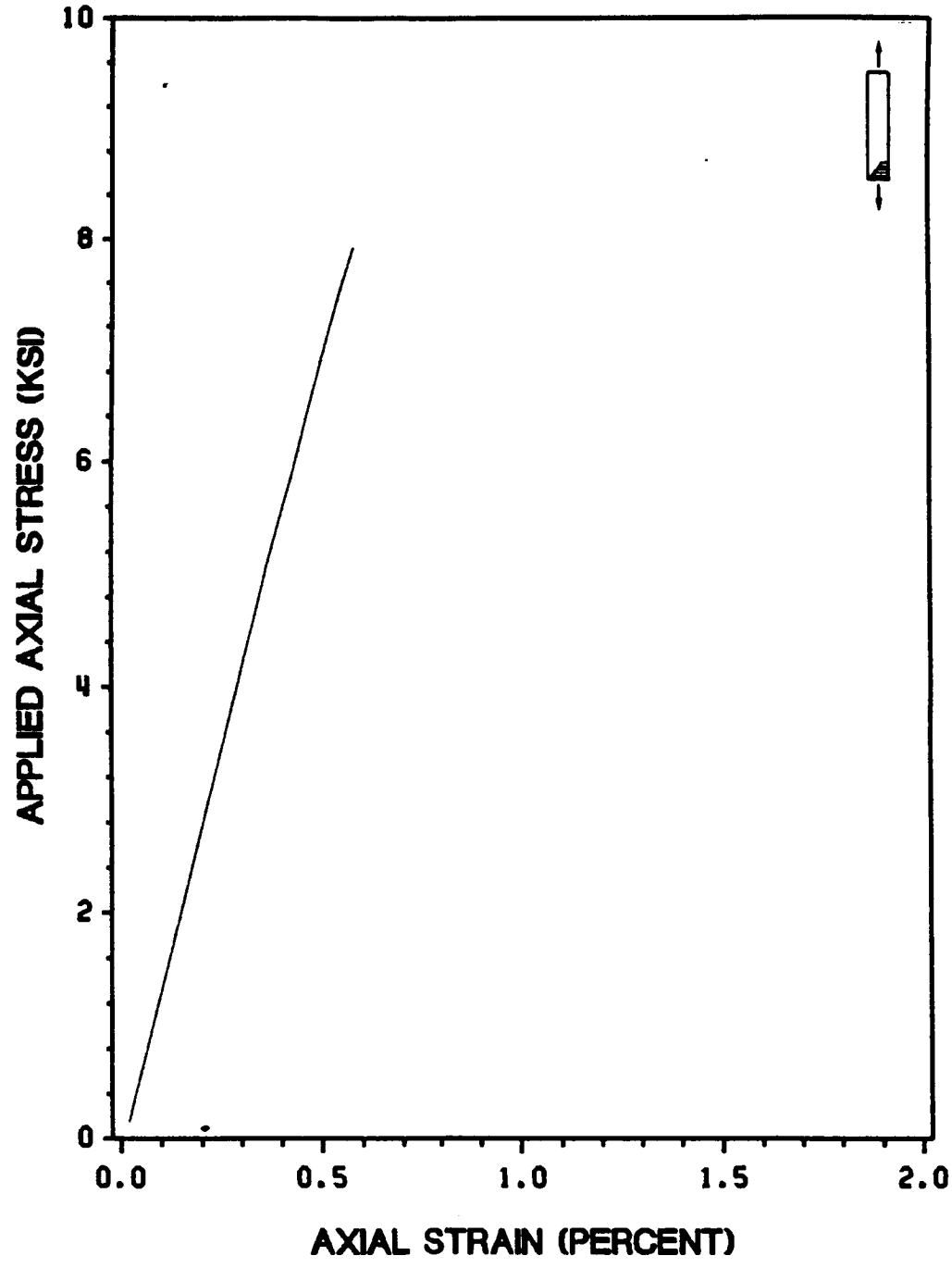

Figure 68. Axial Stress vs. Axial Strain for a Typical 90° Tension Test: AS4/3501-6 Graphite-Epoxy

measure axial and transverse strains. Figure 68 provides a typical plot of axial stress vs. axial strain. As outlined in Table 9, tests 1, 2, and 4 yielded an average value of E_2 = 1.45 msi. Specimen 3 was apparently damaged during specimen preparation and yielded inconsistent modulus and strength results. Also, specimen 1 experienced failure in one of its grip regions at a stress significantly below the ultimate stress exhibited by tests 2 and 4. Because of this, the ultimate stress values from tests 1 and 3 were not used and a supplementary test was run to obtain an ultimate stress value only. Thus, tests 2, 4, and 5 yielded an average value of Y_t = 7.75 ksi.

A.5 Final Material Property Values

The average values for E_1, E_2, ν_{12} , X_t, and Y_t given in Table 9 were used as the final material property values for the AS4/3501-6 graphite-epoxy used in this study. A number of complications presented themselves, however, in determining final values for shear modulus and shear strength from the material property coupon tests. Both the 10° and 45° off-axis tests yielded potential values for G_{12} and S. Before values from either test could be used, however, a proper account had to be made of shear coupling effects due to the material anisotropy and the constraint of grips on the specimen ends. As detailed in Section 3.3.1.2 of this report, such effects cause a shear stress to be applied to the specimen in addition to the applied axial tensile stress. Because the only the axial stress, $\frac{P}{A}$, is measured during a test, experimentally determined values for shear modulus and shear stress in the material coordinate system are not correct. The inaccuracy of experimentally determined shear property values is particularly significant in specimens of small aspect ratio and small off-axis angle.

In [43], Pindera and Herakovich provide a rationale for use in accounting for shear coupling effects in off-axis tensile coupon material property tests. Their analysis of the off-axis test is based upon the centerline stress state predicted by the aforementioned elasticity solution of Pagano and Halpin [28]. The result of their work is a shear modulus and shear strength correction factor that

is a function of specimen aspect ratio, off-axis angle and the material elastic properties. Because the correction factor from [43] is dependent upon the shear modulus value, an iterative approach is needed. This was done in this study by first obtaining a correction factor for each 45° off-axis test. In obtaining the correction factors, the experimentally determined value for G_{12} from the 45° test was used as the material shear modulus. As expected, the correction factors were very close to 1. The correction factors were then used to obtain new values for G_{12}. These corrected values of shear modulus were then used to re-calculate the shear coupling correction factor for each 45° test. Identical correction factors resulted, indicating that no more iterations were necessary. These correction factors were then used to obtain the final corrected values for G_{12} and τ_{ult} given in Table 9 for the 45° tests.. Correction factors for the 10° off-axis tests were obtained using the corrected shear modulus values from the 45° off-axis tests.

The correction factors and resulting corrected shear property values are provided in Table 9. The correction procedure acted to decrease the shear properties obtained from the 10° off-axis tests and to increase slightly the shear properties from the 45° off-axis tests. Based on the corrected shear modulus values from both tests, which should agree with one another, it appears that the correction factors for the 10° off-axis tests may have over compensated for the shear coupling effect that existed in the actual specimens. Another explanation for the discrepancy in the values is not readily apparent. With correction for shear coupling effects, either the 10° or the 45° off-axis tests should provide accurate averaged shear modulus values. Because the averaged corrected values from the two tests do not agree, however, and because the correction factors for the 45° off-axis tests were very close to 1, the average corrected G_{12} value of 0.814 msi from those tests was used as the material property shear modulus value. The value of the material shear strength, S, was originally designated to be taken from the average corrected value for τ_{max} from the 10° off-axis tests. This was initially planned because the 10° off-axis test experiences a more shear-dominated failure than the 45° off-axis test. This is substantiated in the results with the average value of maximum shear stress from the 10° off-axis tests being significantly higher than that from the 45° off-axis tests. Subsequent tests on 0° Iosipescu shear specimens, detailed in Appendix B, yielded significantly higher maximum shear stress values than the 10° off-axis tensile coupons, however. This occurred

because even 10° off-axis coupons are subjected to a significant amount of tensile stress perpendicular to the fiber direction. This σ_2 stress acts to significantly reduce measured maximum shear stress values. Because the 0° Iosipescu tests performed in this study apparently provided much higher maximum shear stress values, their averaged value of 14.4 ksi was used as the material shear strength, S.

Appendix B. Unnotched Iosipescu Test Results

B.1 Isotropic Material Tests

B.1.1 Iosipescu Shear Tests

The first set of unnotched Iosipescu shear tests were performed on 6061-T6 aluminum. Specimen dimensions followed those given in Section 4.2. Strains were measured in the specimen gage section using a Micro-Measurements type WA-06-030WR-120 0.030 gage length stacked 45° strain gage rosette oriented as shown in Figure 69. A total of two aluminum Iosipescu tests were performed. A photograph of the failed specimens is provided in Figure 70. As the figure indicates, both specimens failed in shear in their gage sections. Although not obvious from the figure photograph, a significant amount of deformation occurred in the upper right and lower left portions of each specimen, near the v-notches. This deformation was caused by the significant amount of compressive stress concentration in these regions caused by the test fixture as it applied load to the specimen. The ductile nature of the aluminum allowed the specimens to deform in these regions. As a result, stress concentrations from the fixture did not cause substantial problems in the alumi-

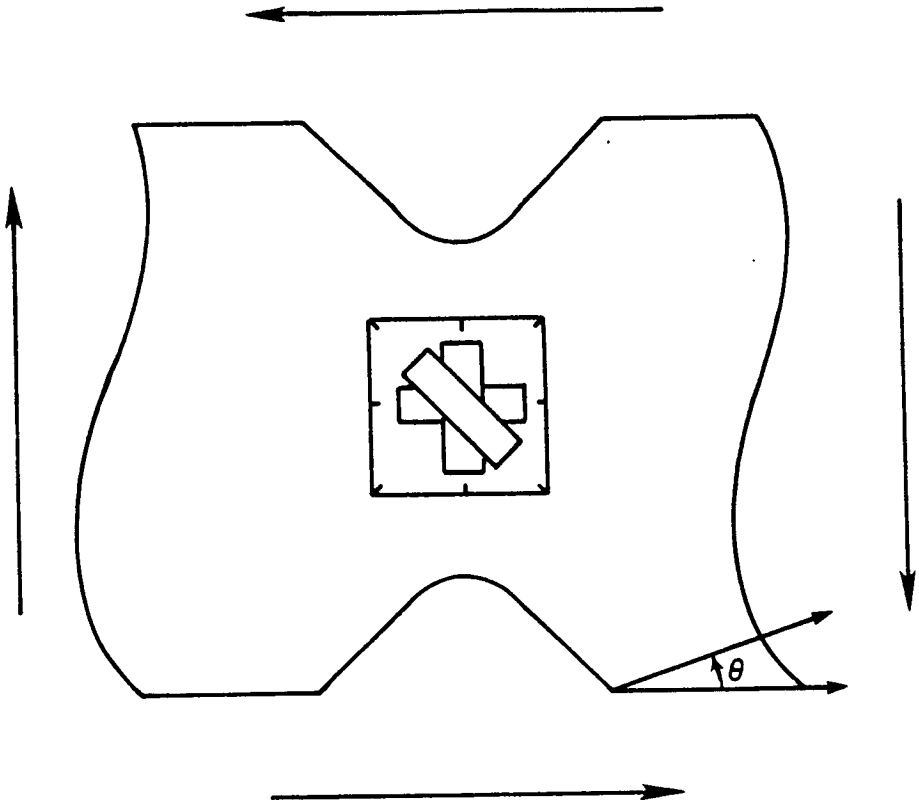

Figure 69. Strain Gage Rosette Orientation Used in Isotropic and Anisotropic Material Iosipescu Tests

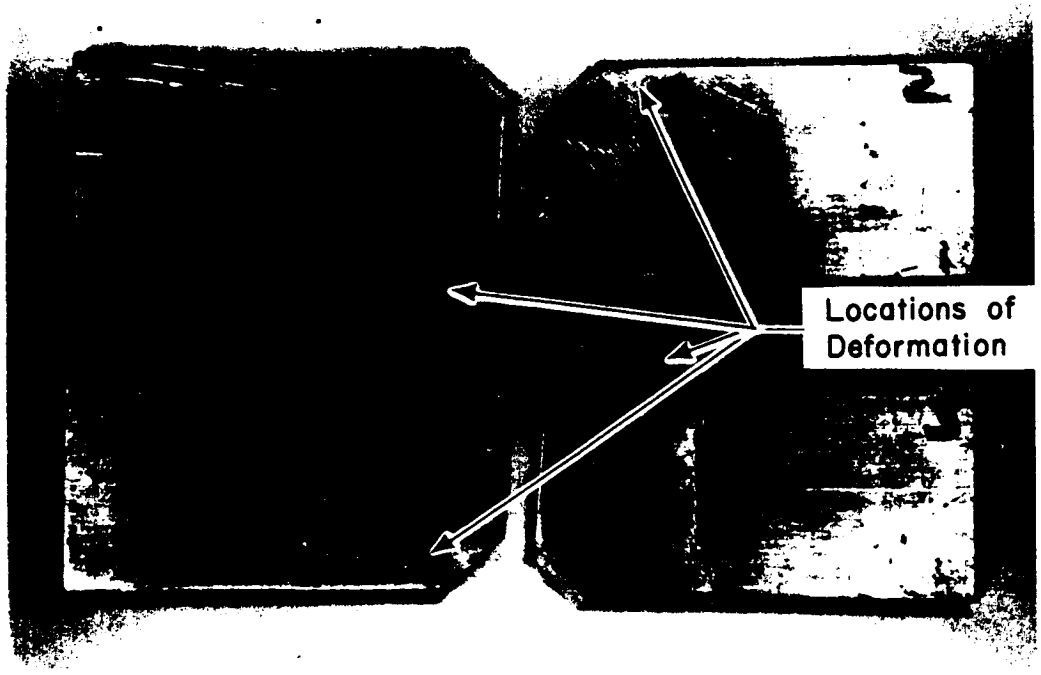

Figure 70. Failed 6061-T6 Aluminum Iosipescu Specimens

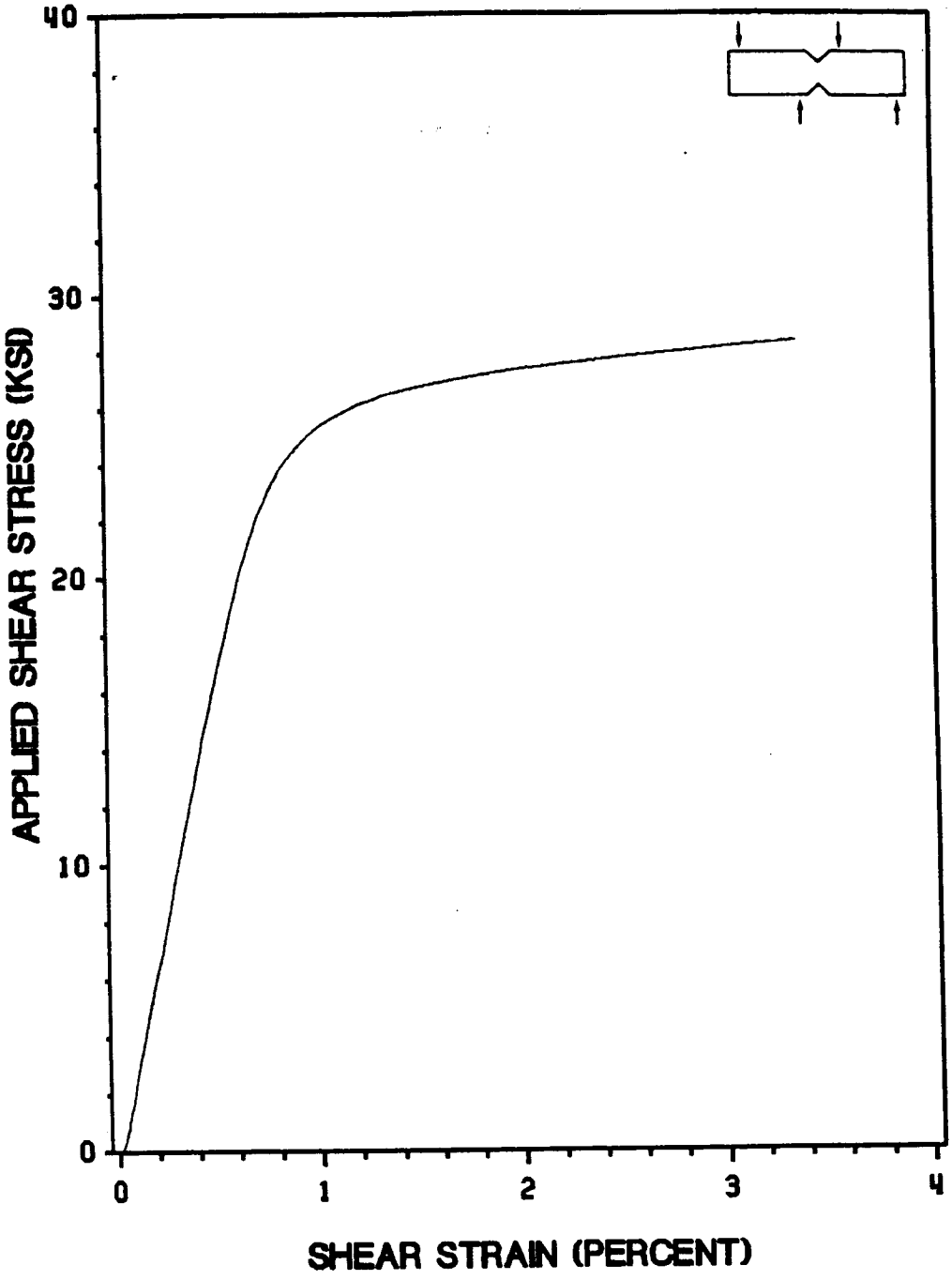

Figure 71. Shear Stress vs. Shear Strain for a Typical Aluminum Iosipescu Shear Test: 6061-T6 Aluminum

Table 10. Isotropic Material Tests

Results of Unnotched Tensile and Iosipescu Tests
6061-T6 Aluminum

Iosipescu Shear Tests

Test Number	G (msi)	τ_{ult} (ksi)
1	3.48	31.0
2	3.47	30.4
Averages	**3.48**	**30.7**

Tensile Test

Test Number	E (msi)	ν	G (msi)	σ_{ult} (ksi)
1	9.24	0.329	3.48	38.93

Literature Values for 6061-T6 Properties [39]

E (msi)	ν	G (msi)	σ_{ult} (ksi)	τ_{ult} (ksi)
10.2	0.345	3.80	45.0	30.0

num Iosipescu tests. As will be outlined in a subsequent section, these stress concentrations did create problems in the Iosipescu tests on AS4/3501-6 graphite-epoxy. Figure 71 provides a typical plot of shear stress vs. shear strain for an aluminum Iosipescu test. As indicated in the figure, in each of the two aluminum Iosipescu tests, the material shear stress vs. shear strain response remained linear up to an applied shear stress level of approximately τ = 20 ksi. The numerical results from the tests are given in Table 10. As the table indicates, the two tests provided highly consistent shear modulus and shear strength values.

B.1.2 Comparative Shear Property Values and Conclusions

A single unnotched tensile test was performed on a 6061-T6 aluminum specimen in order to compare its shear modulus value with that averaged from the two unnotched aluminum Iosipescu tests. The shear modulus values were obtained from the tensile test using the isotropic material relationship $G = \frac{E}{2(1 + \nu)}$. Strains were measured using a single Micro-Measurements type CEA-06-062WT-120 0.062 in. gage length stacked two-way gage, oriented to measure axial and transverse strains. Because only the linear stress vs. strain response was needed for comparison with the Iosipescu tests, a specimen of constant width was used instead of a more complicated dog bone-shaped specimen. The specimen was 1.0 in. in width with a gage length of 8.0 in. Instron grips were used to accommodate the specimen width. During the test, the material axial stress vs. axial strain response was linear up to an applied axial stress level of approximately $\sigma = 30$ ksi.

The numerical results from the aluminum tensile test are given in Table 10. In order to evaluate the accuracy of the τ_{ult} values from the Iosipescu tests, literature values for the properties of 6061-T6 aluminum were obtained from [39]. Comparison of the the averaged aluminum Iosipescu test values of G and τ_{ult} with the value of G from the tensile test and the literature value for τ_{ult} indicates almost almost exact agreement. Although this work with aluminum was brief, it offers a number of conclusions. First, because of the ductile behavior of the aluminum, stress concentrations caused by the loading of the specimen by the fixture do not appear to adversely affect the results of the tests. Second, it appears that the Iosipescu test can offer highly consistent shear modulus and shear strength results from test to test. Finally, it appears that these values are accurate in comparison to results from other sources.

B.2 Composite Material Tests

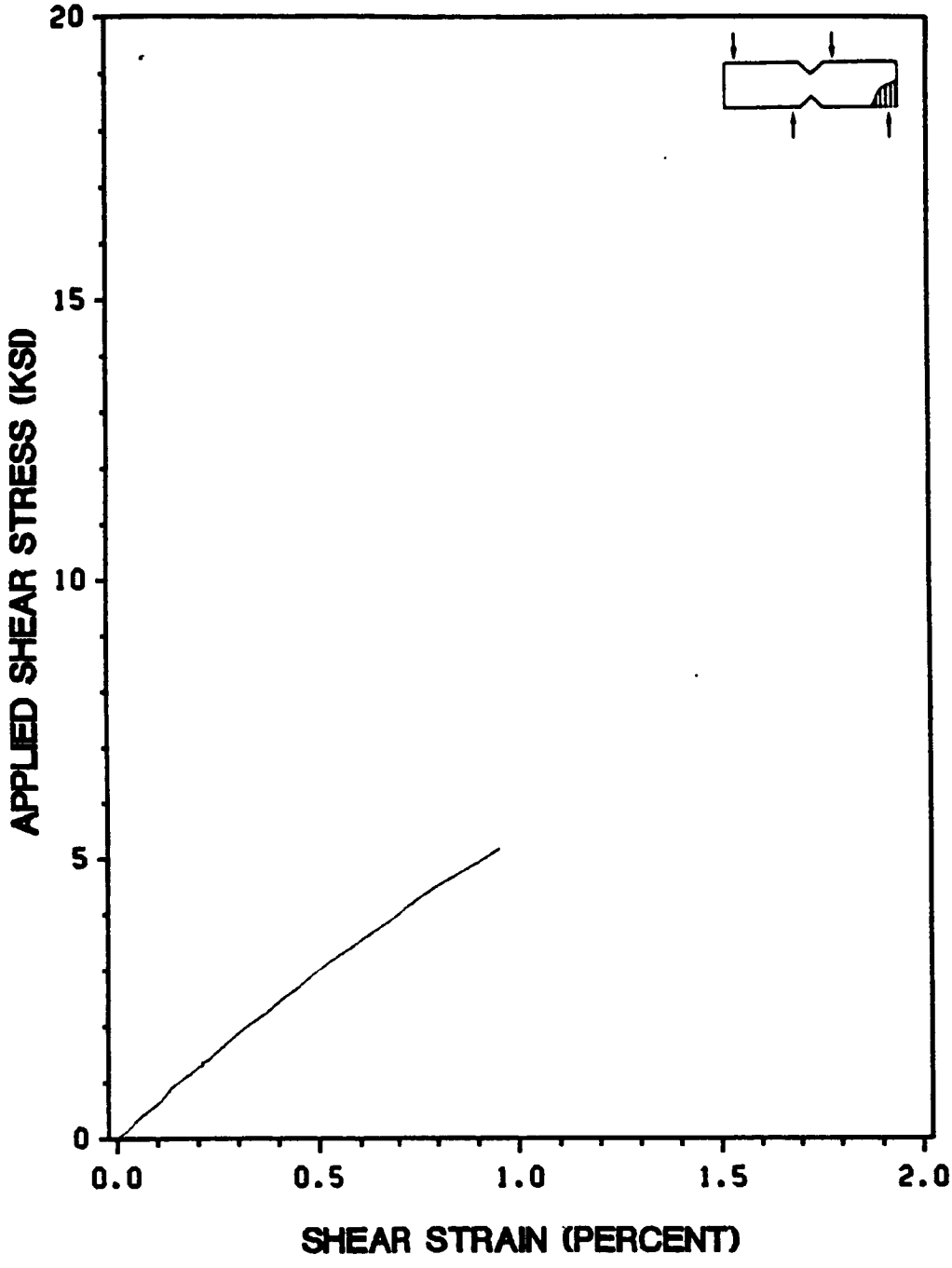

Figure 72. Shear Stress vs. Shear Strain for a Typical 90° Iosipescu Shear Test: AS4/3501-6 Graphite-Epoxy

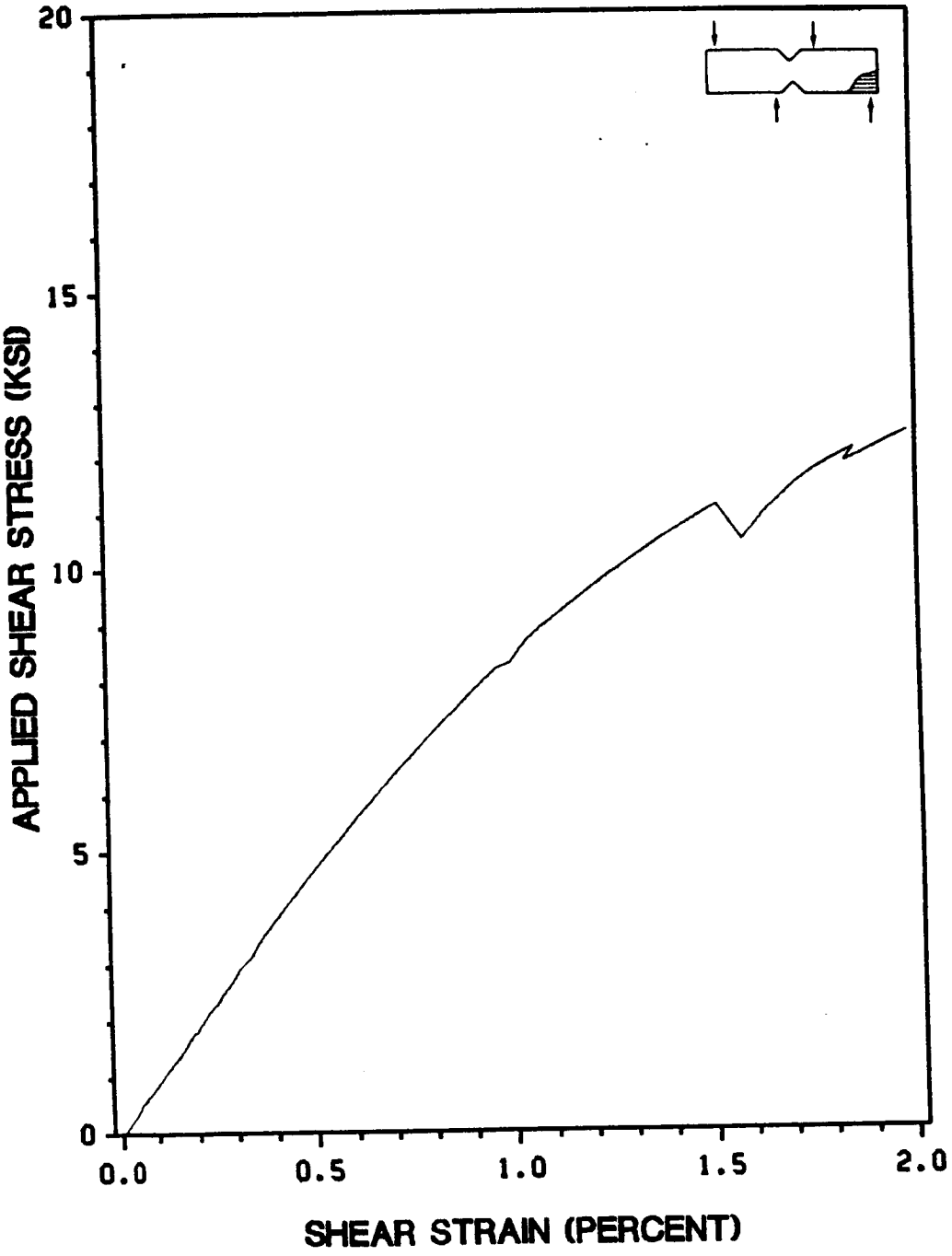

Figure 73. Shear Stress vs. Shear Strain for a Typical 0° Iosipescu Shear Test: AS4/3501-6 Graphite-Epoxy

The second set of unnotched Iosipescu shear tests were performed on 0° and 90° specimens of the unidirectional AS4/3501-6 graphite-epoxy used in this study. Specimen dimensions followed those given in Section 4.2. As with the tests on aluminum specimens, strains were measured in the specimen gage section using a Micro-Measurements type WA-06-030WR-120 0.030 gage length stacked 45° strain gage rosette oriented as shown in Figure 69. A total of eight graphite-epoxy Iosipescu tests were performed, four of each fiber orientation. Figure 72 and Figure 73 provide typical plots of shear stress vs. shear strain for the 90° and 0° Iosipescu tests, respectively. As indicated by the figures, specimens exhibited linear shear stress vs. shear strain response up to approximately $\tau = 4$ ksi.

B.2.1 Maximum Shear Stress Values

The most obvious result from the tests is reflected in the values given for τ_{max} for each test in Table 11. It is obvious from the table that the 90° specimens exhibited maximum shear stress values that were significantly lower than those for the 0° tests. This occurred because the low tensile strength in the direction along the specimen length and tensile stresses that exist in 90° specimens caused them to fail prematurely. This is illustrated in Figure 74, which provides photographs of the failed 90° Iosipescu specimens. In the first specimen tested, failure occurred away from the test section due to stress concentrations caused by the test fixture. In subsequent tests, a compliant material was inserted between the specimen and the fixture. Failures in subsequent specimens typically occurred within the test section along the fiber direction. Because of the problem with premature normal stress-dominated failures, a reasonable value for shear strength cannot be obtained for 90° tests on graphite-epoxy or any other unidirectional composite material with a low value of Y_t.

Although the maximum shear stress values obtained in the 0° tests were much more satisfactory than those obtained from the 90° tests, these tests also exhibited premature failure problems. Two separate failure events occurred. The first premature failure event was cracking that originated

Table 11. Composite Material Iosipescu Tests

Results of Unnotched Iosipescu Tests
AS4/3501-6 Graphite-Epoxy

0° Iosipescu Tests

Test Number	G_{12} (msi)	τ_{cr} (ksi)	τ_{max} (ksi)
1	0.840	12.5	13.7
2	0.898	12.1	14.2
3	0.924	11.1	15.2
4	0.905	11.9	14.4
Averages	**0.892**	**11.9**	**14.4**

90° Iosipescu Tests

Test Number	G_{12} (msi)	τ_{max} (ksi)
1	0.776	2.52
2	0.608	5.18
3	0.612	4.10
4	0.594	4.20
Averages	**0.648**	**4.00**

near the roots of the v-notches cut in the specimens. This cracking was always accompanied by a noticeable drop in applied load to the specimen. In all of the 0° tests, cracking occurred at a shear stress level of approximately 12.0 ksi. Shear stress levels at cracking, designated as τ_{cr}, are given in Table 11 for each 0° specimen. After the initial load drop upon experiencing cracking at the v-notch roots, each 0° Iosipescu specimen continued acquiring load until a second failure event occurred. This was crushing of the specimen edge in the upper right and lower left portions of the specimen near the v-notches (see Figure 75). After crushing occurred, the specimen could no longer acquire additional load. As a result, it is the applied shear stress at crushing that is designated as τ_{max} for the 0° specimens in Table 11.

The problem of specimen cracking is caused by a stress concentration at the v-notch roots. It is likely that this problem is an inherent one for this test method and will present itself in 0° tests

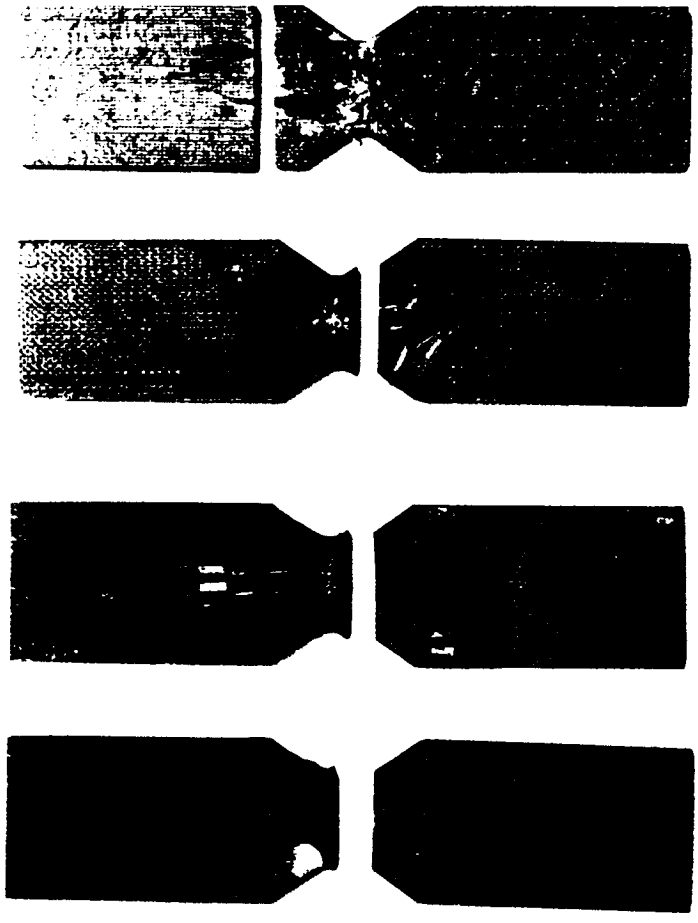

Figure 74. Failed 90° AS4/3501-6 Graphite-Epoxy Iosipescu Specimens

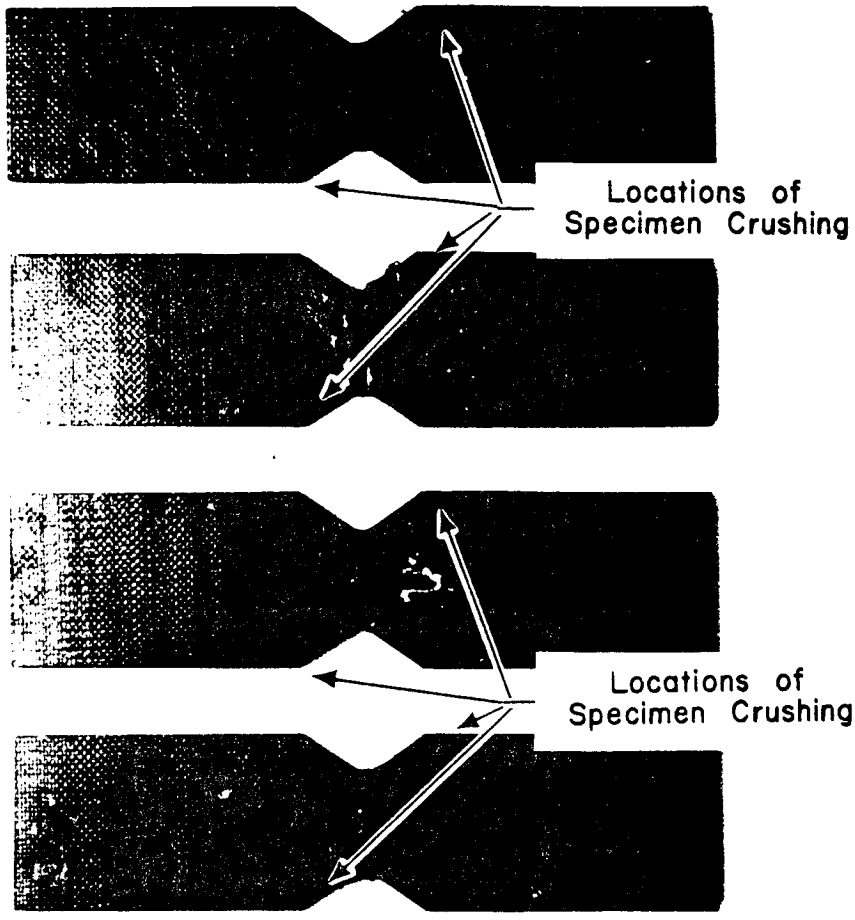

Figure 75. Failed 0° AS4/3501-6 Graphite-Epoxy Iosipescu Specimens

on most composite materials. Fortunately, however, specimen cracking does not act as a final failure event, as specimen edge crushing does. Also, some preliminary finite element modelling of specimens with v-notch cracking by Walrath and Adams [31] indicates that such cracking does not significantly alter the shear stress distribution in the specimen gage section. Their results indicate that, if anything, v-notch cracking serves to reduce the shear stress concentrations at the v-notch root, thus improving the gage section shear stress distribution.

The problem of Iosipescu specimen edge crushing is due to the severe stress concentration imparted to the specimen by the fixture. This is the same stress concentration that caused the areas of severe deformation in the aluminum Iosipescu tests. In 0° graphite-epoxy Iosipescu tests, the material is not ductile enough to reduce the stress concentration. Certainly, in applying the test to more ductile composite materials, the problem of edge crushing may not present itself at all. The problem of a compressive stress concentration was recognized after the first 0° off-axis test was run. In an attempt to eliminate the edge crushing problem, shims of two layers of 0.005 in. thick aluminum were placed inbetween the Iosipescu specimens and the fixture. Shims were also used in all but the first 90° Iosipescu test. Significant increases were noted in the values of τ_{max} obtained from both types of tests. The edge crushing phenomenon could not be eliminated, however. As a result, a true shear failure was not exhibited in any of the graphite-epoxy Iosipescu tests.

The premature failure problems noted in the 0° Iosipescu tests is somewhat discouraging. It is important to note, however, that both of the premature failure events noted in the 0° specimens occurred at a significantly higher applied shear stress than the average maximum shear stress obtained from the 10° off-axis material property tensile coupon tests. Thus, it appears that even with the problems involved with obtaining maximum shear stress values for graphite-epoxy Iosipescu specimens, the test yields better shear strength values than a 10° off-axis test. Because of this, the averaged 0° Iosipescu test τ_{max} value was used as the shear strength, S, in this study.

B.2.2 Shear Modulus Values

A comparison between the values obtained for G_{12} from each Iosipescu test and the value obtained from the material property tensile coupon tests yields two observations. First, it is obvious from the average shear modulus values given in Table 11 that the 90° Iosipescu test provides G_{12} values that are significantly lower than those obtained from the 0° Iosipescu tests. Also, in comparing these values with that obtained from the 10° and 45° off-axis material property tensile coupon tests it appears that the actual value of shear modulus lies somewhere inbetween those obtained from each type of Iosipescu test. This phenomenon is caused by the fact that the Iosipescu specimen gage section stress state is a function of the specimen fiber orientation. The same phenomenon has been noted in [33] in Iosipescu tests on Aramid-Epoxy. It is shown in [33] that a finite element analysis of the specimen indicates significant differences in gage section stress state in 0° and 90° specimens, and that an accurate value of G_{12} can be obtained if an accurate account is made of these differences. The second observation to be made from the values given in Table 11 is that Iosipescu shear modulus values showed significant scatter within each of the two types of tests. Shear modulus values from the much simpler to perform 45° off-axis tension tests given in Table 9 varied much less from test to test.

B.2.3 Summary and Conclusions

The results and observations from the unnotched graphite-epoxy Iosipescu tests performed in this study, offer a number of conclusions. It appears that the 0° test offers significant potential as a test for composite shear strength. Even with the problems of specimen cracking and edge crushing the 0° test yielded maximum shear stress values significantly above the values obtained from the more established 10° off-axis test. Also, the test becomes relatively simple to perform if only a strength value is desired and strain gaging is not necessary. In contrast, use of the Iosipescu

shear test as a method for determining shear modulus appears less attractive. The most detrimental characteristic of the test is the dependence of shear modulus on the type of test (0° or 90°) and the subsequent need to account for it using finite elements. It is shown in [33] that, if such an account is made, a correction factor can be used with measured values to obtain the true value of G_{12} for the material. The finite element runs necessary to obtain such a correction factor, however, make the method cumbersome in comparison to the simple methods needed to obtain values of G_{12} from 45° off-axis tests. In short, the primary advantage of the Iosipescu test in determining composite shear properties is the predominantly shear stress state in its test section. This is a clear advantage in determining shear strength, which can truly be measured only under a pure shear stress state, but not in determining shear modulus, which can be measured in specimens subjected to combined shear and normal stresses

Appendix C. Proposed Experimental Methods for the Verification of Normal Stress Ratio Analysis Assumptions

C.1 Introduction

The work completed in this study has been performed in an attempt to identify the possible limitations of the normal stress ratio theory. The approach that has been taken has been to test the theory's crack growth predictions for simple, but highly varied experiments, using an established stress solution approach. Clearly, further work needs to be completed along these lines. In this appendix, experimental methods are suggested that test the theory and analysis in a different way. Instead of testing the entire analytical approach and theory at once, these methods act to test the validity of some of its individual assumptions. Methods which time has not permitted to be performed and included as a part of this study are suggested for the testing of three specific analytical assumptions.

C.2 *Relation of Initial Notch Length to Critical Stresses*

One assumption inherent in all macroscopic-level analyses using the Lekhnitskii solution for the determination of near-crack-tip stresses is that, for problems having the same original crack orientation with respect to the material fibers, crack initiation stresses will be proportional to the square root of the original crack length. This is a direct consequence of the predicted near-crack-tip stress distribution, and the use of an analysis based solely on original crack geometry to predict critical stresses, even when crack geometry changes at the onset of crack extension. This assumption is not confined to macroscopic-level analyses. As previously noted, the shear-lag analysis of Goree and Wolla [14] predicts essentially identical critical stresses as an analysis explicitly assuming that critical stresses are proportional to the square root of the original notch length.

Despite the number of analytical crack growth models that assume or predict a proportional relationship between critical stresses and the square root of the original notch length, it has never been shown to exist for general composite fracture problems. Until now, only limited comparison has been made with experiment and results have been inconclusive. In [44], for example, Peters attempts to verify the relationship for unidirectional boron-aluminum and boron-epoxy composites and observes that failure stresses are clearly not proportional to the square root of the original crack length. In fact, his results for boron-epoxy indicate that failure stress and crack length are independent of one another. All of the specimens Peters tested, however, experienced significant stable crack extension before failure. As pointed out repeatedly in this report, any crack growth analysis based solely on the original specimen geometry cannot be expected to yield reliable failure strength predictions for specimens experiencing stable crack extension that is not collinear with an original notch. In such cases, only the stress causing crack initiation can be expected to be predictable. It is not surprising that an original crack length/failure stress relationship is not noted in [44]. For such cases, failure stresses are more likely related to the length of the extended cracks just before failure. In contrast to the work of Peters, the experiments from [14] show agreement with an

analysis assuming that critical stresses are proportional to the square root of the original crack length. This is especially significant in that crack initiation stresses were the experimentally determined critical stresses. Again, however, a careful, thorough investigation of the issue remains to be attempted and published in the open literature.

A number of criteria should be fulfilled by a group of tests used to determine the relationship between critical stresses and original notch length in composites. First, the predicted direction of crack extension should not be collinear with the original flaw. In this way, the work by Wu [15] verifying the relationship for collinear crack extension in unidirectional fiberglass would not be duplicated. Second, the tests should be made as arbitrary as possible. Specifically, the notch should be subjected to mixed-mode far-field applied stresses, and/or mixed-mode crack-tip displacements. In the experiments in [14], for example, the near-crack-tip displacements and far-field applied stresses are both pure mode I, thus not fulfilling this requirement. This requirement is important in light of the observation made in [15] that pure mode far-field applied stresses may not necessarily result in pure mode near-crack-tip displacements. This is pointed out as a possible problem in extending isotropic fracture mechanics principles to composites.

The third requirement of tests attempting to validate a proportional relationship between critical stresses and the square root of the original notch length is that no dilemma exist concerning what critical stresses are predictable by theory. This can be done by choosing tests that exhibit only unstable crack extension, thus making the crack initiation stress equal the specimen fracture stress. This also eliminates the cumbersome and potentially difficult task of determining the applied stress at crack initiation. The final requirement of this type of test is that it be easy to accurately determine the near-crack-tip stress state. The best way to do this is to perform simple, established experiments.

Taking all of the above factors into account, a good set of initial experiments for such a study would be a series of tensile tests on 45°, 60°, and 75° off-axis specimens having horizontal notches of various lengths. All of these tests would have mixed-mode near-crack-tip displacements and crack extension at an angle to the original notch. Unnotched tensile specimens of such orientations experience very brittle fractures, making it unlikely that notched specimens experience stable crack

extension. Finally, these tests are well-established and the amount of shear coupling present is small, making analysis of them relatively simple. Given these experiments as a base, more complicated tests could be run, including tests on laminates to help define the limits of the dependence of critical stresses on original notch length.

C.3 Role of Normal Stress in Controlling Crack Extension

As stated in the section describing the normal stress ratio theory, the fundamental assumption in formulating and applying the theory is that mode I crack opening controls crack extension. Although this is a plausible assumption, it remains to be rigorously correlated with experimental observation. The most direct way to gain insight into the fracture mechanism at work is to look at specimen fracture surfaces using a scanning electron microscope. A definitive set of experiments would be notched and unnotched 5°, 10°, and 15° off-axis tensile coupon tests. For the unnotched specimens, fracture surface examinations should indicate fracture predominately due to shear stresses. A direct comparison could then be made with the fracture surfaces of notched off-axis coupons to see if they indeed experienced normal-stress-dominated fractures. A two-part study comparing these experimental results with those from the normal stress ratio theory analysis of notched and unnotched tensile coupons (Section 6.1 of this report) represents a simple, concise, and important investigation into the issue of whether normal stress does indeed control notched composite fracture.

C.4 Functional Relationship of Normal Strength

One of the most important parameters within the normal stress ratio theory is the normal strength parameter, $T_{\varphi\varphi}$. Any error in its assumed functional form has the potential to significantly affect normal stress ratio theory crack growth direction and critical stress predictions. This potential is especially great for tests having a predicted direction of crack extension other than along the material fibers. In such cases, the value of $T_{\varphi\varphi}$ along the predicted direction of crack extension must be approximated using Eq. 6. As a result, any fallacies in the functional form for $T_{\varphi\varphi}$ used in Eq. 6 can be especially detrimental in applications to multidirectional and mildly anisotropic unidirectional composites.

The reason that $T_{\varphi\varphi}$ is defined is that no experimental technique or procedure has been established to determine the normal strength on an arbitrary plane in an anisotropic material. In order to verify the functional form of the variation of normal strength with direction that is assumed by the normal stress ratio theory, a test method must be obtained that can achieve failures perpendicular to the loading axis in off-axis tension specimens. The method suggested in this study is related to crack growth tests performed by Beaumont and Phillips [45]. In their study, an attempt is made to force crack extension to be collinear with the original notch in 0° coupons with horizontal notches. The goal of the study was to determine the notch sensitivity of various unidirectional composite materials. The specimen used is illustrated in Figure 76. At the center of the specimen gage length, two symmetric troughs are cut through the specimen thickness, at 90° to the loading axis. A horizontal notch is then cut along the necked portion of the specimen. In this way, it was hoped that the troughs would channel crack growth along a direction collinear with the original notch. Three materials were tested this way. The method was clearly successful for graphite-epoxy with surface-treated fibers. Specimens of graphite-epoxy with untreated fibers and S-glass epoxy, however, showed some tendency to exhibit crack growth along the fiber direction.

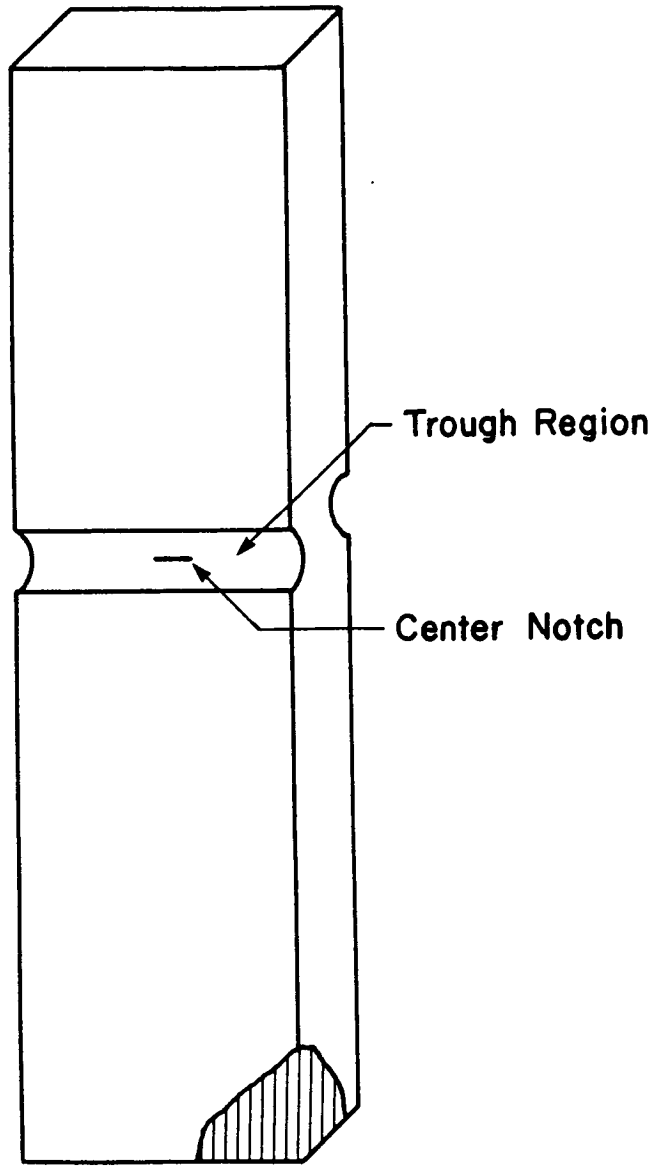

Figure 76. Specimen Used by Beaumont and Phillips [45]: Collinear Crack Extension is Encouraged in Notched 0° Tensile Coupons

An unnotched version of the specimen used by Beaumont and Phillips could potentially be used to determine the normal strength on an arbitrary plane in an anisotropic material. Tensile specimens with fiber orientations ranging from 0° to 90° in, perhaps, 15° increments could be tested, each specimen having a trough cut perpendicular to its tensile loading axis. The troughs could thus be used to encourage normal strength-type failures in the same way that Beaumont and Phillips used them to encourage collinear crack extension. Such failures might be difficult to achieve for all fiber orientations, but could be encouraged by using thick specimens with deeply cut troughs. It would also be advantageous to use a material that is only mildly anisotropic. In order to obtain consistent strength values, it would be important to make sure that as little variation as possible exist in the way the troughs are cut in each specimen, and that no damage be imparted to the specimens by the trough cutting action.

The results of a series of tests like those outlined above could be summarized by a plot of troughed specimen normal strength vs. fiber orientation. As illustrated in Figure 77, this plot could easily be compared with a plot of the variation of material normal strength vs. fiber orientation assumed in the normal stress ratio theory. If it is assumed that the stress concentration caused by the troughs is independent of fiber orientation, then the experimentally obtained values of normal strength on a given plane should differ from the actual normal strength values by a single constant. This assumption can be checked by looking at the strength reduction due to the trough for 0° and 90° specimens, where the normal strengths are known as X_t and Y_t, respectively. The most difficult portion of this investigation would be finding a suitable material and test geometry to consistently achieve normal strength-type failures. Such failures would not have to be achieveable for all fiber orientations, however, and once this problem is solved, the experiments could easily be performed.

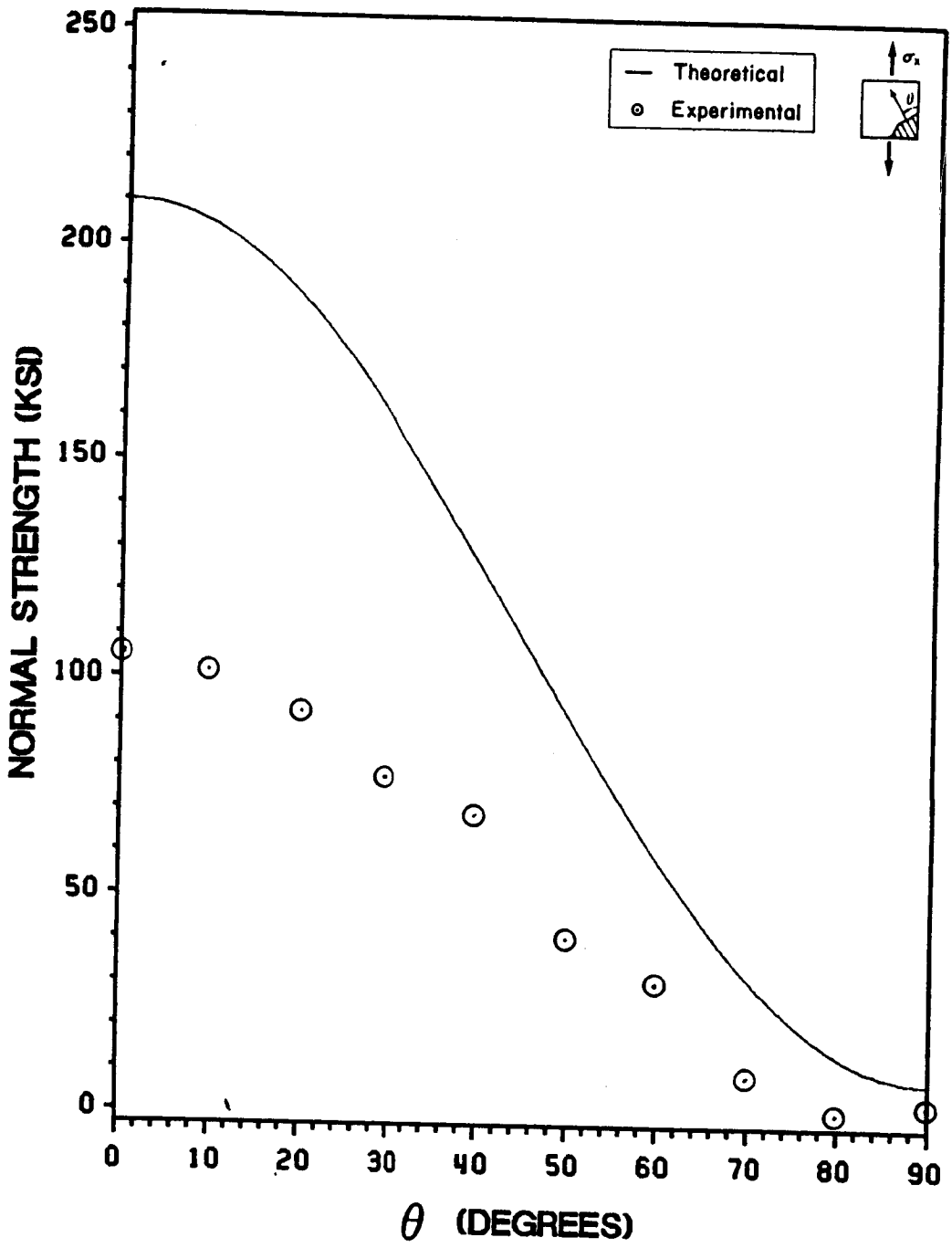

Figure 77. Possible Theoretical and Troughed Specimen Normal Strengths vs. Fiber Orientation

BIBLIOGRAPHIC DATA SHEET	1. Report No. CCMS-87-09, VPI-E-87-10	2.	3. Recipient's Accession No.

4. Title and Subtitle

AN ANALYTICAL AND EXPERIMENTAL STUDY OF CRACK EXTENSION IN CENTER-NOTCHED COMPOSITES

5. Report Date: July 1987

6.

7. Author(s)

J. L. Beuth, Jr. and C. T. Herakovich

8. Performing Organization Rept. No. VPI-E-87-10

9. Performing Organization Name and Address

Virginia Polytechnic Institute and State University
Engineering Science and Mechanics Dept
Blacksburg, Virginia 24061

10. Project/Task/Work Unit No.

11. Contract/Grant No.

NAG-1-343

12. Sponsoring Organization Name and Address

1. National Aeronautics and Space Administration
2. Hercules Incorporated
3. Center for Innovative Technology

13. Type of Report & Period Covered

14.

15. Supplementary Notes

16. Abstracts

The normal stress ratio theory for crack extension in anisotropic materials is studied analytically and experimentally. The theory is applied within a macroscopic-level analysis of a single center notch of arbitrary orientation in a unidirectional composite material. The bulk of the analytical work of this study applies an elasticity solution for an infinite plate with a center line crack to obtain critical stress and crack growth direction predictions. An elasticity solution for an infinite plate with a center elliptical flaw is also used to obtain qualitative predictions of the location of crack initiation on the border of a rounded notch tip. The analytical portion of the study includes the formulation of a new crack growth theory that includes local shear stress. Normal stress ratio theory predictions are obtained for notched unidirectional tensile coupons and unidirectional Iosipescu shear specimens. These predictions are subsequently compared to experimental results.

17. Key Words and Document Analysis. 17a. Descriptors

fracture of composites, graphite-epoxy, anisotropic elasticity, normal stress ratio, tension tests, Iosipescu shear tests

17b. Identifiers/Open-Ended Terms

17c. COSATI Field/Group

18. Availability Statement	19. Security Class (This Report)	21. No. of Pages
unlimited	UNCLASSIFIED	234
	20. Security Class (This Page) UNCLASSIFIED	22. Price

VIRGINIA TECH CENTER FOR COMPOSITE MATERIALS AND STRUCTURES

The Center for Composite Materials and Structures is a coordinating organization for research and educational activity at Virginia Tech. The Center was formed in 1982 to encourage and promote continued advances in composite materials and composite structures. Those advances will be made from the base of individual accomplishments of the forty members who represent ten different departments in two colleges.

The Center functions through an Administrative Board which is elected yearly and a Director who is elected for a three-year term. The general purposes of the Center include:

- collection and dissemination of information about composites activities at Virginia Tech,
- contact point for other organizations and individuals,
- mechanism for collective educational and research pursuits,
- forum and agency for internal interactions at Virginia Tech.

The Center for Composite Materials and Structures is supported by a vigorous program of activity at Virginia Tech that has developed since 1963. Research expenditures for investigation of composite materials and structures total well over seven million dollars with yearly expenditures presently approximating two million dollars.

Research is conducted in a wide variety of areas including design and analysis of composite materials and composite structures, chemistry of materials and surfaces, characterization of material properties, development of new material systems, and relations between damage and response of composites. Extensive laboratories are available for mechanical testing, nondestructive testing and evaluation, stress analysis, polymer synthesis and characterization, material surface characterization, component fabrication, and other specialties.

Educational activities include eight formal courses offered at the undergraduate and graduate levels dealing with the physics, chemistry, mechanics, and design of composite materials and structures. As of 1984, some 43 Doctoral and 53 Master's students have completed graduate programs and several hundred Bachelor-level students have been trained in various aspects of composite materials and structures. A significant number of graduates are now active in industry and government.

Various Center faculty are internationally recognized for their leadership in composite materials and composite structures through books, lectures, workshops, professional society activities, and research papers.

MEMBERS OF THE CENTER

Aerospace and Ocean Engineering
Raphael T. Haftka
Eric R. Johnson
Rakesh K. Kapania

Chemical Engineering
Donald G. Baird

Chemistry
James E. McGrath
Thomas C. Ward
James P. Wightman

Civil Engineering
R. M. Barker

Electrical Engineering
Ioannis M. Besieris
Richard O. Claus

Engineering Science and Mechanics
Hal F. Brinson
Robert Czarnek
David Dillard
Norman E. Dowling
John C. Duke, Jr.
Daniel Frederick
O. Hayden Griffin, Jr.
Zafer Gurdal
Robert A. Heller
Edmund G. Henneke, II
Carl T. Herakovich
Robert M. Jones
Liviu Librescu
Alfred C. Loos
Don H. Morris
John Morton
Ali H. Nayfeh
Marek Pindera
Daniel Post
J. N. Reddy
Kenneth L. Reifsnider
C. W. Smith
Wayne W. Stinchcomb
Surot Thangjitham

Industrial Engineering and Operations Research
Joel A. Nachlas

Materials Engineering
D. P. H. Hasselman
Robert E. Swanson

Mathematics
Werner E. Kohler

Mechanical Engineering
Charles E. Knight

Inquiries should be directed to:

Center for Composite Materials and Structures
College of Engineering
Virginia Tech
Blacksburg, VA 24061
Phone: (703) 961-4969

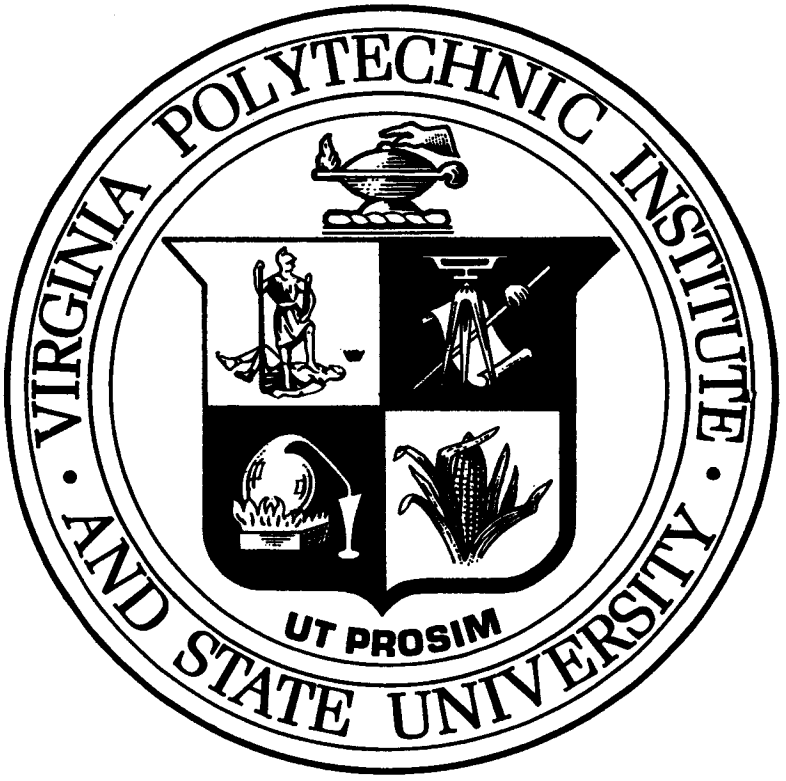
VIRGINIA POLYTECHNIC INSTITUTE
AND STATE UNIVERSITY
UT PROSIM